University of Notre Dame

2019-2020

Notre Dame Rocketry Team
Critical Design Review

NASA Student Launch 2020

Lunar Sample Retrieval System and Air Braking System

Submitted January 10, 2020

365 Fitzpatrick Hall of Engineering
Notre Dame, IN 46556

Contents

List of Tables

List of Figures

Table 1: List of Acronyms

Acronym	Meaning
ABS	Air Braking System
ACCST	Advanced Continuous Channel Shifting Technology
AGL	Above Ground Level
CFD	Computational Fluid Dynamics
CFEA	Competition Future Excursion Area
CPU	Central Processing Unit
CRAM	Compact Removable Avionics Module
DSM	Digital Spectrum Modulation
ESC	Electronic Speed Controller
FEA	Finite Element Analysis
FMEA	Failure Modes and Effects Analysis
FPS	Frames Per Second
FPV	First-Person View
IMU	Inertial Measurement Unit
LED	Light Emitting Diode
LiPo	Lithium Polymer
NDRT	Notre Dame Rocketry Team
OpenCV	Open Source Computer Vision Library
OPTO	Optoisolator
PCB	Printed Circuit Board
PDB	Power Distribution Board
PID	Proportional-Integral-Derivative
PLA	Polylactic Acid
PWM	Pulse-Width Modulation
RC	Radio Controlled
RF	Radio Frequency
UAV	Unmanned Aerial Vehicle

1 Summary of Report

1.1 General Information

School Name:
University of Notre Dame
Team Name:
Notre Dame Rocketry Team
(NDRT)
Address:
365 Fitzpatrick Hall
Notre Dame, IN 46556

Team Lead:
Collette Gillaspie
cgillasp@nd.edu
402.699.736
Safety Officer:
Brooke Mumma
bmumma@nd.edu
314.288.8297

Mentor:
Dave Brunsting
NAR/TRA Level 2
dacsmema@gmail.com
269.838.4275
NAR/TRA Section:
TRA #12340
Michiana Rocketry

1.2 Launch Vehicle Summary

The launch vehicle is 134 in. long with a loaded mass of 798 oz. The final motor choice is a Cesaroni L1395, which will allow the vehicle to attain the target altitude of 4,444 ft after launching from a 12 ft. 1515 rail. The drogue parachute is a FruityChute CFC-24 and will deploy at apogee, and at 600 ft. the the main parachute, a FruityChute Iris Ultra 120 Compact, will deploy.

1.3 Payload Summary

Lunar Sample Retrieval System

The primary payload experiment is a Lunar Ice Sample Retrieval System, which includes a Rover and an Unmanned Aerial Vehicle (UAV). The payload will be secured in the launch vehicle for flight and recovery, and a black powder charge will eject the nose cone at 450 ft. for deployment purposes. The Rover, powered by an eccenctric crank mechanism, will be activated to pull out the UAV upon landing. The autonomous UAV, with a fail-safe manual override system, will ascend and find a Competition Future Excursion Area (CFEA) using computer vision and target detection algorithms. The UAV will then descend to the CFEA, land, and transmit the GPS coordinates of the CFEA to the Rover. The Rover will deploy upon reception of the coordinates, drive to the center of the CFEA, and activate an Archimedes screw sample retrieving system. Finally, the Rover will transport the 10 mL sample 10 ft.

Air Braking System

The secondary payload experiment is an Air Braking System (ABS), which will implement a control system for inducing a variable drag force in order to meet the target apogee of 4,444 ft. A set of drag surfaces will be extended from the body of the launch vehicle to increase the acting drag force, therefore decreasing the projected apogee, until the target has been achieved. The system will use a microcontroller to keep track of altitude and velocity sensor data and run a closed loop PID control algorithm to adjust the extension of the drag tabs until the predicted apogee matches the target apogee. The microcontroller will adjust the extension of the drag tabs by controlling a servo motor, which will drive a mechanism to actuate the drag tabs.

2 Changes Since PDR

2.1 Changes Made to Launch Vehicle Criteria

Table 2: Changes Made to Launch Vehicle Criteria

Decision	Justification
Payload weight increase from 100 oz to 111 oz	Apogee simulations yielded altitudes above the range of the Air Braking System & Lunar Sample Retrieval System CAD mass estimate predicts a system heavier than originally expected
Telemetry for recovery allocated 45 oz in the nose cone	Space available in the nose cone in order to fulfill NASA Requirement 3.12.

2.2 Changes Made to Payload Criteria

Table 3: Payload Criteria Changes

Decision	Justification
LSRS retention via solenoids	Mechanically robust: FEA shows that four friction fitted solenoids can successfully retain the LSRS & Electronically simple: Control of system governed by a simple processor
Nose cone ejection for deployment	Simplicity: Dual-vehicle payload system of rover and UAV makes mechanical deployment complicated

2.3 Changes Made to Project Plan

Table 4: Changes Made to Project Plan

Decision	Justification
Gantt chart software updated	Previous software did not allow for great detail in subsystem project tests, deadlines, etc.
Budget updated	Budget presented in CDR is nearly complete. Both items that have been purchased along with items that the team plans to purchase are listed in the itemized budget (Table 95)

3 Launch Vehicle Technical Design

3.1 Mission Statement

The mission of the Notre Dame Rocket Team is to design and build a launch vehicle to reach a target altitude of 4,444 ft, measured with the use of on-board altimeters and upon landing deploy a UAV and rover for simulated lunar ice sample collection. The launch vehicle will be designed to be recoverable and reusable without need of repair and have four independent sections. A full list of NASA Requirements can be found in Section 6.2.1.

3.1.1 Mission Success Criteria

In order to evaluate mission success, the team has derived a set of criteria as follows:

V.MS.1 The launch vehicle will begin a controlled ascent upon motor ignition and exit the rail with a velocity of 65 ft/s.

V.MS.2 The launch vehicle will reach a burnout without incident at which time the Air Braking System will activate.

V.MS.3 The launch vehicle will reach a target apogee of 4444 ± 44 ft AGL

V.MS.4 The drogue parachute will deploy at apogee and the main parachute will deploy at 600 ft AGL.

V.MS.5 All sections of the launch vehicle will descend safely and be fully reusable on the same day.

3.2 Launch Vehicle Overview

The 2019-2020 Notre Dame Rocketry Team is proud to present this year's launch vehicle. The launch vehicle will will allow the team to safely house, launch to an apogee of 4,444 ft and recover the Rover and UAV. The full-scale launch vehicle will be composed of four independent sections: the nose cone, the payload bay, the recovery bay, and the fin can. This year's vehicle can be found in Figure 1. The nose cone will house the telemetry module while the payload bay and recovery body tube will house their respective subsystems. The fin can contains the secondary payload, motor, and fins. The airframe has a variable diameter with a fore diameter of 8 in. and an aft diameter of 6 in. The center of gravity (CG) is located 75.75 in. from the tip of the nose cone and the center of pressure (CP) is located 96.36 in. from the tip of the nose cone, giving the vehicle a stability of 2.57 calibers as described in Section 3.9.2.

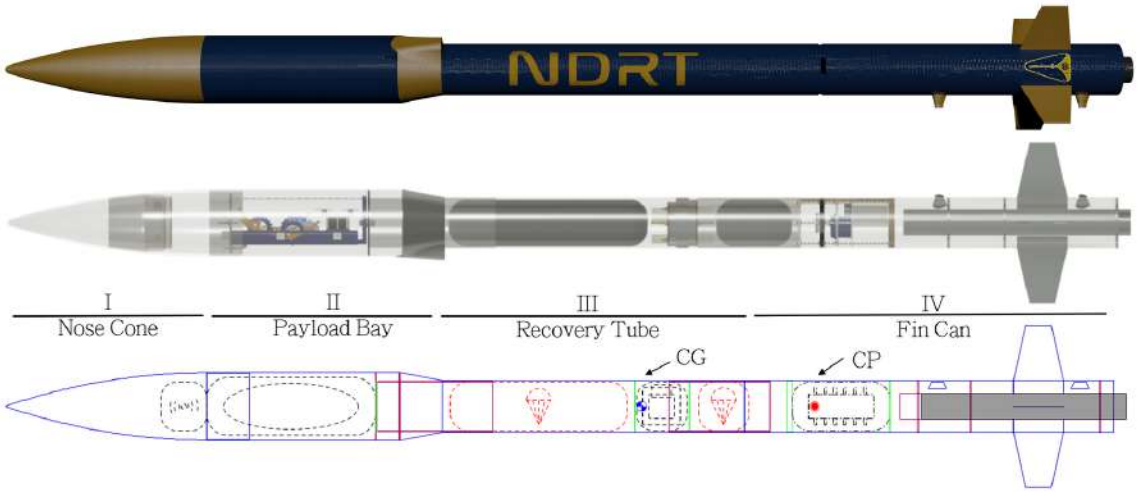

Figure 1: NDRT 2020 Competition Vehicle

Found in Table 5 is a summary of each component and the selected material for the airframe section. Materials were selected based on availability, cost, and weight. Material analysis is further discussed under Section 3.5.1.

Table 5: Component Material Summary

Component	Material
Nose Cone	ASA Plastic
Payload Bay	Fiberglass
Transition Section	ASA PLastic
Recovery Tube	Carbon Fiber
Fin Can	Carbon Fiber
Motor Mount	Carbon Fiber

3.2.1 Size and Mass Statement

The launch vehicle is made of carbon fiber, fiberglass, and 3D printed ASA plastic and has a length of 134 in. with a fore outer diameter of 8.005 in. and an aft outer diameter of 6.122 in., giving the payload, recovery system and flight controls adequate space to function. There are four G10 fiberglass isosceles trapezoid fins. The launch vehicle has a loaded weight of 822 oz and an unloaded weight of 670 oz with an estimated loaded stability margin of 2.63 cal. Figure 2 shows the updated model of the launch vehicle which is followed by a summary of the lengths of each section and component in Table 6.

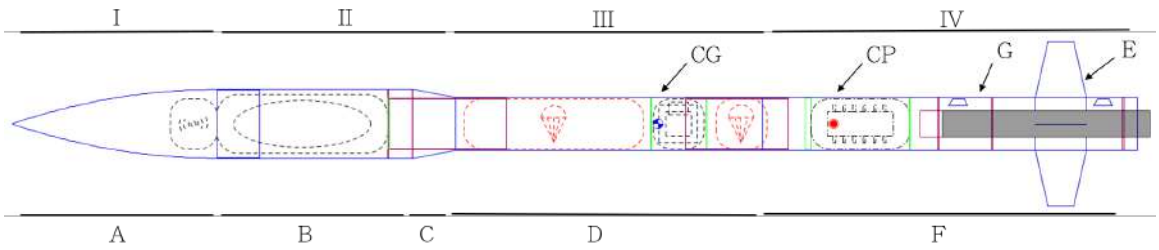

Figure 2: Launch Vehicle Detailed Section Breakdown

Table 6: Section and Component Length Summary. *Does not contribute to vehicle's overall length

Section	Label	Component	Length [in.]	Diameter [in.] (if applicable)
I	A	Nose cone	24	8
		Telemetry*	5.5	
II	B	Payload Bay	23	
	C	Transition Section	5	Variable
III	D	Recovery Tube	36	6.112
		Main Parachute*	21	
		CRAM*	6	
		Drogue Parachute*	6	
IV	F	Fin Can	44	
		ABS*	12	
	G	Motor Mount*	24	3
	E	Fins*	6 (height)	

Figure 3 is a pie chart depicting the weight breakdown of each subsystem of the launch vehicle in oz.

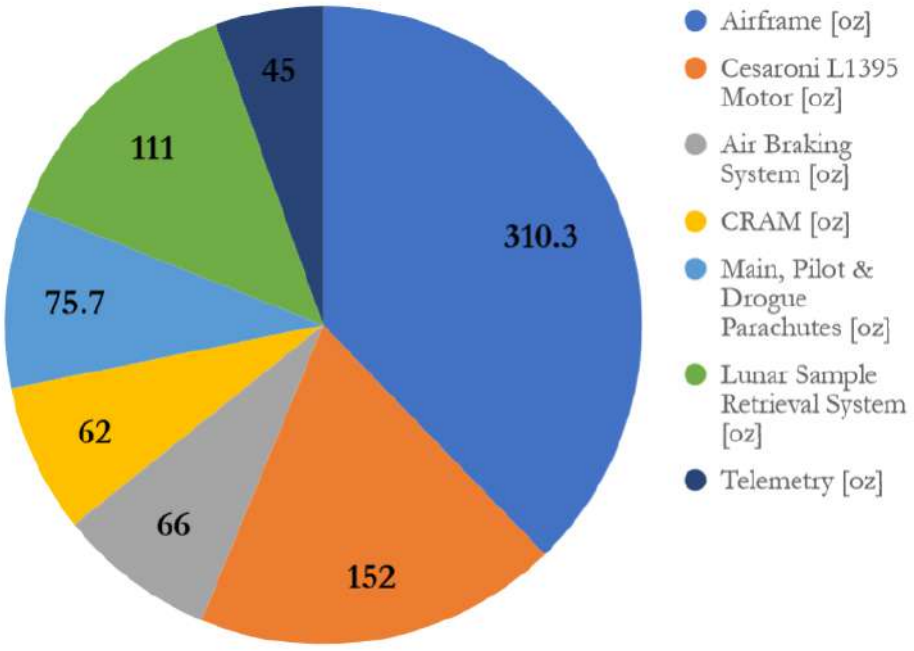

Figure 3: Launch Vehicle Weight Allocation per System in oz

3.2.2 Final Motor Choice

The motor selected for this launch vehicle is the Cesaroni L1395. This motor is at the higher end of total impulse for L-class motors with a total impulse of 4895.4 Ns. When taking conservative estimates for payload and component masses, this motor will exceed the target altitude of 4,444 ft allowing for effective use of ABS to adjust to the target apogee. More detailed information, including the vehicle's performance at different launch angles and wind speeds, can be found in Section 3.9. Additionally, the vehicle will utilize a 12 ft. 1515 launch rail. The selected motor's thrust curve can be found in Figure 4.

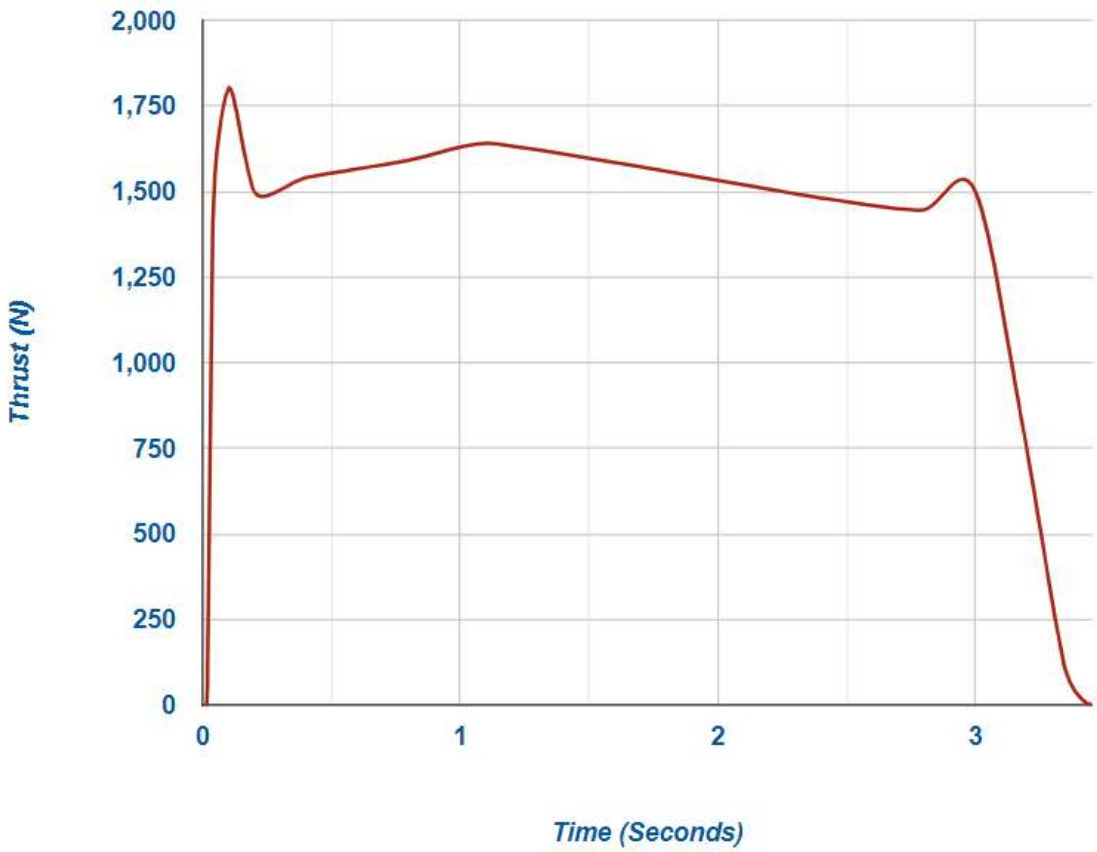

Figure 4: L1395-BS Time-Thrust Curve

3.2.3 Target Apogee

The team has selected a target apogee of 4,444 ft for the launch vehicle. For ideal launch conditions—a launch with 0 mph wind—an OpenRocket simulation for the launch vehicle gave a maximum apogee of 4,939 ft, with 0 mph wind and a launch angle of 5°, and a minimum apogee of 4,354 ft, with 20 mph wind and a launch angle of 10°. The target apogee is achievable in nearly all expected launch conditions using the ABS, which is predicted to be able to reduce apogee by 500 ft.

3.3 Subsystem Design

Each design decision was informed by weight and size restrictions, material properties, and the ability to purchase or manufacture parts. Final decisions were made through trade studies in the Preliminary Design Review. The design of each section of the launch vehicle is discussed in more detail in Sections 3.3.1-3.3.6.

3.3.1 Nose Cone

The nose cone will follow a 3:1 tangential ogive shape with curvature defined by Equation 1. This results in an ogive radius, ρ, of 74 in. The final dimensions of the nose cone are displayed in Table 7.

$$\rho = \frac{R^2 + L^2}{2R} = 74 \text{ in.} \tag{1}$$

ρ	Radius (in.)
L	Nose Cone Length (in.)
R	Base Radius (in.)

Table 7: Nose Cone Dimensions

Dimension	Value
Exposed Length (in.)	24
Shoulder Length (in.)	4
Base Outer Diameter (in.)	8
Base Inner Diameter (in.)	7.815
Weight (oz)	35

Due to the commercial scarcity of a nose cone with the 8 in. base diameter needed to fit the payload bay, the nose cone will be 3D printed in ASA plastic in-house through the Notre Dame IDEA Center Innovation Lab. Due to print size constraints, the 24 in. nose cone will be printed in three separate parts that fit together. The top and bottom parts are joined together with the third part, which acts like a coupler. The central piece also has an integrated mount for the telemetry module. The entire assembly is then epoxied together. This three-part design is depicted in Figure 5, and Figure 6 shows the full part. The outer surface will be smoothed by light sanding and painted to ensure an aerodynamic finish. ASA plastic was selected for the nose cone material because the nosecone is non-load bearing, and therefore does not require high material strength, and is less dense than Garolite G10 fiberglass.

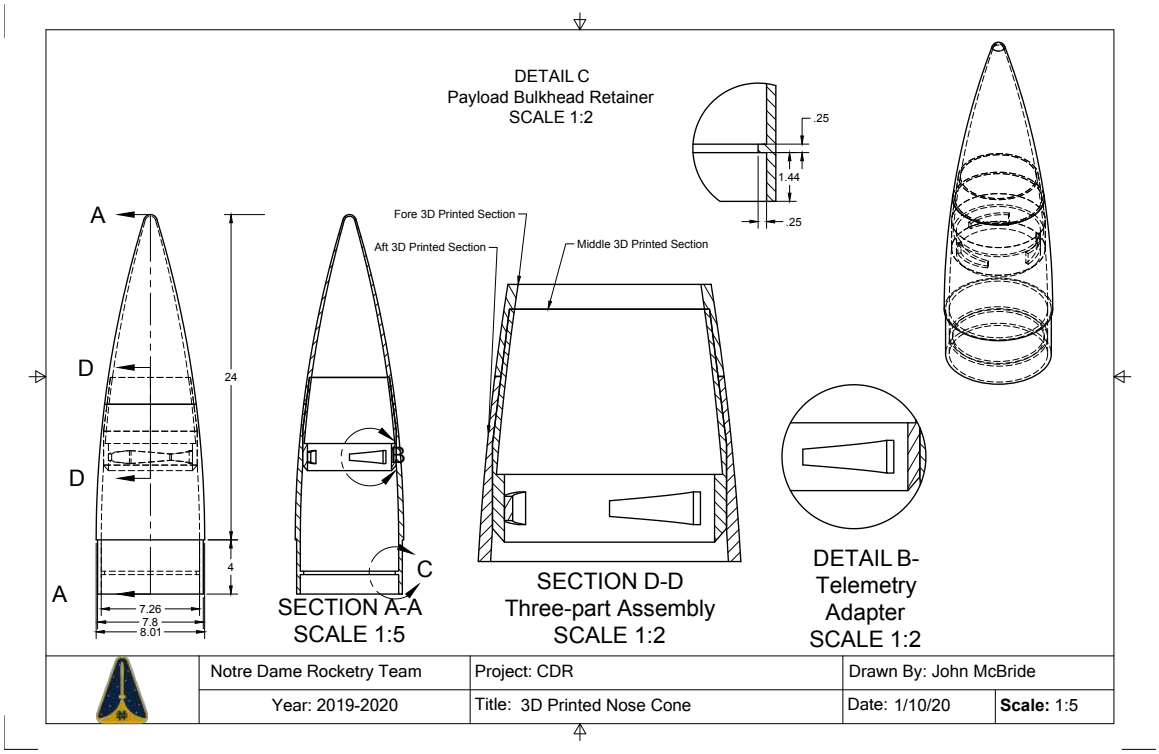

Figure 5: Student Fabricated Nose Cone Engineering Drawing

Figure 6: Student Fabricated Nose Cone

3.3.2 Payload Bay

The payload bay is a 23 in. long fiberglass body tube, which will house the scoring payload to be deployed after landing. The 8 in. diameter body tube was selected to meet the Team Derived Requirement V.5 of radio transparency for the payload. The fore end of the 23 in. long body tube

will be connected to the nose cone and the aft end will be connected to the transition section. The nose cone will be secured with shear pins and the transition section will be secured to the payload bay using a coupler, two centering rings, and epoxy. Figure 7 shows a detailed drawing of this section, and Figure 8 shows the CAD rendering for this section.

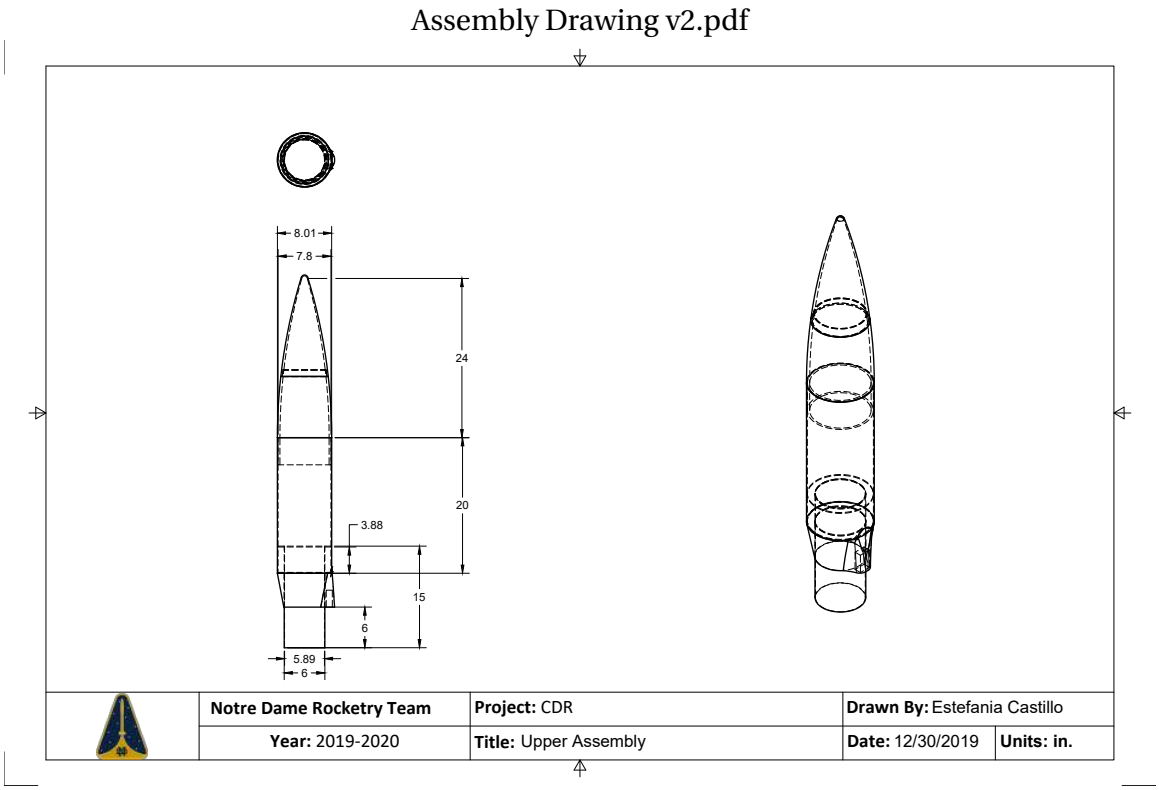

Figure 7: Nose cone, Payload Bay, and Transition Section Drawing

Figure 8: Nose cone, Payload Bay, and Transition Section

3.3.3 Transition Section

Because the launch vehicle has a variable diameter, the transition section must be designed to prevent flow separation. This will reduce drag and decreases turbulent eddies, which could impact altitude barometer readings. The transition section will have a fore diameter of 8 in. and an aft diameter of 6.122 in. with a length of 5 in. The transition section will also house an onboard camera in a built-in shroud designed specifically to hold it. The on-board camera addition allows for visual data of the flight and ABS to be collected, fulfilling Team Derived Requirement V.9. The transition section will be attached to a carbon fiber coupler using epoxy.

Computational Fluid Dynamics (CFD) simulations were run in order to ensure that the transition section angle was shallow enough to prevent flow separation. Simulations were run using Ansys Fluent with a continuity residual convergence criterion of 10^{-3}. The simulation took 430 iterations to converge. A transition SST model solved using a Second Order Upwind method was used for turbulence modeling. The simulation was run with far field pressure boundary conditions and air was modeled as an ideal gas. The Mach number tested was 0.31, which is the average predicted Mach number during flight. A velocity profile produced by the simulation is shown in Figure 9. As shown, the transition section produces effectively no flow separation. There is a small amount of flow separation produced by the camera shroud, but the flow reattaches within 5 in., which has little impact on the flight of the rocket, and will not impact barometric pressure sensors.

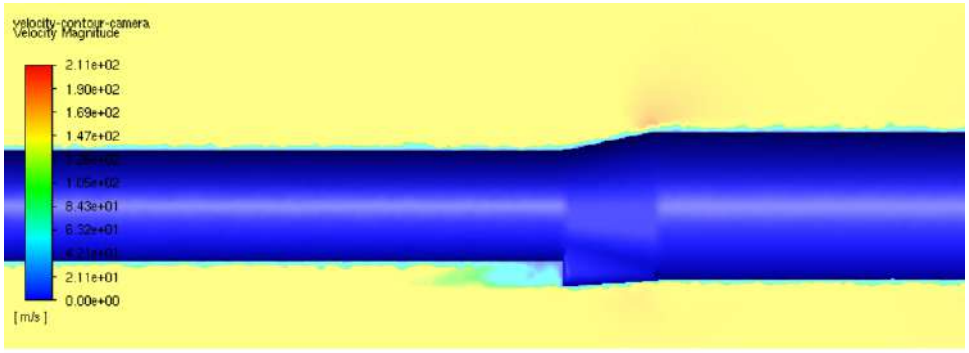

Figure 9: Flow over transiton

Because the transition section is non-load bearing, material selection is very flexible. The team has elected to 3D print it in-house, which allows for customization. The transition section will be printed with Acrylonitrile Butadiene Styrene (ABS) filament, which has higher impact resistance and strength than other filament options available, such as PLA. Figure 10 shows the designed transition section for the vehicle, and Figure 11 shows a rendering of the transition.

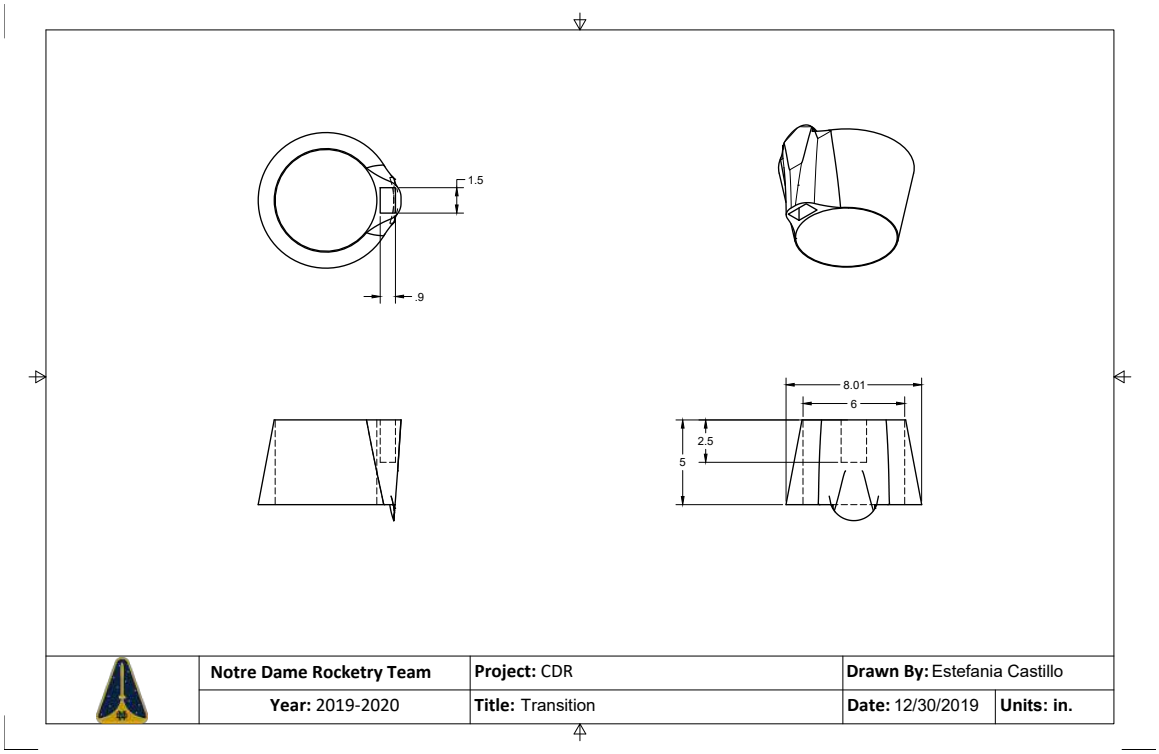

Figure 10: Transition Section Technical Drawing

Figure 11: 3D Printed Transition

3.3.4 Recovery Body Tube

The recovery tube houses the main parachute, the Compact Removable Avionics Module (CRAM), and the drogue parachute. This section is located aft of the transition section and has an outer diameter of 6.122 in. and a length of 36 in. The material selected for the recovery tube is carbon fiber due to its durability and high strength-to-weight ratio. This section of the vehicle is attached to the adjacent sections through carbon fiber couplers. The fore end of the recovery tube is the in-flight separation point for the main parachute and the aft end of the section is the in-flight separation point for the drogue parachute. Additionally, the CRAM is located 7 in. from the bottom of this component. The recovery tube, along with its assembled components, can be found in Figure 12

Figure 12: Assembled Recovery Body Tube

3.3.5 Fin Can

The airframe of the fin can subsystem will also be carbon fiber due to its durability and high strength-to-weight ratio, allowing for a maximum payload weight budget. The fin can will be composed of a 44 in. long body tube, which will be 6.122 in. in diameter, and will house the fins, motor mount, and ABS payload. The ABS payload will rest at the top of the fin can body tube so that the tabs can be within 1 in. of the CP, per Team Derived Requirement V.14. Centering rings will be used to attach the motor mount to the fin can, ensuring that the motor mount remains centered inside the fin can. Additionally, the motor mount will be used as the attachment point for the fins, which will be fabricated according to the specifications laid out in Section 3.3.6. Figure 13 is a drawing of the fin can, and figure 14 shows the fin can assembly. Figure 15 is the drawing for the fully assembled fin can.

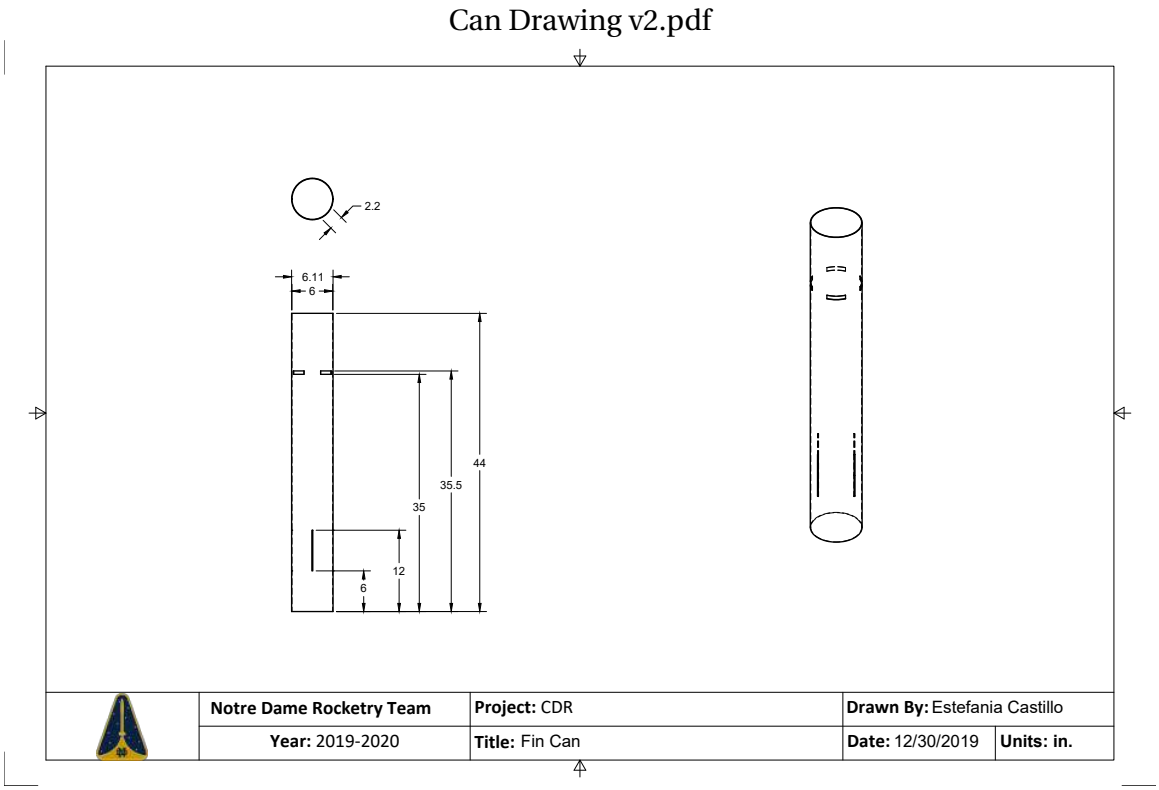

Figure 13: Fin Can Component Drawing

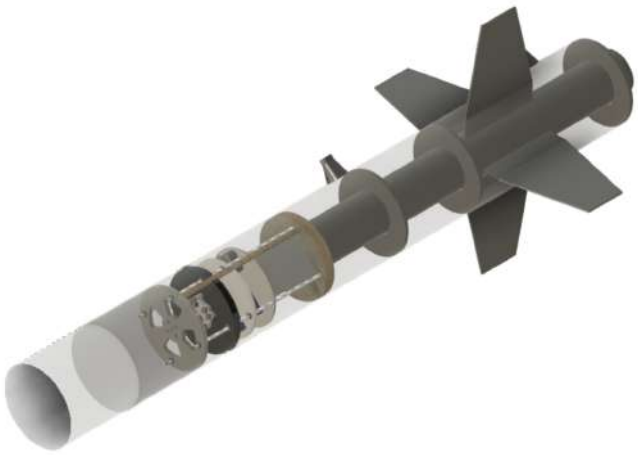

Figure 14: Assembled Fin Can

Fin Can Drawing v2.pdf

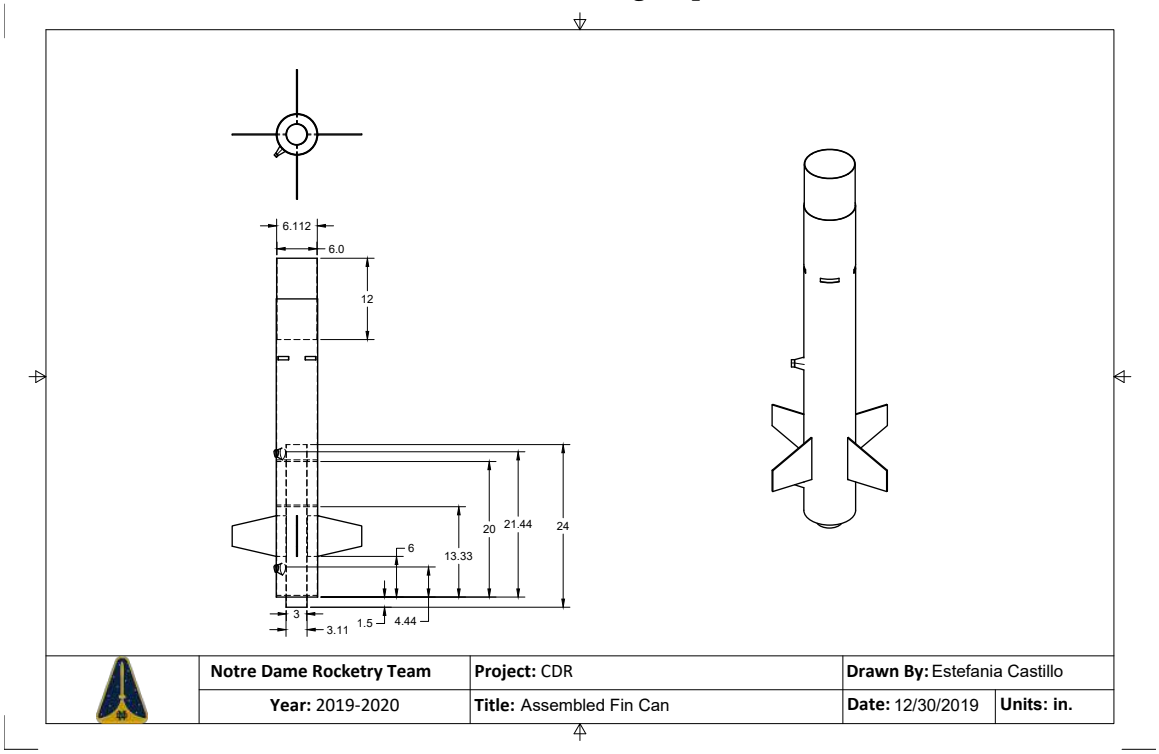

Figure 15: Assembled Fin Can Drawing

3.3.6 Fins

The material, shape, and attachment method were chosen so that the fins could withstand the forces during launch, flight, and landing, while ensuring the stability of the launch vehicle. The fins will be made from 1/8 in. G10 fiberglass because it is durable, commercially available,

and affordable. The fins will be an isosceles trapezoid platform shape, as it results in low drag and is simple to construct. The launch vehicle will have 4 fins, evenly spaced around the base, which creates a higher interface drag and allows for increased stability. An alignment ring used successfully in previous years allows for symmetric attachment of the fins. The alignment ring includes two circular plywood plates with laser-cut slots for the fins that are exactly 90 degrees apart. Figure 16 shows this alignment mechanism. The fins are placed within the slots during construction while the epoxy dries overnight to ensure perfect alignment. Table 8 gives the properties of the fins. Figure 17 below shows the CAD drawing of the fin design and dimensions.

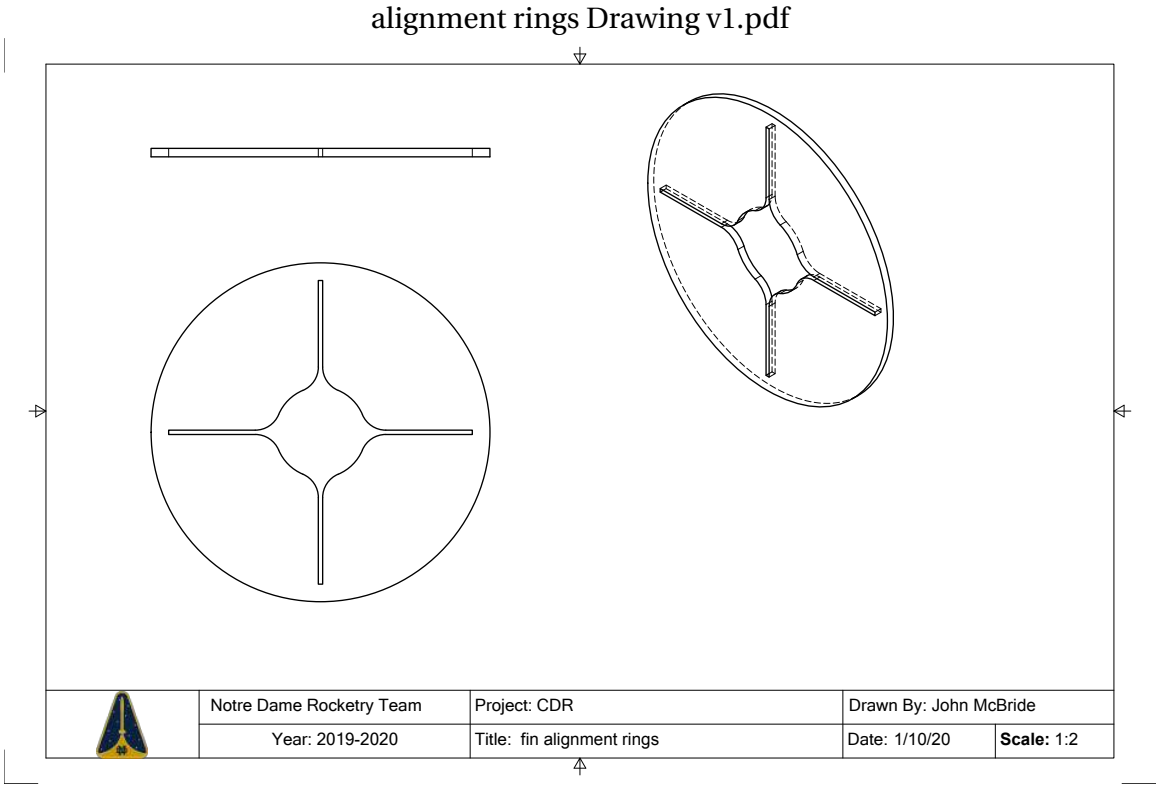

Figure 16: Fin Alignment Rings

The fins will be cut into the designed shape using a CNC router, and the leading and trailing edges will be sanded to reduce drag. Epoxy fillets will be placed inside of the main body to attach the fins onto the fin can. This will ensure the fins will remain perpendicular to the vehicle through the duration of the flight.

Fin Flutter Velocity Calculation

In order to determine whether the fins can withstand the loads during ascent, the velocity at which the fins would flutter was calculated in Equation 2. The fin flutter velocity was calculated using conditions for maximum dynamic pressure, which occurs at burnout. The local speed of sound was calculated at 580 ft, which is the highest simulated burnout altitude, and found to be 1115.5 ft/s. Pressure was found to be 2092.5 lb_f/ft^2, and a shear modulus of 5 GPa was used. From these values, a fin flutter velocity of 800 ft/s was calculated. This value is 220 ft/s above the greatest expected velocity, approximately 580 ft/s, ensuring the fins will not fail during ascent.

Table 8

Dimension	Value
Material	Carbon Fiber
Planform Shape	Isosceles Parallelogram
Root Chord Length	6.0 in
Tip Chord Length	30 in
Sweep Length	1.5 in
Sweep Angle	13°
Tab Length	6 in
Tab Height	1.5 in
Thickness	0.125 in
Number of Fins	4

See Section 3.9 for Mission Performance Prediction details.

$$V_f = a\sqrt{\frac{G}{1.337(\frac{b^2}{S})^3 P(\frac{c_t}{c_r}+1)} \times 2\left(\frac{b^2}{S}+2\right)\left(\frac{t}{c_r}\right)^3} = 800 \text{ ft/s} \tag{2}$$

a	Speed of Sound	1115.5 ft/s
G	Fin Material Shear Modulus	5 GPa
b	Fin Semi-span	0.542 (ft)
S	Fin Area	0.203 (ft^2)
P	Air Pressure at Max. Velocity	2092.5 (lb_f/ft^2)
c_t	Fin Tip Chord	0.25 (ft)
c_r	Fin Root Chord	0.5 (ft)
t	Fin Material Thickness	0.01 (ft)

3.4 Component Design

Sections 3.4.1-3.4.2 describe the various interior parts of the launch vehicle in depth, discussing their purpose, positions, materials, and construction techniques.

3.4.1 Bulkheads

Bulkheads will separate the various sections of the vehicle, maintain the pressure isolation of those sections, and mount components such as the parachute's shock cord or electronics. There are a total of seven bulkheads in the vehicle. Six bulkheads will be made out of G10

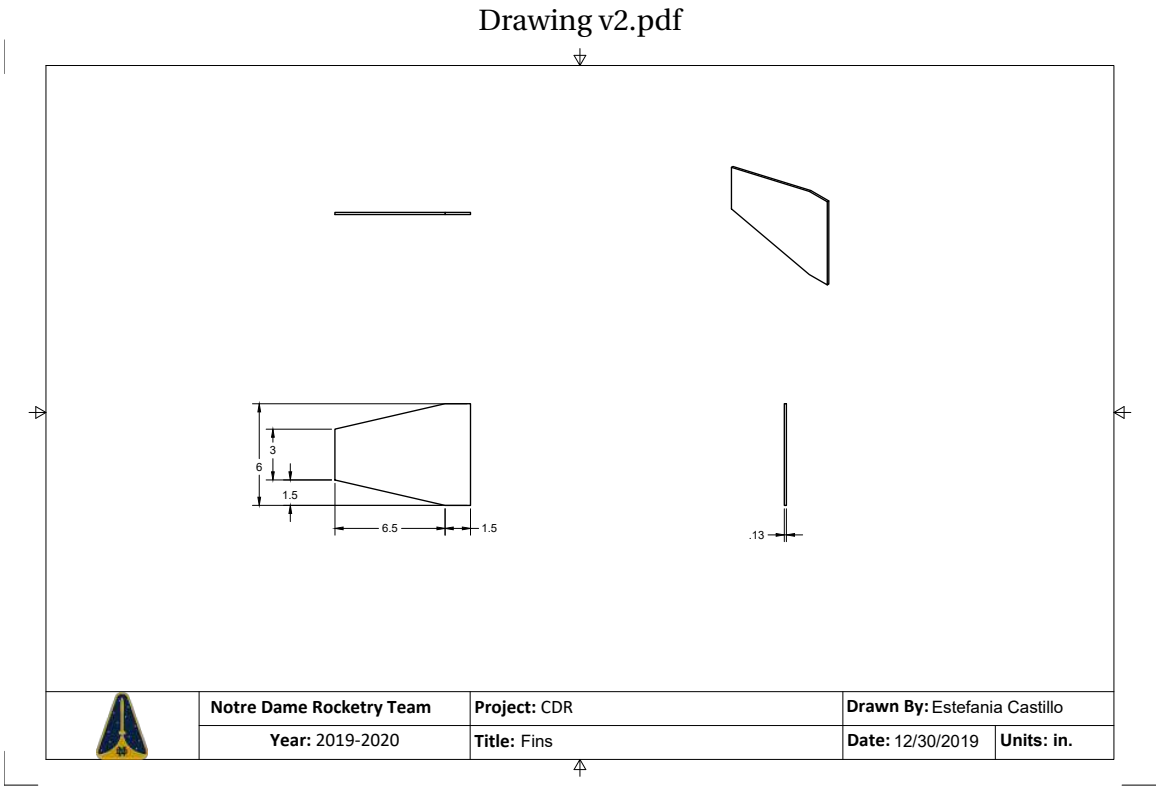

Figure 17: Fin Design and Dimensions

fiberglass. This decision was made based on FEA and historical experience and will be verified with solid testing from January 15-24 (see Vehicle Timeline in Figure 141). The G10 fiberglass bulkhead fore of the motor mount has a diameter of 6 in. and a thickness of 1/8 in. An aluminum bulkhead at the fore end of ABS is 6 in. in diameter and has a thickness of 3/8 in. Two G10 bulkheads keep the Compact Removable Avionics Module within the recovery tube and distribute loads from parachute deployment. These bulkheads are 1/8 in. thick and have a diameter of 6 in. (see Figures 66 and 67 for top and bottom bulkhead drawings, respectively). The main parachute will be attached to a 3/16 in. thick G10 bulkhead that is 5.88 in. in diameter. The fore payload bulkhead is used to eject the nose cone for Lunar Sample Retrieval System deployment. This G10 bulkhead is 1/8 in. and 7.26 in. in diameter. The foremost bulkhead in the launch vehicle is to protect telemetry from the black powder charge. This G10 bulkhead is 6.15 in. in diameter and is 1/8 in. thick.

3.4.2 Centering Rings

Centering rings will connect tubes of different diameters together: between the recovery tube and payload bay, and between the motor mount and fin can. Around the motor mount, the centering rings are also responsible for translating thrust from the motor mount to the rest of the vehicle body. Figure 18 demonstrates how the motor mount will be held in place using centering rings.

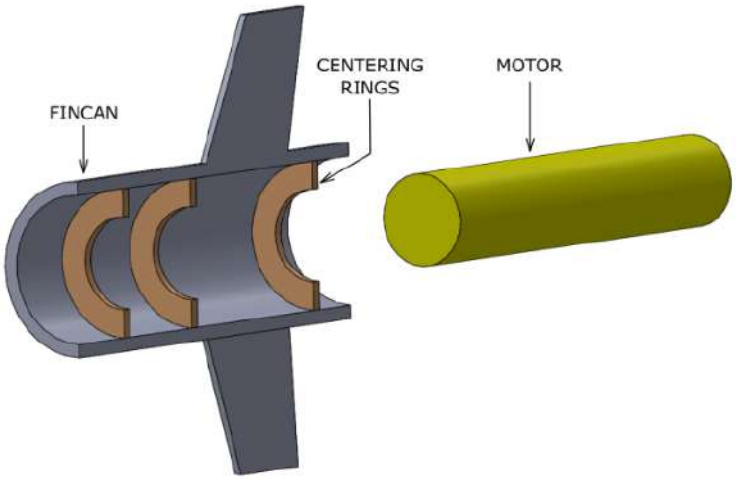

Figure 18: Centering Rings

The centering rings in the fin can will have an inner diameter of 3 in. an outer diameter of 6 in. and a thickness of 0.125 in. Centering rings will also be used to connect the nose cone to the payload bay. The rings used in this part of the rocket will have an inner diameter of 6 in., an outer diameter of 7.812 in., and a thickness of 0.125 in.

Although plywood is cheaper, the centering rings will be made out of fiberglass because it is significantly stronger material and thus compensates for the higher costs.

G10 fiberglass centering rings securing the motor mount were analyzed under the maximum motor load of 400 pounds. Figure 19 shows the results of this analysis. A minimum FoS is 3.037 and hence safe.

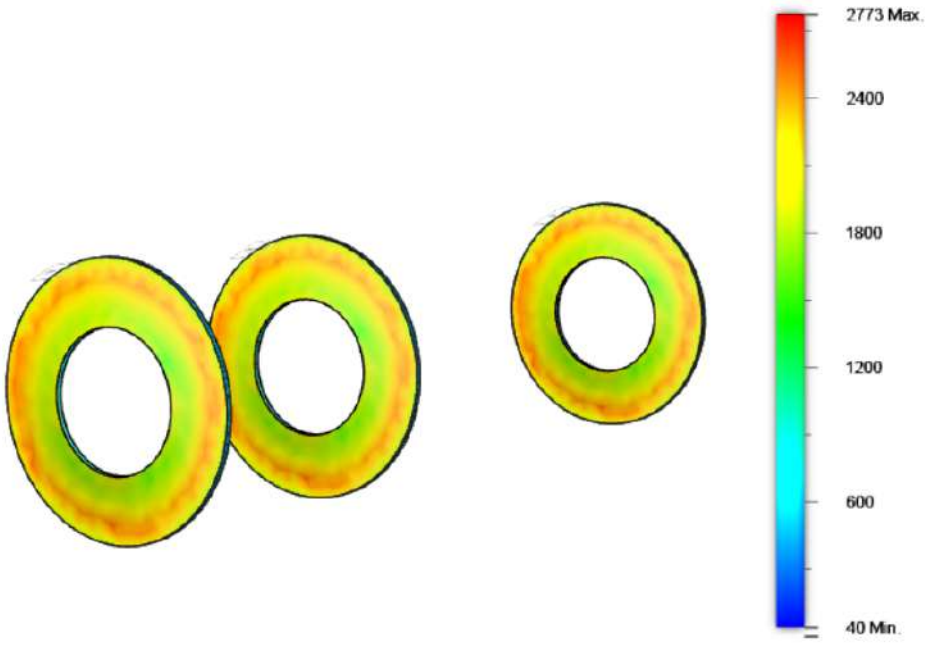

Figure 19: FEA of Centering Rings in Motor Mount

3.4.3 Motor Retention

The motor will be mounted into a carbon fiber tube which will be centered using centering rings, shown in Section 3.4.2, and secured to the launch vehicle with a retaining ring attached to the aft side of the motor mount.

The aluminum casing that will contain the launch vehicle motor is a Cesaroni 75mm 4-grain hardware set. It has a length of 23.95 in. and an outer diameter of 2.965 in. It consists of thin-wall 6061-T6 aluminum, and the forward closure is retained by a formed ring at the head end of the casing. The rear casing has internal threads to hold it steady. Figure 20 shows an image of the Cesaroni aluminum casing.

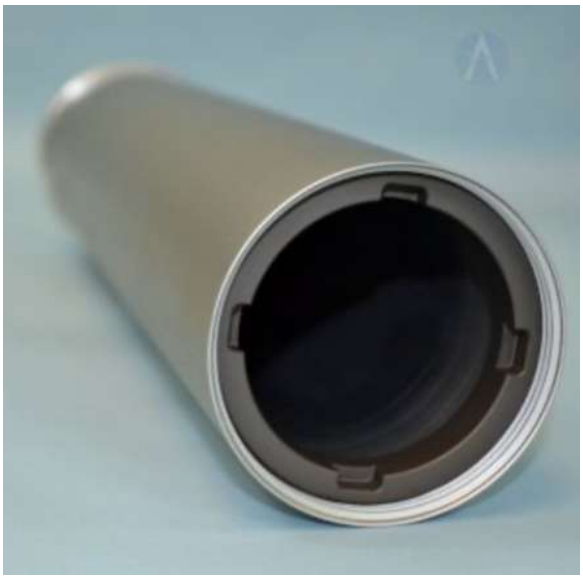

Figure 20: Cesaroni 75mm, 4g Aluminum Casing

The Cesaroni aluminum casing will be restricted in the rocket so that its radial center axis is coincident with the launch vehicle's radial center axis. This will be accomplished using three fiberglass centering rings. The centering rings will have an outer diameter of 6 in., an inner diameter of 2.965 in., and will be 1/8 in. thick. The aluminum casing will be attached to the centering rings using JB Weld epoxy, due to its high heat tolerance, as discussed in section 3.5.3.

The launch vehicle motor itself is a Cesaroni 4-grain L1395 motor, which will be screwed into the aluminum casing, and secured using retaining rings and closures. As these specific parts were designed for the aluminum casing and for a motor of this size, NDRT did not find it necessary to run FOS testing on these parts.

3.5 Material Analysis

In order to ensure that the vehicle airframe and its components would not fail under expected loads, the team considered various properties in making material selection, such as strength, density, availability, cost, among others.

3.5.1 Airframe Components

Materials for the vehicle's airframe were selected based on strength, cost, system-specific requirements (such as radio transparency), along with other considerations. The nose cone and transition section will be 3D printed using ASA plastic, which allows for customization. Since each component only has to withstand the aerodynamic loads of flight, the strength of ASA is sufficient.

The payload bay must be radio transparent so that payload components can communicate with the team without interference. This requirement eliminates carbon fiber from consideration. G12 Fiberglass is a suitable choice for this requirement as it is also relatively durable.

All other sections of the airframe will be fabricated out of carbon fiber. This includes the fin can, fins, recovery tube, and motor mount. Carbon fiber was selected for its durability and strength to help fulfill NASA Requirement 2.4, which states that the launch vehicle be reusable on the same day without repairs. A summary of these materials selections is provided in Table 9.

Table 9: Summary of Material Selection for Airframe Components

Subsystem	Material	Justification
Nose Cone	ASA Plastic	Customizable through student fabrication
Transition Section	ASA Plastic	Non-load bearing, light weight
Payload Bay	Fiberglass	Radio transparent, durable
Recovery Tube	Carbon Fiber	High strength-to-weight ratio
Fin Can	Carbon Fiber	Durable for load bearing
Fins	Carbon Fiber	Durable
Motor Mount	Carbon Fiber	Durable

3.5.2 Load Bearing Structures

Because the centering rings and bulkheads are load bearing, the team elected to conduct solid testing on two bulkhead materials. The testing involved epoxying bulkheads into carbon fiber couplers in the same way in which they would be secured into the vehicle. The bulkheads were then put under a slow-loading force in order to calculate at what force they would fail. The two materials available for bulkhead construction are fiberglass and plywood. Both options been used in previous team projects and are strong, durable, and low cost. Plywood testing procedures may be found in Test VT??? in Section ???, and future fiberglass testing procedures may be found in Test VT??? in Section ???.

Solid testing with a load cell verifies the strength of those materials and also demonstrates the strength of the epoxy used. The test completed on plywood revealed that bulkheads would first start to fail at around 750 N, cracking and splintering, before the epoxy began to fail. In a few of the tests, the epoxy itself was cracked, with a clean break between the coupler and bulkhead.

Those trials, along with the data collected, show that a high quality epoxy connection between the bulkhead and vehicle airframe is crucual to structural integrity. Figures 21 and 22 show the procedure the team completed with plywood bulkheads.

The Compact Removable Avionics Module bulkheads will each experiencing a force of 320 lbs, and the payload section bulkhead will experience a force of 794 lbs. In other words, the bulkhead material needs to withstand forces greater than 750 N (169 lbs). Thus, the team has opted for Garolite G10 fiberglass bulkheads. Garolite G10 fiberglass its excellent impact strength and good strength-to-weight ratio. FEA has demonstrated the material's durability. Nonetheless, solid testing next semester will verify this choice.

Figure 21: Load Cell Setup

Figure 22: Plywood Failed Bulkhead

3.5.3 Adhesives

In order to assemble the launch vehicle, Glenmark RocketPoxy and JB Weld Epoxy will be used. Couplers, bulkheads and twist and lock mechanisms will be secured using a ring of RocketPoxy which should cover the greatest amount of contact surface area between the secured parts. For the motor mount, JB Weld will be used, as JB Weld has a maximum temperature threshold of approximately 600°F and the components in the fin can will be the ones exposed to the greatest temperatures. Every joint is filleted for added strength.

3.6 Subscale Vehicle

A 2:5 scaled variable diameter launch vehicle was developed in order to determine the stability of the proposed launch vehicle as well as to verify calculations for the apogee and the drag coefficient. The most important considerations in designing the subscale vehicle were that the geometry and stability remain consistent. If the subscale launch vehicle represents a true scale model of the full-scale vehicle, the results of the subscale launch can be used to reasonably predict full-scale performance. Figure 23 shows the variable diameter subscale vehicle. Three successful flights of the subscale vehicle were performed.

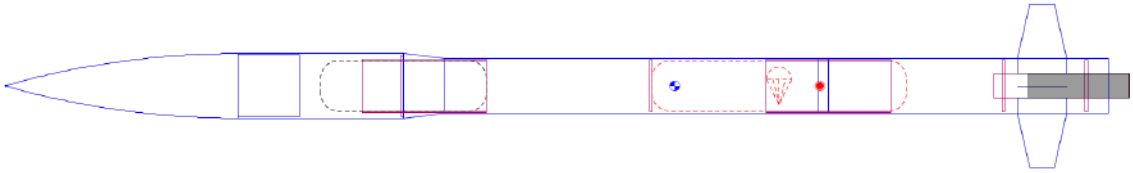

Figure 23: View of the Subscale Vehicle

The subscale vehicle and the final launch vehicle differed significantly in material selection. The body tube of the subscale vehicle consisted of Kraft Paper, the fins were made from plywood, and the nose cone was made from poly-prolene plastic. These differences was not considered significant, as the team focused on stability margin and geometry for subscale. Differences in material do not affect flight dynamics as long as the stability margin remains the same and the geometry resembles that of the full scale vehicle.

Sensors and altimeters were placed inside the subscale launch vehicle to record apogee, velocity, and acceleration data from each subscale test flight. The G80 motor with a 7 s delay deployed the Fruitychute CFC-24 parachute. Figure 24 shows the as-built subscale vehicle.

Figure 24: As-built Subscale Vehicle

The G80 motor was selected for the subscale as it has a total impulse of 136.6Ns, which was sufficient to accelerate the subscale launch vehicle into a compressible flow regime. With this, the team was able to verify performance of the ABS tabs and estimate average values of the coefficient of drag for the full scale launch vehicle.

3.6.1 Scale Justification

The subscale vehicle was scaled to 40% of the full-scale vehicle in length, diameter, CG, and CP. Scaling these variables allows for an accurate analysis of the stability of the full-scale vehicle. The mass of the subscale vehicle was not scaled because its accuracy would not impact flight dynamics. Table 10 shows the exact scaling factor that was used for the subscale vehicle. Actual values are not an exact 2:5 scale due to material availability.

Table 10: Comparison Between 2:5 of Fullscale Vehicle and Actual Subscale Vehicle

Vehicle Property	Exact 2:5 Scale	Sub scale	% Difference
Length (in.)	53.2	53.25	0.09%
Upper Diameter (in.)	3.2	3.1	3.13%
Lower Diameter (in.)	2.4	2.555	6.46%
Center of Gravity (in. from nose cone)	30.3	32.2	6.2%
Center of Pressure (in. from nose cone)	38.6	39.3	1.92%
Stability (cal)	2.62	2.26	13.7%

The most important factors that were tested in the subscale vehicle were the overall design of the vehicle and the ABS. Flight profile data was collected on the flights with different variations of ABS tab extension in order to verify that the tabs are effective in inducing drag. The results from the flights can be seen in Section 3.6.3.

3.6.2 Subscale Testing

The team used the subscale launch vehicles for test flights and wind tunnel testing in order to predict the performance of the full scale vehicle. The wind tunnel testing, shown in Figure 25, was performed in order to find a drag coefficient to use for full scale predictions as well as to test how effective the ABS tabs are in inducing drag on the airframe.

The vehicle was tested in a 2 ft by 2 ft by 6 ft subsonic wind tunnel in Hessert Laboratory. A schematic of the wind tunnel may be found in Figure 26.

Drag force was measured at various speeds with and without 40% scale tabs to represent the tabs of the ABS. Since the wind tunnel was at a low speed, the boundary layer generated was larger than the tabs' width, hence, no reliable data was recorded for the ABS system. Figure 27 below shows the drag coefficient versus Reynolds number curve generated from the wind tunnel results.

Figure 25: Wind tunnel testing November 11-12.

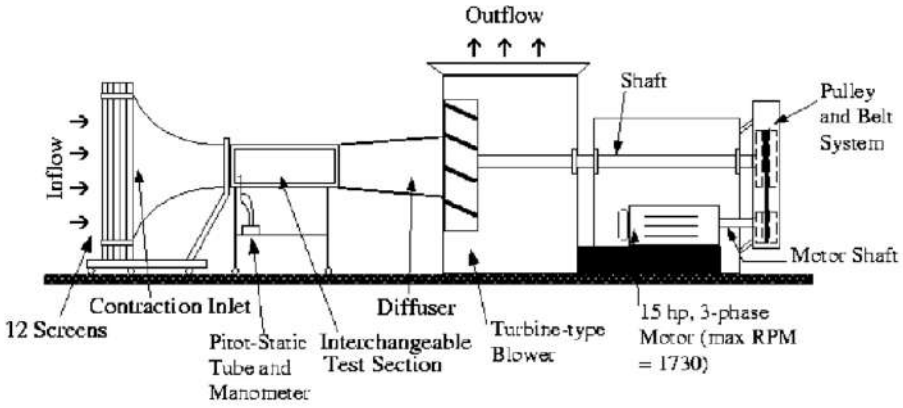

Figure 26: Wind tunnel diagram

Additionally, the team had three successful sub scale test launches which took place on December 7. These demonstrate viability of the team's design and ability for rapid reuse of the launch vehicle. By comparison of Matlab models, OpenRocket, and subscale test launch apogees, the team found that the vehicle's drag coefficient lines up with the drag coefficient found from the wind tunnel testing, and therefore can be reliably used for full-scale simulations.

3.6.3 Subscale Results

The subscale vehicle was successfully launched three times on December 7th, 2019 in Three Oaks, Michigan. It fulfilled its purpose of testing the launch vehicle design and construction techniques, as well as providing data to verify the effects of the ABS tabs. The first launch had no ABS tabs, the second had the tabs fully extended, and the third had tabs half extended.

Launch conditions stayed consistent over the three launches. The weather was cloudy with a high of 39°F and a low of 32°F. At the time of the first launch, the temperature was 34°F with the

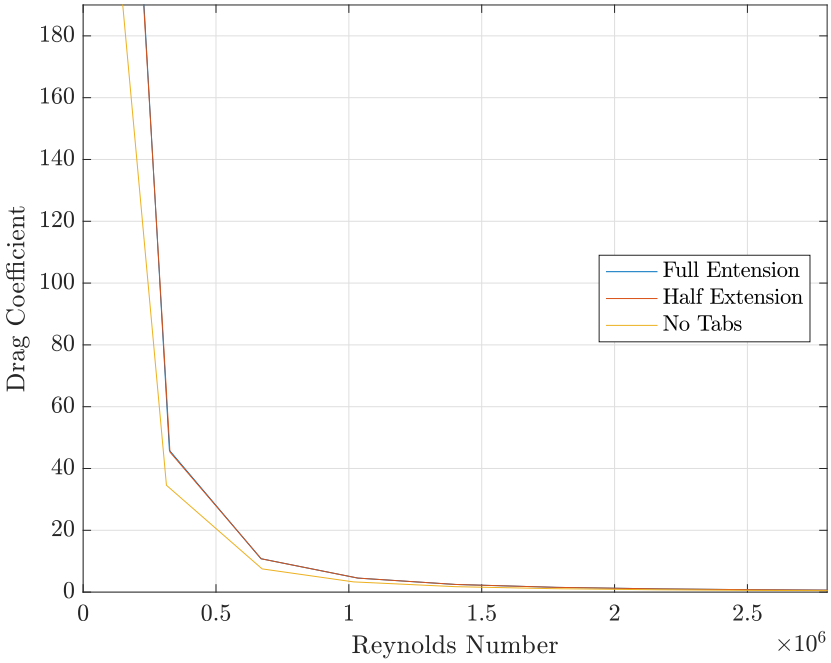

Figure 27: Drag Coefficient data from Wind Tunnel testing

wind coming from the south at 6 mph. During the second and third launches, the temperature was 34°F with a south wind of 8 mph.

Table 11: Subscale Launch Condition

Launch	Temperature	Wind
1	34°F	S at 6 mph
2	34°F	S at 8 mph
3	34°F	S at 8 mph

In between launches, there were a few tasks that had to be completed before the subscale vehicle was ready for its next launch. This included refolding and repacking the parachute and confirming its connection to the two sections of the vehicle that separate at apogee. The spent motor had to be removed and replaced with a new motor, and the ABS section had to be interchanged with one of the other two sections. The ABS sled with the various altimeters also had to be removed and reset. The time between launches was around 20 min. This verified the team's ability to relaunch within the same day without repairs or modifications, per NASA Requirement 2.4.

The predicted apogee for the subscale launch was 1,100 ft with the ABS tabs, and 1,256 ft without them. These predictions were obtained via simulations run in OpenRocket and RockSim. There were two altimeters on board the subscale vehicle: the Recovery squad's altimeter Raven and the ABS squad's altimeter Stratologger. The subscale results are summarized in Table 12

Table 12: Subscale Test Flight Results

Launch	Apogee (Raven)	Apogee (Stratologger)
No Tabs	1367 ft	1365 ft
Full Tabs	1011 ft	1009 ft
Half Tabs	1127 ft	1126 ft

The results from the three subscale launches show that the ABS tabs were successful in lowering the apogee of the vehicle. Both altimeters showed a 26% decrease in apogee from the first launch to the second, and a 17.5% decrease from the first launch to the third. However, some of the decrease in apogee from the first launch to the second was attributed to the ignition cord, which did not detach until the subscale vehicle had nearly cleared the rail, causing the vehicle to pitch and spiral, eventually stabilizing, and subsequently lowering the apogee. The issue with the igniter cord was three-fold: the cap used to hold the igniter in place was too tight, igniter wires were wrapped around the alligator clips to ensure a good connection, and the cord was not wrapped around the launch pad. These issues will be avoided in the full-scale launch because the ignition method will be entirely different. Despite this error, the third launch with the half tabs also showed a significant decrease in apogee, so it is reasonable to assume that the second launch's lower apogee was caused both by the full tabs and the pitch experienced on takeoff.

3.6.4 Flight Analysis

Figure 28 shows the altitude vs. time plots for the three subscale flights. Simulations were run using a fourth order Runge-Kutta method approximating the forces on the launch vehicle during flight. As shown, the simulations, which only differ in their approximated drag coefficient for the launch vehicle, predict the flight path in all three cases. Noise in the altitude data can be attributed to parachute deployment.

In addition, the simulated velocity was compared to the velocity of the subscale launch. The velocity was calculated using a fourth order finite difference method on the altitude data. A smoothing filter was then applied to the velocity data to account for noise produced by the barometric sensor. Figure 29 shows the velocity data for the no tabs flight. As shown, the simulation has a maximum error at burnout of 15%. This is due to the fact that the simulation approximates the thrust as a constant force over the burn of the motor. However, the simulation follows the trend of the flight well, and does not deviate from actual flight data by more than 3% except at burnout. Again, noise in the data can be attributed to deployment and parachute opening.

Additional simulations were run using OpenRocket. As shown in Figure 30, the altitude predicted by OpenRocket is about 100 ft short of the actual apogee. This is due to difficulty in modelling the actual viscous forces on the rocket in flight. This underestimation is noted for future OpenRocket simulations.

The velocity profile predicted by OpenRocket was very similar to that predicted by the

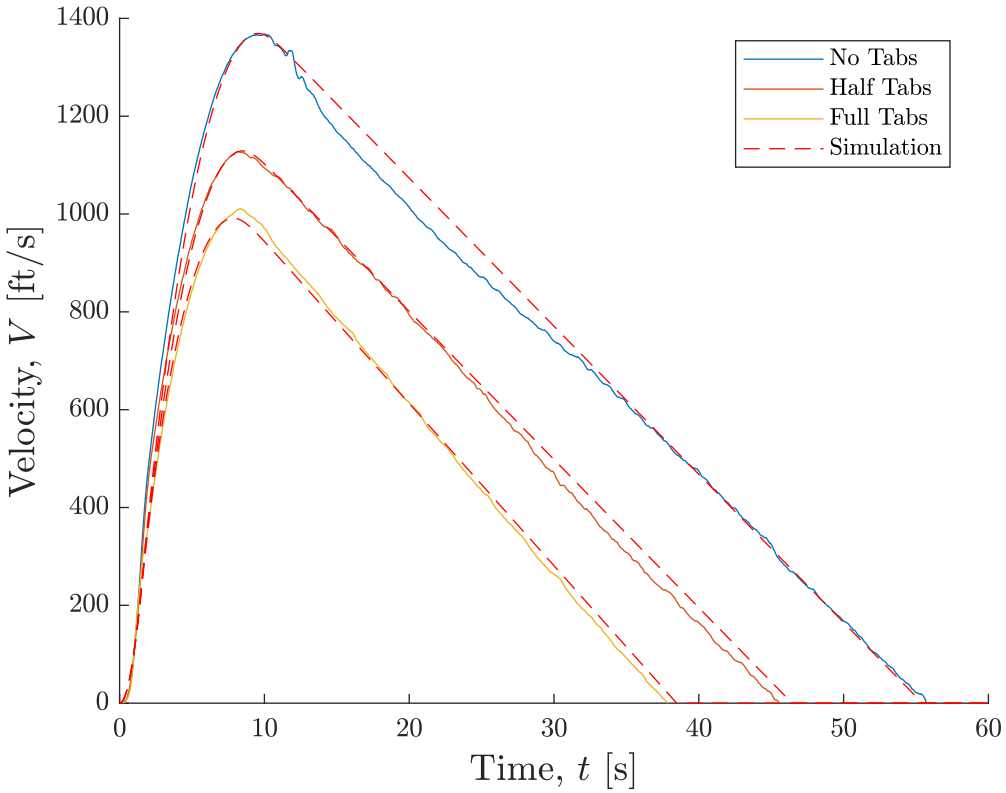

Figure 28: Subscale launches compared to simulated flights

Runge-Kutta simulation and agreed well with the actual flight data, as shown in Figure 31. Again, the maximum error of 13% occurred at burnout, possibly due to differences in the modeled thrust curve and the thrust curve actually produced by the motor.

3.6.5 Full Scale Implications

The subscale test launches successfully demonstrated that the drag-inducing tabs can lower the altitude of the launch vehicle. No vehicle design changes were made based on the results of the subscale vehicle. Additionally, the sensors and altimeters flown on the subscale vehicle were able to record data and are therefore viable choices for the full scale vehicle.

3.7 Air Braking System

In order to reach apogee at the target altitude of 4,444 ft, the launch vehicle will utilize an Air Braking System (ABS), with the goal of inducing a controlled variable drag force during flight. ABS will consist of an on-board closed-loop control system that simultaneously tracks flight data and alters the extension of a set of four drag surfaces, called drag tabs. The drag tabs will extend radially outward from the CP of the launch vehicle such that they act as flat plates normal to the direction of airflow. For the duration of flight from burnout to apogee, the actuation

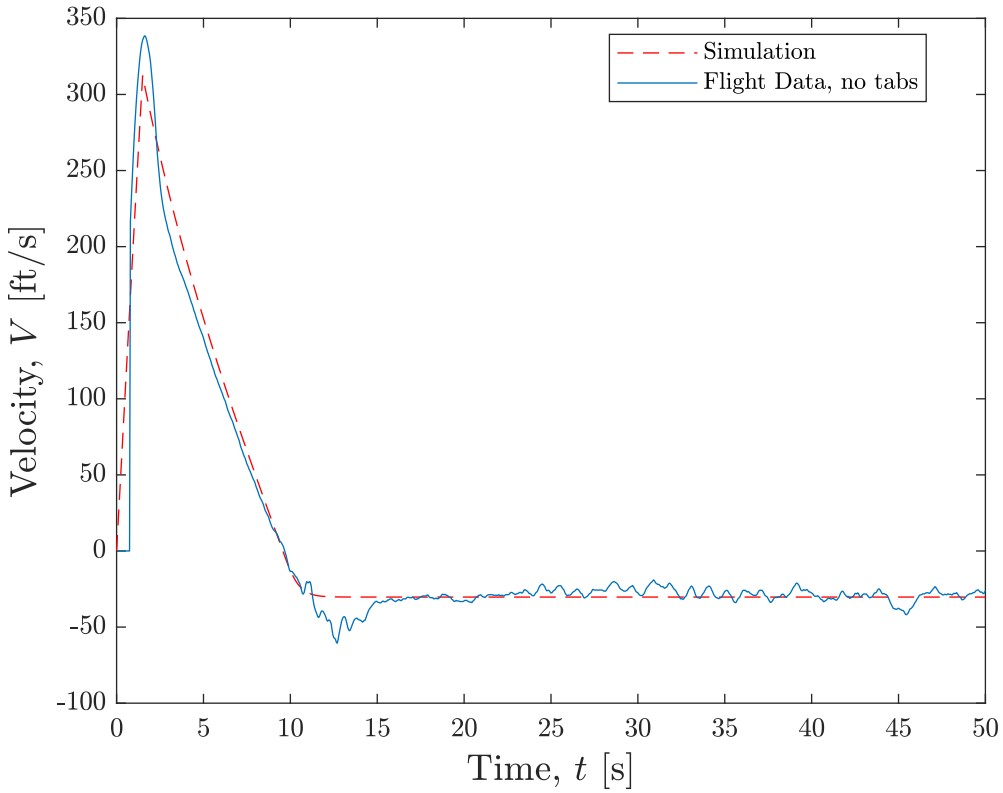

Figure 29: Subscale velocity compared to simulated flight

of these drag tabs will be altered according to a PID control algorithm, and they will remain retracted for the remainder of the flight.

3.7.1 Mission Success Criteria

In a successful flight, ABS will bring the launch vehicle to the target apogee of 4,444 ft, within an acceptable margin of error, in a manner that does not compromise safety or stability. To verify that this objective is met, the following specific set of success criteria must be met:

ABS.MS.1 On-board sensor data shall indicate that the launch vehicle reaches apogee at an altitude of 4,444 ± 25 ft.

ABS.MS.2 Actuation of the drag tabs shall be visually confirmed by footage from the onboard camera.

ABS.MS.3 The drag tabs shall actuate at a location within ± 1 in. of the CP to ensure that they do not significantly alter the static stability margin.

ABS.MS.4 The drag tabs shall extend simultaneously and symmetrically to ensure that no destabilizing moments are generated.

ABS.MS.5 The drag tabs shall only actuate during flight from burnout to apogee, and shall remain fully retracted for the remaining duration of flight.

ABS.MS.6 No components of the system shall experience structural failure at any stage of

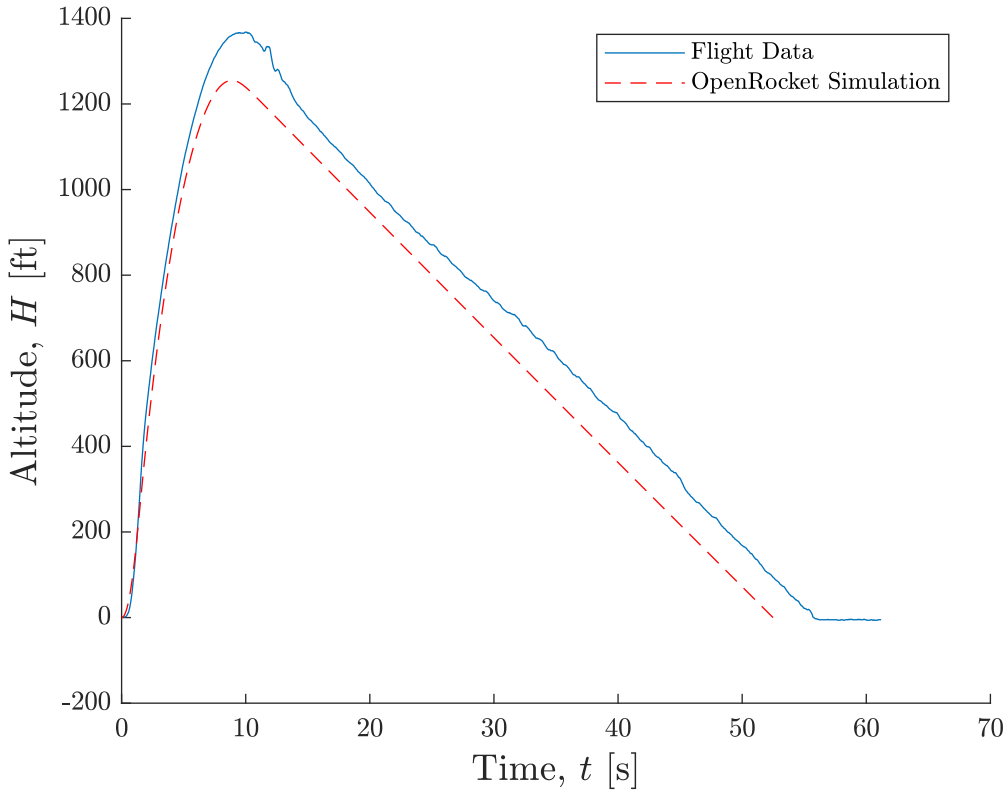

Figure 30: OpenRocket simulation for subscale flight altitude

flight.

3.7.2 Mechanical Design

The CP of the launch vehicle is 2.75 in. aft of the forward end of the section in the fin can allotted to ABS. At the forward side of the section sits a removable bulkhead that is screwed into the launch vehicle body. Four threaded rods run through this removable bulkhead and are mounted to it through a set of threaded holes. Nuts screwed onto each threaded rod on either side of the bulkhead prevent them from moving. All components are supported by these threaded rods with nuts on either side of the components, clamping them in place.

Aft of the removable bulkhead sits the drag tab deployment mechanism. This mechanism is designed to deploy four drag tabs through slots cut in the launch vehicle body. Contained within a deck with four slots cut into it sits a central hub and the four drag tabs. Four linkages connect the central hub to the drag tabs allowing the rotation of the central hub to push the drag tabs out through the slots in the fin can. At full extension the drag tabs will extend approximately 1 in. out from the launch vehicle body in the radial direction. This deck is mounted to the threaded rods using nuts allowing for its position to be adjustable, which will ensure that the drag tabs align with the slots cut in the launch vehicle body.

The central hub is rotated by a Hitec D845WP servo motor mounted to a deck aft of the

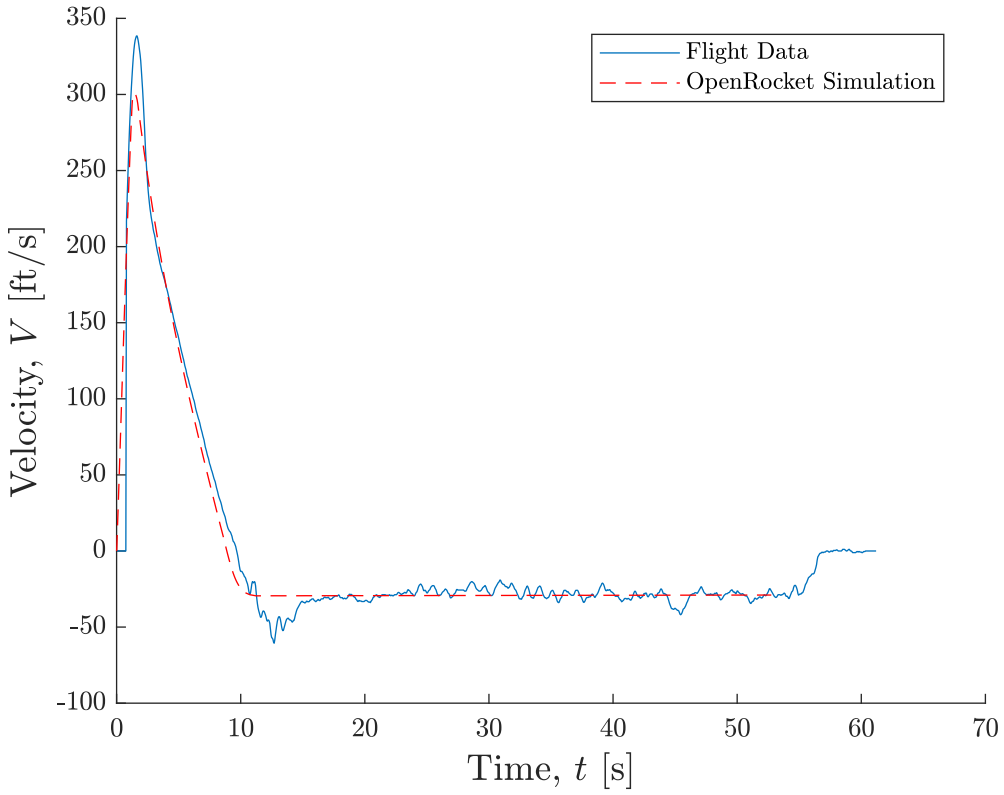

Figure 31: OpenRocket simulation for subscale flight velocity

mechanism, which also sits on the threaded rods allowing for the height of the servo to be adjusted. A LiPo battery to power this servo also sits on this deck within a 3D printed box, epoxied to the deck. The central hub from the mechanism runs through the center of the slotted deck and connects directly to the servo head.

A third deck sits aft of the servo deck, which is also supported by the threaded rods. Connected to this deck sit two vertical HDPE walls that hold the remaining electronics, namely a LiPo battery (within another 3D printed box), a Rasberry pi, BNO055 ccelerometer, and MPL3115A2 barometer, and an ADXL345 accelerometer are all mounted and connected to these plates.

At the aft-side of the ABS is a plywood deck, which rests on the fiberglass bulkhead epoxied into the launch vehicle body to separate the ABS from the launch vehicle motor. This deck ensures that the threaded rods do not bend or twist, causing the tabs to come out of alignment. A dowel rod runs the length of the section adhered to the launch vehicle body. Slots are placed in each deck to the system to slide onto the dowel rod, thus ensuring that all decks and the components attached to them are aligned as intended. A CAD model of the entire system is shown in Figure 3.7.6, and the dimensions of the system are shown in Figure 33.

3.7.2.1 System Integration

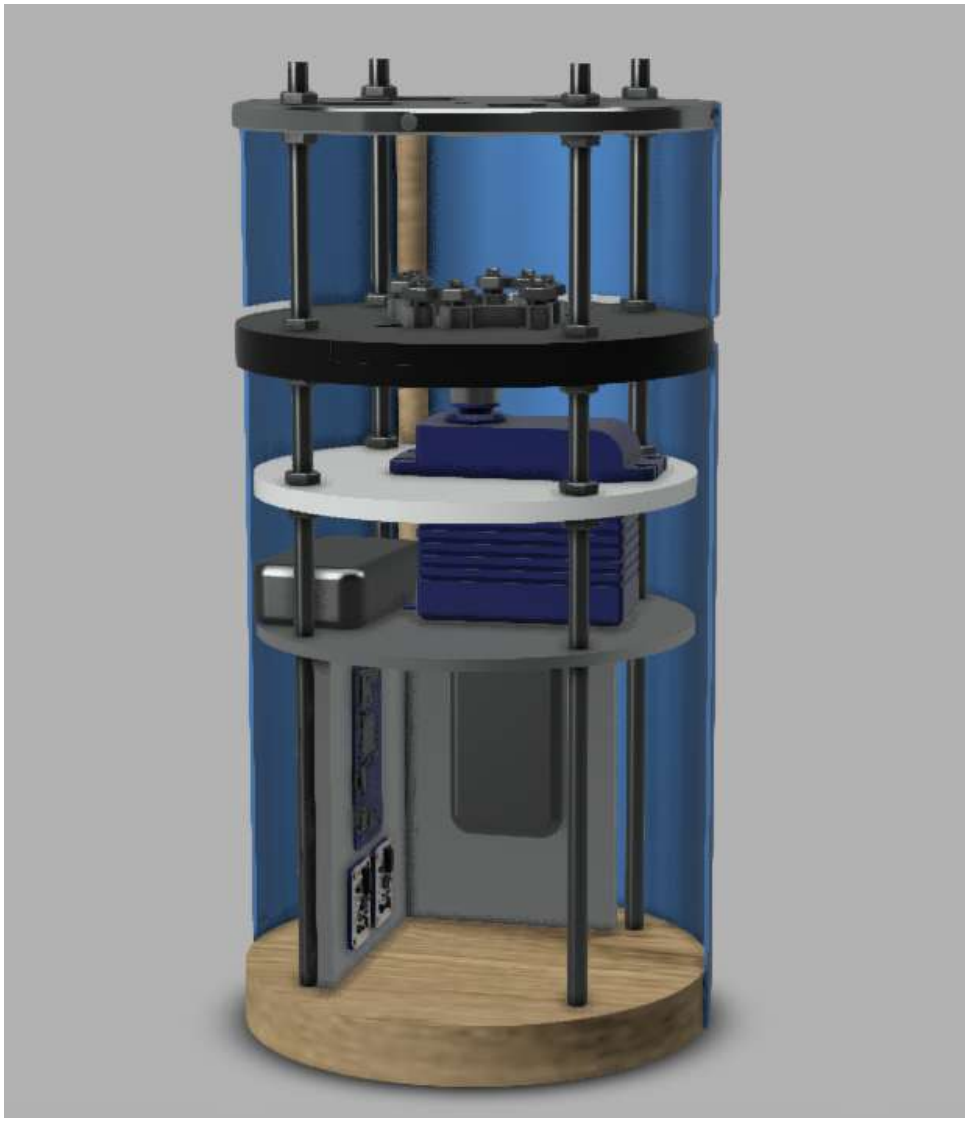

Figure 32: Model of ABS within a section of the fin can

ABS must be integrated into the fin can of the launch vehicle in such a way that it can be easily inserted and removed to make modifications and preparations before and between flights. To make this feasible while ensuring that the system is aligned properly to the slots in the fin can, all decks of the system will be attached to four threaded rods that run down the length of the ABS section of the fin can. The decks will each be secured in their respective locations on the threaded rods by toothed locknuts, which will ensure that vibrations do not cause components to come loose. The rods will be inserted into threaded holes in the aluminum removable bulkhead at the fore end of the ABS section, as well as threaded holes in the plywood deck at the aft end. This will allow for the entire system to be removed in one piece when the fore removable bulkhead is unscrewed. To ensure alignment of the drag tabs with the fin can slots in the radial direction, the system will slide up and down a dowel rod that runs the length of the inner wall of the ABS section of the fin can.

The 3/8 in. thick aluminum removable bulkhead will be included fore of the ABS as a strong

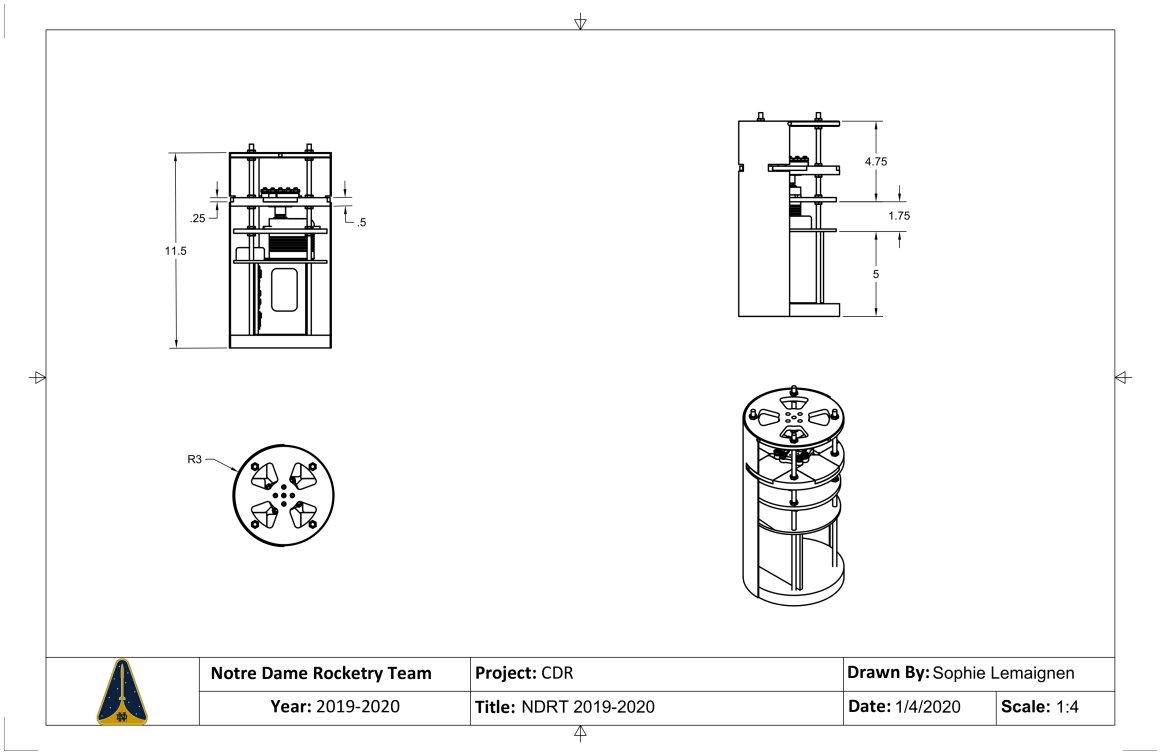

Figure 33: Technical Drawing of Full ABS with Dimensions

structural component that simultaneously enables access to ABS. This bulkhead attaches to the launch vehicle body using four machine screws that go through small holes in the body of the launch vehicle and into threaded holes in the bulkhead. These screws are easily removable, allowing for ABS to be pulled from the launch vehicle body for modifications, data collection, and battery replacement. The bulkhead also supports the parachute shock-chord for the Recovery subsystem. The need to support both crucial systems necessitated the use of exterior mounting screws and the material choice of aluminum. The bulkhead will be cut to a slip-fit within the fin can to ensure that it is centered within it, ensuring that all parts mounted to it are symmetric about the central axis of the launch vehicle. The in-house machining of the bulkhead will also ensure that the threaded rods that hold the entirety of the ABS are parallel with the length of the launch vehicle and symmetric about its central axis.

The drag tabs must be positioned so that the flow separation induced by the drag tabs does not interfere with the flow over the fins or the avionics bay bleed hole. To achieve this, the tabs will be placed at 45°angles relative to the fins. For repeatable and easy alignment of the tabs with their slots in the fin can, a dowel will be epoxied to the inner side of the launch vehicle. Each deck of the ABS bay will have a small notch cut into it, so that they can easily slide down the dowel rod, ensuring proper axial orientation. This dowel positioning system is shown in Figure 34.

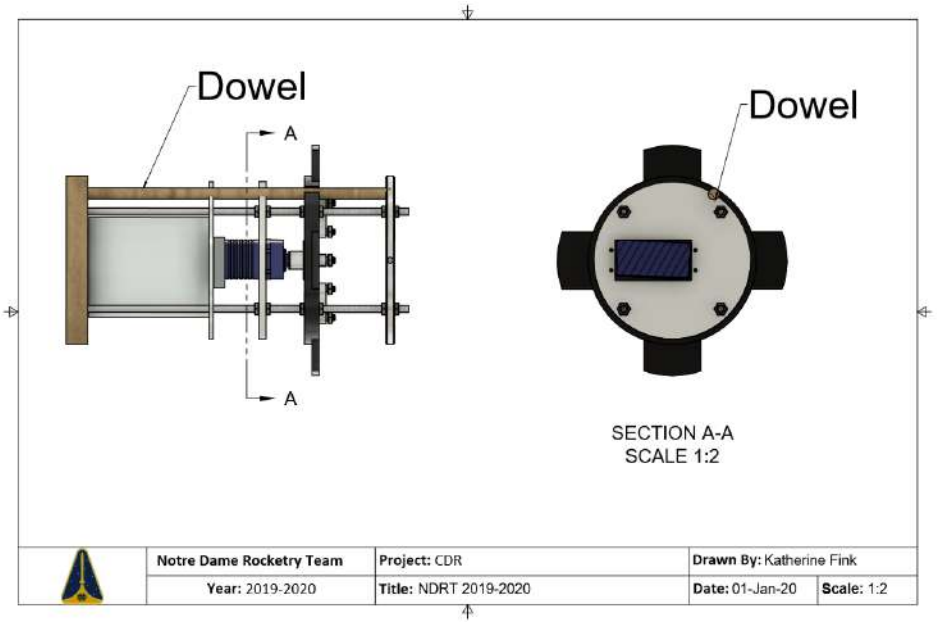

Figure 34: Dowel rod for drag tab orientation

3.7.2.2 Component Integration

All electrical components of the system will need to be secured to the HDPE decks and walls such that they will withstand the forces and vibrations experienced during flight. Conveniently, the PCB holding the microcontroller and sensors, and the servo motor both include holes that provide the ability to easily screw them into threaded holes in the HDPE. For this, 10-32 nylon screws and lock nuts will secure each component to the HDPE. Unfortunately, the batteries do not provide convenient means of integration as part of their structures, so custom battery boxes will be 3D printed out of ABS plastic, and will be epoxied to the HDPE to secure the batteries in place. Each of these will include a snap-lock lid, and a hole to allow the wires to reach the necessary electronics.

3.7.3 Fabrication

Aside from the shoulder screws and the ball bearing, the team has decided to fabricate the remaining mechanism components in-house to provide control over dimensions and tolerancing. The drag tabs and the slotted deck for the drag tabs will both be machined out of sheets of Nylon 6/6 using Techno Mill CNC cutters available through the Notre Dame Student Fabrication Lab. Similarly, the decks and walls that provide housing for all electronics in the system will be machined out of sheets of HDPE that are available from previous years, as this material has proven reliable for such structures. Finally, the central hub and linkage components of the mechanism will be machined out of aluminum 6061 to ensure they meet the required strength. These components will also be fabricated using the Techno Router to ensure tight tolerances in the mechanism.

3.7.3.1 Drag Tab Design

When fully retracted, the tabs are designed to sit flush with the outer casing of the system, which places a space constraint on them. The area of each drag tab exposed to airflow at maximum extension is 2.055 in.^{2}, which was the maximum that could be achieved using four tabs and the inner diameter of the fin can. This area was proven sufficient by flight simulations, as outlined in depth in the PID section. The final design and dimensions of the tabs are shown in Figure 35.

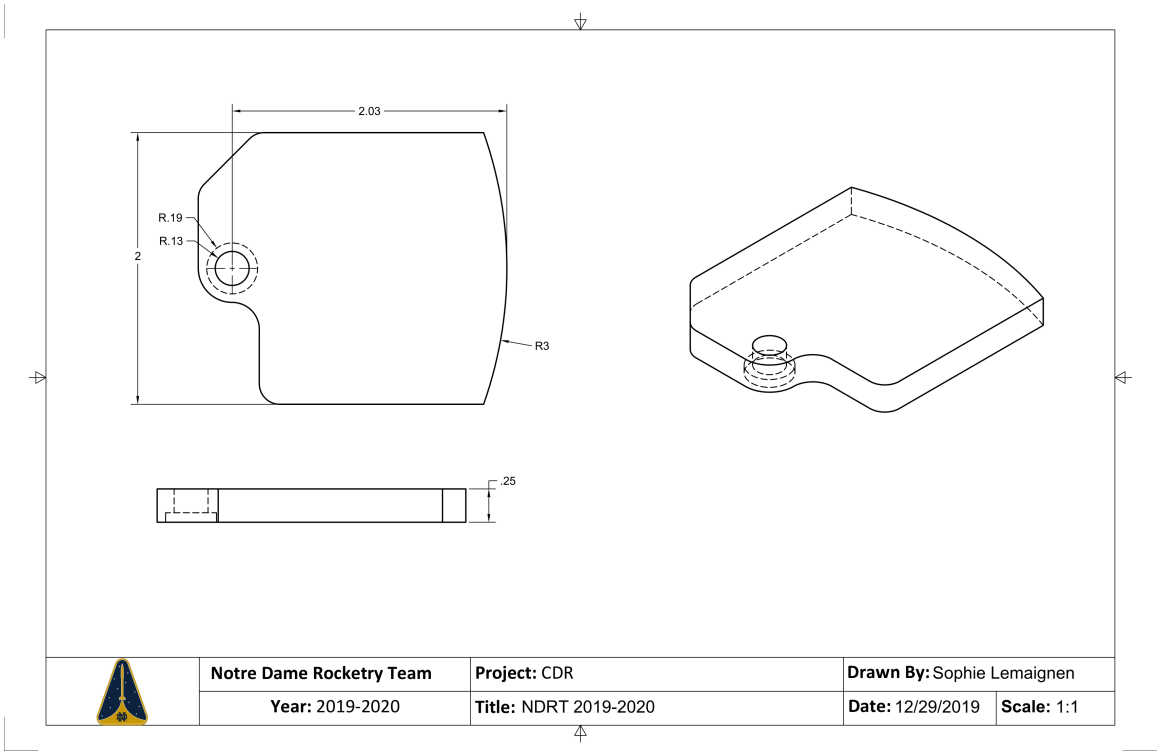

Figure 35: Technical Drawing of Drag Tabs

The dynamic force balance on the launch vehicle during vertical flight with drag tabs deployed is shown in Equation 3. Taking the drag equation, shown in Equation 4, and substituting it for the drag forces, and taking into account the flight angle of the launch vehicle with respect to the vertical, yields the equation of motion of the launch vehicle, as shown in Equation 5.

$$m\ddot{y} = -F_{drag,rocket} - F_{drag,tabs} - mg \tag{3}$$

$$F_{drag} = \frac{1}{2} C_d \rho A \dot{y}^2 \tag{4}$$

$$\ddot{y} + \left(C_{d,tabs} A_{tabs} + C_{d,rocket} A_{rocket}\right)\left(\frac{\rho}{2m\cos\theta}\right)\dot{y}^2 + g = 0 \tag{5}$$

m	Mass of Vehicle (lb_m)
$\ddot{y}$	Vertical Acceleration (ft/s)
$F_{drag,rocket}$	Drag Force on Launch Vehicle (lb_f)
$F_{drag,tabs}$	Drag Force on Drag Tabs (lb_f)
C_d	Drag Coefficient
ρ	Fluid Density ($slug/ft^3$)
A	Incident Area (ft^2)
$\dot{y}$	Vertical Velocity (ft/s)
θ	Angle of Launch Vehicle WRT Vertical (degrees)

Since the equation of motion is a non-linear second order differential equation, it needed to be solved numerically, which was done for flight simulations using the code shown in Appendix B.3. Full deployment of the tabs will not be necessary throughout the time period when the air braking system is active, as verified by the flight simulations in the PID section. Instead, the design requires a control system to adjust the drag tab extension as necessary, thereby adjusting the resultant drag force.

The team selected Slippery MDS-Filled Wear-Resistant Nylon 6/6 sheeting for the drag tabs and the slotted deck they sit within. Nylon 6/6 was chosen for its low coefficient of friction, as it is more slippery than regular Nylon and self-lubricating, so that the friction between the drag tabs and their slots is minimized to avoid stalling the servo motor. The coefficient of friction will be further lowered with the aid of Krytox, an industrial lubricant. Nylon 6/6 also provides a high yield stress and low cost compared to plastics with similar properties. For reference, Table 13 lists the material properties of Nylon 6/6.

Table 13: Material Properties of Nylon 6/6

Cost at 1/4 in. Thick ($/ft^2)	Yield Stress (psi)	Density (g/cm^3)	Coefficient of Friction
30.31	11750	1.135	0.26

The team will purchase the Nylon in 1/4 in. thick sheets, because this is the desired thickness of the fabricated drag tabs, so that the coefficient of friction of the faces of the tabs can be retained at the factory value.

3.7.3.2 Drag Tab Analysis

To estimate the force exerted by the drag tabs on the launch vehicle, Computational Fluid Dynamics (CFD) simulations were performed using Ansys Fluent ^{TM}. A volume mesh of the launch vehicle was created in Pointwise ^{TM}. The Fluent simulations were run using far field pressure boundary conditions with Mach numbers 0.52, 0.3, and 0.042. The simulations were

run for 1000 iterations with a continuity residual convergence criteria of 10^{-3}. The CFD simulation was configured under the parameters presented in Table 14.

Table 14: CFD Simulation Parameters

CFD Parameter	Value
Axial Mach number	0.52, 0.3, 0.042
Angle of attack (°)	0
Far field static pressure (kPa)	101.3
Fluid temperature (K)	280

For both Mach numbers simulated, the maximum pressure on 90% of the drag tab surface is 98.7% of the total (stagnation) freestream pressure. The minimum absolute pressure on the tabs, however, varied based on the Mach number and was 66.7% of the freestream total pressure for the Mach 0.52 case and 94.4% of the freestream total pressure for the Mach 0.3 case. A curve fit based on the simulation provides an estimate for the drag on the tabs at any Mach number as expressed in Equation 6.

$$F_{drag,tabs} = P_s A \left(1 + \frac{\gamma - 1}{2} M^2\right)^{\frac{\gamma}{\gamma-1}} \left[1 - (1 - M^2)^{3/2}\right] \tag{6}$$

$F_{drag,tabs}$	Net Force on Drag Tabs (lb_f)
M	Freestream Mach Number
P_s	Freestream Static Pressure (Pa)
γ	Ratio of Specific Heats

Since the average Mach number during flight as estimated by OpenRocket is 0.31 (Section 3.9), the average coefficient of drag for the tabs was estimated to be 2.06 based on the CFD results. This is higher than the standard 1.28 coefficient of drag for a flat plate perpendicular to flow, but this is expected due to compressibility effects. Figure 36 shows the pressure distribution on the forward face of the drag tabs for a Mach 0.3 simulation.

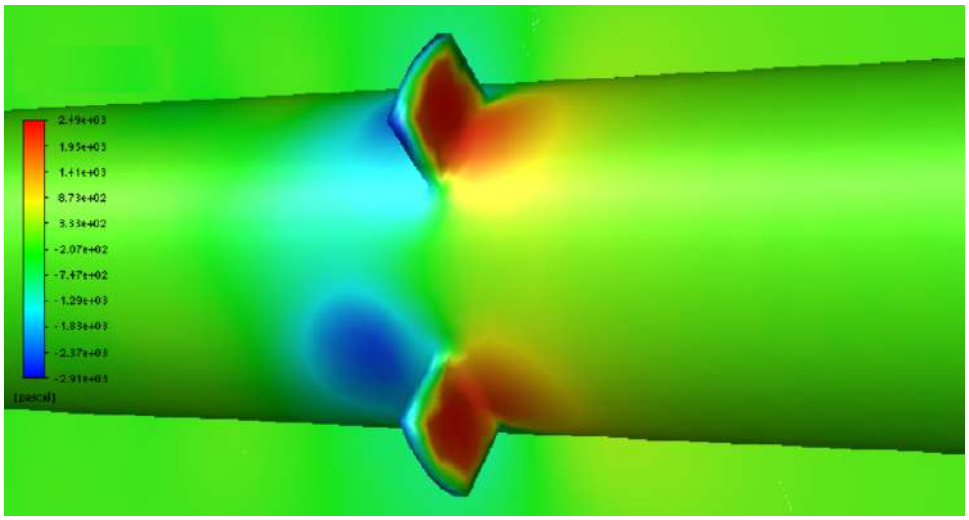

Figure 36: Pressure Profile on Drag Tabs for Mach Number 0.3

A highly incompressible simulation (Mach number 0.042) was run in order to compare simulation results with wind tunnel tests. Again, the continuity residual convergence criteria was 10^{-3} and the simulation was run for 1000 iterations. For these slower speeds, a wake develops after the transition section, which reduces the drag force on the tabs. The incompressible simulation estimated the pressure on the forward faces of the drag tabs to be only 64.29% of the stagnation pressure of the freestream flow, substantially less than that at higher Mach numbers. This leads to a drastically reduced force on the drag tabs, such that it would not have been able to be resolved by the force gauge in wind tunnel tests, which explains why the tests did not show any added force when the drag tab models were added, as discussed in the test results section. Figure 37 shows the velocity profile over the launch vehicle for the incompressible simulation. The wake produced by the transition section is shown as the lower velocity section of the flow. It is substantially more prominent coming off the camera shroud on the transition section.

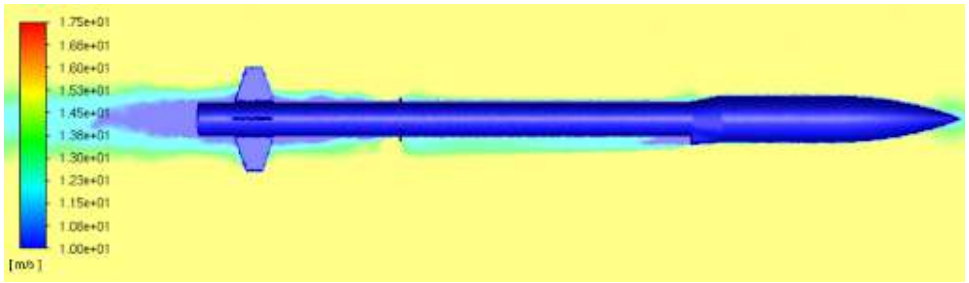

Figure 37: Velocity Profile for Incompressible Simulation

In order to ensure the structural integrity of the drag tabs during flight, a static FEA was performed on the CAD model of one drag tab using Ansys Structural^{TM}. The boundary conditions applied model the conditions experienced by a drag tab that is fully deployed at burnout, when the velocity of the launch vehicle is highest, as this is the moment when the drag tabs are expected to experience the highest stress due to drag. More specifically, the

model included a pressure force acting on the portion of the face of the drag tab that will extend from the body of the launch vehicle with a magnitude of 3.55 psi, the pressure at the maximum expected velocity of approximately 580 ft/s (see Section 3.9). A cylindrical support was applied to the interior of the pin hole, fixing its walls in the tangential direction to model the constraint of a shoulder screw. Additionally, frictionless supports, constraining the walls from moving in the normal direction, were applied to the side walls where they will contact the insides of the mechanism slots, and another frictionless support was applied to a portion of the surface above the pin hole to model the normal reaction force from the mechanism linkage. The boundary conditions described are shown in Figure 38. The analysis settings were set to measure von-Mises stress and total deformation, and the assigned material was Nylon 6/6. The analysis was run for three mesh refinement levels to ensure that the results converged. The final results are shown in Figure 39 and Figure 40. Given that the maximum stress predicted by the analysis was 3920.4 psi and the tensile strength of Nylon 6/6 is 11,750 psi, yielded a factor of safety of 3.00 for the drag tabs.

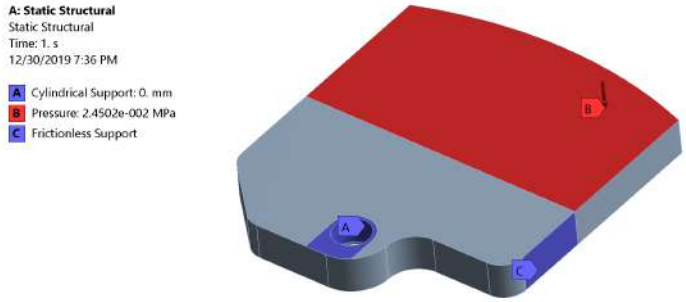

Figure 38: Boundary conditions for drag tab FEA

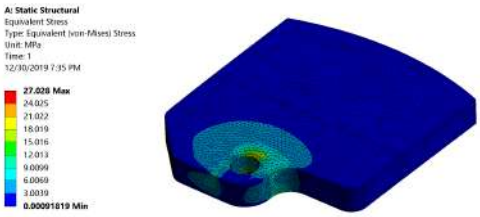

Figure 39: FEA- Max. von Mises Stress for Drag Tabs

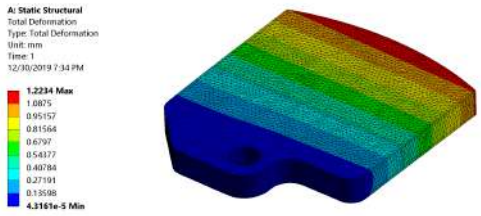

Figure 40: FEA- Deformation of Drag Tabs

3.7.3.3 Mechanism Components

The mechanism that will deploy the drag tabs from the fin can converts rotation of a central hub via a servo motor to the linear motion of the drag tabs, which sit in grooves that guide them linearly outward through slots in the launch vehicle body. Four linkages connect a central hub, which is attached to the servo motor, to the drag tabs such that rotation of the servo motor straightens the linkages to actuate the drag tabs. The slots that the drag tabs move within are cut into a Nylon deck, which provides the structure for the mechanism. This slotted deck is

secured to four threaded rods that run through it, with nuts and washers to prevent movement, while allowing the deck position to be adjusted so that the drag tabs can be easily lined up with the holes cut in the launch vehicle body. The motion provided by the mechanism can be seen in Figure 41, where the tabs are fully retracted on the left, and partially deployed on the right. For visibility, the drag tabs are shown in red, the linkages in yellow, the central hub in green, and a section of the launch vehicle body is in blue.

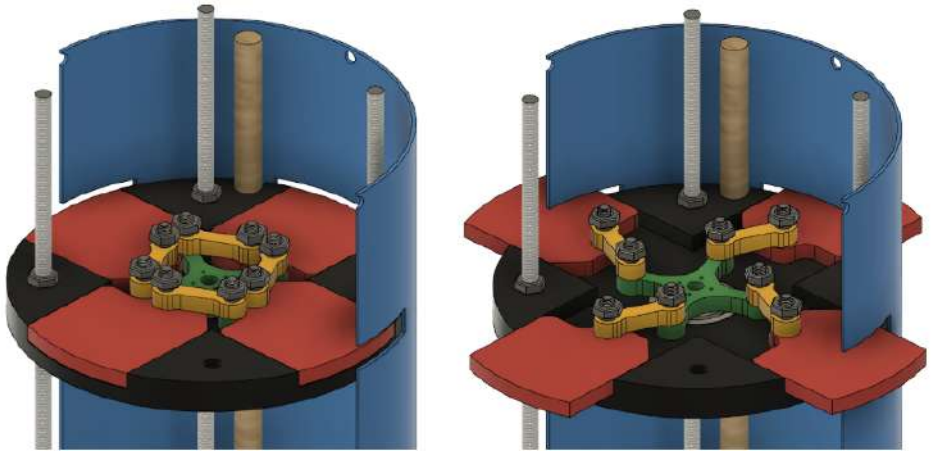

Figure 41: Motion of ABS mechanism

To ensure tight tolerances are achieved, the central hub and linkages will all be machined out of aluminum. The holes in the central hub and linkages will both be cut to slip fit to minimize the friction during movement. The pins will be ultra-low profile precision shoulder screws. This will allow them to sit within counterbored holes in the bottoms of the drag tabs and central hub arms, as to prevent them from interfering with the slotted deck. A dimensioned drawing of the central hub is shown in Figure 42, and the linkage is shown in Figure 43, both of which are to be fabricated out of aluminum.

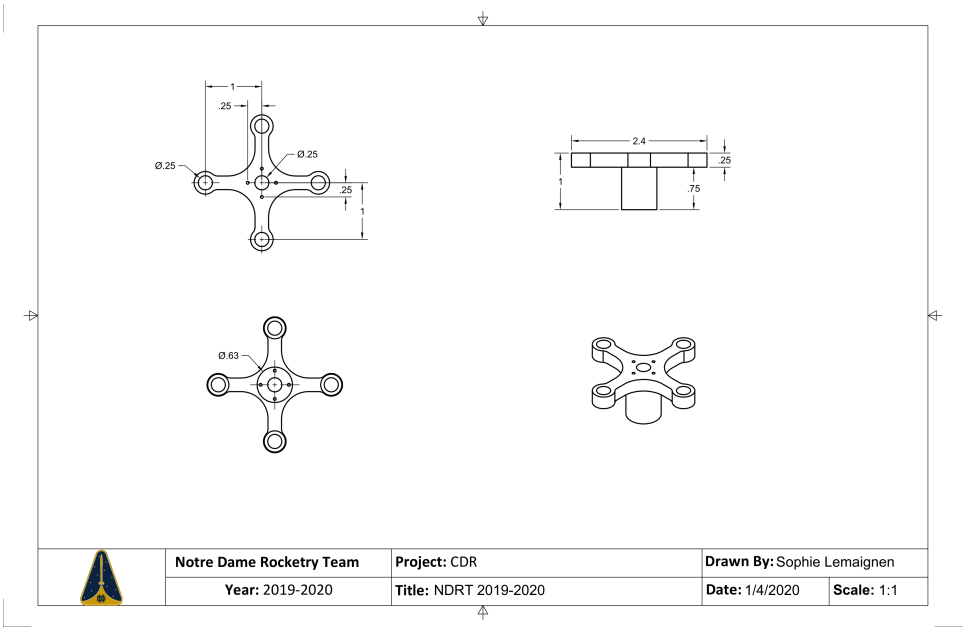

Figure 42: Central hub component of ABS mechanism

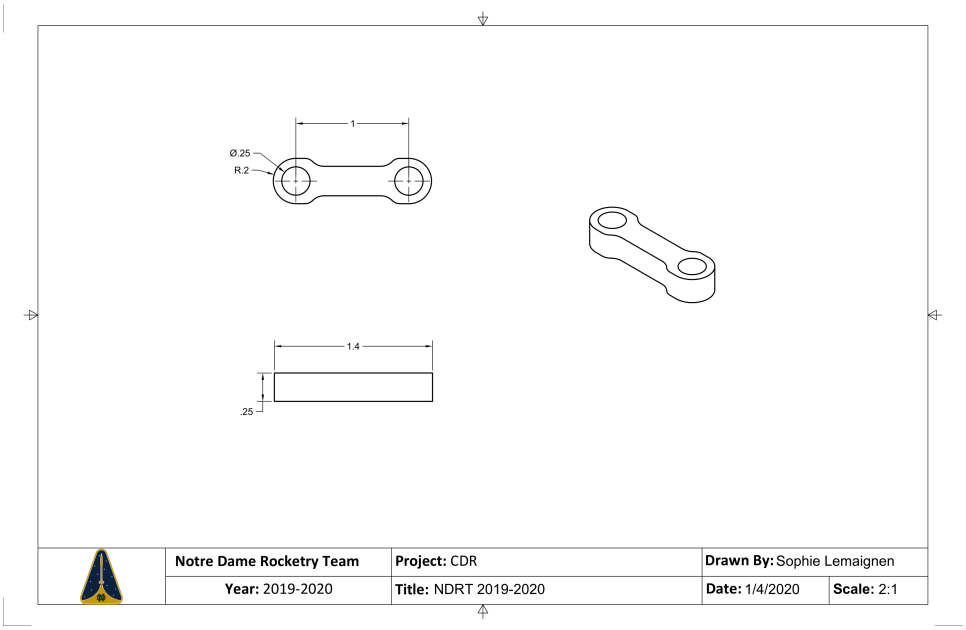

Figure 43: Linkage component of ABS mechanism

The central hub will be attached directly to the servo head via four low profile socket head screws. The servo sits below the mechanism, mounted to a HDPE deck. This deck will have a completely adjustable height as it is mounted to the threaded rods running the length of the ABS. These bolts can be adjusted to ensure that the servo does not push or pull excessively on the central hub. The central hub will run through a ball bearing that is press fit and glued into the mechanism deck. This ball bearing will ensure that the central hub is perfectly centered and will rotate on only one axis without added friction. The friction created between the drag tabs

and the sides of the slots that they run in must not stall the motor. The maximum amount of torque required by the servo occurs when the tabs are fully retracted and the servo first starts to turn, so a static analysis was performed to ensure that the servo motor can overcome the torque at this point, yielding Equation 7 for the angle at which the linkage will cause the servo motor to stall.

$$\theta_{max} = \tan^{-1}\left(\frac{1}{\mu_{static}}\right) = 75.96° \tag{7}$$

μ_{static}	Coefficient of Static Friction of Nylon 6/6
θ_{max}	Max. Angle of Drag Tab Movement

At this maximum angle, the force from the servo motor on the linkage will equal the opposing friction force, and no movement will occur, thus stalling the servo motor. Therefore, the maximum angle the linkage may make with the axis of drag tab motion is 75.96°, and all angles smaller than this will yield movement of the drag tabs. The mechanism design uses a maximum linkage angle of 63.0°, so the current configuration will not stall the servo motor.

Since the mechanism converts the rotational motion of the servo motor into the linear motion of the tabs, a mechanical analysis was performed on the design to determine the relation between rotation angle and linear displacement. This was done by treating the mechanism as a three-bar linkage with shaft rotation as the input, and Newton's method was applied to generate a plot of linear displacement as a function of shaft angle. Additionally, a motion analysis of the mechanism CAD model was performed to verify the result, and both are shown plotted in Figure 44. The similarity between the two plots verifies that the correct relation between servo angle and linear displacement for the mechanism design has been obtained. For use in the control software, a third-degree polynomial fit on the result of the Newton's method analysis produced Equation 8. The fully retracted state is at $\phi = 0$.

$$x = (-9.16 \times 10^{-7})\phi^3 - (1.66 \times 10^{-4})\phi^2 + 0.0317\phi - 0.00131 \tag{8}$$

x	Linear Displacement (in.)
ϕ	Servo Motor Rotation Angle (°)

3.7.4 Electrical Design

3.7.4.1 Sensors

Two accelerometers will serve to extrapolate the velocity of the rocket using the Kalman filter, determine when the launch vehicle has entered a new stage in the launch cycle, and track absolute orientation. The team decided to use both the Adafruit BNO055, which will provide orientation data in the form of Euler angles, and the ADXL345, which will provide triple-axis linear acceleration (without gravity) and acceleration with gravity. The BNO055 is the only commercially available accelerometer that provides 3-axis orientation data, but this mode restricts its acceleration range to 4 g's, which is insufficient to track linear acceleration.

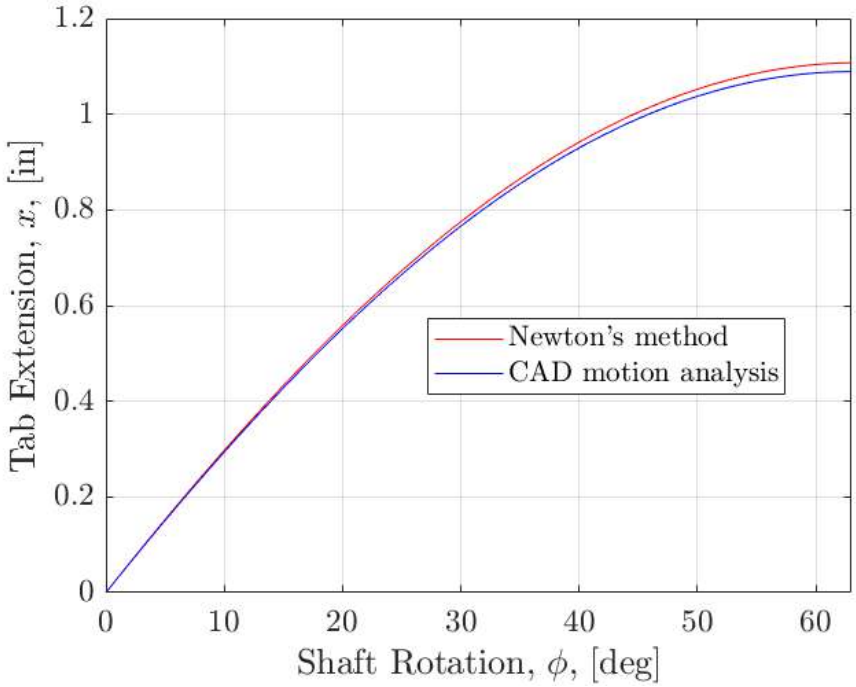

Figure 44: Drag Tab Extension vs. Servo Motor Rotation

This led to the decision to include the ADXL345, which will provide linear acceleration data within a lower error range than a second BNO055 could. Refer to Table 15 for the specifications on the BNO055, and Table 16 for the specifications on the ADXL345.

Table 15: BNO055 Accelerometer Technical Specifications

Specification	Value
Output frequency (Hz)	100
Acceleration range (g's)	2 - 16
Supply voltage range (V)	2.4 - 3.6
Average supply current (mA)	12.3
Weight (oz)	0.1058
Dimensions (in.)	0.8 x 1.1 x 0.2

Table 16: ADXL345 Accelerometer Technical Specifications

Specification	Value
Output frequency (Hz)	800
Acceleration range (g's)	2 - 16
Supply voltage range (V)	2.0 - 3.6
Supply current range (μA)	30 - 140
Weight (oz)	0.0448
Dimensions (in.)	0.95 x 0.75 x 0.12

The team is choosing the BNO055 for the primary accelerometer for a variety of reasons. This sensor provides data at 100 Hz, which will provide enough samples for the system to alter the drag if necessary, and it provides more than just 3-axis acceleration. This sensor provides useful information such as orientation, linear acceleration (without gravity), and acceleration with gravity. These values are going to be critical in the algorithms that are going to be used in ABS, and the BNO055 is a well respected inertial measurement unit reasonably priced within the team budget allowance. It is possible to calculate some of these values by utilizing a 3-axis accelerometer and calibrating it with respect to gravitational acceleration, but the team decided that it would be much more efficient and reliable to find a sensor that can present absolute orientation as raw data, as orientation is critical for predicting the motion of the launch vehicle. This accelerometer is also highly programmable, and different sensors can be activated/deactivated if necessary. These different metrics can be used to improve the systems accuracy, and all of these data points are provided at 100 Hz.

The team decided to use the MPL3115A2 - I2C as the barometer in order to determine the altitude of the rocket. It was chosen for its comparatively low margin of error on pressure readings, low cost, and high output frequency. Table 17 shows the specifications of the MPL3115A2.

Table 17: MPL3115A2 Barometer Technical Specifications

Specification	Value
Pressure measurement range (kPa)	50 - 110
Pressure accuracy (Pa)	± 1.5
Output frequency (kHz)	400
Weight (oz)	0.0423

3.7.4.2 Servo Motor

The ABS mechanism is going to be driven by the HiTec D845WP servo motor. This servo motor was chosen for its high torque capability to ensure that it can overcome the friction

forces that will occur within the mechanism. Additionally, this servo utilizes an internal feedback potentiometer to verify that it has rotated to the correct angle. In order to provide this high torque, it has a very large current draw and is relatively heavy, but these drawbacks were deemed acceptable considering the benefits. The specifications for the D845WP can be seen in Table 18. To account for the high current draw of this motor, a switch will be

Table 18: D845WP Servo Motor Technical Specifications

Specification	Value
Weight (oz)	8
Rotation speed	.17 sec/60°
Torque (oz-in)	694
Cost	$100
Maximum rotation angle	202.5°
Idle current draw (mA)	30
Operating current draw (A)	1.6
Operating voltage range (V)	4.8 - 8.4

implemented in the servo circuit to ensure that no unnecessary current will be drawn from the 7.4 V LiPo Battery. This switch will not be activated until the vehicle is on the launch pad. An advantage of the D845WP is that it is highly programmable. The team will be able to adjust many aspects of the servo's function prior to launch, such as the travel range. In the table above, the maximum travel range is shown to be 202.5°, which is much too wide for practical application in the system. The team will be able to lessen the maximum range to 63.0°, which will allow for more precise movement of the servo and prevent it from extending too far. This programming will be done through the DPC-11 servo programmer, which will allow the team to interface a PC directly with the motor. In flight, the servo is going to be directly controlled by the Raspberry Pi. One of the Pi's GPIO pins will output a PWM signal to the center pin of the servo, which will alter the angular position of the motor, resulting in the actuation of the drag tabs. The circuit that the servo motor will be using is shown in Figure 45.

3.7.4.3 Microcontroller

To integrate all of the sensors and actuators in ABS, the team will be using a Raspberry Pi Zero. The Raspberry Pi Zero provides the power necessary for the system's data processing algorithms while being small and light enough to fit properly in the ABS. The specifications of the Raspberry Pi can be seen in Table 19. The Raspberry Pi Zero is highly versatile: it is a miniature computer, running on an altered version of Linux called Raspbian. This makes data storage much easier, because rather than needing to write to an external SD card, the program can save the flight data as a file on the Pi itself. There are Python packages that can be downloaded onto the Pi that are specifically designed to interface with the Adafruit sensors that will be used in the system, making data collection very simple and straightforward. The Pi

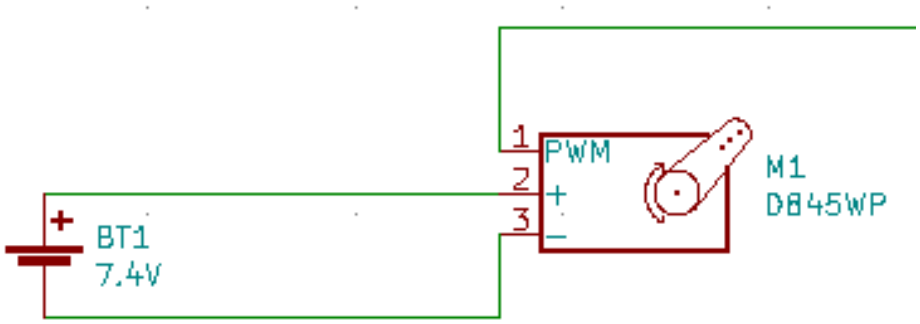

Figure 45: Servo motor circuit schematic

Table 19: Raspberry Pi Zero technical specifications

Specification	Value
System Clock (GHz)	1
RAM (MB)	512
Number of pins	40
Micro USB Supply Voltage (V)	5

can also output PWM signals that will be used to control the servo. Two different hardware techniques will be used to connect the sensors to the microcontroller: I2C and UART. I2C utilizes two buses, SDA and SCL, to connect up to 128 sensors to the microcontroller through the use of a Master/Slave communication protocol. SDA is the data bus and SCL is the I2C clock. Both the MPL3115A2 and the BNO055 being utilized for raw acceleration data are going to be connected to the Raspberry Pi in this way; in subscale, sampling rates of over 50 Hz were attained.

For full-scale, the BNO needs to be connected in a different way. When being used to collect absolute orientation data the BNO055 needs to integrate data taken from several of its sensors, which results in a slower sampling rate. In order to function properly on the I2C bus, the SCL clock would need to be slowed down by a factor of 10. This was not deemed acceptable, and ended up slowing down sampling rates by a significant margin. In order to avoid this issue, this BNO055 is going to be connected to the Pi through the use of the UART serial protocol. UART allows for two devices to communicate with each other directly. This configuration was designed to maximize the sampling rate, which is crucial to the success of ABS. The wiring can be seen more clearly in the Section 3.7.4.4.

3.7.4.4 Printed Circuit Board

In order to optimize the hardware of the system, the ABS is going to utilize a printed circuit board (PCB). This PCB was designed using KiCAD, and will allow for all of the electrical

components of the system to be connected to each other with ease. Figure 46 shows the schematic of the system, and Figures 47 and 48 show the PCB that will be printed from this schematic. The PS0 pin on the UART BNO055 will need to be connected to the 3.3 V pin via a wire (not included on the PCB Schematic).

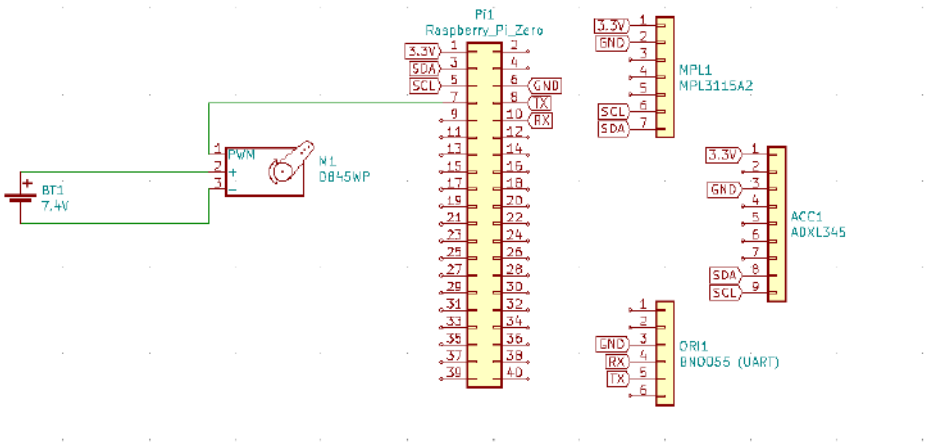

Figure 46: ABS Electronics Wiring Schematic

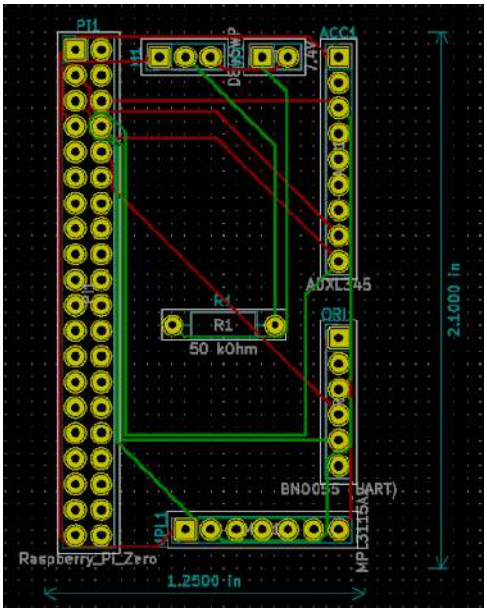

Figure 47: PCB Schematic

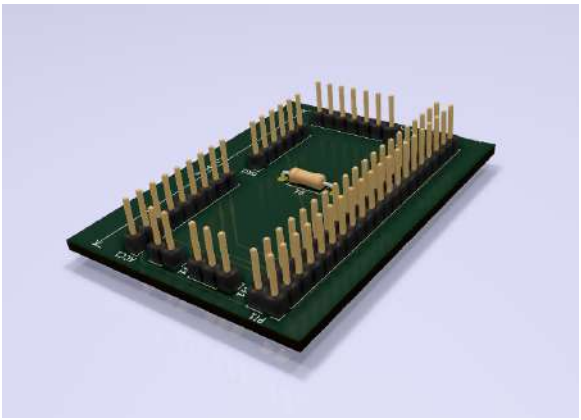

Figure 48: CAD Model of PCB

3.7.4.5 Batteries

The team has chosen a 450 mAh 3.7 V YDL LiPo battery to power the Raspberry Pi, and a 350 mAh 7.4 V CBB LiPo battery to power the servo motor. Neither of these batteries needs to have a very large capacity, as the Raspberry Pi has a low current draw, and the servo motor will only need to be operating at its maximum current draw for a very short duration during flight. The idle current of the servo motor is 30 mA, the operating current of the servo motor is 1.6

A, and the stall current is 10 A. If the servo is only operating after burnout and the flight time is approximately 20 s, then the servo will drain a maximum of 56 mAh from the battery if the motor is stalled the entire time, which is the worst-case scenario. This would leave 294 mAh for the servo while idle, which provides 10 hours of life, significantly more than the required 2 hours. The Raspberry Pi Zero draws an average current of 100 mA, and each GPIO pin can draw an additional 16 mA of current. Assuming that 5 pins are drawing this maximum current, the Raspberry Pi will be able to function for 2.5 hours, which also exceeds the required 2 hours.

In order to power the Raspberry Pi with a 3.7 V battery, a power booster will be implemented. The Raspberry Pi requires a consistent 5V, 100 mA power supply, and will reboot itself if this supply varies. In order to ensure this does not occur in flight, the team purchased an Adafruit PowerBoost 500 to directly convert the power supplied from the battery.

3.7.5 Control Structure

The ABS control code first activates on the launchpad through the flipping of the power switch, giving visual confirmation through LED status lights that it is acquiring sensor data. The system will be able to write to an SD card in order to provide detailed logs of the flight data and filtered outputs. This connection to an SD card will also be indicated by an LED. Upon activation of the arming switch, a third LED will indicate that the system is armed. Sensor data will then be collected continuously after passing through a Kalman filter. The system then waits to detect when liftoff has occurred, as indicated by the spike in acceleration. Once in this stage, the system will use filtered data to determine when burnout has occurred. Once burnout is detected, the filtered data will be read into a proportional-integral-derivative (PID) control algorithm to determine the optimal drag tab extension length. During this stage, the system will act as a closed-loop controller, continuously recalculating a new drag tab extension and communicating it to the servo motor. This process terminates when sensor data indicates that the launch vehicle has reached apogee, as indicated by a change to negative velocity, at which point the drag tabs will retract for the remainder of the flight. A flow chart of the ABS control structure is shown in Figure 49, and a description of each stage of the control cycle is given in Table 20.

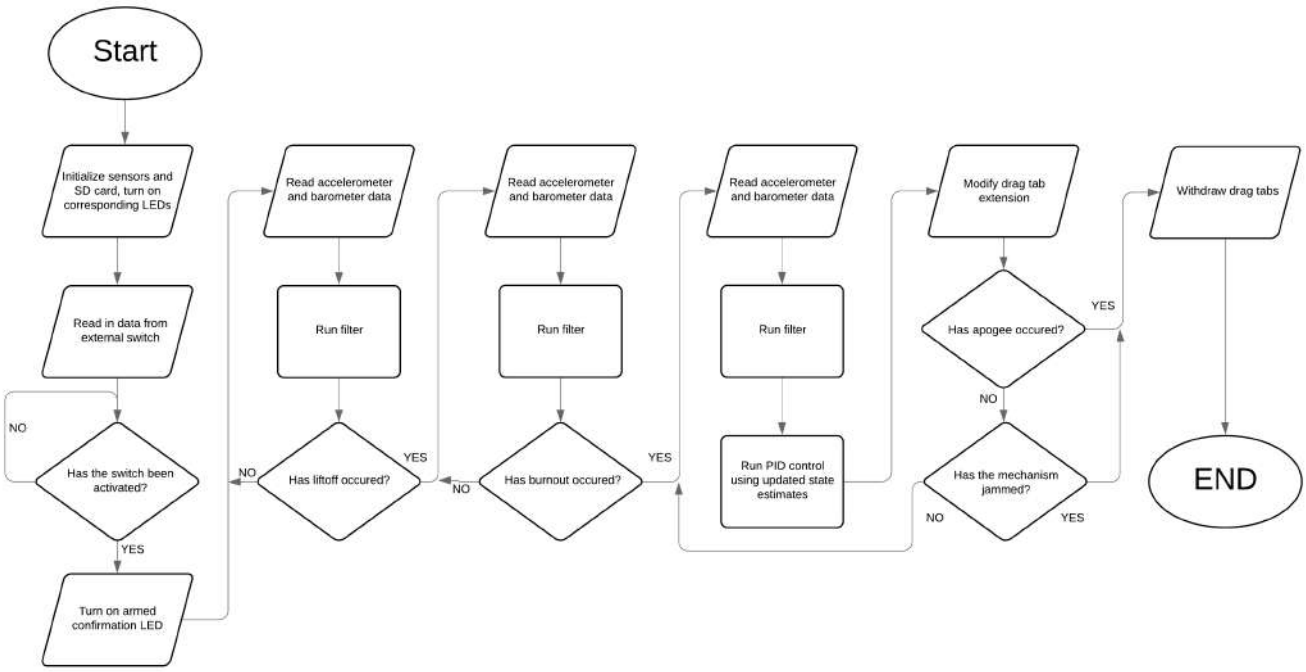

Figure 49: ABS Control Structure

Table 20: Control Stages

Stage	Description
Armed	When the external switch for sensors is activated, turn on the armed confirmation LED, the module changes to Armed, starts to read data from sensors and runs the filtering module.
Liftoff	When either the acceleration is greater than the threshold acceleration for a lift-off or the altitude is greater than the threshold altitude, the module changes from Armed to Liftoff.
Burnout	When the acceleration is smaller than the threshold acceleration for Burnout, the module changes from Liftoff to Burnout module and the PID control algorithm is run.
Apogee	When the altitude is greater than the threshold altitude for the designated height of apogee, the module changes from Burnout to Apogee and the PID control module is stopped.
Landed	When the altitude is smaller than the designated altitude, or the velocity is smaller than the threshold, the module changes from Apogee to Landed.

3.7.5.1 Data Filtering

One important stage of the control flow is data filtering. The goal of this stage is to combine data from each different sensor into reliable altitude and velocity data. In designing the ideal filter, the team has decided to implement a Kalman filter. The Kalman filter maintains an internal state of the system which combines sensor data with a physical model describing how

the system is expected to evolve over time. The algorithm has two broad steps: a prediction step and an update step, and a system of matrices go into the definition of these steps. The X vector stores the internal state, Z stores the sensor data, Φ projects the state forward, H translates from state to sensor data, Q stores the state covariance, R stores the measurement covariance, P stores the error covariance, and K is the Kalman gain. These matrices combine to form Equations 9-13:

$$\hat{X}_{k(-)} = \Phi_{k-1(+)} \tag{9}$$

$$\hat{X}_{k(+)} = \hat{X}_{k(-)} + K_k \left[Z_k - H_k \hat{X}_{k(-)} \right] \tag{10}$$

$$P_{k(-)} = \Phi_{k-1} P_{k-1(+)} \Phi_{k-1}^T + Q_{k-1} \tag{11}$$

$$P_{k(+)} = \left[I - K_k H_k \right] P_{k(-)} \tag{12}$$

$$K_k = P_{k(-)} H_k^T \left[H_k P_{k(-)} H_k^T + R_k \right]^{-1} \tag{13}$$

$\hat{X}$	Stores Internal State
Z	Stores Sensor Data
Φ	Projects State Forward
H	Translates from State to Sensor Data
Q	Stores the Covariance
R	Stores the Measurement Covariance
P	Error Covariance
K	Kalman Gain

The specific construction of these matrices determines how the filter operates. The standard Kalman filter only works for linear systems, so several simplifying assumptions have to be made. In constructing the state transition matrix Φ, the team will use Kinematic Equations 14-16.

$$a_{t+\Delta t} = a_t \tag{14}$$

$$v_{t+\Delta t} = v_t + a_t \Delta t \tag{15}$$

$$y_{t+\Delta t} = y_t + v_t \Delta t + a_t \frac{\Delta t^2}{2} \tag{16}$$

a	Acceleration (ft/s^2)
v	Velocity (ft/s)
y	Position (ft)
Δt	Time (s)

This is a very basic kinematic model that assumes no drag. However, it provides a good model and removes noise from the position and velocity estimates explicitly, and it factors in all of the relevant information. While a rough approximation to vertical acceleration can be

taken by only considering one of the three axes of acceleration, a better estimate can be obtained using the absolute orientation data gathered from the BNO055 to construct a rotation matrix, which transforms from the reference frame of the launch vehicle to an inertial frame, and multiplying the ADXL acceleration by that matrix, which is shown in Equation 17.

$$R_I^B(\phi,\theta,\psi) = \begin{pmatrix} c(\psi)c(\theta) & c(\psi)s(\phi)s(\theta) - c(\phi)s(\psi) & s(\phi)s(\psi) + c(\phi)c(\psi)s(\theta) \\ c(\theta)s(\psi) & c(\phi)c(\psi) + s(\phi)s(\psi)s(\theta) & c(\phi)s(\psi)s(\theta) - c(\psi)s(\phi) \\ -s(\theta) & c(\theta)s(\phi) & c(\phi)c(\theta) \end{pmatrix} \tag{17}$$

Where ϕ is roll, θ is pitch, and ψ is yaw. The team combined these steps into a Python script, found in Appendix B.1, which implements the Kalman filter and the data transformation. Figure 50 shows the output of this program when applied to the sub-scale launch data.

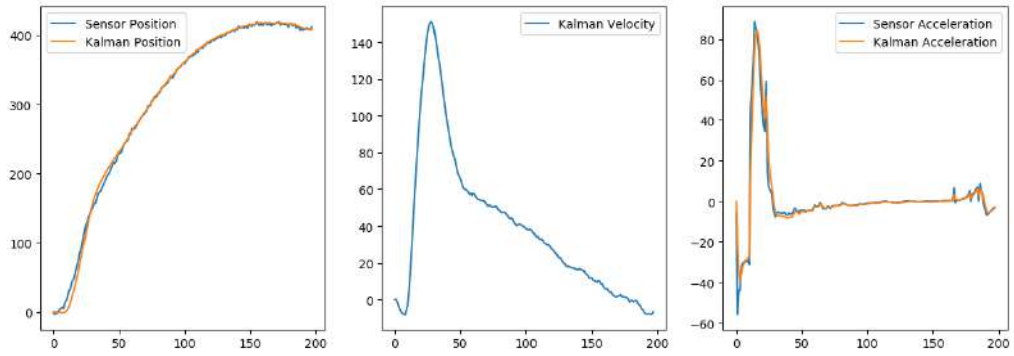

Figure 50: Kalman Filter Applied to Sub-scale Flight Data

This model is powerful for its relative speed and robustness, along with its ability to provide both position and velocity to the PID control algorithm. While the equations do not account for drag, it will not be completely ignored, as the sensor data will inevitably show its effects.

3.7.5.2 PID Algorithm

After the system has detected burnout, the actuation of the drag tabs will be actively controlled by a PID algorithm until apogee is detected. The algorithm alters the rotation angle of the servo motor, thus adjusting the extension of the drag tabs as governed by the previously derived Equation 8. To serve as an input, an ideal flight path was generated by combining simulation data from OpenRocket for liftoff to burnout with a flight simulation from burnout to apogee generated using MATLAB. The MATLAB generated flight path numerically solves the derived equation of motion for the rocket, Equation 5 using 4th Order Runge-Kutta for a second order differential equation, and can be seen in Appendix B.3. The drag coefficient for the ideal flight was adjusted until the launch vehicle reached the target apogee of 4,444 ft. In the algorithm, the altitude and velocity data from this ideal flight are compared to the real-time altitude and velocity of the launch vehicle as indicated by the sensor data after being passed through the Kalman filter, which is then used to determine an ideal servo motor

rotation angle. The resulting closed-loop process carried out by the control system from burnout to apogee is shown in the diagram in Figure 51.

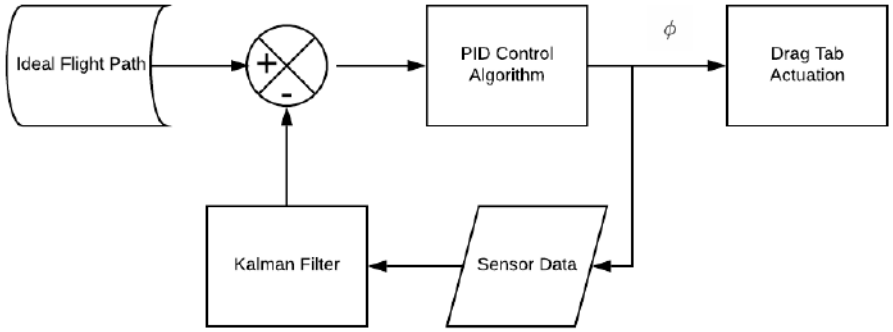

Figure 51: Control Flow Algorithm from Burnout to Apogee

For each altitude after burnout, the PID algorithm actively calculates error as the difference between the measured velocity of the launch vehicle and the ideal velocity from the simulated flight path, and estimates derivative error using the first order backward finite difference method, as well as integral error using a Riemann sum. Using these inputs, it then outputs a new angle of rotation for the servo motor according to the PID control law, shown in Equation 18.

$$\phi(e) = kPe + kD\frac{de}{dt} + kI\int(e)dt \tag{18}$$

ϕ	Angle of Rotation of Servo Motor (°)
e	Error
kP	Proportional Gain
kD	Derivative Gain
kI	Integral Gain

The algorithm includes constraints that ensure that ϕ does not exceed the 63°maximum rotation angle allowed by the mechanism, or the maximum rotation speed of the servo motor, 352.9 °/s. In order to choose values for the gains, the algorithm was tested in MATLAB by simulating flights of the launch vehicle, for a launch angle of 10°and a wind speed of 0 mph. A reasonable set of gain values was found to be kP = 2, kD = 0.5, and kI = 0.05, but these will be verified during control algorithm ground testing before a full-scale flight is attempted. For comparison, simulated flights were also generated for tabs at full extension and without drag tab actuation. The results of the simulated flights are shown in Figure 52.

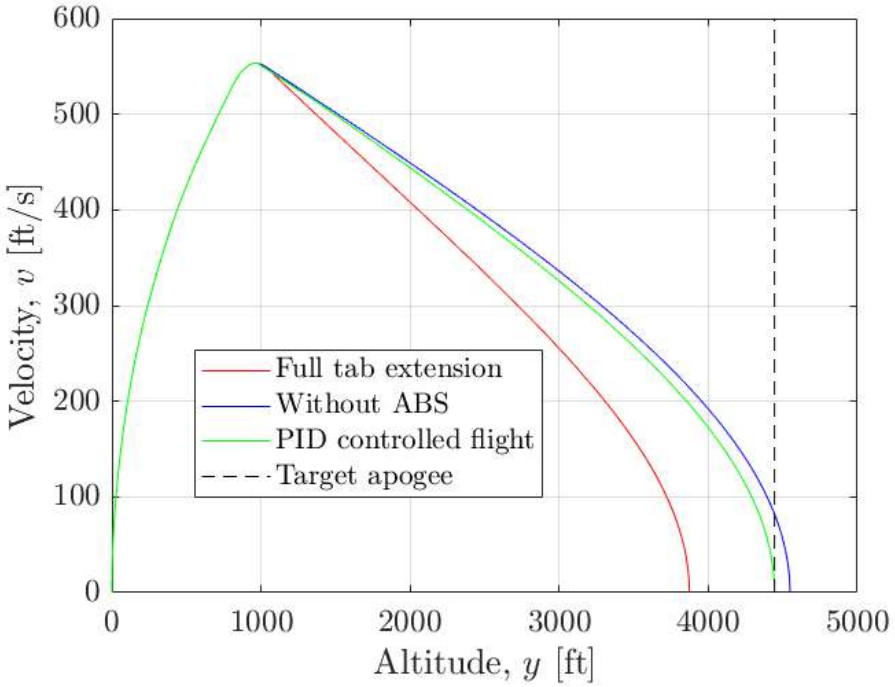

Figure 52: Simulated flight paths verifying the PID control algorithm

The entire functional PID algorithm can be seen in Appendix B.2-B.4.

3.7.6 Sub-scale Results

The team completed a successful sub-scale flight test on December 7, 2019. The launch vehicle flew three times, first with no drag tabs, then with the tabs at full extension, and finally with the tabs at half extension. Table 21 shows the altitude recorded at each apogee by the onboard MPL3115A2.

Table 21: Average Altitude at Apogee

Flight	No Tabs	Half Tabs	Full Tabs
Altitude (ft)	1366	1126.5	1010

The trend of the data verifies that the drag tabs effectively lower the apogee of the launch vehicle. The team was also able to complete a series of wind tunnel testing with no drag tabs, drag tabs at half extension, and drag tabs at full extension in one of the subsonic wind tunnels at Notre Dame's Hessert Laboratory. The wind tunnel could only produce wind speeds of up to 115 ft/s, which is far lower than the maximum expected in-flight velocity. The relevant dimensionless quantity for wind tunnel testing is the Reynolds Number, shown in Equation 19.

$$R_e = \frac{\rho v D}{\mu} \tag{19}$$

R_e	Reynolds Number
ρ	Fluid Density (lbs/ft^3)
v	Fluid Velocity (ft/s)
D	Launch Vehicle Diameter (in.)
μ	Fluid Viscosity $lb/ft/s$

Both ρ and μ only differ marginally between the higher and lower altitude, and since D was at 40% of the full-scale value, the velocity during the wind tunnel test would have needed to be nearly 740 ft/s to achieve dynamic similarity. Since the flow velocity in the wind tunnel was nowhere near this speed, the wind tunnel Reynolds number was much lower than it will be during flight, resulting in a boundary layer that extended past the edge of the drag tabs, as was shown in the CFD analysis in Section 3.7.3.2. Because of this, a drag coefficient for the tabs could not be obtained from the wind tunnel data. For future calculations and control software, the team will use the average drag coefficient of 2.06 extracted from the CFD analysis.

3.8 Recovery System

In order to recover the launch vehicle, a removable recovery system has been designed. At vehicle apogee, a set of independently powered altimeters will ignite black power ejection charges, separating the vehicle into two tethered sections and deploying a 2 ft drogue parachute to control descent. The vehicle will then descend to an altitude of 600 ft AGL, at which point the altimeters will ignite another set of black powder charges that will separate the vehicle into three tethered sections and deploy a 10 ft main parachute. At 400 AGL, an altimeter in the nose cone will separate the nose cone from the payload section, into a total of four tethered sections, descending under a single main parachute.

As it is not required for safe recovery of the vehicle, the nose cone separation system will be treated as a payload subsystem. The design of this system is described in Section 5.3.2.

3.8.1 Parachutes, Harnesses, and Attachment Hardware

A FruityChutes CFC-24 elliptical parachute will be deployed at apogee as a drogue parachute. Deploying a small drogue a parachute at apogee allows for a stable, controlled descent until main parachute deployment while limiting drift and descent time. See Table 22 for the manufacturer specifications of the drogue parachute.

Table 22: FruityChutes CFC-24 Specifications

Specification	Value
Diameter	24 in.
C_d	1.5
Shape	Elliptical
Canopy Material	1.1 oz Ripstop Nylon
Shroud Lines	220 lb Nylon
Weight	2.2 oz

The drogue parachute is protected from the black powder charges using a 24 in. Nomex blanket, which is tied to the recovery harness. Nomex is fire-resistant, preventing the hot gasses produced by the black powder from burning the nylon parachute canopy or shroud lines. Figure 53 shows an example of such a blanket.

Figure 53: Nomex blanket

A FruityChutes IFC-120-S parachute will be deployed at 600 ft AGL to slow the vehicle to its landing velocity. The parachute was chosen due to its low packing volume and high drag coefficient. The performance of the parachute is analyzed in Section 3.9.4. See Table 23 for the manufacturer specifications of the main parachute.

Table 23: FruityChutes IFC-120-S Specifications

Specification	Value
Diameter	120 in.
C_d	2.2
Shape	Toroidal
Canopy Material	1.1 oz Ripstop Nylon
Shroud Lines	400 lb Spectra
Weight	22 oz

To protect the main parachute from the hot gasses produced by the black powder, the parachute is packed in a 16 in. Nomex deployment bag. In addition to black powder protection, the deployment bag slows the parachute's deployment sequence and keeps the shroud lines from tangling during parachute unfolding. A FruityChutes CFC-24 will be attached to the deployment bag as a pilot chute in order to pull the deployment bag off of the main parachute after vehicle separation. Figure 54 shows an example of a deployment bag.

Figure 54: Nomex deployment bag

To slow the deployment of the main parachute, and reduce the forces induced in the rest of the vehicle, a stainless steel reefing ring is placed around the main parachute shroud lines. During parachute opening, this ring will slide down the shroud lines, slowing down the opening sequence and reducing the shock of a large parachute opening at drogue-parachute velocities. The reefing ring has an inner diameter of 1 9/16 in. and a thickness of 1/8 in. At the bridle of the parachute, a 3/8 in. stainless steel swivel will prevent the parachute from imparting torque to the recovery eyebolts.

Shock cords will tether the separated sections of the vehicle in flight, as well as connect the parachutes to the rest of the vehicle. Two cords will be used, one connecting the payload section to the recovery tube, along which the main parachute will be attached, and one connecting the recovery tube to the fin can, along which the drogue parachute will be attached. Both cords will be OneBadHawk 1 in. tubular nylon harnesses, each with a length of 35 ft and loops sewn into the cord at either end. The harness has a breaking strength of 4000 lbs according to the manufacturer. Using the expected force calculated in Section 3.9.3, and the manufacturer-rated strength, the shock cord has an expected factor of safety of 2.3. Figure 56 shows the recovery shock cord, and Figure **??** shows how the shock cords, parachutes, and Nomex are arranged during terminal descent.

Figure 55: Tubular Nylon shock cord

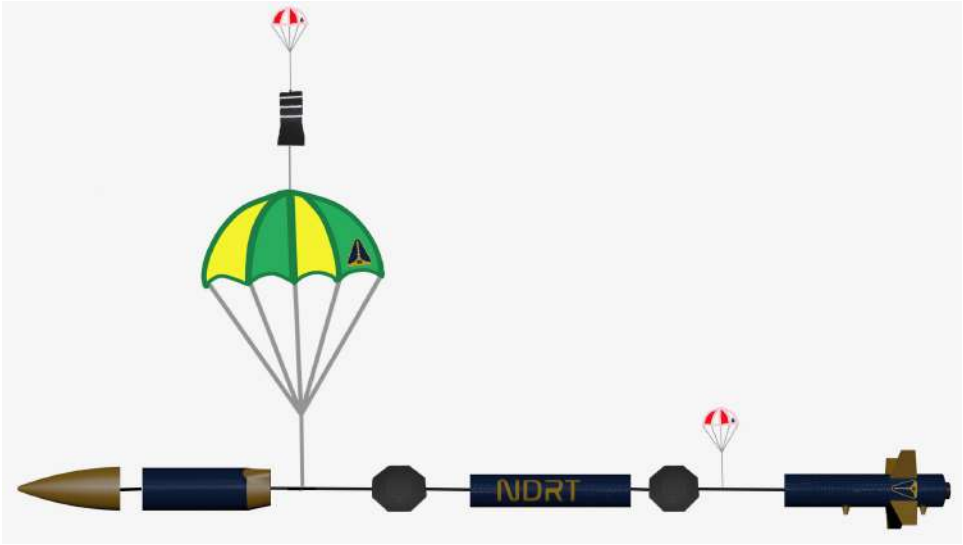

Figure 56: Parachute arrangement on descent

Eyebolts will transfer the parachute load from the shock cord to the recovery bulkheads. The eyebolts are 3/8-16 threaded galvanized steel, of forged construction, with a lifting shoulder and 2 1/2 in. shank. The eyebolts are rated for 1400 lbs of static and up to 3100 lbs of shock load, giving a factor of safety of 4.1 when comparing against the peak expected loads calculated in Section 3.9.3. Galvanized steel was selected for its strength, availability in the required lengths, and resistance to corrosion. These eyebolts will be mated using a 4 in. coupling nut, positioned in the center of the CRAM core. Oversized steel washers between the eyebolt shoulder and the CRAM bulkheads help to spread the load of parachute deployment, and split lock washers prevent the eyebolts from backing out of the coupling nut in flight.

Stainless steel locking quick links connect the parachutes to the shock cords and the the shock cords to the recovery eyebolts. These quick links are constructed from 3/8 in. 316 stainless steel, for strength and corrosion resistance, and feature a threaded sleeve that screws in place on the link shackle to prevent the link from opening in flight. The quick links have a manufacturer-rated working load of 2700 lbs and a maximum shock load of 6000 lbs, giving a factor of safety of 3.4 when comparing against the peak expected loads calculated in Section

3.9.3 . A total of six of these will be used, one to connect each parachute to the shock cord, and two to connect each end of the shock cord to its mounting location within the vehicle. An example of the quick links can be seen in Figure 57.

Figure 57: Stainless steel quick link

3.8.2 Recovery Electronics

The black powder ejection charges that separate the vehicle and deploy the parachutes during descent are controlled using three independent, commercial flight computers, two Featherweight Raven 3 altimeters and one PerfectFlite Stratologger SL100. Both the Raven and Stratologger were chosen due to their small size and power requirements, demonstrated reliability, and quality of recorded data. Using two separate models of altimeter brings additional redundancy to the recovery system, as the system will not fail due to a design flaw inherent to one type of altimeter. Each altimeter controls its own drogue ejection charge and main ejection charge, and is independently powered by its own 3.7 V LiPo battery. Both of the altimeters connect to their respective batteries and e-matches through screw terminals. Both types of altimeters can be seen in Figure 58.

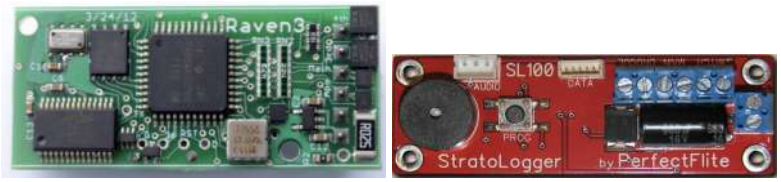

(a) Raven3 (b) Stratologger SL100

Figure 58: Recovery Altimeters

Ejection charge ignition is staggered to avoid damage to the vehicle due to over-pressurization of the parachute bays. The primary Raven altimeter is programmed to deploy its drogue charge immediately at apogee, and its main charge at 600 ft, the secondary Raven altimeter is programmed to deploy its drogue charge 1 s after apogee and its main charge at 550 ft, and tertiary altimeter, a Stratologger, is programmed to deploy its drogue charge 2 s after apogee and its main charge at 500 ft. Any failure to transition state in one of the altimeters has no effect on the other two altimeters, meaning that it would take three independent altimeter faults to cause recovery failure. Figure 59 shows the process that each of the altimeters undergoes during flight.

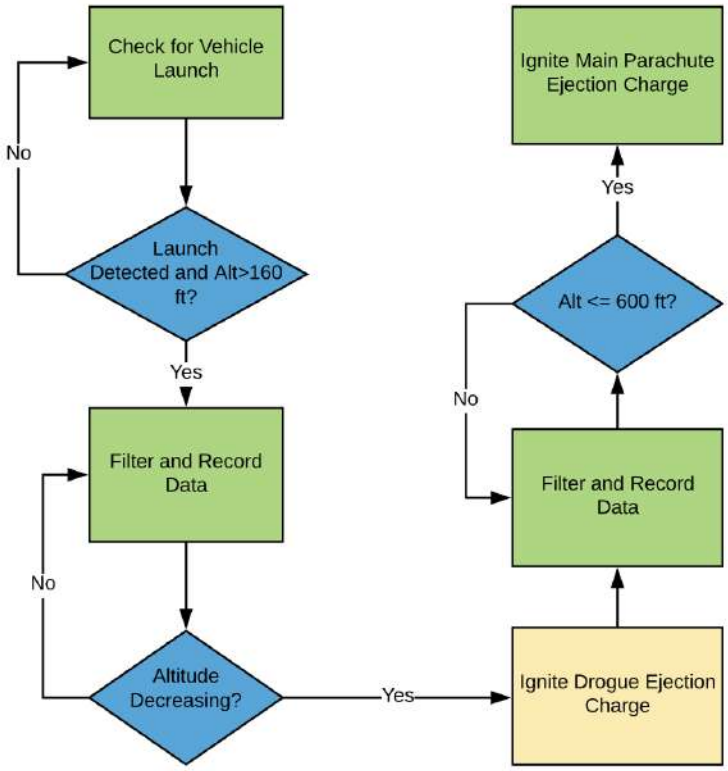

Figure 59: Altimeter Deployment Logic

The altimeters are powered using YDL 170 mAh, 1S LiPo batteries, one for each altimeter. The batteries have a nominal voltage of 3.7 V, which is within the operating range of both the altimeters used. Both the altimeters draw less than 5 mA during standby, giving the altimeters a theoretical maximum on-pad wait time of 34 hrs. The batteries were chosen for their extremely light weight (approximately .21 oz) and high current output, assuring e-match ignition. The batteries feature a robust 2mm PH JST connector, allowing strong yet removable connection to the rest of the recovery electronics and easy recharging before flights. The battery type that will be used can be seen in Figure 60.

Figure 60: Lithium-Polymer Battery

Two types of switches arm the recovery system. The altimeters are powered on using Featherweight magnetic switches, which allow the altimeters to be turned on and off from outside the vehicle using only a magnet. The altimeters are connected to the black powder

e-matches using Aerocon ThroughMount slotted switches. These single-pole, double-throw switches can be activated using a small screwdriver inserted in a hole drilled through the vehicle. Both switches were selected due to their light weight and resistance to vibration. The slotted rotary switch requires an appreciable amount of torque to arm, negating the chance of accidental recovery activation or deactivation through vibration or shock. The magnetic switches are entirely solid-state, eliminating any chance of accidental activation or deactivation through flight or assembly forces. The circuit locations of the two switches require that both be activated before the recovery system is fully armed, giving extra safety to personnel during assembly and launch preparation. Figure 61 shows both types of switches to be used.

(a) Magnetic switch (b) Slotted Rotary switch

Figure 61: Recovery Switches

Three solderable perfboards connect the batteries and switches to each of the altimeters. Solderable perfboards were chosen for electrical connection due to the strength of soldered wire connections and the small size of perfboards when compared to wire crimps or other connection systems. In addition, soldered perfboards can be quickly modified and repaired if they undergo damage, unlike PCB connections. Figure 62 shows how the two Raven3 altimeters are connected on the perfboard, and Figure 63 shows how the Stratologger altimeter is connected on the perfboard.

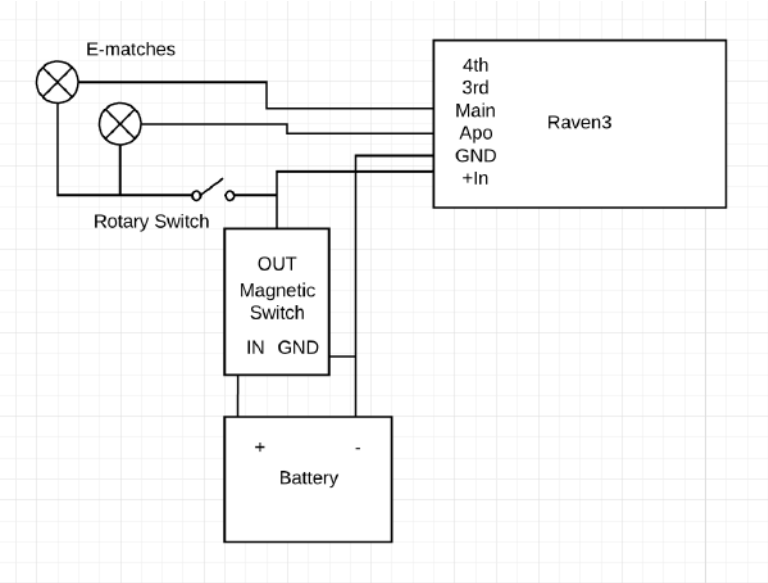

Figure 62: Raven3 Circuit Diagram

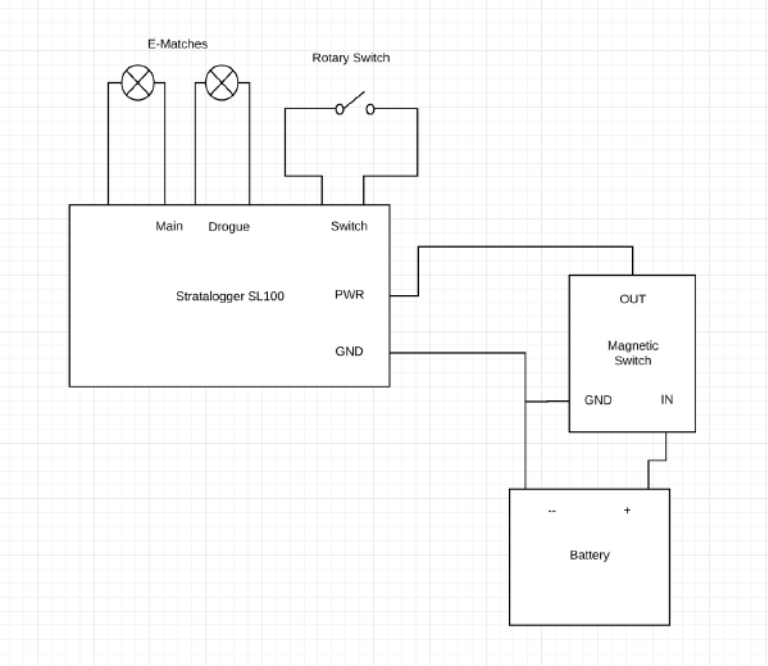

Figure 63: Stratologger Circuit Diagram

3.8.3 Altimeter Bay Design

The altimeters that control ejection charge deployment, as well as the associated batteries and switches, are contained in the Compact Removable Avionics Module, or CRAM. The primary feature of the CRAM is a twist-to-lock retainment system that allows for robust mounting inside the vehicle while still being easily removable for data retrieval and replacement of ejection charges. Figure 64 shows the full CRAM assembly.

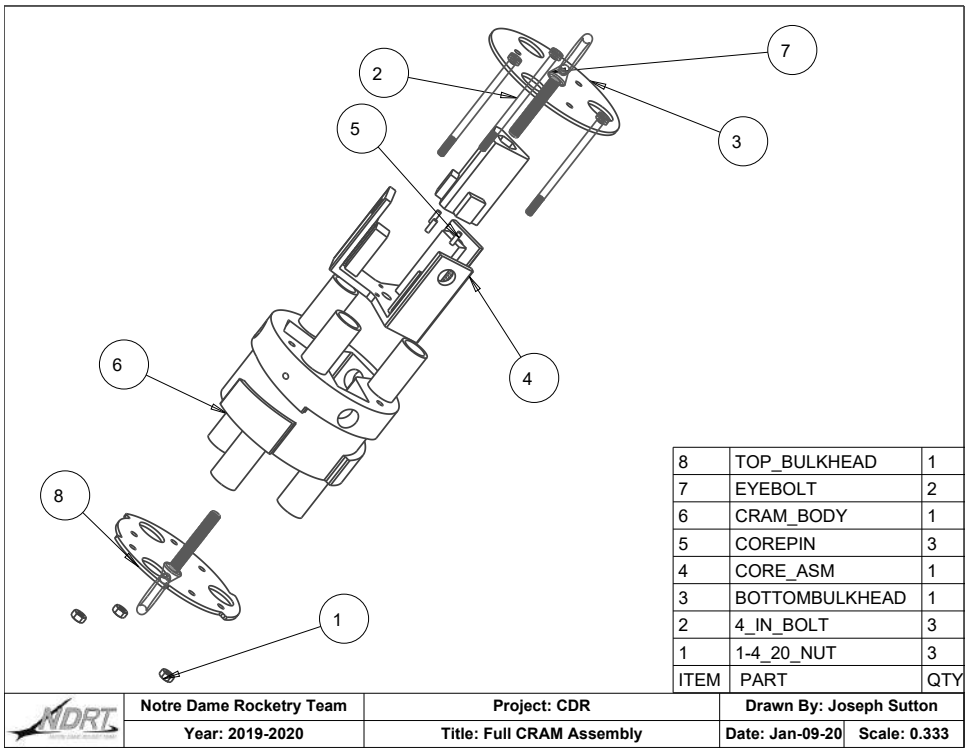

Figure 64: Full CRAM Assembly

The CRAM core is the central component of the CRAM to which the altimeters and other electronics are mounted. The CRAM core will be 3D printed from PLA due to its availability and ease of manufacturing. The low strength of 3D printed PLA is not a detriment in this application, as the CRAM core is entirely non-load bearing. The core will be printed in two sections a top and bottom, and joined by press-fit steel pins. The altimeters and soldered breadboards will be secured to the core by 2 #2-56 screws and nuts each, while the rotary switch will be epoxied into its mounting hole. The batteries will be secured to the core via semi-permanent foam mounting tape. The CRAM eyebolts will be secured to the steel coupling nut in the CRAM core. Figure 65 is a drawing of the assembled core.

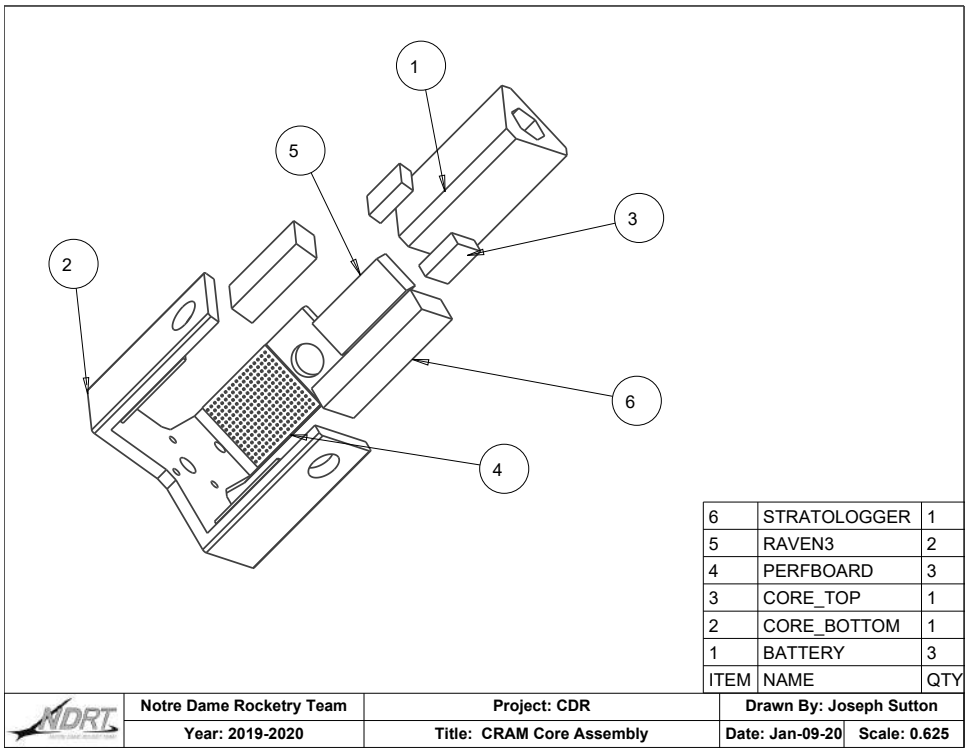

Figure 65: Assembled CRAM core

Bulkheads on either side of the CRAM distribute the loads from parachute deployment and keep the CRAM core inside the body. The 1/8 in. bulkheads feature multiple holes to allow for the PVC charge wells and space for wires to run from the CRAM to the charge wells. The bulkheads will be CNC milled from Garolite G10 fiberglass, chosen because of its good strength-to-weight ratio, excellent impact strength, and overall durability. Three 4 in. long, 1/4-20 bolts with nuts are used to secure the bulkheads to the CRAM body and retain the core.

During parachute deployment, the CRAM bulkheads will transfer load between the recovery eyebolts and the CRAM body. The worst-case forces experienced by the bulkheads are calculated in Section 3.9.3. The forces calculated were entered into a Fusion360 static simulation study to analyze the stresses that the bulkheads undergo. Figures 68 and 69 display the results of the studies. The top bulkhead features a Von Mises Stress FOS of 5.9, while the bottom bulkhead features a FOS of 4.0, given the peak found in the analysis and a material tensile strength of 40000 psi.

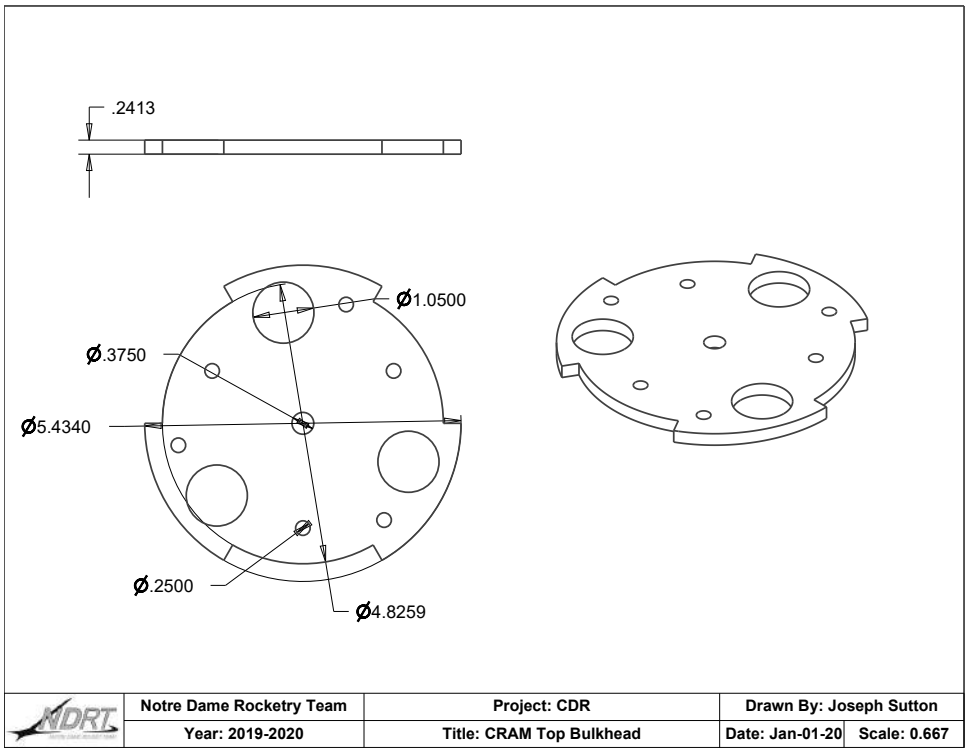

Figure 66: Drawing of CRAM top bulkhead

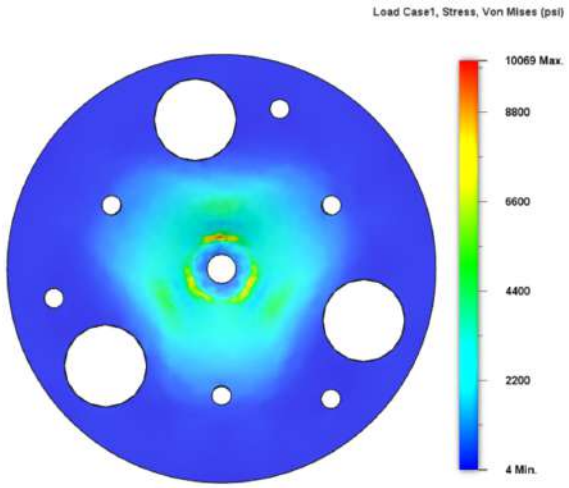

Figure 69: Finite Element Analysis of CRAM bottom bulkhead

The CRAM body retains the ejection charges and transfers load from the CRAM bulkheads to the ring adapter and the recovery tube. The tapered cutouts on the exterior of the CRAM interface with a ring adapter mounted in the recovery tube, allowing the whole CRAM to be secured into the body tube with a 60 degree twist. Hardwood screws inserted from the outside of the body tube keep the CRAM body from twisting free in flight. Holes in the exterior of the body allow for access to the altimeter arming switches, as well as airflow for proper altimeter function. These holes match holes drilled in the vehicle body tube to allow for access from the

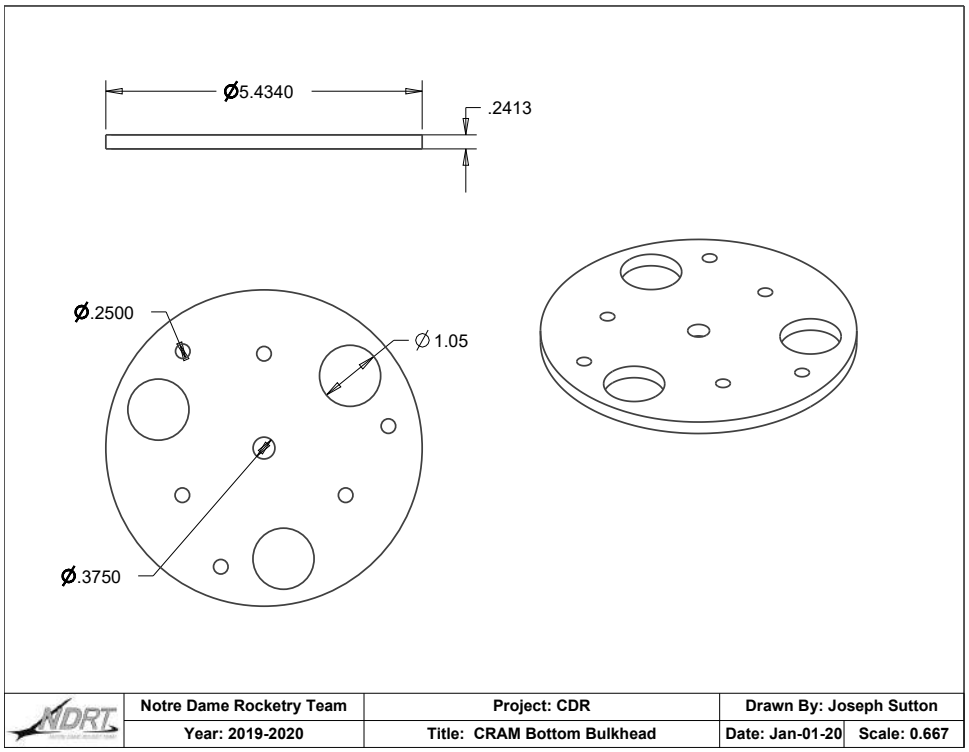

Figure 67: Drawing of CRAM bottom bulkhead

exterior of the vehicle. On the top and bottom of the CRAM are 1 in. diameter, 2.5 in. long PVC pipes that function as charge wells, holding the black powder ejection charges in place during launch. The CRAM body will be CNC milled from 3/4 in. oak common board in four pieces, and permanently assembled using JB-Weld epoxy. Wood was chosen due to its good strength-to-weight ratio ease of manufacturing, and low cost. Alignment dowel pins ensure that the twist-to-lock tapers remain aligned.

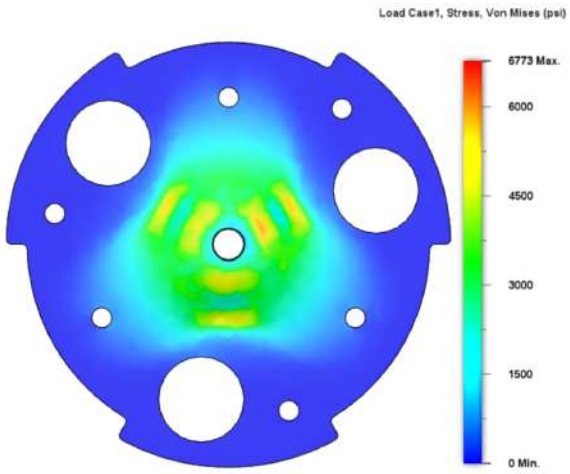

Figure 68: Finite Element Analysis of CRAM top bulkhead

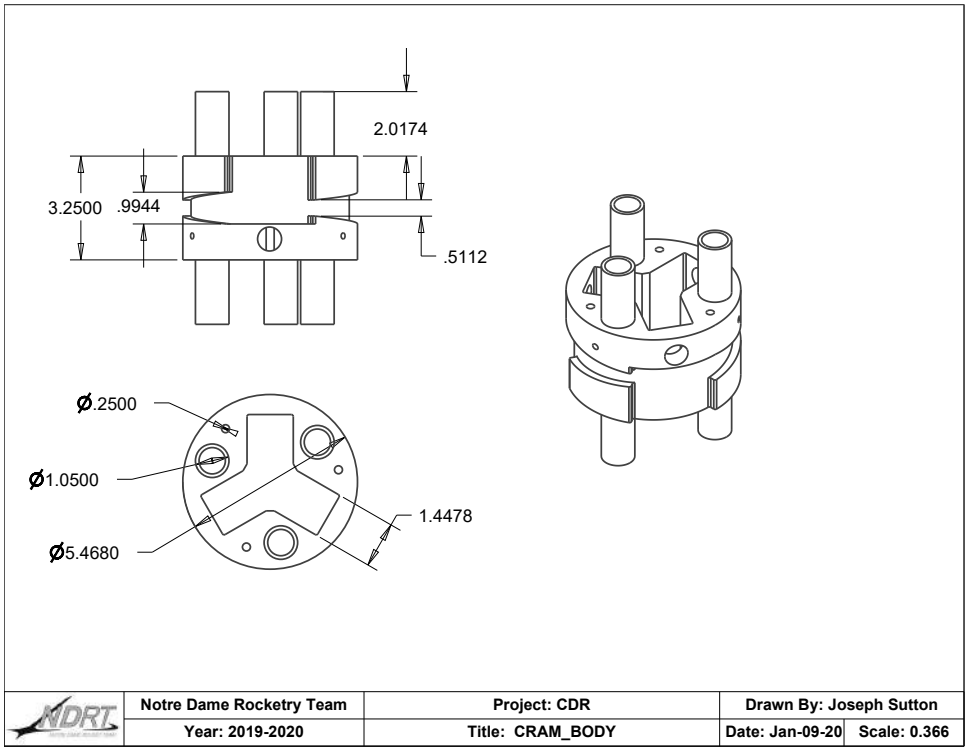

Figure 70: Drawing of CRAM body

To protect the altimeters and other electrical components of the recovery system from electromagnetic interference, electromagnetic shielding in the form of copper foil tape is added to the interior of the CRAM body and the altimeter-facing sides of the CRAM bulkheads. The pieces of copper tape will overlap when the CRAM is fully assembled, forming a contiguous Faraday cage to protect from electromagnetic signals. During parachute deployment, the CRAM body will transfer the parachute force from the bulkheads to the vehicle body tube. The worst-case forces experienced by the CRAM body are calculated in Section 3.9.3. The forces calculated were entered into a Fusion360 static simulation study to

analyze the stresses that form. Figure 71 displays the results of the static study. From this study, the bulkhead features a Von Mises FOS of 6.2, given the peak stresses found in the analysis and oak's against-the-grain tensile strength of 6760 psi.

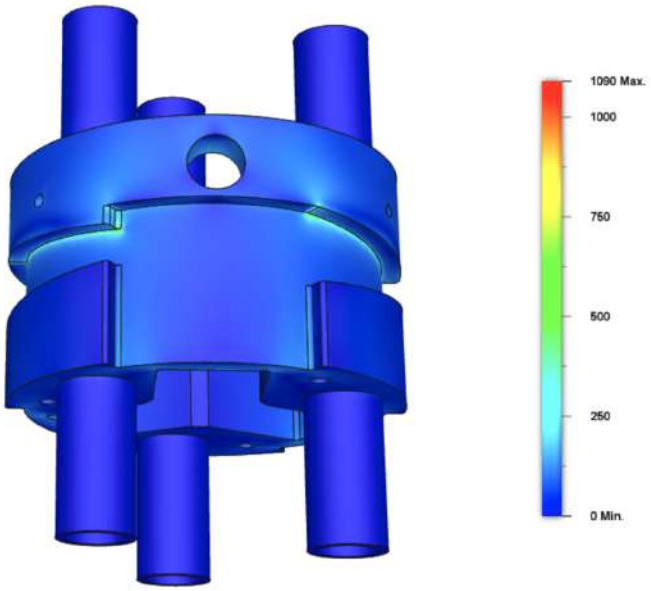

Figure 71: Finite Element Analysis of CRAM body

The ring adapter that connects the CRAM to the vehicle's body tube is a 1/4 in. thick ring with internal protrusions that match the external cutouts of the CRAM body. The adapter will be machined from oak board in two pieces and epoxied together, in a manner similar to the CRAM body. The adapter is permanently epoxied into the recovery tube, 6 in. forward of the aft end of the tube.

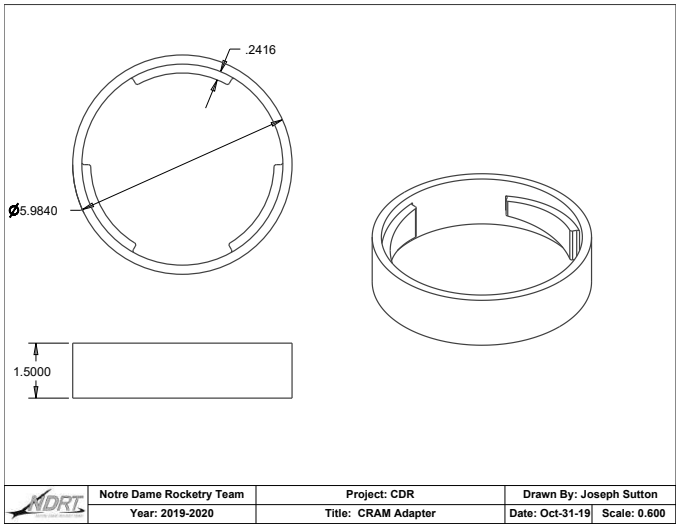

Figure 72: Drawing of CRAM tube adapter

During parachute deployment, the ring adapter will transfer load from the CRAM body to

the rocket body tube. Figure 73 displays the results of a Finite Element study done on the ring adapter, using expected peak forces calculated in Section 3.9.3. The ring adapter has a Von Mises FOS of 20.6, given the peak stresses found in the analysis and oak's against-the-grain tensile strength of 6760 psi.

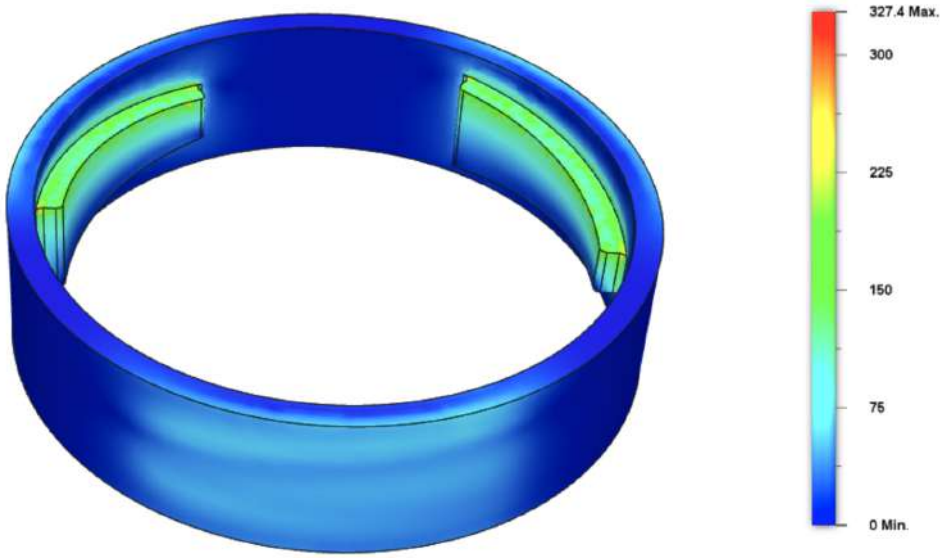

Figure 73: Finite Element Analysis of CRAM Ring adapter.

3.8.3.1 Rocket Separation

In order to determine the amount of 4F black powder needed for separation, the force necessary to break the shear pins can be calculated with Equation 20. The friction between vehicle sections is assumed to be negligible in comparison to the force of the shear pins. The pressure necessary to break the shear pins can then be calculated from Equation 21.

$$F = \tau A_s n \tag{20}$$

F	Force (lb_f)
τ	Shear Strength (psi)
A_s	Shear Pin Area ($in.^2$)
n	# of Shear Pins

$$P = \frac{F}{A_b} \tag{21}$$

P	Pressure (psi)
F	Force (lb_f)
A_b	Bulkhead Area ($in.^2$)

Because the combustion reaction of black powder occurs at high temperatures (1837 K) and relatively low pressures (less than one atmosphere), the ideal gas law can be used to find the number of moles of gas needed to produce the necessary pressure with Equation 22.

$$n_g = \frac{PV}{RT} \tag{22}$$

n_g	Moles of Gas (mol)
P	Pressure (atm)
V	Chamber Volume (L)
R	Gas Constant (L*atm/mol/K)
T	Combustion Temperature (K)

A simplified balanced equation for the combustion of black powder is given in Equation 23.

$$2KNO_3(s) + S(s) + 3C(s) \rightarrow K_2S(s) + N_2(g) + 3CO_2(g) \tag{23}$$

The moles of gas needed can be converted into moles of each solid component of the black powder using stoichiometry, and the moles can be converted to grams using the molar mass of each component, shown in Equations 24-26.

$$\frac{\text{mol gas}}{1} \times \frac{2 \text{ mol } KNO_3}{4 \text{ mol gas}} \times \frac{101.1 \text{ g } KNO_3}{1 \text{ mol } KNO_3} = \text{g } KNO_3 \tag{24}$$

$$\frac{\text{mol gas}}{1} \times \frac{1 \text{ mol S}}{4 \text{ mol gas}} \times \frac{32.1 \text{ g S}}{1 \text{ mol S}} = \text{g S} \tag{25}$$

$$\frac{\text{mol gas}}{1} \times \frac{3 \text{ mol C}}{4 \text{ mol gas}} \times \frac{12.0 \text{ g C}}{1 \text{ mol C}} = \text{g C} \tag{26}$$

Adding the grams of each component together gives the total mass of black powder needed for the separation event, shown in Equation 27.

$$\text{g } KNO_3 + \text{g S} + \text{g C} = \text{g Black Powder} \tag{27}$$

A FOS of 25% is then added to give a total amount of black powder needed. This calculation is performed for each separation event to determine the amount of black powder needed for each charge. The calculated value is then rounded up to the nearest half gram for measurement simplification.

Summary of Black Powder Charge Calculations

Tables 24, 25, and 26 contain a summary of the expected black powder forces, pressures, moles of gas, and mass of powder used to separate the drogue parachute compartment, the main parachute compartment, and the nosecone, respectively. Full calculations can be seen in Appendix A.

Table 24: Drogue Parachute Black Powder Ejection Charge Summary

Separation	$F(lb_f)$	P (atm)	n_g (mol gas)	$Mass\,4F$ (g)
Initial	181	0.438	0.0148	1.0
Secondary	273	0.657	0.0222	1.5
Tertiary	273	0.657	0.0222	1.5

Table 25: Main Parachute Black Powder Ejection Charge Summary

Separation	$F(lb_f)$	P (atm)	n_g (mol gas)	$Mass\,4F$ (g)
Initial	273	0.699	0.0665	4.5
Secondary	323	0.777	0.0741	5.0
Tertiary	323	0.777	0.0741	5.0

3.8.4 Telemetry

In order to track the position and status of the vehicle in real time during its flight, a telemetry system has been designed. The telemetry system gathers data during flight, packages it, transmits it to a relay station, and receives it at a ground station where the position and status of the vehicle are displayed. The portion of the telemetry system onboard the vehicle is located in the nose cone, and transmits at 250 mW of power and a frequency of 433 MHz using a dipole antenna. The main function of the telemetry system is transmission of GPS data; however, the transmission of pressure and acceleration data will also be included to give a more accurate estimation of the vehicle's position. For an illustration of the overall system design, see Figure 74.

Table 26: Nose Cone Black Powder Ejection Charge Summary

Separation	$F(lb_f)$	P (atm)	n_g (mol gas)	$Mass\,4F$ (g)
Nose Cone	286	0.387	0.0148	1.0

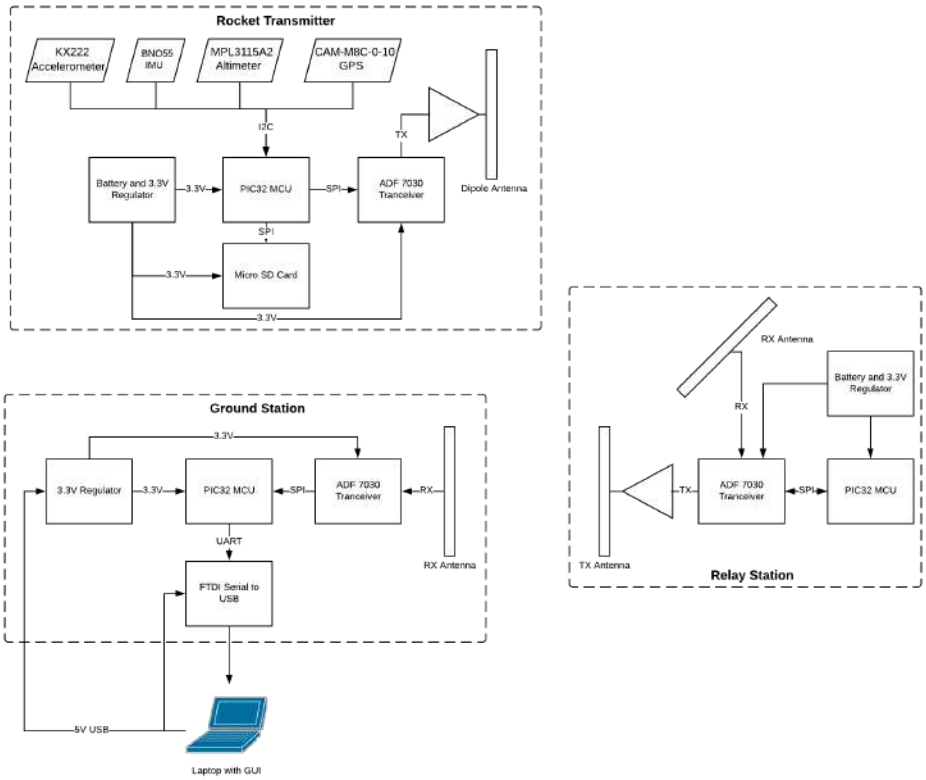

Figure 74: Telemetry System Block Diagram

3.8.4.1 Subsystem Design

The telemetry system is comprised of five subsystems: the vehicle sensor management system, the vehicle transceiver, the relay station transceiver, the ground station transceiver, and the ground station user interface. The vehicle sensor management system is responsible for collecting data from the telemetry sensors on-board the vehicle, packaging the data, and providing this package to the vehicle transceiver. The vehicle transceiver then transmits data to the relay station transceiver, which in turn forwards the data to the ground station transceiver. The ground station user interface receives data from the transceiver and reports it to observers.

3.8.4.1.1 Onboard Vehicle System

Vehicle Sensor Management System The telemetry system has a GPS, accelerometer, and barometric altimeter onboard the vehicle. Each sensor is sampled at a minimum frequency by a microcontroller in order to maintain an optimal resolution for the data that is being gathered

so that it is accurate enough to be considered nominally correct. The sensors were selected because they possess desired characteristics needed for system performance, shown in Table 27.

Table 27: Vehicle Sensor Specifications

Sensor	Product Name	Max. Sampling Freq. (Hz)	Max. Operating Altitude (ft)	Interface
GPS	CAM-M8C-0-10	10	50,000	I2C
IMU	BNO055	100	N/A	I2C
Accelerometer	KX222-1054	25.6 (kHz)	N/A	I2C
Altimeter	MPL3115A2	160	11,775	I2C

Two accelerometers, the BNO055 and KX222-1054, are integrated into the telemetry system to serve different functions. The BNO055 has a fusion mode that performs sensor fusion calculations on measurements from the accelerometer, gyroscope, and magnetometer to obtain an absolute orientation measurement. While in fusion mode, the BNO055 clips at an acceleration of 129 ft/s^2 and is therefore not a reliable accelerometer. To compensate for this, the BNO055 serves exclusively as an orientation sensor, whereas the KX222-1054, capable of operating at accelerations up to 1029 ft/s^2, serves as the accelerometer of the telemetry system. The KX222-1054 is useful because of its high maximum sampling rate. While it is possible to derive acceleration from GPS measurements, the low sampling rate of the CAM-M8C-0-10 does not provide the desired resolution for acceleration data. Conversely, with a maximum sampling rate of 25.6 kHz, the KX222-1054 can achieve the minimum sampling requirement of 800Hz.

The GPS sensor must be sampled at a minimum of 10Hz, as this frequency is a standard for GPS readings and provides a minimum resolution of 59 ft. In order to achieve a resolution of approximately 6 ft, the altimeter is sampled at a minimum rate of 100 Hz. The data rates of each sensor are shown in Table 28

Table 28: Calculated Sensor Data Rates

Device Type	Device	# Measurements	# Bits	Frequency (Hz)	Data Rate (bits/s)
Altimeter	MPL3115A2	1	24	160	3840
GPS	CAM-M8C-0-10	3	32	10	960
Accelerometer	KX222-1054	3	16	800	38400
Accelerometer	BNO055	N/A	243	100	24300
				Total	**67500**

Managing this system of sensors requires the use of a microcontroller that can accommodate four I2C interfaces to read from each device. The PIC32 MCU family from

Microchip is suitable for this requirement given the number of I/O ports that are available to support the necessary interfaces. Since this family of microcontrollers requires a 3.3 V input, a voltage regulator, such as the LD1117, is required to downconvert the 3.7 V-4.2 V range from the battery. Additionally, the sensor readings are performed using timer interrupts due to the sampling frequency requirements. In order to ensure a sufficient timing accuracy, an external oscillator is used by the microcontroller.

To store each data packet locally, the microcontroller must write data to an SD card. The SanDisk Ultra microSDXC is a suitable option due to its memory capacity of 128GB and ease of removal for analysis.

Vehicle Transceiver

The transceiver module selected for use in the design is the ADF7030 from Analog Devices, which is capable of operating between 426 MHz and 470 MHz. Because of the data rate requirement of the system, an operating frequency in the 433 MHz band was selected to decrease path losses and increase effective range. In addition, none of the other transmitters located in the payload of the vehicle operate in the 433 MHz band, ensuring that the vehicle transceiver will not interfere.

The vehicle transceiver must be capable of transmitting between 200-250 mW of radiated power. The ADF7030 is capable of outputting -20 dBm to 17 dBm (0.01 mW to 50 mW) of power from its transmit ports. For this reason, an external 20 dB power amplifier is placed on the output of the ADF7030, and the tunable output power of the transceiver is used to adjust the exact radiated power of the antenna to be in the range of 23 dBm to 24 dBm. The ADF7030 is capable of operating with either a 2FSK or 4FSK modulation scheme. Because extremely high data rates are not required, 2FSK was selected in order to maximize possible range. When transmitting with the 2FSK modulation scheme, the maximum data rate of the ADF7030 is 150kbps, which meets the requirement of 67.5 kbps.

Assuming that the relay station is placed approximately 2,500 ft from the launch site, the line-of-site distance from vehicle transceiver to relay receiver is 5,500 ft. Future testing will confirm that the vehicle transceiver is capable of transmitting the required distance at the specified transmission angle of 63°, shown in Section 6.1.2. However, due to the design decision to set the transceiver to the maximum allowed transmission power of 250 mW, as well as other design decisions made to maximize the effective range, the system is expected to be able to meet the transmission range requirement.

In order to guarantee that the transceiver is able to maintain a connection to the relay station throughout the entire duration of the vehicle's flight, a half-wave dipole antenna has been selected for the design: the ANT-433-MHW-SMA-S, designed for use in the 433 MHz band. The radiation pattern of this antenna is symmetrical about the X-Z plane, as shown in Figure 75. This allows the antenna to have an approximately equal gain of 0 dB regardless of the roll orientation of the vehicle. The radiation pattern for this antenna is approximately equivalent regardless of whether the antenna is pointing upwards or downwards. For this reason, when mounted in the nose cone, the transmitter antenna will be able to maintain an approximately equal gain of -5 dB when oriented upwards and downwards at the maximum transmission angle of 63°.

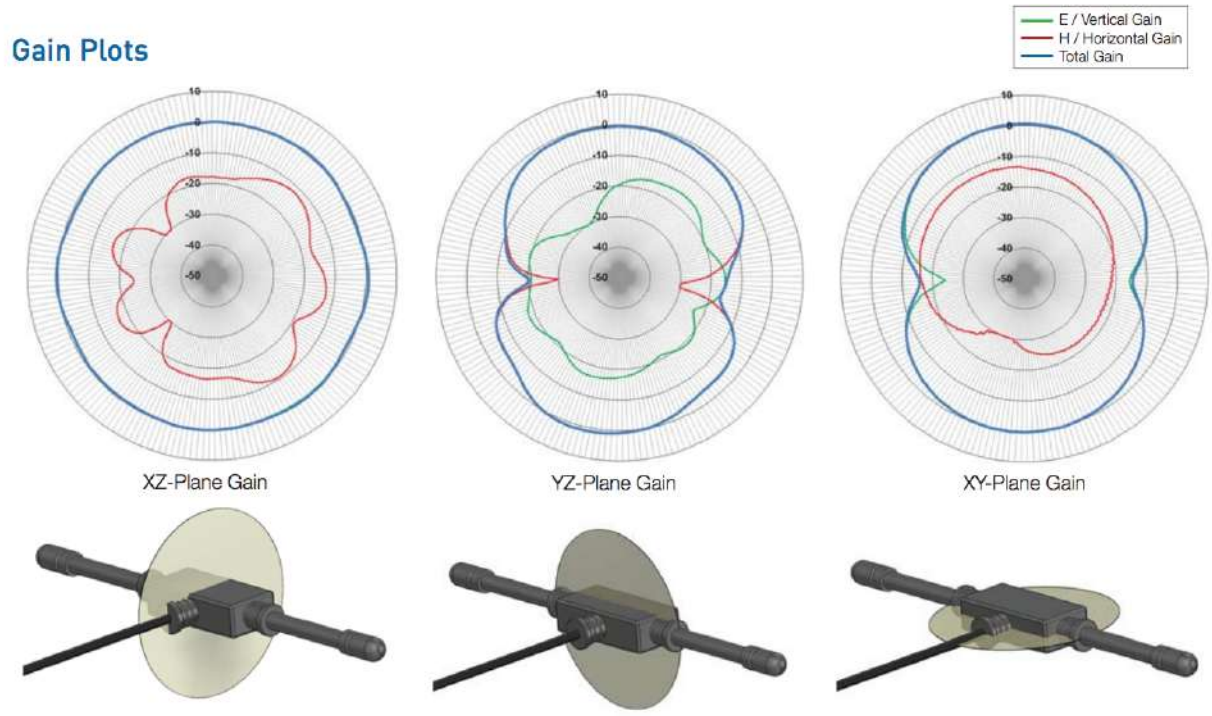

Figure 75: Gain Plots for the ANT-433-MHW-SMA-S Antenna

Vehicle Subsystem Power Considerations

The subsystems onboard the vehicle are required to run on independent power and are limited by what weight and size constraints allow for in terms of battery selection. The system must have an effective life which exceeds the length of the mission, as well as any potential standby time the vehicle may experience while sitting on the pad. Full Recovery Requirements can be seen in Table 90. To estimate the running time of the vehicle subsystems while powered by the selected Adafruit Lithium Ion 3.7 V 2500 mAh battery, calculations were performed as shown in Table 29.

Table 29: Estimated Power Budget

Device/State	ADF7030	GPS	Accel. (KX222)	IMU (BNO055)	Altimeter	PIC	Total Current
Current Draw (mA)	65	71	0.145	12.3	2	100	**250.445**

The power budget calculations were estimated using the current draw for each device on the vehicle subsystem board, assuming that the ADF7030 is in the transmit state for the entirety of operation to produce a conservative estimate.

3.8.4.1.2 Relay Station Transceiver

In order to achieve an ideal radiation pattern with proper directivity, a cross-polarized patch

antenna is used at the relay station. The radiation pattern of this antenna captures the position of the vehicle throughout its flight. The transmission to the ground station is achieved with a second identical antenna set to transmit. An ADF7030 transceiver is used to both receive data from the vehicle and transmit data to the ground station. A PIC32 microcontroller controls this radio chip via an SPI interface by sending timed radio commands.

3.8.4.1.3 Ground Station Transceiver

In order to maintain directivity towards the relay station, the design uses a cross-polarized patch antenna at the ground station. A patch antenna has ideal directivity, and the cross-polarization allows for better communication between the antennas regardless of orientation. Additionally, the design uses the ADF7030-1 transceiver at the ground station to maintain consistency with the relay station and vehicle transceivers. This allows the system to maintain a consistent data rate of 67.5 kbps.

In addition, to receive the data from the ADF7030, the ground station subsystem includes the same microcontroller from the PIC32 family specified in Section **??**, along with a similar external oscillator to ensure accurate timing. This microcontroller is capable of communicating with the transceiver chip via an SPI interface, and is able to process the data stored in each of the packets. In addition, an FTDI FT230XS-R USB to serial UART converter chip is used to allow the PIC32 microcontroller to send the received data to the ground station user interface over USB.

Because the PIC32 microcontroller, ADF7030, and FTDI FT230XS-R require 3.3 V power, an LD1117 linear regulator is used to convert the 5 V input from the USB connection supplied by the laptop down to the required 3.3 V.

3.8.4.1.4 Ground Station User Interface

Since the ground station UI must report data from four different sensors in near-real time, this data must be presented clearly and intuitively. This means that instead of reporting purely numerical values, figures and plots are also utilized. For example, the GPS readings will be plotted on a map to provide a visual interpretation of where the vehicle is located. Measurements from the orientation sensor, accelerometer, and altimeter will be plotted continuously to demonstrate the trajectory and altitude of the vehicle respectively throughout the flight. Following the conclusion of the test, these figures and plots can be saved locally for future analysis and reporting.

3.8.4.2 Telemetry Housing

The telemetry vehicle subsystems are housed in the nose cone of the vehicle through the use of a 3D printed ASA Plastic, twist-to-lock retainment system, similar in form to that shown in Section 3.8.3. The adapting ring is integrated directly into the nosecone assembly, as shown in Figure 5, and the removable cylinder piece has been resized to the dimensions of the nose cone, as shown in Figure 76.

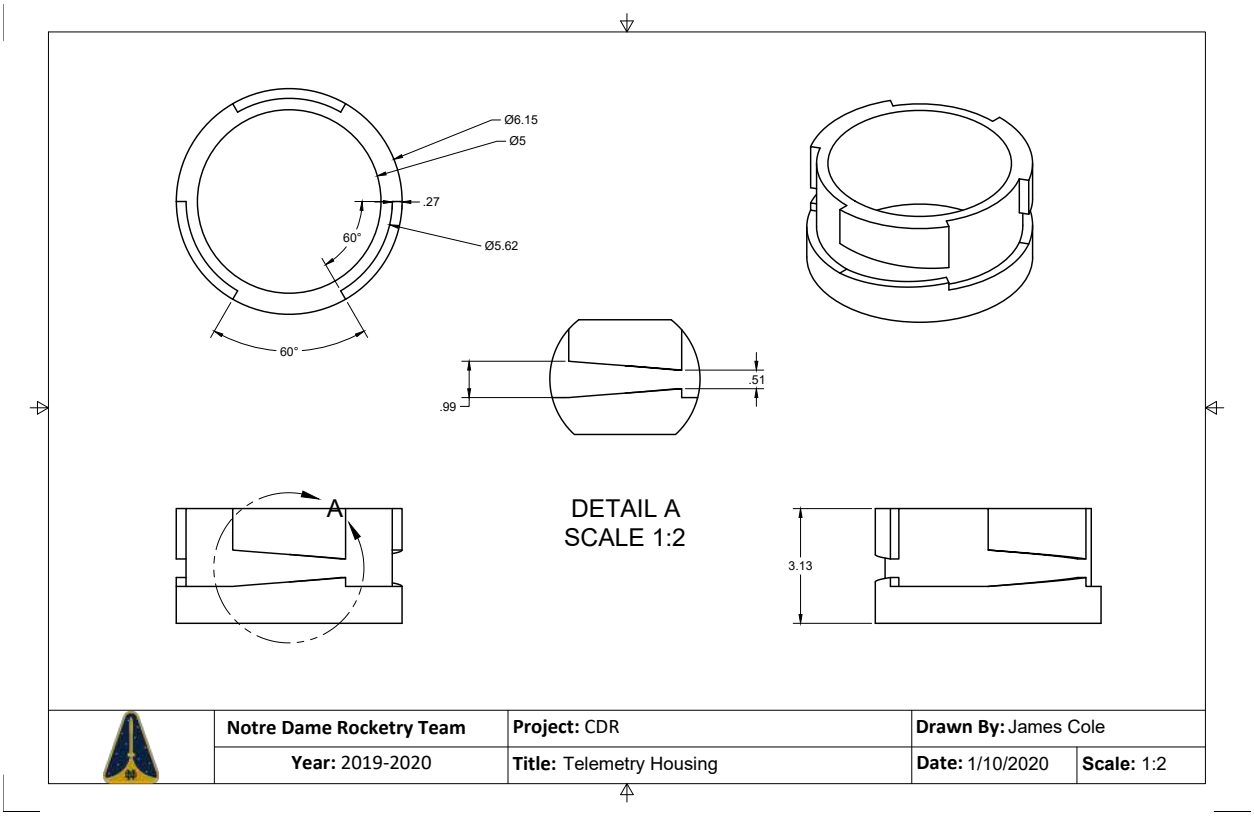

Figure 76: Drawing of Telemetry Housing Cylinder

A 0.125 in G10 Garolite bulkhead is secured to the bottom of the housing cylinder with epoxy. An eyebolt is secured through the center of the bulkhead with a nut and washer to allow for the nose cone to be ejected by a black powder charge during the decent of the vehicle, but will remain tethered to the vehicle as described further in Section 5.3.2. The loads that the twist-to-lock system and retention assembly are expected to experience will be low enough that the bulkhead and 3D printed ABS cylinder are well within safe limits. To ensure that this is the case, Finite Element Analysis was conducted on the part. With a load case of 300 lb, which is significantly higher than the maximum expected force of 188 lb, the resulting factor of safety, with a minimum S of 7.35, is significantly large enough to assuage any causes for concern of structural failure.

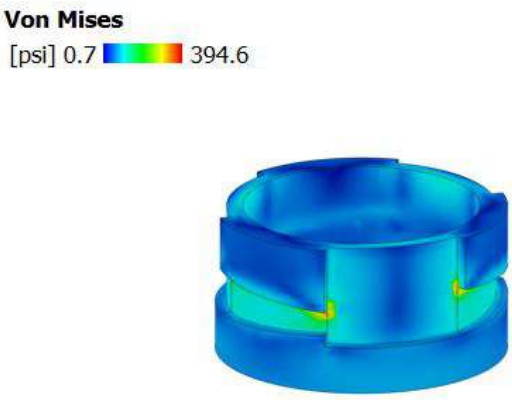

Figure 77: Finite Element Analysis for Stresses in Telemetry Housing Cylinder

3.8.4.2.1 RF Transparency

One major concern during the design and integration of the telemetry system is reducing sources of RF interference. As such, materials surrounding the vehicle onboard subsystem were selected for both strength and RF transparency. The nose cone is made out of 3D printed ASA plastic, while the telemetry housing cylinder is made from 3D printed ABS plastic and the telemetry bulkhead is made from G10 Garolite, all of which are RF transparent. Aft of the telemetry vehicle subsystem, RF opaque materials and structures like carbon fiber and faraday cages respectively are utilized to assist in RF shielding vulnerable subsystems like e-matches and altimeters. However, it is unlikely that these constructs will interfere with the ability of the telemetry system to transmit vehicle data during flight.

3.9 Mission Performance Predictions

To ensure that the vehicle performs as expected and meets all mission requirements, a number of simulations and calculations were performed. The next few sections will go in depth on how the design of the launch vehicle will affect its performance as well as the purpose of these simulations.

3.9.1 Flight Simulations

The launch vehicle's flight is governed by major events such as ignition, rail exit, burnout, among others. The expected flight profile was simulated in two separate ways in order to build confidence in design choices for target apogee. The team first simulated the flight using OpenRocket, as shown in Figure 78. The predicted apogee is 4921 ft. Because the ABS is predicted to be able to reduce the apogee of the launch vehicle by 500ft, this makes the target apogee of 4444 ft achievable.

The team also used a fourth order Runge-Kutta Method and the coefficient of drag estimated from CFD simulations and subscale tests to estimate the predicted flight profile. The results of this simulation are shown in Figure 79. As shown, the maximum and minimum predicted

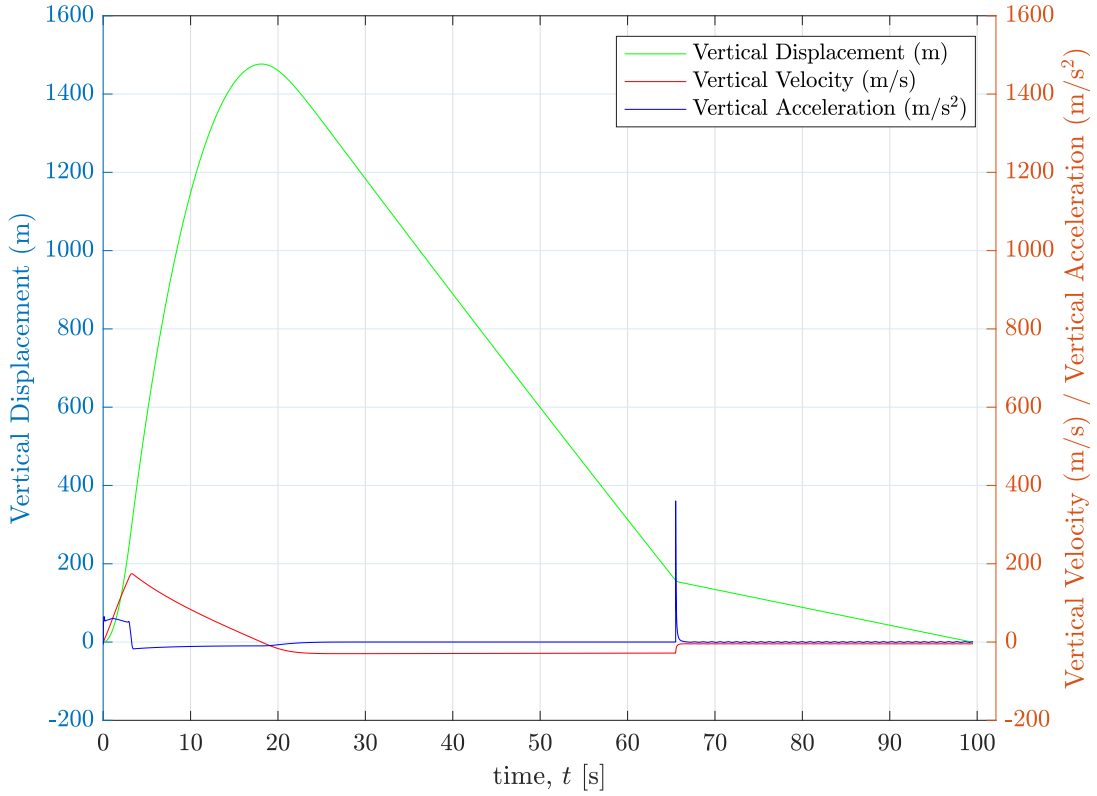

Figure 78: Launch Vehicle Flight Profile OpenRocket Simulation

apogees are 4940 ft and 4464 ft AGL respectively. Again, because the ABS is predicted to be able to reduce the apogee of the launch vehicle by 500 ft, this again confirms that the target apogee is achievable for any possible launch conditions.

3.9.2 Stability

According to NASA Requirement 2.14, the off rail static stability margin of the launch vehicle is required to be above 2.0. Additionally, Team Derived Requirement V.10 states that the static stability must be between 2 and 3 calibers in order to prevent an over stable launch vehicle that tilts into the wind. Two different methods were used to calculate the center of pressure in order to find the static stability margin. OpenRocket software predicted that the off-rail center of pressure was located 96.36 in from the tip of the nose cone. In addition to OpenRocket, the team used an Ansys Fluent simulation to estimate the center of pressure. The simulation relied on farfiled static boundary conditions, a continuity residual convergence criteria of 10^{-3}, 1000 iterations, and a Mach number of 0.045, which corresponds to the estimated off-rail velocity for the launch vehicle. The simulation yielded a center of pressure 94.16 in from the tip of the nose cone. The center of gravity was calculated to be 75.75 in from the nose cone with the motor and 69.93 in without it. A summary of the static stability parameters are shown in Table 30.

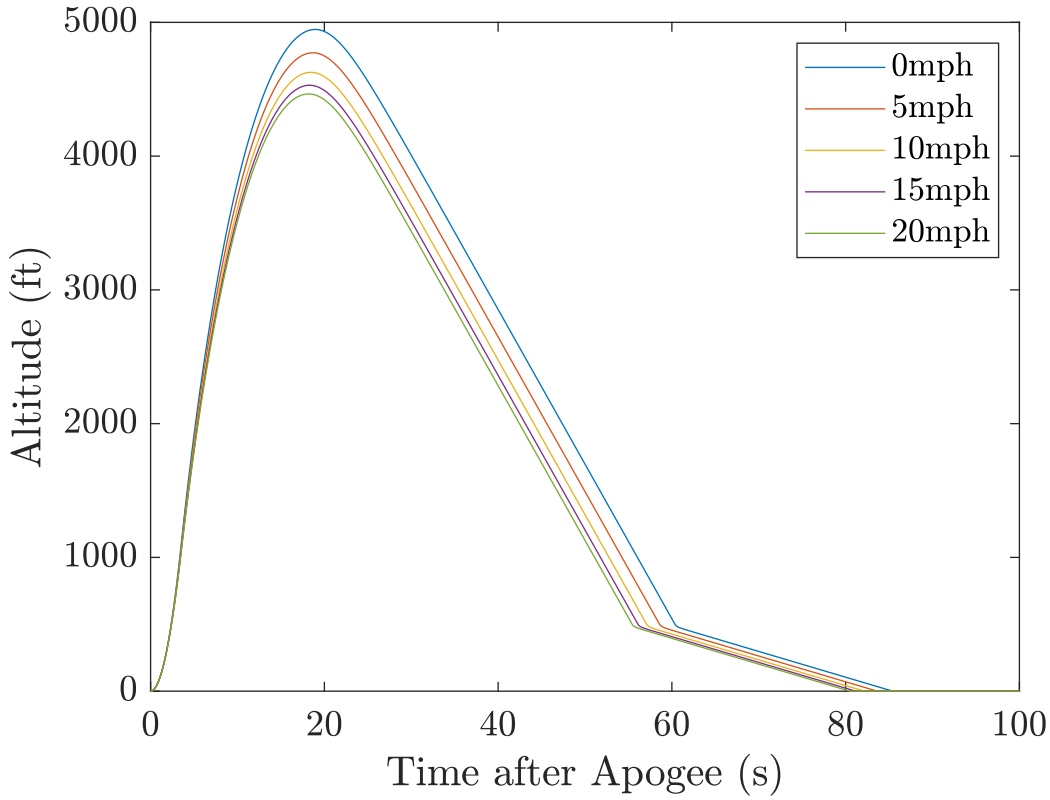

Figure 79: Runge-Kutta Flight Profile Simulation for various wind conditions

Table 30: Static Stability Margin Parameters

Method	Cp (in)	Cg (in)	Static Margin
OpenRocket	96.36	75.75	2.57
Ansys Fluent	94.16	75.75	2.30

As shown, the static stability margin is at a minimum of 2.3, well within the team derived requirements. However, the center of gravity and center of pressure shift over the course of the flight and so OpenRocket was used to verify that the launch vehicle remained stable over the course of the entire flight. A plot of the stability margin over the course of the predicted flight is shown in Figure 80.

The center of gravity is measured prior to all launches to ensure that the static margin is sufficient for a successful mission.

3.9.3 Main Parachute Opening Force

The drag forced induced on the vehicle by main parachute opening was modeled using a simple Euler's method. Using the terminal velocity of the rocket under the drogue parachute as an initial velocity, the instantaneous force induced by the main parachute was found using

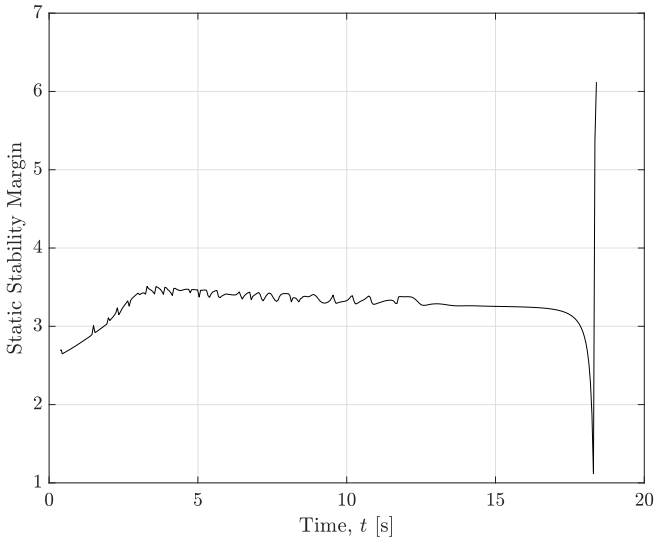

Figure 80: OpenRocket Stability Plot for predicted flight

the drag equation, described in Equation 28, using the parachute parameters provided by the manufacturer.

$$F_d = \frac{1}{2}\rho V^2 C_d A \tag{28}$$

F_d	Drag Force (lb_f)
ρ	Density of Air ($slugs/ft^3$)
V	Velocity (ft/s)
C_d	Parachute Coefficient of Drag
A	Parachute Area (ft^3)

The acceleration of the vehicle was then found using Newton's second law described in Equation 29, and the target dry mass of the vehicle.

$$a = \frac{F_d}{m} \tag{29}$$

F_d	Drag Force (lb_f)
a	Vehicle Acceleration (ft/s^2)
m	Vehicle Dry Mass (slugs)

The initial velocity of the vehicle for the next time step was then found using the calculated vehicle acceleration and the simulation time step, as described in Equation 30.

$$V_{next} = V_{current} + a * dt \tag{30}$$

V_{next}	Velocity of Next simulation step (ft/s)
$V_{current}$	Velocity of Current simulation step (ft/s)
a	Vehicle Acceleration (ft/s^2)
dt	Simulation Time Step (s)

The calculation was then repeated, using V_{next} as the initial velocity in calculating the drag force for the next time step. The simulation was carried out for a total of 0.15 seconds, using a time step of 0.0001 seconds. Figure 81 shows the main parachute drag force and vehicle acceleration, as a function of time, as calculated through this iterative method. The calculated maximum acceleration during parachute opening is 44.4 g. This method of force calculation is conservative, as it assumes that the parachute instantaneously changes from closed to open. In reality, the parachute will take time to open, which will reduce the peak drag forces and vehicle acceleration.

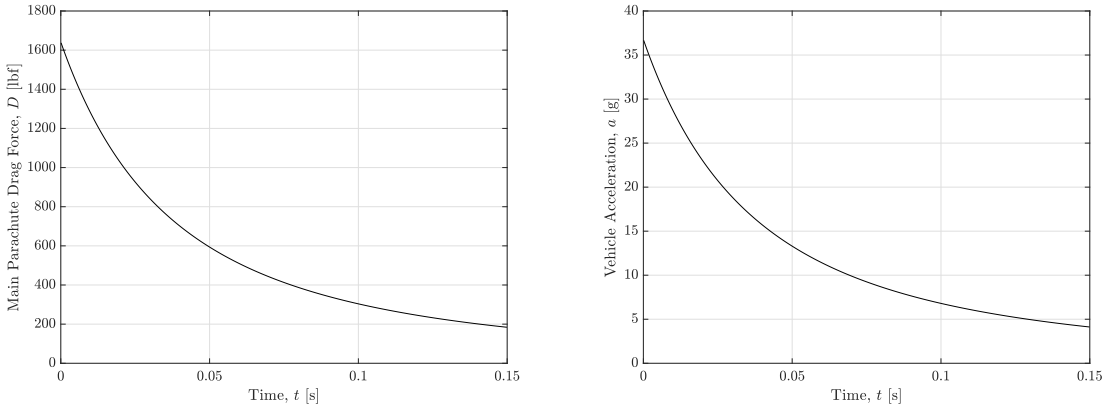

(a) Main Parachute Drag Force (b) Vehicle Acceleration

Figure 81: Vehicle Dynamics during Main Parachute Opening

From the results of this simulation, the peak forces on the various load bearing components of the vehicle were calculated. The quicklink that connects the main parachute to the recovery harness is expected to bear the full parachute drag forces. The load-bearing portion of the ABS is expected to bear the inertial forces induced in in the fin can, the CRAM body and bulkheads are loaded with the inertial forces induced in the recovery tube and avionics bay, and the payload bulkhead is loaded with the inertial forces of both the payload section and nosecone. Table 31 shows the expected loads and factors of safety of the load bearing components of the vehicle, during main parachute deployment.

Table 31: Main Parachute Load Summary

Component	Expected Peak Load (lbs)	FOS
Quicklink	1741	3.4
Shock Cord	1741	2.3
Eyebolts	757.5	4.1
ABS Bulkhead	452.0	11.9
CRAM Top Bulkhead	269.3	5.9
CRAM Bottom Bulkhead	269.3	4.0
CRAM Body	269.3	6.2
CRAM Adapter	269.3	20.6
Payload Section Bulkhead	677.7	3.7

3.9.4 Descent Rate and Kinetic Energy

To find an accurate measure of the kinetic energy the vehicle sections will have on landing, three calculations of the vehicle's descent rate were performed. The first is calculated using an OpenRocket simulation of the vehicle, at a variety of different launch angles and wind speeds. The highest descent rate the OpenRocket simulation recorded was at a launch angle of 10 degrees, with a 0 mph wind. The second calculation was made using the parachute manufacturer's descent rate calculator, and the third was performed using the terminal velocity equation, Equation 31, in a rudimentary MATLAB simulation. Table 32 shows a summary of the worst-case vehicle descent rates, as well as the worst-case section kinetic energy on landing.

$$V_t = \sqrt{\frac{2mg}{C_d A \rho}} \tag{31}$$

m	Vehicle Mass (slugs)
ρ	Density of Air (slugs/ft^3)
V_t	Vehicle Terminal Velocity (ft/s)
C_d	Parachute Coefficient of Drag
A	Parachute Area (ft^3)

All the different kinetic energy calculations are within 10 percent of each other, and all are at least 17 percent from the NASA designated maximium of 75 ft-lbs.

Table 32: Vehicle Descent and Kinetic Energy Summary

Simulation Method	Descent Rate (ft/s)	Kinetic Energy (ft-lbs)
OpenRocket Simulation	15.6	61.6
FruityChutes Calculator	15.22	58.7
MATLAB Simulation	15.0	57.1

3.9.5 Vehicle Descent Time

The time that the vehicle takes to descend from its apogee to the ground was calculated using the same calculation methods. The worst-case descent time predicted by the OpenRocket simulation was 85.7 seconds, using a launch angle of 0 degrees and a wind speed of 0 mph. The FruityChutes descent rate calculator predicts a descent time of 86.9 seconds, 47.4 seconds under the drogue parachute and 38.5 seconds under the main parachute. MATLAB simulations, using Equation 31 as a base, showed a vehicle descent time of 88.3 seconds. Table 33 shows a summary of the descent time calculations.

Table 33: Vehicle Descent Time Summary

Simulation Method	Descent Time (s)
OpenRocket Simulation	85.7
FruityChutes Calculator	86.9
Hand Calculation	88.3

3.9.6 Vehicle Drift

The total drift the rocket would experience was calculated using two different methods: an OpenRocket simulation and a team-developed 4th order Runge-Kutta simulation in MATLAB. In both simulations, the highest drift was recorded using a launch angle of 0 degrees and a wind speed of 20 mph. The OpenRocket simulation predicted a drift distance of 2226 ft. under those launch conditions, while the MATLAB simulation predicted a drift distance of 2184 ft., both under the 2500 ft. maximum drift designated by the handbook. Figure 82 shows the flight profile provided by the OpenRocket simulation at a variety of wind speeds, and a launch angle of 0 degrees.

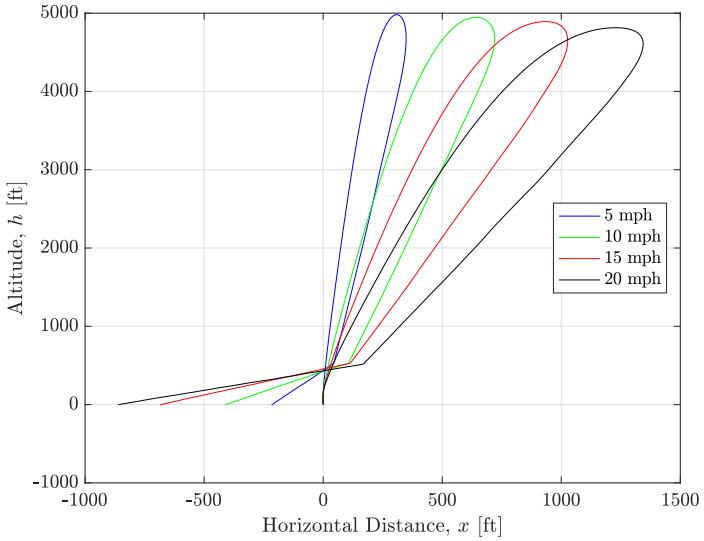

Figure 82: OpenRocekt simulated flight profile, at 0° launch angle and wind speeds of 5-20 mph.

4 Safety

4.1 Checklists

The team will make use of checklists on launch day to ensure that all components are properly assembled and prepared for flight. These checklists will be explicitly followed by all team members. Signatures will be used to ensure that necessary personnel have reviewed the checklist and verified that all steps have been completed in each list.

University of Notre Dame
NASA SLI Launch Checklist

General

Required Personnel

NAR Certified Launch Manager: Dave Brunsting
Safety Officer: Brooke Mumma
Team Captain and Vice Captains: Collette Gillaspie, Jed Cole, Eric Dollinger
Vehicles Lead: Estefy Castillo
ABS Lead: Ben Tompoles
Recovery Lead: Joe Sutton
LSRS Lead: Greg Bracht
A team member may fill in for one of these leads if approved by the Safety Officer.

Tools

- ☐ **1 hand drill, fully charged**
- ☐ **Drill bit case with standard range of bits**
- ☐ **Standard wrenches**
- ☐ **Standard Alan wrenches**
- ☐ **Screwdriver set**
- ☐ **Electrical tape**
- ☐ **Duct tape**
- ☐ **Masking tape**
- ☐ **Scissors**
- ☐ **2 folding tables**
- ☐ **Hot glue gun**
- ☐ **Garbage bags**
- ☐ **Rocket stands**
- ☐ **Rocketpoxy**
- ☐ **JB Weld**
- ☐ **Soldering iron**
- ☐ **Lead solder**
- ☐ **Digital multimeter**
- ☐ **Pens/pencils**
- ☐ **Exacto knives**
- ☐ **Metal files**
- ☐ **Assorted screws**
- ☐ **Wire cutters**
- ☐ **Wire strippers**
- ☐ **Bluntnose pliers**
- ☐ **Needlenose pliers**
- ☐ **Dial caliper**
- ☐ **Tape measure**
- ☐ **Sandpaper**
- ☐ **Epoxy applicators**

Personal Protective Equipment

- ☐ **Box of nitrile gloves**
- ☐ **Pair of cut resistant gloves**
- ☐ **Fire resistant battery bags**
- ☐ **First aid kit**
- ☐ **Dusk masks**
- ☐ **Pair of heat resistant gloves**
- ☐ **Safety glasses**
- ☐ **Leather gloves**

Vehicles

Vehicles Pre-Departure Checklist

Required Personnel: Vehicles Lead
Required PPE: None

Equipment

- ☐ **Nose cone**
- ☐ **Payload bay**
- ☐ **Transition Section**
- ☐ **Recovery Tube**
- ☐ **Fin can**
- ☐ **Shear pins**
- ☐ **Locking screws**
- ☐ **Motor (2)**
- ☐ **Motor Casing**
- ☐ **Motor Retainer**
- ☐ **Eyebolts**
- ☐ **Camera**
- ☐ **Washers**
- ☐ **Nuts**
- ☐ **Screws**
- ☐ **Motor retainer**

Inspection

⚠ **Failure to complete the following steps could result in an unidentified failure mode and thus a failed launch**

- ☐ Inspect each body tube for deformations or cracks to ensure there is no damage
- ☐ Check adhesives and connectors at each connection to make sure they are strong
- ☐ Inspect fins for any cracks or deformations

Vehicles Pre-Flight Checklist

Required Personnel: Vehicles Lead, Safety Officer, Launch Manager
Required PPE: Leather gloves, Heat resistant gloves, Safety glasses

⚠ **Failure to complete the following steps in order could result in an unidentified failure mode and thus a failed launch**

⚠ **Leather gloves should be used at any step where two components are connected in order to avoid pinch points**

- ☐ Recovery Integration (See Recovery Checklist)
  - ☐ Pack main parachute below the transition section. Ensure that the parachute is not packed so tightly that is cannot be pulled out
  - ☐ Pack drogue parachute above the fin can. Ensure that the parachute is not packed so tightly that is cannot be pulled out

- ☐ Ensure that all shock cords are attached and eye bolts are secured. **One end of the drogue shock cord should still be loose**
- ☐ Secure the recovery tube to the payload bay with shear pins

☐ ABS Integration

- ☐ Insert ABS into fincan by matching the notches to the internal dowel rod in the body tube
- ☐ The removable bulkhead at the top of the system is then secured using four button head screws.
- ☐ Inspect the drag tab cutouts in the fin can to ensure that the tabs are visible and have clearance to extend
- ☐ Place one 10 washer and lock nut on each of the threaded rods at the top of the forward ABS bulkhead to secure them to the fin can
- ☐ Inspect through the barometric vent holes to ensure that the LEDs are still lit and indicate the system is not prematurely in the launched state
- ☐ If the LEDs indicate a premature launched state, the system must be removed and reset.
- ☐ Make a final inspection of the system's installation for any obvious defects or abnormalities

☐ Attach loose end of drogue shock cord to the ABS top bulkhead eyebolt

☐ Secure fin can to recovery tube using shear pins

☐ Telemetry Integration

- ☐ Use twist to lock mechanism to screw telemetry system into nose cone
- ☐ Secure the lock by aligning the two eye bolts and tying them with Kevlar cord

☐ Payload Integration

- ☐ Slide sliding platform into slots on stationary platform
- ☐ Thread nuts and bolts through holes on platform

⚠**The next steps should ONLY be performed by the Launch Manager Dave Brunsting. Gloves and safety glasses should be worn.**

☐ Prepare nose cone ejection charge LM: _____

- ☐ Create one ejection charge using an e-match and black powder. Ensure that the e-match loose wires are shunted together to prevent accidental ignition of the black powder
- ☐ Re-check to ensure that the battery box switch is in the "off" position
- ☐ Connect the loose ejection charge wire to its corresponding lever wire
- ☐ Place the ejection charge in its corresponding PVC charge well
- ☐ Cover each charge well with painters tape to keep the charge in place

- ☐ Ensure all wire holes are plugged with sealing clay

⚠This concludes the steps that must be performed by the Launch Manager

- ☐ Press fit nose cone between the sliding bulkhead and the inner diameter of the payload bay body tube. Be careful to align the shear pin holes.
- ☐ Place shear pins in holes

☐ Flight Camera Integration

- ☐ Insert the MicroSD card into the back of the camera
- ☐ Press power button
- ☐ Wait for steady yellow light from camera
- ☐ Press the recording button (button with the camera symbol).
- ☐ If camera is flashing yellow, then the camera is recording
- ☐ Insert the camera into the transition section slot so that the lens is facing downward
- ☐ On the edge closest to the lens, place three small washers and loosely fit a lock nut onto the tie rod
- ☐ On the edge further from the lens, place the medium washer and then two small washers and loosely fit the lock nut on the tie rod
- ☐ If the camera does not fit, or has too much space to move, repeat previous four steps
- ☐ If a proper fit is achieved, tighten the lock nuts with crescent wrench
- ☐ Perform shake test of assembly to ensure secure connection

⚠The next steps should ONLY be performed by the Launch Manager Dave Brunsting. Gloves and safety glasses should be worn.

☐ **Motor Assembly** LM: _____

- ☐ Remove the motor from its packaging
- ☐ Check that the motor is properly assembled according to manufacturer's instructions and inspect the motor for defects
- ☐ Insert the propellant into the casing, ensuring that the two spacers precede the propellant
- ☐ Screw on the rear closure
- ☐ Insert the motor into the rocket, ensuring proper motor direction
- ☐ Attach the motor retainer
- ☐ Check for a secure fit

⚠This concludes the steps that must be performed by the Launch Manager

⚠The Cg and stability check should be performed by the Vehicles lead

☐ Center of gravity and stability check VL: _____

- ☐ Perform center of gravity (Cg) test to ensure the center of gravity matches the simulated Cg by placing the fully assembled vehicle on a thin wooden stand so that it is cantilevered on both sides. Move the vehicle until it perfectly balances.
- ☐ Mark the measured Cg and simulated Cg on the vehicle
- ☐ Mark the simulated center of pressure (Cp) on the vehicle
- ☐ Ensure calculated stability corresponds to predicted value
- ☐ Ballast as necessary to maintain a stability margin of >2 calipers or within 10% of predicted margin (whichever is greater)

☐ **Vehicle Setup and Launch Pad Preparation**

- ☐ Register with LCO and RSO at the launch site
- ☐ Lower the launch rail such that it is parallel to the ground
- ☐ Align the rail buttons with the rail and slide the vehicle onto the rail with the fin can towards the ground
- ☐ Set rail angle to be perpendicular to the ground with an added maximum 7 degrees into the wind Allow payload and subsystem teams to activate systems

⚠ **The next steps should ONLY be performed by the Launch Manager Dave Brunsting. Heat resistant gloves and safety glasses should be worn.**

☐ **Igniter Installation** LM: _____

- ☐ Clear all personnel except for the Launch Manager
- ☐ Check that the ignition wires, connected to the launch control system, do not have a live voltage across them. This can be done by lightly touching the clips to each other while away from the vehicle, watching for sparks. If no sparks are thrown it is safe to proceed.
- ☐ Remove the igniter clips from the igniter
- ☐ Ensure that the igniter has properly exposed ends which are split apart
- ☐ Insert the igniter into the motor
- ☐ Attach the clips to the igniter, ensuring good contact
- ☐ Clear the launch are of all personnel and maintain the distance as designated by the RSO in accordance with NAR/TRA regulations
- ☐ If motor does not ignite when planned, wait for RSO instruction to approach

Vehicles Post-Flight Checklist

Required Personnel: Vehicles Lead, Safety Officer, Launch Manager
Required PPE: Heat resistant gloves

⚠ **Team members should wait for RSO approval to approach vehicle and enter the launch field**

⚠**After landing the motor still may be hot or batteries could catch fire. It is important to assess the landed components carefully**

- ☐ Assess the landing site and vehicle for potential hazards such as fire or smoke
- ☐ Examine recovery and payload sections for unexploded black powder charges, if any are found, see troubleshooting procedures
- ☐ Document state of vehicle with photographs before moving any part
- ☐ Disconnect quick links where possible to transport the vehicle

⚠**The next step should ONLY be performed by the Launch Manager Dave Brunsting. Heat resistant should be worn.**

- ☐ Motor Removal LM: _____
  - ☐ Remove the motor retainer from the vehicle
- ☐ Ensure that each subsystem completes their Post-Flight Checklist

I certify and attest that the above checklists have been fully and properly completed

Safety Officer: _____ Date: _____

Air Braking System (ABS)

ABS Pre-Departure Checklist

Required Personnel: ABS Lead
Required PPE: Fire proof battery case

Equipment

- ☐ **Assembled ABS**
- ☐ **Assembled ABS electronics**
- ☐ **ABS electronics toolbox**
- ☐ **Fire-proof battery case**
- ☐ **Fully charged batteries**
- ☐ **6-32 nylon screws**
- ☐ **10-32 nylon screws**
- ☐ **6-32 nylon lock nuts**
- ☐ **10-32 nylon lock nuts**
- ☐ **Tenergy LiPo charger**

Inspection

⚠ **Failure to complete the following steps could result in an unidentified failure mode and thus a failed launch**

- ☐ Inspect ABS for material defects. After ensuring battery is disconnected, inspect the mechanical system for loose screws and bent components, particularly the drag tabs
- ☐ With the battery disconnected from the circuit board, inspect electronics for secure connections and mounting
- ☐ Verify batteries are fully charged based on LED status of Tenergy LiPo charger
- ☐ Ensure the proper control code has been installed on the Raspberry Pi

ABS Pre-Flight Checklist

Required Personnel: ABS Lead, Safety Officer
Required PPE: Fire proof battery case

⚠ **Failure to complete the following steps in order could result in an unidentified failure mode and thus a failed launch**

⚠ **LiPo batteries are a potential fire risk and should always be inspected for swelling to punctures before use. When not in use batteries should be housed in the fire proof battery case.**

- ☐ For both batteries, install the battery and ensure the snap cover battery case cover is secured
- ☐ Ensure the SD card is inserted in the Raspberry Pi prior to powering the system
- ☐ Connect the battery's molex connector to the circuit board and flip the power switch

- ☐ Confirm that the power-LED has lit
- ☐ Inspect the status LEDs for the sensors and SD card to ensure the Raspberry Pi controller is properly receiving sensor data and writing to the SD card
- ☐ In the event that these lights do not turn on, notify the ABS lead immediately
- ☐ If ABS is to be active for this flight, turn on the arming switch. Ensure the arming LED turns on
- ☐ Check that the drag tabs are flush with the support plates

ABS Post-Flight Checklist

Required Personnel: ABS Lead, Safety Officer
Required PPE: Fire proof battery case

⚠ **Team members should wait for RSO approval to approach vehicle and enter the launch field**

⚠ **After landing the motor still may be hot or batteries could catch fire. It is important to assess the landed components carefully**

- ☐ Use a screwdriver to unscrew the button head screws from the forward bulkhead of the ABS.
- ☐ Check that the drag tabs are fully retracted to avoid jamming the ABS in the fin can while removing.
- ☐ Carefully remove the ABS from the fin can by lifting with the Recovery system eyebolt at the forward bulkhead of the ABS
- ☐ Inspect the avionics system for power and status LED indication to determine if power was lost during flight or landing
- ☐ Flip the power switch to turn off the system
- ☐ Inspect the batteries for damage. If damaged, place in the fire-proof battery case for safe storage
- ☐ Inspect and note any damage to the mechanical system or payload assembly
- ☐ Remove the micro SD card form the Raspberry Pi
- ☐ Insert the micro SD card into the SD card adapter and plug into a laptop. Open the data log file on the SD card and verify successful flight metrics

I certify and attest that the above checklists have been fully and properly completed

Safety Officer: _____ Date: _____

Recovery

Recovery Pre-Departure Checklist

Required Personnel: Recovery Lead, Vice Captain, Safety Officer
Required PPE: Fire proof battery case, nitrile gloves, safety glasses

Equipment

- ☐ **CRAM body**
- ☐ **CRAM core, both pieces**
- ☐ **CRAM core pins**
- ☐ **Raven3 altimeters (2)**
- ☐ **Stratologger SL100 Altimeter**
- ☐ **Fully Charged 3.7v, 170 mah Batteries (3)**
- ☐ **Assembled altimeter wiring perfboards**
- ☐ **CRAM top bulkhead**
- ☐ **CRAM bottom bulkhead**
- ☐ **4 in, 1/4-20 Grade 8 bolts (3)**
- ☐ **1/4-20 hex nuts (3)**
- ☐ **1/4 in washers (6)**
- ☐ **3/8 in washers (2)**
- ☐ **3/8 in split lock washers (2)**
- ☐ **Lever nut wire connectors (6)**
- ☐ **E-matches (6)**
- ☐ **Black powder (mentor, 19.5g)**
- ☐ **3/8 in Eyebolts (2)**
- ☐ **3/8 in Quick links (6)**
- ☐ **Slider Ring**
- ☐ **1 in Nylon shock cord (35 ft, x2)**
- ☐ **Main parachute (10 ft)**
- ☐ **Drogue parachute (2 ft)**
- ☐ **Pilot Chute (2 ft)**
- ☐ **Main Parachute Deployment Bag**
- ☐ **24 in Nomex blanket (2)**
- ☐ **Laptop with Featherweight Interface Program and Perfectflite DataCap installed**
- ☐ **Data cable for Raven altimeters**
- ☐ **Data cable for Stratologger altimeter**
- ☐ **Fire-retardant cellulose wadding**
- ☐ **Talcum powder**
- ☐ **Sealing clay**
- ☐ **Telemetry Housing Assembly**
- ☐ **Telemetry Vehicle Electronics**
- ☐ **Telemetry Relay Station**
- ☐ **Telemetry Ground Station**
- ☐ **1/8 in kevlar chord**

Inspection

⚠ **Failure to complete the following steps could result in an unidentified failure mode and thus a failed launch.**

- ☐ Inspect main parachute bulkhead (in transition section of vehicle) for fatigue or failure in bulkhead and epoxied seal.
- ☐ Lay out the shock cord and tie knots in the locations where the drogue and main parachutes will be attached to mark their locations.
- ☐ Ensure that the ends of the main shock cord have loops to accept quick links. Check for

holes or wear.

- ☐ Check the LiPo batteries to ensure a full charge.
- ☐ Connect each altimeter to a battery through the mounted screw terminals and connect the altimeter to a laptop through the data cable. Check the programming of the altimeters to confirm proper deployment programming.
- ☐ Ensure that 6 lever nut wire connections are properly epoxied to the upper CRAM bulkhead

Recovery Pre-Flight Checklist

Required Personnel: Recovery Lead, Vice Captain (Jed Cole), Safety Officer, Launch Manager
Required PPE: Fire proof battery case, safety glasses

⚠ **Failure to complete the following steps in order could result in an unidentified failure mode and thus a failed launch**

⚠ **LiPo batteries are a potential fire risk and should always be inspected for swelling to punctures before use. When not in use batteries should be housed in the fire proof battery case.**

- ☐ Telemetry Activation and Uplink
  - ☐ Insert SD card into telemetry vehicle system
  - ☐ Connect power to telemetry vehicle system
  - ☐ Turn on telemetry relay system
  - ☐ Connect power to telemetry ground station
  - ☐ Activate uplink between telemetry vehicle system and relay station
  - ☐ Activate uplink between relay station and ground station
  - ☐ Ensure that ground station is properly receiving data package
  - ☐ Place relay station approximately 2500 ft away from pad
- ☐ Main Parachute Folding
  - ☐ Suspend the parachute by its shroud lines, shaking the parachute lightly to untangle the cords.
  - ☐ Line all of then shroud lines up such that they are the same length. Tape the shroud lines at this position to make folding easier. MAKE SURE TO UNTAPE THE PARACHUTE SHROUD LINES PRIOR TO INSTALLATION IN THE VEHICLE.
  - ☐ Flatten out the canopy of the parachute, such that there are an even number of gores on either side of the centerline, where the shroud lines are. Ensure all of the gores are flat, folded in an accordion-like fashion.
  - ☐ Fold both sides of the parachute inwards toward the center line, forming a rectangular parachute shape.

- ☐ Feed the slider ring up from the parachute bridle all the way to the beginning of the canopy.
- ☐ Quicklink the crown of the parachute to the deployement bag tether.
- ☐ Z-fold the deployment bag tether and insert it in the bag, pushing it all the way to the top.
- ☐ Push the canopy of the parachute into the open deployment bag, starting with the top and working down the folded canopy.
- ☐ Z-fold and lace the shroud lines of the parachute along the straps mounted to the outside of the deployment bag. Ensure that the shroud lines are capable of easily pulling out of the straps.
- ☐ Untape the shroud lines.
- ☐ Quicklink the pilot chute to the deployment bag.
- ☐ Add a quicklink to the main parachute bridle.

☐ Drogue and Pilot Chute Folding

- ☐ Suspend the parachute by its shroud lines, shaking the parachute lightly to untangle the cords.
- ☐ Line all of then shroud lines up such that they are the same length.
- ☐ Flatten out the canopy of the parachute, such that there are an even number of gores on either side of the centerline, where the shroud lines are. Ensure all of the gores are flat, folded in an accordion-like fashion.
- ☐ Fold one side of the parachute towards the other, forming a flat triangle with shroud lines protruding from one corner.
- ☐ Fold the parachute shroud lines upwards into the middle of the triangle, with the parachute bride sticking out the bottom.
- ☐ Fold the parachute in half longways, then Z-fold it.
- ☐ Attach a quicklink to the parachute bridle and loosely wrap in Nomex blanket.

☐ CRAM Assembly

- ☐ Check to ensure all of the solder joints on the altimeter perfboards are solid, and that the board is securely screwed to the CRAM core.
- ☐ Secure each the altimeter to its respective perfboard with screws and ellectrically connect it using the on-board screw terminals.
- ☐ Plug each altimeter battery into its respective JST port on the perfboard.
- ☐ Place the CRAM core in the CRAM body.
- ☐ Four wires protrude from each perfboard, two upwards and two downwards. Feed the upward-facing wires through the CRAM top bulkhead and the bottom-facing wires through the CRAM bottom bulkhead. Connect them to the Wago lever nuts on the

oustide face of the bulkheads.

- ☐ Bolt the bulkheads onto the CRAM body.

⚠The next steps should ONLY be performed by the Launch Manager Dave Brunsting. Gloves and safety glasses should be worn.

- ☐ Ejection charges LM: _____
  - ☐ Create six ejection charges using e-matches and black powder. Ensure that the e-match loose wires are shunted together to prevent accidental ignition of the black powder.
  - ☐ Re-check to ensure that the recovery activation switches are all in the "off" position
  - ☐ Connect each loose ejection charge wire to its corresponding lever wire connector.
  - ☐ Place each ejection charge in its corresponding PVC charge well, covering the full well with painter's tape.
  - ☐ Ensure all wire holes in the CRAM upper bulkhead are plugged with sealing clay.

⚠This concludes the steps that must be performed by the Launch Manager

- ☐ CRAM Integration Preparation
  - ☐ Thread the eyebolts into place on either side of the CRAM.
  - ☐ Twist the CRAM into place in its adapter in the recovery tube.
  - ☐ Ensure that the switch ports and air holes in the CRAM are visible from the holes in the airframe.
  - ☐ Screw the CRAM in place from the outside to keep it from rotating.
- ☐ Parachute Installation
  - ☐ Ensure that all both the parachutes are properly connected to the shock cords and enclosed in the Nomex parachute protectors
  - ☐ Connect the fore end of the shock cords to the prepared eyebolts in the recovery tube, fin can, and transition section using quicklinks.
  - ☐ Fold the excess shock cord together in an accordion fashion and loosely tape it together with a single layer of painters tape.
  - ☐ Place several handfuls of cellulose recovery wadding in the recovery tube near the top of the CRAM
  - ☐ Lightly coat the outside of the main and drogue parachutes with talcum powder
- ☐ Arming the System
  - ☐ Use a magnet to activate the magnetic switches on all three altimeters
  - ☐ Listen for each altimeter's starting sequence.
  - ☐ Use a screwdriver to switch each altimeter's second switch.
  - ☐ Listen to the continuity beeps of the altimeters to confirm both main and drogue charges are active for all three altimeters.

Recovery Post-Flight Checklist

Required Personnel: Recovery Lead, Vice Captain, Safety Officer, Launch Manager
Required PPE: Fire proof battery case

⚠**After landing the ejection charges may not have detonated or batteries could catch fire. It is important to assess the landed components carefully**

- ☐ Before touching the rocket, take pictures in landed state, paying specific attention to the positions of the shock cord and parachutes
- ☐ Ensure all three ejection charges have properly fired
- ☐ Bring launch vehicle back to staging table and remove the CRAM. Turn off all but the main altimeter and invert the CRAM
- ☐ Listen to and record the altitude provided by the Raven altimeter
- ☐ Inspect the parachutes, chute releases, shock cords, CRAM, bulkheads, connectors, and launch vehicle for any damage sustained during the flight

I certify and attest that the above checklists have been fully and properly completed

Safety Officer: _____ Date: _____

LSRS

LSRS Pre-Departure Checklist

Required Personnel: LSRS Lead
Required PPE: Fire proof LiPo Bag, Nitrile Gloves, Safety Glasses

Equipment

- ☐ **2 1/8 inch kevlar chord**
- ☐ **Fore Bulkhead**
- ☐ **Stratologger SL100 Altimeter**
- ☐ **Fully Charged 3.7v, 170 mAh Battery**
- ☐ **Stationary Platform**
- ☐ **Sliding Platform**
- ☐ **UAV Sled**
- ☐ **Platform nut and bolt (2)**
- ☐ **Solenoid (4)**
- ☐ **Stability Rod and Stopper**
- ☐ **Orientation Bearing**
- ☐ **Aft Bulkhead nut and bolt**
- ☐ **Fully charged 1800 mAh, 11.1 V Battery (2)**
- ☐ **Fully assembled Rover**
- ☐ **Fully assembled UAV**
- ☐ **Fully charged 5000 mAh, 11.1 V Battery**
- ☐ **Fully assembled Sample Retrieval System**

Inspection

⚠ **Failure to complete the following steps could result in an unidentified failure mode and thus a failed launch**

⚠ **LiPo batteries are a potential fire risk and should always be inspected for swelling to punctures before use. When not in use batteries should be housed in the fire proof battery case.**

- ☐ Ensure that all batteries are fully charged for all systems
- ☐ Check wiring connections on UAV, Rover, and ROD to ensure that all electronics are secure
- ☐ Check UAV, Rover, and ROD ASA plastic components for cracks or defects
- ☐ Ensure that bearing is able to rotate freely when solenoids are not in place
- ☐ Ensure solenoids fully extend

LSRS Pre-Flight Checklist

Required Personnel: LSRS Lead, Safety Officer, Launch Manager
Required PPE: Fire proof battery case, nitrile gloves, safety glasses

⚠ **Failure to complete the following steps in order could result in an unidentified failure mode and thus a failed launch**

⚠**LiPo batteries are a potential fire risk and should always be inspected for swelling to punctures before use. When not in use batteries should be housed in the fire proof battery case.**

- ☐ UAV Activation
  - ☐ Connect power to UAV System
  - ☐ Ensure connection with Ground Station via the LED
  - ☐ Ensure UAV is in low power mode via LED
- ☐ Rover Activation
  - ☐ Connect power to Rover System
  - ☐ Ensure connection with Ground Station via LED
  - ☐ Ensure Rover is in low power mode via LED
  - ☐ Ensure proper sample retrieval system connection via LED
- ☐ Placement into Payload Bay
  - ☐ Properly slide UAV into UAV Sled
  - ☐ Place UAV Sled on platform such that pins go through UAV Struts
  - ☐ Ensure solenoid pins are inserted into UAV sled by sending a signal to the system
  - ☐ Place Rover body onto platform and insert solenoid pins by sending a signal to the system
- ☐ Retention Activation
  - ☐ Connect ROD system to Rover using detachable cables
  - ☐ Ensure communication with rover via LED on deployment

LSRS Post-Flight Checklist

Required Personnel: LSRS Lead, Safety Officer
Required PPE: Fire proof battery case

⚠**After landing the ejection charges may not have detonated or batteries could catch fire. It is important to assess the landed components carefully**

- ☐ Ensure nose cone charge has proerly fired
- ☐ Document state of LSRS with photographs
- ☐ Make any notes regarding mission success/failure
- ☐ Inspect batteries for any damage
- ☐ Inspect all systems for any damage
- ☐ Empty sample retrieval system

- ☐ Turn off the ROD solenoids, UAV, and rover
- ☐ Properly store LiPo batteries

vspace5 pt I certify and attest that the above checklists have been fully and properly completed

Safety Officer: _____ Date: _____

Troubleshooting Checklist

Altimeter Issue on the Launch Pad

The Raven altimeter performs a continuity check before flight to ensure that all ejection charges are properly connected. Should the altimeter fail this check on the launch pad, the altimeters may need to be removed and examined.

⚠**Ensure that the battery box switches are in the "off" position. Failure to turn off the altimeters could result in unintentional black powder ignition.**

- ☐ Take the rocket off of the launch pad and back to the preparation table.
- ☐ Remove the shear pins from the rocket and separate the sections.
- ☐ Remove the parachute, Nomex protector and shock cords from the rocket.
- ☐ Separate the fin can and recovery tube
- ☐ Unbolt the CRAM from the aft recovery bulkhead.
- ☐ Slide the CRAM out of the rocket.

⚠**Recheck to ensure that the battery box switches are in the "off" position. Failure to do so could result in unintentional black powder ignition.**

- ☐ Disconnect the black powder charges from the lever nut wire connections.
- ☐ Unbolt and remove the CRAM upper bulkhead and filler.
- ☐ Remove the CRAM core and examine the altimeter wire connections for defects. If none are detected, plug the Raven altimeters into a computer for diagnostics. Consult the user's manual for more information.

Tight Fitting Parachute

If the folded parachute is too tight inside the parachute bay, it may not slide out upon separation, which will result in the vehicle descending much faster than normal.

⚠**DO NOT attempt to force the parachute into the bay. This can prevent clean separation at apogee and potentially damage the rocket or parachute.**

- ☐ Remove the parachute from the vehicle
- ☐ Unfold the parachute and refold according to the procedure outlined in the Recovery Checklist.
- ☐ Ensure that all folds are crisp and that the finished parachute is very tightly rolled.
- ☐ Reattach the chute releases. Ensure that the chute releases are turned on.
- ☐ Re-wrap the parachute in Nomex.
- ☐ Proceed to re-install the parachute in the rocket using the procedure outlined in the

Recovery Checklist. A layer of talcum powder on the parachute and coupler may also help the parachute to slide out.

Ignition failure

Occasionally, a rocket motor will fail to ignite on the pad. This can be caused by numerous issues, such as faulty igniters, incorrect installation, faulty launch equipment, and damaged motor.

- ☐ After a failed ignition, the LCO of a launch range will typically attempt another ignition. If this fails, proceed to the next step.

⚠The remaining steps should only be performed by the Launch Manager.

- ☐ Disconnect the igniter from the ignition clips.
- ☐ Carefully remove the igniter from the motor.
- ☐ Install another igniter, paying careful attention to standard procedure, and attempt another ignition.
- ☐ If this ignition fails, take the rocket off the pad, take the motor out and inspect it for damage or incorrect assembly.
- ☐ If the motor appears in good condition and properly assembled, inspect the launch system to ensure that it is properly set up, in good condition, and has a charged battery. The range LCO should perform this inspection.
- ☐ Put the rocket back on the pad and attempt another ignition with a fresh igniter. If this fails, consult the Launch Manager for further troubleshooting.

Removing Black Powder Charges

In the unlikely event that a black powder charge remains intact during descent, the charge must be removed before regular post-launch procedures can commence.

⚠Ensure that all altimeters are fully powered off by flipping the switches on the attached battery boxes into the "off" position. Failure to do so could result in an unintentional ignition.

⚠These next steps should only be performed by the Launch Manager.

- ☐ Separate the fin can and recovery tube
- ☐ Unbolt the CRAM from the aft recovery bulkhead.
- ☐ Remove the CRAM from the body tube.

⚠Re-check to ensure that the battery box switches are in the "off" position.

- ☐ Unhook the black powder charges from the level nut wire connections. Remove the charges from the charge wells.

☐ Dispose of the charges through University Hazardous Waste procedures.

Punctured or damaged battery

Extremely dangerous, if believed to be damaged at all, battery should not be used AT ALL. While the team is still at the launch site, the battery should be housed in a fire proof battery case. The battery should then be disposed of according to University Standards upon return.

⚠PPE required are heat resistant gloves and safety glasses

☐ If battery is believed to be damaged, approach with caution, as it should be considered an exploding hazard. PPE must be worn when handling the defective battery.

☐ Battery should be handled with care, and held away from face and body.

☐ Place battery in fireproof battery disposal bag

☐ Bring battery to qualified and authorized disposal site

4.2 Safety Analysis

Hazards are evaluated at a level of risk based on their severity and probability of occurrence. Risks will be evaluated at each subsystem level as well as the project management level. The Systems and Safety team will continue to re-evaluate the risks, mitigations, and verifications as the project continues. Probability of occurrence will be evaluated and designated with values 1 through 5, with 5 being that the event in question is almost certain to happen under present conditions, and 1 being that it is improbable the event occur. The criteria for this scoring is outlines in Table 34 below.

Table 34: Probability of hazard occurrence classification

Description	Value	Criteria
Improbable	1	Less than 5% chance that the event will occur
Unlikely	2	Between 5% and 20% chance that the event will occur
Moderate	3	Between 20% and 50% chance that the event will occur
Likely	4	Between 50% and 90% chance that the event will occur
Unavoidable	5	More than 90% chance that the event will occur

As mentioned, this probability is evaluated according to present conditions, meaning two assumptions were made. The first is that if the conditions change, the probability will be re-evaluated and changed accordingly. The second assumption is that all personnel involved in the activity will have undergone proper training and clearly acknowledged understanding of the rules and regulations outlined in safety documentation. This may include, but is not limited to, the safety manual, compiled SDS document, FMEA tables, most recent design review, and lab manual if applicable. The evaluation of occurrence probability will also assume that proper PPE was used, all outlined procedures were correctly followed, and all equipment was inspected before use. Severity of the incident is evaluated on a scale of 1 through 4, where 4 is that the incident will prove catastrophic, and 1 is that the incident will prove negligible. Severity is evaluated according to the incident's impact on personal health and well-being, impact on mission success, and the environment. The score shall be based off of whatever the worst case scenario for the types of impacts being considered. These considerations will be re-evaluated anytime new hazards are identified. The criteria used to evaluate severity of each hazard is outlined are Table 35.

Table 35: Severity of hazard classification

Description	Value	Criteria
Negligible	1	Could result in insignificant injuries, partial failure of systems not critical to mission completion, project timeline or outcome possibly affected and might require corrective action, or minor environmental effects.
Marginal	2	Could result in minor injuries, complete failure of systems not critical to mission completion, project timeline or outcome affected and requires corrective action, or moderate environmental .
Critical	3	Could result in severe injuries, partial mission failure, severe impact to project requiring significant and immediate corrective action for project continuity, or severe and reversible environmental effects.
Catastrophic	4	Could result in death, total mission failure, complete failure of project rendering project unable to continue, or severe and irreversible environmental effects.

By combining the severity and probability values, a risk score will be assigned to each hazard. Risk scores will have a value from 1 to 20 where is lowest risk and 20 is the highest risk. Risk levels can be reduced through mitigating actions which will lower either the severity score or the probability score. Actions will be taken starting with the highest risk level hazards, and will continue through the lower levels until all hazards have been reduced as much as possible. All hazards pose a risk and will not be ignored, but the classifications help the Safety officer prioritize resources to those that require the most immediate attention. Mitigations can take the form of design considerations to reduce severity or probability of failure, verification systems created to ensure proper operating conditions, and better handling procedures to follow. Risk scores and the risk levels that correspond with each score are outlined in the risk assessment matrix shown in Table 36, and the description of each risk level is listed in Table 37.

Table 36: Risk Assessment Matrix

Probability Level	Severity Level			
	Negligible (1)	Marginal (2)	Critical (3)	Catastrophic (4)
Improbable (1)	1	2	3	4
Unlikely (2)	2	4	6	8
Moderate (3)	3	6	9	12
Likely (4)	4	8	12	16
Unavoidable (5)	5	10	15	20

Table 37: Description of Risk Levels and Management Approval

Risk Level	Acceptable Level/Approving Authority
High Risk	Highly Undesirable. Must be approved by Team Captain, Safety Officer, and supervising squad lead.
Medium Risk	Undesirable. Must be approved by Safety Officer and supervising squad lead.
Low Risk	Acceptable. Must be approved by supervising squad lead or Safety Officer.

In order to properly assess the risks facing the mission, key areas for assessment were identified: project risks, personnel hazards, failure modes and effects, and environmental concerns. Each one of these areas was then broken down further into more specific categories of interest and analyzed in the same manner. Each risk is assigned a risk value prior to mitigations and then a risk value after mitigations are in place.

4.2.1 Project Risk Analysis

Table 38: Project Risk Analysis

Hazard	Cause	Outcome	Probability	Severity	Mitigations	Verification
Complete destruction or loss of full scale or subscale vehicle	1. Uncontrolled descent 2. Energetics improperly contained	Team must build an entirely new vehicle causing project delays and doubling the costs of the project	Medium	High	1. All components will be tested individually prior to full-scale assembly 2. Construction procedures will be written prior to construction	1. Tests will be logged and documented; multiple sources (calculations, simulations) and trials will be used to verify the results 2. Construction procedures will be available prior to construction
Failure to conduct subscale launch by January 10th full scale launch by March 2nd	1. Weather conditions 2. Construction is incomplete 3. Failure to find a date that works with both the team and mentor	Inability to participate in competition	Medium	High	1. Multiple dates will be chosen for a possible launch 2. The team will implement a Technology Readiness Level schedule to ensure that all the subsystems are meeting each deadline 3. The team will push to meet the first available date for launch	1. The team has chosen February 1st, 15th, and 22nd in order to meet the demonstration flight deadline 2. The team has a chart to track the individual subsystems TRLs in order to identify any issues with meeting deadlines 3. The team will begin full scale construction two weeks prior to the first available launch date
Lack of funds/exceeding budget	1. Allocation of funds to a subsystem is insufficient 2. Parts are not properly sourced	Team takes on debt or funds from travel or other subsystems diminish	Medium	High	1. The allocation of funds are based off of previous years' spending and design. 2. Parts will be sourced to find the best quality at the lowest cost. Each part should be considered from at least three vendors if possible.	1. This years' budget has been set in Section 6.3 according to previous need and consultation with each design lead 2. Team members must submit their receipts and add to the budget to ensure they are tracking their spending
Delay in receiving parts/issues with vendors	1. Parts (especially custom) ordered have an anticipated arrival date that will not work with the team deadlines 2. The part shipped by a vendor is incorrect or does not meet the needs of the team	Project delays and/or mission failure	Medium	High	1. Custom parts will be ordered early in order to avoid project delays and if they are critical the team will order an additional component in the case one is damaged 2. NDRT has compiled a trusted vendor list to ensure quality of parts	1. Any custom parts will be ordered at least three weeks in advance of the start of construction and the design lead will determine whether or not multiples should be ordered 2. All team members ordering parts will consult the trusted vendor document

Team member leaves team	1. Injury or illness 2. Member has other commitments	Project delays and/or incomplete work	Medium	Medium	All tasks on the team will have multiple members assigned or at least multiple members aware of the details of the task	All designs and tests will be well documented in case someone should have to take over
Safety violations	1. Insufficient PPE 2. Insufficient training	Injury to personnel and the potential for the workshop space to be revoked	Medium	High	1. PPE will always be stocked in the workshop and a part of the Systems & Safety budget 2. All personnel that will be participating in construction must be certified in the Student Fabrication Lab according to university regulations	1. The Safety Officer will check for PPE in the workshop prior to all construction; the Safety Officer will be notified when certain PPE items are almost out of stock. 2. Students must show their certification card before entering the workshop during construction
Insufficient materials	Parts to complete the project are not ordered	Project delays	Medium	Medium	Personnel will make an itemized list of parts in their designs	Construction procedures will provide a good check to make sure all the parts need for fabrication are ordered
Violation of FAA by exceeding approved altitude	Launch site does not have proper waiver for the team's altitude requirement	Potential legal action	Low	High	The team will not use any launch sites without the proper waiver	The NDRT leadership will confirm with prospective launch sites that they have the proper waiver for NDRT's selected altitude.
Improper testing equipment	1. Test equipment is faulty 2. Inability to use University resources for more complex testing	Incorrect data could lead to faulty analyses and/or design decisions	Low	Medium	1. The team will confirm all tests with calculated results and simulations 2. The team will reach out to test facilities early to ensure lab time and comply with regulations at each facility	1. All test results will be documented and shared with the team 2. The team will reach out to test facilities at least three weeks in advance of the anticipated testing date

4.2.1.1 Construction

Table 39: Personnel Hazard Analysis-Construction Operations

Hazard	Cause	Outcome	Probability	Severity	Pre	Mitigations	Verification	Probability	Severity	Post
Skin contact with strong adhesive materials, such as epoxy or glue	Not using proper gloves necessary for safe glue/epoxy application	Severe allergic reactions, severe irritation to skin, and damage to skin	3	2	6	Mandating safety gloves and safety training for all team members who will work with adhesives	1. All team members participating in construction are trained in the workshop according to University standards 2. MSDS sheets are readily available in the workshop	1	2	2
Contact with the spinning bit of a portable drill or drill press	Improper technique regarding drill use	Severe damage to fingers and/or other body parts that including cutting, scraping, breaking, amputation, or other injury	3	4	12	Mandatory safety training for all team members who will work with drills	All team members participating in construction are trained in the workshop according to University standards	2	4	8
Loose workplace materials when drilling, sanding, or cutting	Not securing part properly with vise, clamps, or hands during machine use	Blunt bodily damage, cuts, or impalement to the body	2	4	8	Mandatory general workshop safety training for all team members	All team members participating in construction are trained in the workshop according to University standards	1	4	4
Contact with the spinning bit of a dremel	Improper technique and poor hand placement	Severe damage to fingers and/or other body parts including cutting, scraping, breaking, amputation, or other injury	2	4	8	Mandatory safety training will be conducted for all members who use the dremel	All team members participating in construction are trained in the workshop according to University standards	1	4	4
Contact with the cutting blade of a bandsaw or scroll saw	Improper sawing techniques, which includes footing, cut speed, and hand placement	Severe damage to fingers and/or other body parts including cutting, scraping, breaking, amputation, or other injury	2	4	8	Mandatory safety training will be conducted for all members who use the bandsaw	Team members will be specially certified for proper use of the bandsaw through the review and signing of a safety form and hands-on training with members certified for bandsaw use	1	4	4
Contact with the sanding surface of a belt sander or a palm sander	Improper sanding techniques	Damage to fingers including scraping, burning, and severe cuts	3	3	9	Mandatory safety training will be conducted for all members who use the sanders	Team members will be specially certified for proper use of sanding equipment through the review and signing of a safety form and hands-on training with certified members	1	3	3

Projectiles, shrapnel, or other hazardous materials launched into eyes	Not wearing protective eye gear at all times in the workshop	Temporary or permanent damage to eyes which may lead to future or immediate blindness or degradation of vision	4	4	16	All team members in the workshop will be required to wear safety glasses at all times	1. Team members will not be allowed to work in the workshop without proper eye protection 2. All team members participating in construction are trained in the workshop according to University standards	2	4	8
Inhalation of airborne particulates resulting from cutting, machining, or sanding parts	Not wearing respirator when generating harmful airborne particulates	Temporary or permanent damage to the lungs which could cause intense pains and long-term health issues	4	4	16	Team members working with potentially harmful fumes will be required to wear proper protective breathing gear	1. Team members will be certified for proper sanding safety through the review and signing of a safety form and hands-on training with members certified for sanding of materials such as carbon fiber and fiberglass 2. Team members will not be allowed to work in the workshop without proper breathing protection when generating harmful particles 3. MSDS sheets are readily available in the workshop	2	4	8
Extended inhalation of toxic fumes from glue or epoxies	Not wearing protective breathing gear	Damage to the lungs that could cause long or short term health effects	4	4	16	Team members working with potentially harmful fumes will be required to wear proper protective breathing gear	1. All team members participating in construction are trained in the workshop according to University standards 2. MSDS sheets are readily available in the workshop	2	4	8
Baggy clothes getting caught in machinery and causing bodily harm	Baggy clothing that hangs too close to machinery when working on parts	Parts of the body could be pulled into machines, causing extensive bodily damage and potentially death	4	4	16	Mandatory general workshop safety training for all team members	1. All team members participating in construction are trained in the workshop according to University standards 2. Members must wear proper attire to enter the workshop	2	4	8
Blunt bodily damage	Not wearing protective footwear and clothing to protect from falling objects that are blunt or sharp	Damage to the hands and feet that results in breakage or blunt damage	3	3	9	Mandatory general workshop safety training for all team members	All team members participating in construction are trained in the workshop according to University standards	1	3	3
Burns	Poor 3D printer operational procedures	Hands could receive painful burns that could lead temporary or lasting scarring	2	3	6	Mandatory general workshop safety training for all team members	All team members participating in construction are trained in the workshop according to University standards	1	3	3

4.2.1.2 Launch Operations

Table 40: Personnel Hazard Analysis-Launch Operations

Hazard	Cause	Outcome	Probability	Severity	Pre	Mitigations	Verification	Probability	Severity	Post
CATO	Imperfections in motor	Motor explodes causing personnel injury	2	4	8	1. The Launch Manager, Dave Brunsting, will inspect all motors prior to launch 2. Dave Brunsting will install the motor prior to launch to ensure it is installed correctly.	Dave Brunsting will be the only individual to install any motor or energetics and will obey NAR/TRA guidelines and procedures when doing so	1	4	4
Vehicle impact with personnel	1. Launch vehicles tips over towards personnel during launch sequence 2. During recovery the Launch vehicles lands on personnel	Personnel injured by launch vehicle's impact	2	4	8	1. The launch platform will be built properly and checked to ensure structural integrity 2. Stability of the vehicle off the rail is verified by simulations and testing 3. Personnel will be trained in launch proper procedures	1. All launch equipment will be verified by the Launch Manager 2. Vehicle stability simulations can be seen in Section 3.9 3. Pre-launch briefings will be held before each launch	1	4	4
High temperature of motor when ignited	1. Motor is still hot after landing 2. Personnel are too close to launch pad	Burns to personnel	3	3	9	1. Personnel will not touch the motor after landing 2. Personnel will stand a safe distance as designated by the RSO at launch (at least 300 ft. as required by the NAR)	1. All team members attending a launch will attend a pre-launch briefing prior to any launch 2. All team members must follow instructions from the RSO	1	3	3
Pinch-points	Pinch-points created during Launch vehicles assembly	Personnel are pinched/cut on their hands	4	1	4	The team leads will enforce the use of hand PPE	The team will provide and keep hand PPE (gloves, etc) in stock	2	1	2
Excessive sunlight	Direct exposure to sun for an extended period of time	Sunburn, increased risk of skin cancer	5	2	10	The team leads will inform personnel attending the launch that they must wear proper clothes for long term exposure to inclement weather.	1. Written announcements about potential weather hazards for team personnel will be sent in the full team email 2. The Safety Officer will provide a reminder during pre-launch training sessions	2	2	4
Sharp tools for system assemblies	System assemblies may require pliers, scissors, and other sharp tools	Cuts to personnel	3	2	6	1. The team leads will enforce the use of hand PPE and proper usage of all sharp tools 2. All team personnel will be trained in proper tool handling	1. The team will provide and keep hand PPE (gloves, etc) in stock 2. Leads will verify that personnel using tools have received training.	1	2	2

Car accident to/from the launch site	Bad traffic/road conditions to and from the launch site	Personnel injury	2	4	8	Only drivers who are properly certified will be allowed to drive personnel	Leads will confirm driver certification before leaving for the launch	1	4	4
Extreme cold	Inclement weather conditions	Hypothermia	2	4	8	Leads will inform all those attending the launch that they must wear proper clothes for long term exposure to inclement weather	Leads will ensure that everyone leaving has proper attire	1	4	4
Payload impact	1. Payload dislodged during launch 2. UAV falls during mission	Personnel injury via impact	2	3	6	NDRT members will be attentive during the launch and trained in proper launch procedures	1. The "finger-pointing" technique will be enforced 2. Pre-launch training sessions will be conducted before each launch	1	3	3
Battery chemical burn	Battery for payloads malfunctions during assembly	Personnel recieves chemical burn	3	3	9	1. Leads will enforce the use of proper eye and hand PPE during the handling of chemical batteries 2. All batteries not in use will be stored in a battery-safe container	1. NDRT will provide and keep in stock both hand and eye PPE 2. Leads will visually check to make sure all batteries are properly stored and that PPE is in use during handling	1	3	3

4.2.2 Failure Modes and Effects Analysis

4.2.2.1 Vehicles Flight Mechanics

Table 41: FMEA- Vehicles Flight Mechanics

Hazard	Cause	Outcome	Probability	Severity	Pre	Mitigations	Verification	Probability	Severity	Post
Failure of motor to ignite	1. Malfunction in e-match 2. Imperfections in motor	The vehicle will not takeoff	2	3	6	All energetics will be handled by Dave Brunsting	Dave Brunsting will inspect all components involving energetics prior to launch	1	3	3
Vehicle fails to clear launch rail	1. Deformation of launch rail. 2. Insufficient motor burn 3. Rail buttons deform or break during motor burn due to incorrect manufacturing.	Overall mission failure with potential dangers to property and people nearby who may endure injuries due to damages or destruction to the vehicle	2	4	8	1. Launch rail will be inspected prior to launch 2. Motor selection is chosen based on simulations and calculations 3. Rail buttons are carefully connected to vehicle	1. The Launch Manager will verify launch equipment 2. Motor selection can be seen in Section 3.2.2, and predicted rail exit velocity can be seen in 3.9 3. Construction procedures will be available in workshop prior to construction	1	4	4
Failure of vehicle to reach sufficient velocity upon exiting launch rail	1. Improper motor selection 2. Excessive weight	Vehicle moves along an unintended line of motion causing potential harm to vehicle or personnel	2	4	8	1. Motor selection is chosen based on simulations and calculations 2. Weight budgets have been allocated to each subsystem	1. The Launch Manager will verify launch equipment 2. Motor selection and calculations can be seen in Sections 3.2.2 and 3.9	1	4	4
Fin Flutter	1. Fin material is inadequate for withstanding flight velocities 2. Vehicle velocity exceeds the expected max. velocity	Vehicle moves along an unintended line of motion causing potential harm to vehicle or personnel	1	4	4	1. Fins design and material are chosen to minimize drag and maximize strength 2. Fin flutter velocity is calculated and proven to be above expected max. vehicle velocity 3. Fin design and material are chosen based on calculations, simulations and testing to reach a static stability margin of 2.0	1. Fins will be made from 1/8 in. G10 fiberglass in an isosceles trapezoid platform shape; see Section 3.3.6 2. Fin flutter velocity is calculated to be below max. vehicle velocity, shown in Section 3.3.6 3. Expected static stability margin is above 2.0, shown in Section 3.9.2	1	2	2

4.2.2.2 Vehicles Structures

Table 42: FMEA - Vehicles Structures

Hazard	Cause	Outcome	Probability	Severity	Pre	Mitigations	Verification	Probability	Severity	Post
Bulkhead failure	1. Improper construction 2. Insufficient adhesives to secure bulkheads 3. Material cannot withstand shear stress	1. Components are not properly retained causing damage internally to the vehicle and its components 2. Components are not protected from blasts 3. Vehicle unitentionally separates	3	3	9	1. Materials are selected carefully to withstand flight forces 2. Testing will be conducted to ensure material strength is sufficient for flight	1. Material selections for bulkheads can be seen in Section 3.4.1 2. Testing plans for solids testing can be seen in Section 6.1.1.	1	3	3
Nose cone detachment	1. Shear pin failure 2. Premature black power charge ignition	1. Unpredictable flight path leads to crashing and damage of vehicle components 2. Loss of payload components	2	4	8	1. Nose cone and vehicle body materials will be chosen carefully and tested to ensure functional capabilities 2. All components of the nose cone and payload bay that connect the two entities will be tested and constructed according to the correct procedures	1. 1. Retention FEA can be seen in Figures 91 and 92 2. Retention testing plan can be seen in Section 6.1.3	1	4	4
Structural failure at touchdown	Improper materials are selected structural strength	1. The vehicle may be damaged or entirely destroyed upon impact 2. Potential for damage to nearby property and people	3	2	6	Materials have been chosen based on expected forces and have demonstrated functional capabilities, seen in Section 3.3	Solids testing plan can be seen in Section 6.1.1	1	2	3
Motor explosion	1. 1. Improper installation of motor casing 2. Imperfections within the motor	1. Vehicle and payload sustain considerable damages during flight 2. People nearby are potentially injured	2	4	8	1. The Launch Manager, Dave Brunsting, will inspect all motors prior to launch 2. Dave Brunsting will install the motor prior to launch to ensure it is installed correctly	Dave Brunsting will be the only individual to install any motor or energetics and will obey NAR/TRA guidelines and procedures when doing so	1	4	4
Fin integrity failure	Fins are improperly connected the vehicle body	Flight path becomes unpredictable and vehicle does not follow the intended trajectory	2	3	6	1. The vehicle will be constructed using proper procedures 2. Proper techniques will be used when attaching fins to the fin can and vehicle body	1. Testing and construction procedures will be written for the fins and followed by all members involved in each task 2. Fin material selection can be seen in Section 3.3.6	1	3	3

Fin Flutter	1. Fins are not manufactured to specifications. 2. Fins are not made of the correct material. 3. Fins and fin can are not adequately secured to the vehicle due to failures of adhesives or load-bearing bulkheads.	Vehicle will move along an unintended flight path potentiallly damaging property and endangering bystanders. Vehicle may impact the ground in a nonoptimal fashion further endangering porperty and bystanders.	1	4	4	Fins will be composed of strong, lightwieght material. All adhesives and construction techniques will ensure the fins are secruely attached to the vehicle body. Fins will be selected to ensure a mininum stability margin of 2.0.	Construction and testing procedures will be written and approved by a safety team member, as well as team leadership. Fin design will meet requirements.	1	2	2
Transition section separates from body	Poor construction techniques lead to the separation of centering rings from the vehicle body	Vehicle flight path becomes unpredictable, and the payload section may sustain considerable damages	2	4	8	Centering rings and adhesives are specifically chosen to meet anticipated forces	1. The solids testing plan can be seen in Section 6.1.1. 2. Material selections for the transition section can be seen in Section 3.3.3	1	4	4
Dropping vehicle	Carelessness of team members when transporting the vehicle to and from launch destinations	Potential damages to payload and vehicle components, especially exterior components such as fins or the nose cone	2	2	4	Team members will use great care when transporting the vehicle	No less than 5 team members will be involved on transporting the vehicle, and an additional member will aid in ensuring a clear path for transportation	1	4	4
Shearing of bulkheads and twist-and-lock mechanisms	1. Parachutes anchored to bulkheads create too much stress for the adhesives securing them to the body tube 2. Materials strength of twist-and-lock mechanism is insufficient	1. Parachutes separate from the vehicle body and fails to sufficiently slow the descent of the vehicle 2. The twist-and-lock mechanism will fail and allow the CRAM to move within the body tube 3. The parachutes may tangle, leading to a more rapid descent speed than expected 4. Separated vehicle body sections may collide in air, leading to damages to the vehicle body and/or the payload	3	3	9	1. Bulkhead and twist-and-lock mechanisms are carefully selected for anticipated forces, seen in section 3.4.1 2. Construction procedures will be followed to ensure proper connections	1. The solids testing plan can be seen in Section 3.4.1 2. Construction procedures will be available in the workshop during construction	1	3	3

4.2.2.3 Air Braking System

Table 43: FMEA- Air Braking System

Hazard	Cause	Outcome	Probability	Severity	Pre	Mitigations	Verification	Probability	Severity	Post
Power failure in electrical system	1. Broken circuits from poor construction 2. Damage from launch forces 3. Batteries are insufficiently charged	Shutdown of the electrical system and loss of control of ABS tabs causing an overshoot of target apogee	3	4	12	1. Checking of the battery, circuit connections, and electronic components before launch 2. Only fully charged batteries will be used	1. Procedures for properly constructing/testing circuits will be created and properly adhered to by all members 2. Procedures for properly charging and checking the batteries will be created and adhered to by all members 3. Connections will be tested prior to launch with a multimeter	2	4	8
Incorrect or unavailable sensor data	1. Improper installation and programming of the sensors 2. Loss of power to the electrical system	Improper data transmission to flight computer that causes improper deployment of ABS	3	4	12	The ABS code and electrical components of the launch vehicle will be tested prior to launch.	Testing plans for ABS hardware and software will be implemented and utilized to verify the integrity of flight hardware before launch, shown in Section 6.1.6	1	4	4
Improper command signals from microcontroller	1. Improper coding of the electronic system 2. Unexpected errors when computing live sensor data	ABS not fully deploying or partially deploying the flaps, causing loss of proper ABS functionality	2	4	8	The code for the system and components will be tested before launch in a proper testing environment	Testing plans for ABS hardware and software will be implemented and utilized to verify the integrity of flight hardware before launch, shown in Section 6.1.6	1	4	4
Broken mechanical system for the ABS	1. Material strength is insufficient 2. Improper construction techniques	The ABS gets stuck open or closed and causes the launch vehicle to not reach or pass the targeted altitude	2	4	8	1. Materials are chosen based on simulations and calculations, shown in Section 3.7.3.3 2. Construction procedures will be written prior to construction	1. The mechanical system will be tested prior to launch, shown in Section 6.1.6 2. Construction procedures will be available in the workshop prior to construction	1	4	4
Loss of structural integrity of drag tabs	1. Material strength is insufficient 2. Improper construction techniques	Drag tabs are unable to deploy or break off the outer casing of the launch vehicle, causing the complete loss of the ABS system	2	4	8	1. Materials are chosen based on simulations and calculations 2. Construction procedures will be written prior to construction	1. Drag tab analysis can be seen in Section 3.7.3.2 2. Construction procedures will be available in the workshop prior to construction	1	4	4

Shearing of screws or bulkheads that anchor the ABS within the launch vehicle	1. Material strength is insufficient 2. Improper construction techniques	The ABS fails to properly deploy and potentially shifts within the body tube of the launch vehicle, causing severe changes to the mass distribution of the launch vehicle	3	5	15	1. Materials are chosen based on simulations and calculations 2. Construction procedures will be written prior to construction	1. Materials chosen for integration components can be seen in Section 3.7.2.1 2. Construction procedures will be available in the workshop prior to construction.	1	5	5

4.2.2.4 Recovery

Table 44: FMEA- Recovery

Hazard	Cause	Outcome	Probability	Severity	Pre	Mitigations	Verification	Probability	Severity	Post
Vehicle separation failure at apogee or at main deployment	1. Black powder charges are insufficient for separation 2. Avionics are not turned on or malfunction.	1. Vehicle impacts ground at high velocity damaging vehicle and/or personnel 2. Delayed ignition could result in large forces that could damage the vehicle	2	4	8	1. The black powder charges and altimeters are triple redundant 2. Each black powder charge and altimeter combination are independent of the other three 3. Altimeters are supplied from trusted vendors; see section 3.8.2	1. See Section 3.8.3 for redundant charge layout 2. See Section 6.1.2 for black powder testing 3. Altimeters chosen for full scale were verified in the subscale flight as seen in Section 3.6.3. 4. Black powder charge calculations are summarized in Section 3.8.3.1 and presented fully in Appendix A	1	4	4
Parachute fails to reduce descent velocity	1. Improperly sized parachute 2. Parachute is deployed at an improper time 3. Parachute is tangled and does not deploy correctly 4. Black powder charges damage some or all of the parachute upon deployment at apogee	Vehicle impacts ground at high velocity damaging vehicle and/or injuring personnel	2	4	8	1. Calculations and simulations were performed to determine proper parachute size 2. Altimeters are trusted models and redundant 3. Parachute folding is practiced and verified by recovery lead 4. Nomex cloth and insulation is used to protect the parachute, shown in Section 3.8.1	1. Calculations and simulations for parachute size can be seen in Section 3.9.4 2. Altimeter selection and redundancy is in Section 3.8.2 3. Altimeter testing can be seen in Section 6.1.2.	2	2	4
Parachute separation from vehicle	1. Component failure due to stresses	1. Vehicle impacts ground at high velocity damaging vehicle and/or personnel	2	4	8	1. Structural components will be rated for the anticipated forces with a FOS	1. Solids testing for structural components can be seen in Section 3.4.1	1	4	4
Vehicle drift exceeds allowed drift radius	1. Parachute deploys earlier than expected. 2. Parachute is an improper size.	1. Vehicle could encounter unexpected obstructions out of the drift radius causing personnel or property damage 2. Payload mission success is compromised.	3	2	6	1. Altimeters are from a trusted vendor 2. Parachute sizing is based on multiple calculations and simulations.	1. Altimeter selection can be seen in 3.8.2 and testing can be seen in Section 6.1.2 2. Parachute sizing calculations and simulations can be seen in Section 3.9.4	2	2	4

Vehicle separation during motor burn	1. Altimeter malfunction 2. Black powder ignites prematurely	1. Vehicle shears causing the interior components to be damaged 2. Personnel could be harmed	2	4	8	1. Altimeters are from a trusted vendor 3. Black powder and altimeters are tested	1. Altimeter selection can be seen in 3.8.2 and testing can be seen in Section 6.1.2 2. Black powder testing can be seen in Section 6.1.2	1	4	4
CRAM separates from vehicle body	1. Material strength is insufficient for main and drogue parachute loads	1. Internal components of vehicle shear 2. Vehicle impacts ground at high velocity	2	4	8	1. CRAM is manufactured with birch wood 2. CRAM locking mechanism has been a success in NDRT's past launches	1. CRAM material selection and analysis can be seen in Section 3.8.3.	1	4	4

4.2.2.5 Payload Vehicles

Table 45: FMEA- Payload Vehicles

Hazard	Cause	Outcome	Probability	Severity	Pre	Mitigations	Verification	Probability	Severity	Post
Fire	1. LiPo batteries on the UAV or the Rover vibrate during flight or are punctured 2. Wires within the UAV or rover systems short	Payload vehicles, nose cone, and payload bay are damaged or destroyed	2	4	8	1. Batteries will be checked prior to launch 2. Batteries will be housed so that they are unlikely to become damaged	1. The LSRS Pre-Launch Checklist can be seen in Section 4.1 2. The UAV and Rover design can be seen in Sections 5.4 and 5.5.	1	4	4
UAV power failure	1. Team member fails to turn the power on 2. Electronics failure 3. Battery insufficiently charged	UAV is not able to deploy or function, resulting in mission failure	2	4	8	1. A pre-lauch checklist will be followed to ensure electronics are set up properly 2. Only fully charged batteries will be used	1. The LSRS Pre-Launch Checklist can be seen in Section 4.1 2. Batteries not in use will be charged	1	4	4
Rover power failure	1. Team member fails to turn the power on 2. Electronics failure 3. Battery insufficiently charged	Rover is not able to deploy or function, resulting in mission failure	2	4	8	1. A pre-lauch checklist will be followed to ensure electronics are set up properly 2. Only fully charged batteries will be used	1. The LSRS Pre-Launch Checklist can be seen in Section 4.1. 2. Batteries not in use will be charged	1	4	4
UAV Unable to Operate	1. Weight of UAV is too great for stable flight 2. Wires on the UAV detach and disconnect the power supply 3. UAV is unable to detach from the platform	UAV is not able to fly correctly and likely results in a mission failure	3	4	12	1. Calculations will be made to determine the amount of weight needed and the sustainable flight time 2. Wires will be securely attached and checked with test flights 3. UAV deployment system will be tested prior to launch	1. Weight allocations can be seen in Section 5.4.1. 2. The LSRS Pre-Launch Checklist can be seen in Section 4.1 3. The test plan for retention can be seen in Section 6.1.3	1	4	4
Battery failure	UAV or Rover battery is not capable of powering the respective system for the duration of the mission	The UAV or Rover cannot complete mission	2	4	8	1. Battery life will be calculated to ensure the mission can be completed 2. Each system will be tested	1. Battery life calculations can be seen in Sections 5.4.2 and 5.5.2. 2. Testing plans for the UAV and Rover can be seen in Sections 6.1.5 and 6.1.4.	1	4	4

Radio transmission signal disruption	1. Transmitters are functioning at an improper frequency and are disrupted by other nearby transmitters 2. Transmitters lose signal due to a shielding material, such as carbon fiber, inhibiting signal transmissions.	UAV is unable able to become beacon for Rover and the Rover will be unable to reach the target	1	4	4	1. All transmitting frequencies will be carefully chosen to avoid overlap with other teams or nearby signals 2. The material selected surrounding the transmitters must be RF transparent	1. Transmitting frequencies can be seen in Section 5.4.3.3. 2. The material surrounding the payload bay is fiberglass which is RF transparent.	1	2	2
Rover movement mechanism failure	1. Rover component breaks due to impact 2. Wires on the Rover detach	Rover is unable to function correctly	2	4	8	1. The retention system will be designed to constrain the rover in all three axes. 2. Wires will be securely fastened and checked prior to launch.	1. The testing plan for the retention system can be seen in 6.1.3. 2. The pre-launch checklist for the LSRS can be seen in Section 4.1.	1	4	4
Sample retrieval mechanism failure	1. Sample retrieval components are damaged or break upon impact or due to a high-force event during flight 2. Sample retrieval mechanism is unable to support a sufficient load.	Rover is unable to retrieve a sufficient amount of the provided sample.	2	3	6	1. The sample retrieval system will be made of robust materials. 2. Tests will be conducted to verify the maximum retrieval force of the system. 3. The UAV and Rover will have RF transparent materials for the deployment signal	1. The sample retrieval system materials and rationale can be seen in Section 5.5.3. 2. The testing plan for the sample retrieval system can be seen in Section 6.1.4 .	1	2	2
Target detection failure	UAV detection algorithm does not recognize or encounter a sample site.	Rover has no target site to approach, resulting in mission failure.	2	4	8	Multiple detection algorithms will be compared to find the most efficient and successful.	The testing plan for target detection can be seen in Section 6.1.5.	1	4	4

4.2.2.6 Payload Deployment and Integration

Table 46: FMEA - Payload Deployment and Integration

Hazard	Cause	Outcome	Probability	Severity	Pre	Mitigations	Verification	Probability	Severity	Post
Nose cone removal failure	Black Powder charges do not generate sufficient force.	Vehicles are unable to exit the payload bay and consequently cannot complete the mission.	2	4	8	1. Black powder quantities are based on calculations. 2. Black powder will be tested prior to launch.	1. Black powder calculations can be seen in Appendix A. 2. Black powder test plans can be seen in 6.1.2.	1	4	4
Nose cone removal partial failure	The black powder charges generate less force than required to sufficiently separate the nose cone from the vehicle body.	Vehicles are unable to fully exit the nose cone and are unable to orient to complete the task. The mission is a failure.	2	3	6	1. Black powder quantities are based on calculations. 2. Black powder will be tested prior to launch.	1. Black powder calculations can be seen in Appendix A. 2. Black powder test plans can be seen in Section 6.1.2.	1	3	3
Damage from vehicle impacting ground at high velocity	1. The vehicle descends at unintentionally high speeds. 2. Supports securing the payload do not function as intended.	1. Vehicles are unable to function as intended. 2. Vehicles may not be able to deploy.	2	4	8	1. The retention system is designed to be robust. 2. The retention system will be tested.	1. Material selection for the deployment system can be seen in Section 5.3.1. 2. Testing plans for the retention system can be seen in Section 6.1.3.	1	4	4
Premature vehicle deployment	1. The securing mechanism fails to keep the vehicles from deploying at the incorrect time. 2. Bulkheads are not installed into the payload bay correctly.	Vehicles are not able to complete the mission successfully due to damages to essential components of the vehicles.	1	4	4	1. The securing mechanism will be designed to retain the vehicles in all three axes. 2. Construction procedures will be written prior to construction.	1. The mechanism design can be seen in Section 5.3. 2. Construction procedures will be available in the workshop prior to construction. 3. The testing plan for the retention system can be seen in Section 6.1.3.	1	3	3
Delayed vehicle deployment	The black powder system mechanism takes more time than intended to operate.	1. Vehicles are unable to perform the mission within the established time constraints 2. The batteries powering the vehicles likely run out of power before completing the mission.	1	4	4	1. Black powder quantities are based on calculations 2. Black powder will be tested prior to launch.	1. Black powder calculations can be seen in Appendix A. 2. Black powder test plans can be seen in Section 6.1.3.	1	3	3
Orientation correction failure	1. Vehicle platform does not have sufficient room to rotate 2. The platform cannot move because of friction.	Vehicle is not properly oriented, leading to mission failure	2	4	8	1. The orientation system will be extensively tested prior to launch	1. Testing plans for the orientation system can be seen in Section 6.1.3.	1	4	4

Vehicle platform or rover becomes unconstrained	1. Pin mechanism is not properly set 2. Pin breaks	Vehicles experience more forces than expected, which could lead to damage	2	3	6	1. The pin connection from the solenoid will be checked prior to launch 2. The pin material has been selected to withstand forces during flight.	1. The payload lead will confirm pin attachments before launch as seen in the Launch Procedure for the LSRS. 2. The pins are made of stainless steel for its durability and strength as see in Section 5.3.	1	3	3
UAV not properly secure to platform	Supports either break or are not attached correctly	Vehicles experience more forces than expected, which could lead to damage	2	3	6	1. Supports will be carefully constructed following construction procedures.	1. Construction procedures will be available in the workshop prior to construction. 2. Rention testing plans can be seen in Section 6.1.3.	1	3	4
UAV sled failure	1. Sled material strength is insufficient for forces 2. Sled connection cannot withstand forces during flight 3. Sled connection cannot withstand forces upon landing	The UAV vehicle is unable to exit the payload bay and is therefore unable to deploy to locate the target.	2	3	6	1. The sled is material is sufficient for its application 2. The retention will be tested	1. Sled material selection and FEA can be seen in Section 5.3.1. 2. The retention testing plans can be seen in Section 6.1.3.	1	3	3

4.2.2.7 Launch Support Equipment

Table 47: FMEA- Launch Support Equipment

Hazard	Cause	Outcome	Probability	Severity	Pre	Mitigations	Verification	Probability	Severity	Post
Launch rail is at an improper angle	1. Launch equipment is improperly set up 2. Vehicle is improperly placed on launch pad	Vehicle does not reach apogee	2	3	6	1. Launch equipment will be set up according to NAR standards 2. The NDRT mentor and RSO recommendations will be followed when setting up the vehicle	1. The RSO will verify that launch equipment is properly set up in accordance to Section 9 of NAR's High Powered Rocketry Safety Code 2. The vehicle set up will be verified by the NDRT mentor before launch	1	3	3
Launch controller fails to ignite motor	1. Wire connection or controller is faulty	Motor does not ignite	2	2	4	1. NDRT will use an official Rocketry club's controllers	NDRT will ensure that the clubs the team launches with are reliable and have a consistent record of successful launches	1	2	2
Launch ignition wires are live during set up	1. Launch controller unit is faulty	Premature motor ignition may injure personnel	2	4	8	1. All launch equipment will be inspected prior to use	The NDRT mentor along with the local Rocketry club will assist in inspecting equipment prior to set up	1	4	4

4.2.3 Environmental Hazards

4.2.3.1 Environmental Hazards to Vehicle

Table 48: Environmental Hazards to Vehicle

Hazard	Cause	Outcome	Probability	Severity	Pre	Mitigations	Verification	Probability	Severity	Post
Rain	Local weather patterns	Potentially severe water damage to electrical circuits, batteries, payload, and the launch vehicle motor	3	5	15	Flight readiness will be evaluated the day of launch after carefully monitoring the weather and following the NAR Weather Safety Code, which states that launch vehicles will not be launched into clouds, unsafe weather conditions, or in winds exceeding 20 miles per hour.	NDRT will comply with NAR regulations in regards to launching in inclement weather	1	5	5
Lightning	Local weather patterns	Could damage the electrical components, batteries, payload, and change the course of the launch vehicle after launch	2	4	8	Flight readiness will be evaluated the day of launch after carefully monitoring the weather and following the NAR Weather Safety Code	NDRT will comply with NAR regulations in regards to launching in inclement weather	1	4	4
High Winds	Local weather patterns	Potentially severe structural damage in the event of the launch vehicle falling over, as well as launch trajectory issues with very powerful winds	3	4	12	Flight readiness will be evaluated the day of launch after carefully monitoring the weather and following the NAR Weather Safety Code	NDRT will comply with NAR regulations in regards to launching in inclement weather	1	4	4
Snow	Local weather patterns	Potentially severe water damage to electrical circuits, batteries, payload, and the launch vehicle motor	2	4	8	Flight readiness will be evaluated the day of launch after carefully monitoring the weather and following the NAR Weather Safety Code	NDRT will comply with NAR regulations in regards to launching in inclement weather.	1	4	4
Extreme Temperatures	Local weather patterns	Potential damage to the battery and weakening of bonding materials within the launch vehicle	2	4	8	Flight readiness will be evaluated the day of launch after carefully monitoring the weather and following the NAR Weather Safety Code	NDRT will comply with NAR regulations in regards to launching in inclement weather	1	4	4

Low Cloud Cover	Local weather patterns	Turbulent air that could make launch and recovery operations difficult	3	2	6	Flight readiness will be evaluated the day of launch after carefully monitoring the weather and following the NAR Weather Safety Code	NDRT will comply with NAR regulations in regards to launching in inclement weather	1	2	2
High Humidity Levels	Local weather patterns	Could affect the bonding materials of the launch vehicle as well as the launch vehicle propulsion material	4	4	16	Flight readiness will be evaluated the day of launch after carefully monitoring the weather and following the NAR Weather Safety Code	NDRT will comply with NAR regulations in regards to launching in inclement weather	1	4	4
UV exposure from the Sun	No cloud cover over launch area	Potentially severe damage to the electronics and sensors within the launch vehicle if significant exposure occurs	3	4	12	Flight readiness will be evaluated the day of launch after carefully monitoring the weather and following the NAR Weather Safety Code	NDRT will comply with NAR regulations in regards to launching in inclement weather	1	4	4
Hail/Sleet	Local weather patterns	Potentially severe water damage to electrical circuits, batteries, payload, and the launch vehicle motor	2	4	8	Flight readiness will be evaluated the day of launch after carefully monitoring the weather and following the NAR Weather Safety Code	NDRT will comply with NAR regulations in regards to launching in inclement weather.	1	4	4
Local Terrain and Man-Made Structure Interference	Local terrain and the natural environment around the launch site	Could interfere with the course of the launch vehicle and cause destruction of the launch vehicle	2	5	10	Closely monitoring local natural topography and man made structures near the launch area	Team leads and the Launch Manager will inspect the launch site to confirm that it is safe to launch	1	5	5
Animal Interference	Local animal population in and around the launch site	Potential structural damage to the launch vehicle and potentially lethal damage to the animal	2	3	6	Closely monitoring local animal movements and local species in the launch area	Team leads and the Launch Manager will inspect the launch site to confirm that it is safe to launch	1	3	3

4.2.3.2 Vehicle Hazard to Environment

Table 49: Vehicle Hazard to Environment

Hazard	Cause	Outcome	Probability	Severity	Pre	Mitigations	Verification	Probability	Severity	Post
Fiberglass particulates (styrene gas)	Sanding of bulkhead or other fiberglass materials	1. Cause skin, eye, and respiratory tract irritation to surrounding individuals 2. Emission of toxins depletes air quality	3	3	9	Quantity of styrene gas emitted has negligible effects on environment	1. All members involved in sanding will be certified prior to entering lab and will wear proper equipment 2. Sanding will be conducting in ventilated area and the workshop vacuum will be utilized	3	1	3
Excessive carbon dioxide emission	1. Motor produces CO_2 emissions when ignited 2.The black powder charges in the recovery system produces CO_2 emissions when ignited	Contribute to greenhouse effect and increase global warming	5	1	5	1. CO_2 emissions from the motor are negligible 2. CO_2 emissions from black powder charges are negligible	Motors and black powder charges will be inspected by the Launch Manager	4	1	4
Hydrogen chloride emmission	Ammonium perchlorate motor produces hydrogen chloride	HCl reacts with water to form hydrochloric acid, contaminating water	4	1	4	Launches will take place away from water sources in order to prevent contamination	1. Leads will survey the land to ensure the launchpad is placed away from water sources 2. Motors will be disposed of according to SDS and local standards	2	1	2
Components come loose from vehicle	Improper retention of components	Wildlife could potentially ingest or be harmed by materials	3	3	9	Exterior and interior of launch vehicle will be inspected prior to launch	The Vehicle Pre-Launch Checklist can be seen in Section 4.1	1	3	3
Battery leakage	Defective batteries that fail to enclose the acid in its appropriate space	1. Absorption of acid contaminates soil 2. Pollution of groundwater	2	4	8	Batteries are housed in battery bag when not in use and are inspected by leads before and after each use	Batteries will be inspected by a team lead or the Safety Officer and if a defect is found, the battery will be disposed of according to the SDS and local regulation	1	4	4
Spray paint on vehicle	Use of spray paint to paint exterior of vehicle	Release of toxic emissions into the atmosphere	4	2	8	Spray painting is executed in a ventilated area to reduce concentration of air contamination	1. Members involved in spray painting will be certified prior to entering workspace and will wear proper PPE 2. Painting area will be well ventilated and only contain personnel participating in painting.	4	1	4

Plastic Waste	Plastic waste can be produced by 3D printing and other construction procedures	Wildlife could potentially ingest or be harmed by plastic	5	2	10	Disposal of plastics according to SDS and local standards	The workshop will contain a specific bin for recycling certain plastics in order to reduce waste	4	1	4
Wire Waste	Excessive wire scraps as a result of electrical component construction	Wildlife could potentially ingest or be harmed by wire waste	5	2	10	Wire will be disposed of according to SDS and local standards	The workshop will contain a specific bin for recycling certain electronic components in order to reduce waste	4	1	4
Soldering Material Waste	Excess materials improperly disposed of during the soldering of wires	Soldering releases toxic that can contaminate the air quality	4	2	8	Proper ventilation will be used to negate release of toxins into environment	Members involved in soldering will be certified. Disposal will be monitored according to SDS and local guidelines	4	1	4
Grass fire	1. Motor burnout 2. Electrical components short circuit	1. Damage to surrounding grass 2. Damage to animals' natural habitats 3. Greenhouse emissions as a result of combustion	2	3	6	1. Bring appropriate extinguishing devices on site of launch 2. Leads inspect wire connections and electronics before launch	1. A fire extinguisher must be available at each launch 2. Pre-launch checklists can be seen in Section 4.1.	1	3	3
Damage to nearby property	1. High wind speeds knock vehicle out of expected trajectory 2. Recovery fails to deliver vehicle safely to the ground	Damage to private property and/or damage power lines or environment	3	4	12	1. Launch equipment will be inspected Stability of the vehicle will be confirmed through simulations and testing 2. Leads ensure redundant and reliable systems for recovery	1. Simulations confirming vehicle stability can be seen in Section 3.9 2. The recovery system will employ three redundant altimeters and black powder charges that will be tested prior to launch, shown in Section 3.8.2	2	4	8
Noise Impacts	Excessive noise generation from the launch vehicle's motor on launch	Noise could harm wildlife, bystanders, and potentially vibrate structures	1	4	4	Impact will be temporary and will not exceed EPA regulations	Personnel will stand at least 300 ft. away from launch site as required by the NAR	1	2	2

5 Technical Design: Lunar Sample Retrieval System

5.1 Overview

The Notre Dame Rocketry Team will design, build, and test a payload system that will simulate retrieving lunar ice for the 2019-2020 NASA Student Launch Competition. The system will be comprised of an Unmanned Aerial Vehicle (UAV) that will locate the sample and a Rover that will retrieve and transport the sample.

5.1.1 Mission Success Criteria

The payload must accomplish 8 main tasks: (1) withstand forces experienced during vehicle flight and recovery, (2) activate remotely via a signal from the ground station, (3) orient and deploy, (4) locate the closest Competition Future Excursion Area (CFEA), (5) transmit the coordinates of the closest CFEA, (6) traverse to the sample area, (7) retrieve and secure a 10 mL lunar sample, and (8) transport the sample 10 ft away.

The mission will be considered successful if it meets all Payload and Safety Requirements outlined in the 2020 NASA Student Launch Handbook and the following criteria:

P.MS.1 The payload shall be powered off until the launch vehicle has safely landed and has been approved for remote-activation by the RSO.
P.MS.2 The payload shall remain retained inside the vehicle during vehicle flight and recovery.
P.MS.3 The payload shall self orient to within 5°of its upright position for deployment.
P.MS.4 The payload shall deploy from inside the launch vehicle from a position on the ground.
P.MS.5 The UAV shall locate, fly to, and land at the closest FEA.
P.MS.6 The UAV shall send its coordinates to the Rover and activate the Rover.
P.MS.7 The Rover shall traverse to the UAV coordinates and locate the sample area.
P.MS.8 The Rover shall recover and secure a 10 mL lunar ice sample.
P.MS.9 The Rover shall move 10 linear ft away from the sample area.

5.1.2 Summary of Payload

The Lunar Sample Retrieval System (LSRS) is comprised of three main systems: the UAV, the Rover, and the Retention Orientation and Deployment (ROD) system. The UAV is integrated with the Target Detection subsystem and the Rover is integrated with the Sample Retrieval subsystem. The LSRS will remain inactive during vehicle flight and recovery. To facilitate deployment of the UAV and Rover, the nose cone of the vehicle will be jettisoned at 400 ft above ground level and will be attached to the vehicle via a shock chord. See Section 5.3.2 for nose cone ejection details. The ROD system will be able to freely rotate when the nose cone is ejected and will properly orient the system due to an off-center CG. Upon successful recovery, the Ground Station will transmit an initiation signal to the Rover and initiate the deployment sequence. The ROD system will retract the solenoid pins allowing the Rover to translate and tow the UAV out of the payload bay. The UAV will take off, search for, locate, and land at the

nearest CFEA. The coordinates of the CFEA will be transmitted to the Rover and the Rover will travel to the coordinates. When the Rover is within 15 ft of the coordinates, the Rover will use computer vision to locate the sample on the CFEA and translate onto the sample. The sample retrieval system will deploy the Archimedes screw into the sample and collect a 10 mL sample. When the Archimedes screw has been retracted, the Rover will translate 10 linear ft from the sample and complete the mission.

5.2 Layout

5.2.1 Full Assembly

The LSRS is located in the fore section of the vehicle. Figure 83 shows renderings of the complete LSRS within the payload bay. The LSRS is 16 in. long and there is a 7 in. gap between the nose cone bulkhead and the fore bulkhead of the payload bay. This space is used as a pressure chamber when jettisoning the nose cone during recovery. Additionally, the retaining platform will be able to freely rotate within the payload bay due to a 0.5 in. clearance between the platform and the inner wall of the payload bay. The UAV and UAV sled are located in the aft section of the payload bay so the Rover can tow the UAV out of the payload bay. A total weight of 111 oz was allocated to the LSRS. A summary of the weight distribution of each system is shown in Table 50.

(a) Fore End (b) Aft End

Figure 83: CAD Model of full LSRS within the Payload Bay

Table 50: Summary of LSRS subsystem weight

System	Weight
UAV	17 oz
Rover	41 oz
Sample Retrieval	2 oz
Deployment	49 oz
Total	109 oz

5.2.2 Launch Vehicle Integration

The LSRS is integrated into the launch vehicle using a rail and sled system to satisfy NASA Requirement 4.2. The system is comprised of two platforms shown in figures 85 and 86. This grants easy access to the payload and ensures the proper placement of the UAV and Rover into the ROD system. An exploded view of the vehicle integration can be seen in Figure 84. The stationary platform is permanently attached to the aft bulkhead using a nut and bolt. The sliding platform attaches to the stationary platform by inserting the two “rails" of the stationary platform into the respective slots on the sliding platform. When the sliding platform is fully placed on the stationary platform, two nuts and bolts are placed in the fore section of the platforms to secure them together.

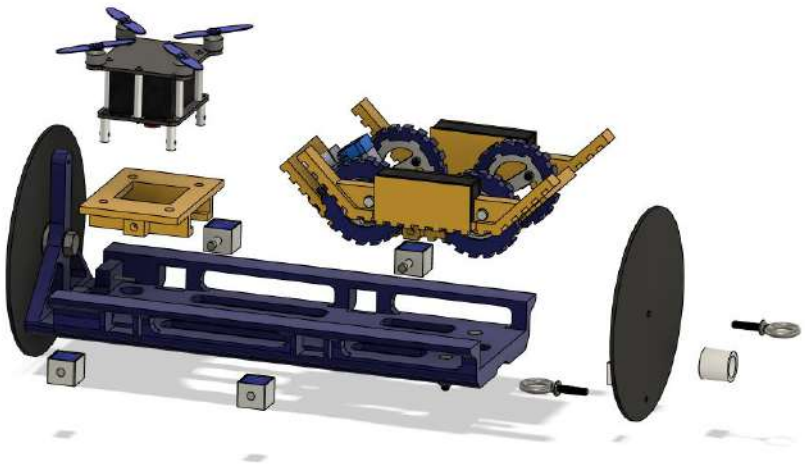

Figure 84: LSRS Exploded View of Vehicle Integration

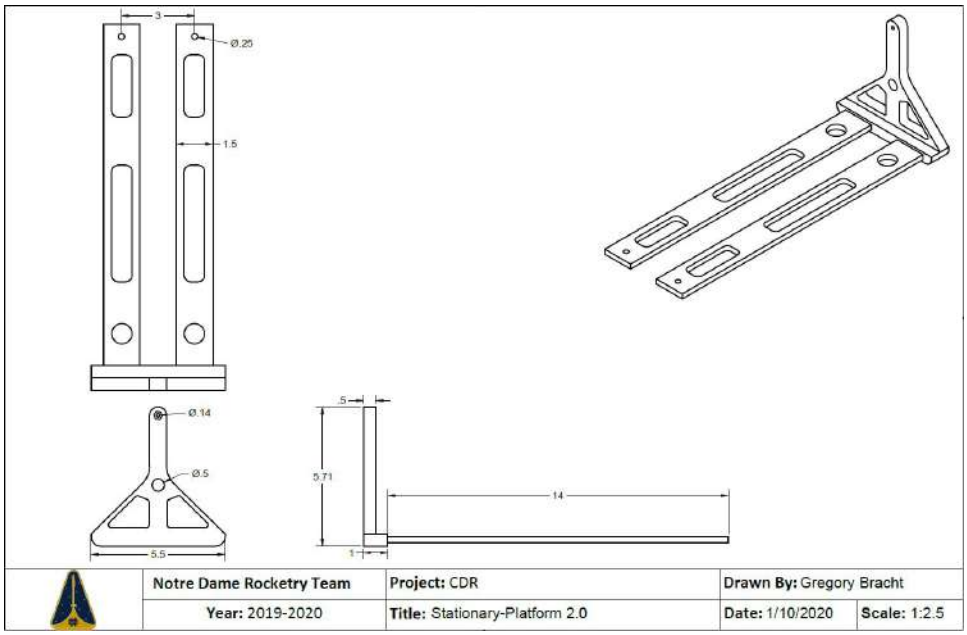

Figure 85: Drawing of Stationary Platform

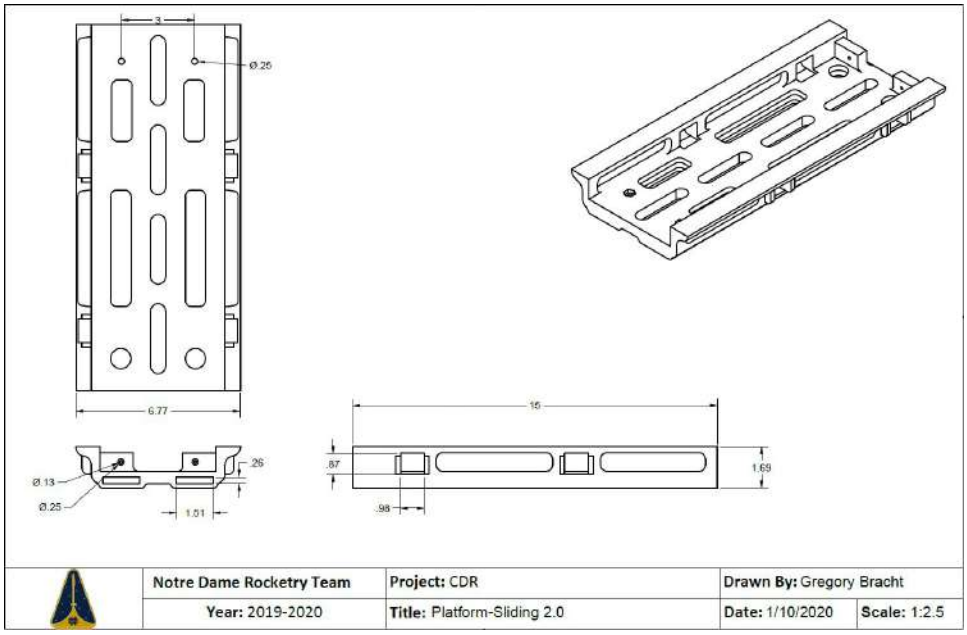

Figure 86: Drawing of Sliding Platform

5.3 ROD System

The Retention, Orientation, and Deployment (ROD) System is a critical component for the success of the LSRS payload. The ROD System combines retention, orientation, and deployment in one mechanism to efficiently use the space within the payload bay and to create a simple, elegant system that fulfills multiple requirements. The system is integrated

with the sled and rail platform system and is shown in Figure 87.

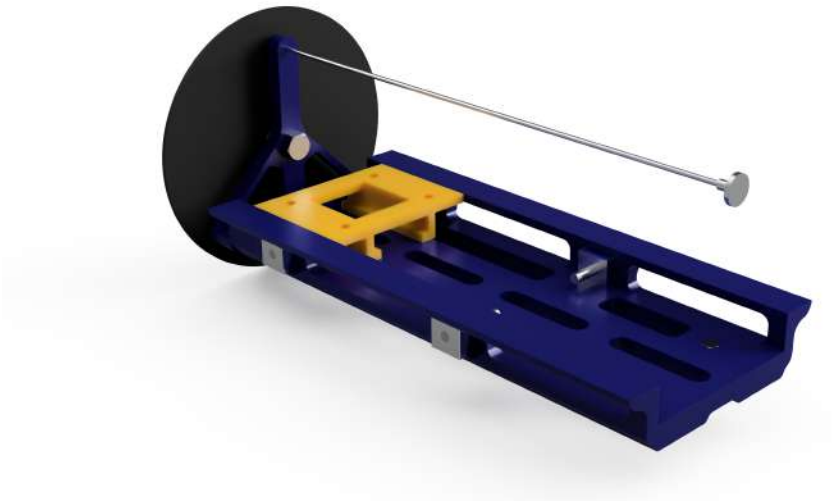

Figure 87: ROD System

5.3.1 Payload Retention

The retention of the LSRS during vehicle flight is accomplished using four solenoids that are friction fit into the sliding platform of the sled and rail integration system as seen in Figure 88. Two solenoids are used to restrict motion of the Rover and are inserted into holes within the Rover body, restricting motion in all directions. The other two solenoids are inserted into two holes within the UAV Sled, restricting motion of the sled in all directions. The landing struts of the UAV slide through two holes in the UAV sled allowing the bottom platform of the UAV frame to rest on the sled. The UAV is prevented from lifting out of the sled during flight by two pins in the aft section of the sliding platform as seen in Figure 89. These pins go through the rear struts of the UAV preventing any translation of the UAV out of the sled.

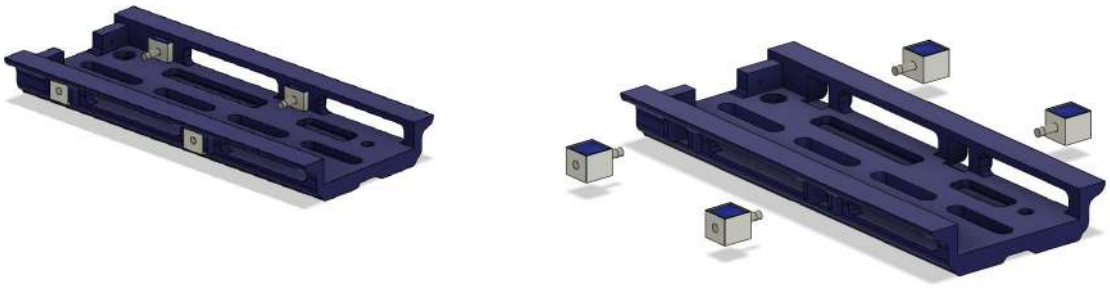

(a) Assembled (b) Exploded

Figure 88: CAD Model of Full LSRS within the Payload Bay

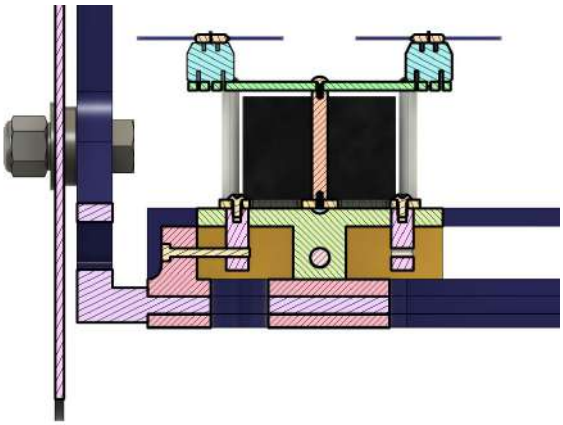

Figure 89: UAV Sled

The solenoid for the retention of the payload is the Adafruit Medium Push-Pull Solenoid shown in Figure 90. This solenoid was chosen for its long throw length and large diameter pin as well as the other parameters outlined in Table 51. The pin of the solenoid is made of stainless steel and will withstand forces experienced during flight and successfully retain the UAV and Rover. The solenoid also provides a mechanical fail-safe for the system. When no power is running to the solenoid, a linear spring provides an outward force on the pin that holds the pin in the extended position. This force will ensure the pin remains extended into the holes of the Rover body and UAV sled during vehicle flight and recovery. This design satisfies NASA Requirements 4.3.7.1-4.

Table 51: Solenoid Parameters

Parameter	Value
Dimensions	1.02 x 0.98 x 0.86 in.
Weight	2.4 oz
Throw Length	0.39 in.
Pin Diameter	0.27 in.
Voltage	6 V

Figure 90: Retention Solenoid

To ensure that the various components involved in the retention system will withstand all forces experienced during vehicle flight and recovery, FEA studies were performed. The maximum force experienced by the retention system is during main deployment, and a 37 g acceleration was estimated from vehicle flight simulations in Section 3.9. This estimate was used when conducting the FEA studies. Figures 91 - 93 show the results of the FEA studies.

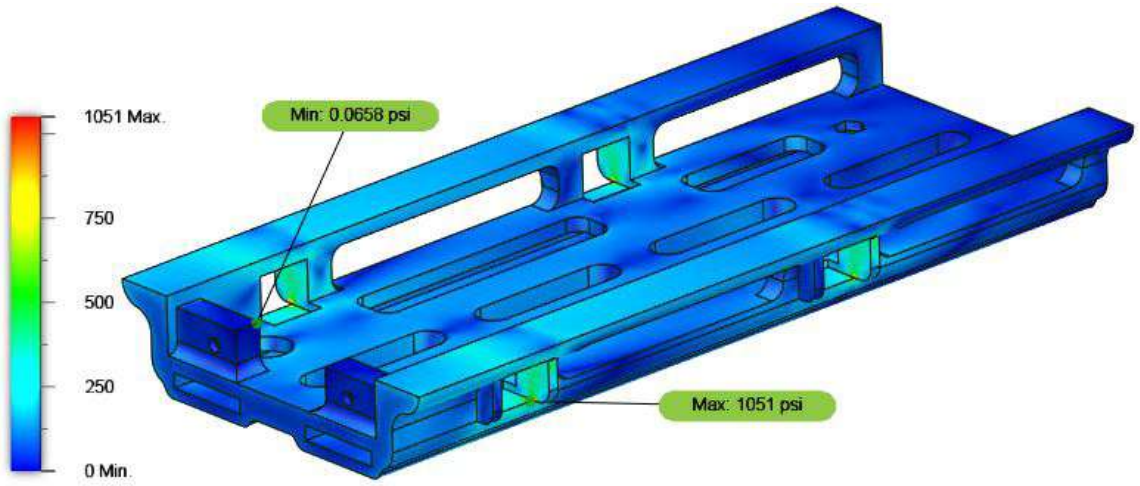

Figure 91: FEA of Sliding Platform

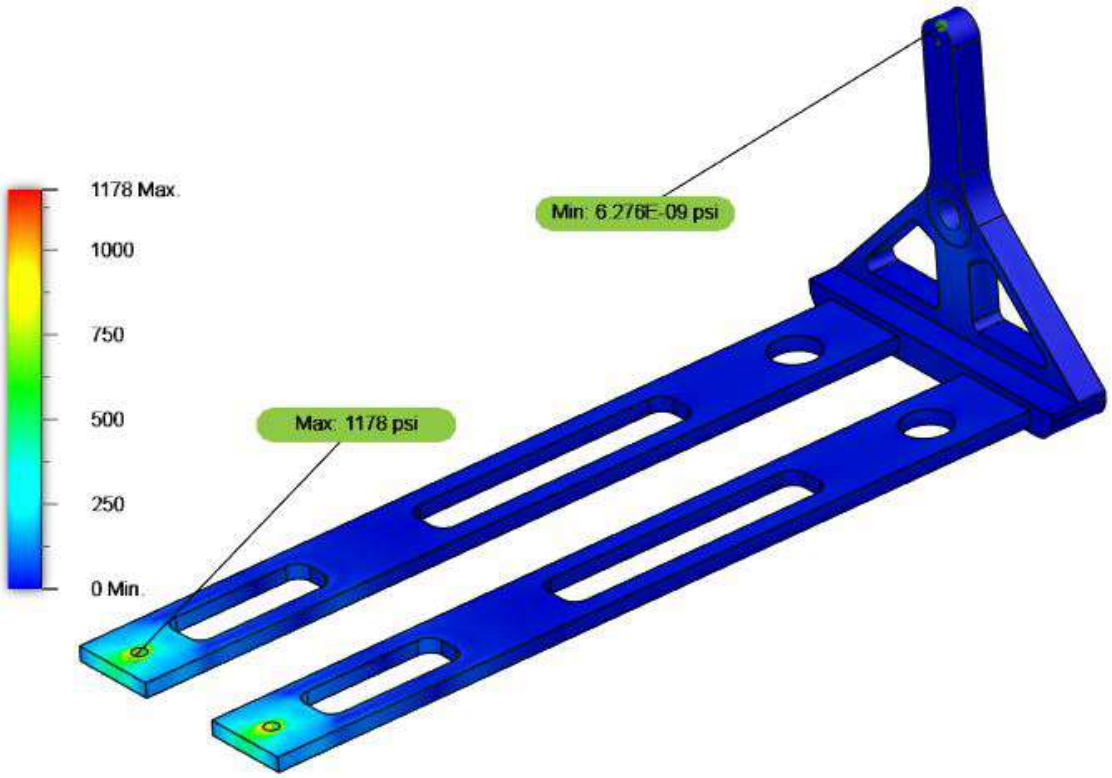

Figure 92: FEA of Stationary Platform

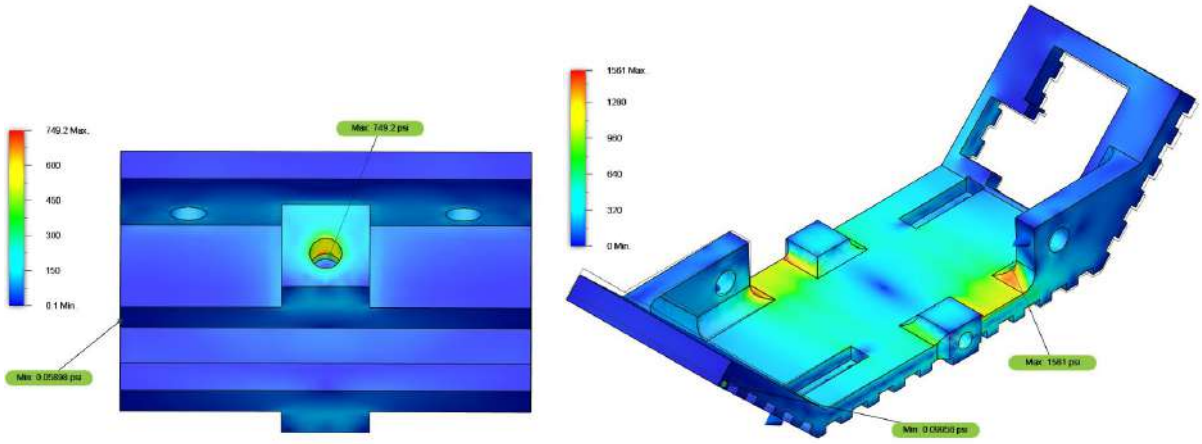

(a) UAV Sled (b) Rover Body

Figure 93: FEA of Primary LSRS Vehicles

The results of the FEA studies are summarized in Table 52. Factors of Safety were calculated for ASA plastic using a yield stress of 5,000 psi. The lowest factor of safety was 3.20 for the Rover Body. These results confirmed a robust design that will succeed in retaining the LSRS during vehicle flight.

Table 52: Finite Element Analysis of the Payload Retention Summary

Component	Material	Max Stress (psi)	Factor of Safety
Sliding Platform	ASA	1051	4.75
Stationary Platform	ASA	1178	4.24
UAV Sled	ASA	749.2	6.67
Rover Body	ASA	1561	3.20

5.3.1.1 Retention Electronics

The retention of the Rover and UAV consists of solenoids which must remain locked until deployment has been approved by the RSO. In order to control this system, a simple processor will receive a control signal from the Rover system initiated by a radio transmission to the rover. The retention processor will then trigger the solenoids to retract.

The Adafruit Itsy Bitsy 3 V microcontroller board was selected due to its low profile, 3 V logic matching the rover's 3 V logic, and ample GPIO pins for connecting the solenoids. Because the solenoids can draw up to 1 A of current, transistor switches must be used to control the current into the solenoids. The GPIO pins of the Itsy Bitsy will be used to set the gates of the transistors high or low, allowing 5 V from an L7805 regulator to flow into the solenoids. A 7.4 V LiPo battery will power the circuit as it can safely supply the peak current draws of 1 A per solenoid. The

Itsy Bitsy utilizes an internal voltage regulator while each solenoid will have a dedicated 5 V regulator. The circuit schematic can be seen in figure 94.

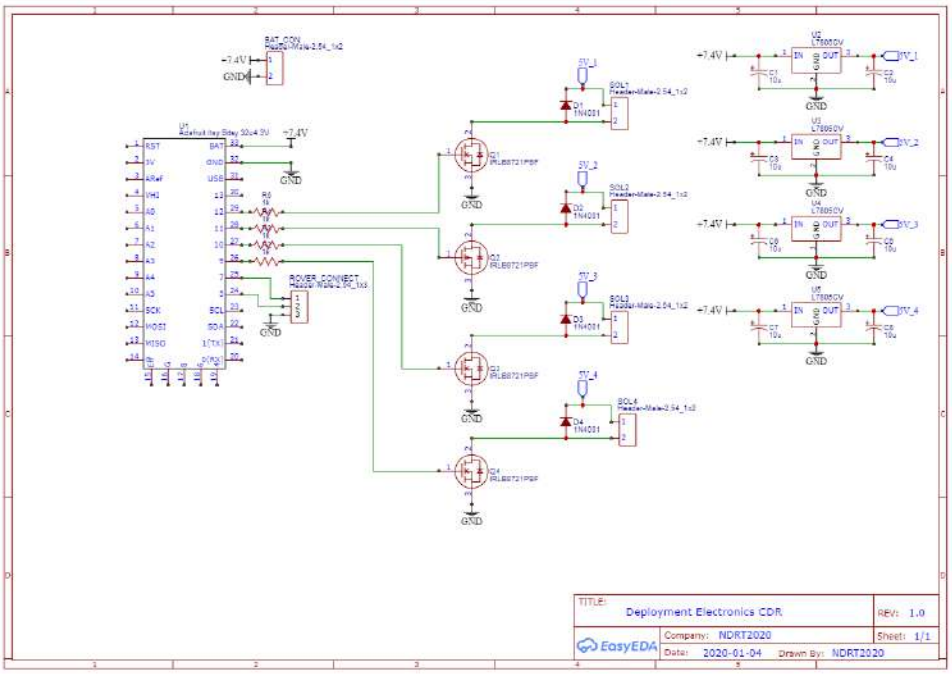

Figure 94: Retention Electrical Schematic

A 3 pin header will connect the Rover and the retention electronics via a quick disconnect terminal. As the rover drives out of the payload bay, it will pull on the connector which will be securely fastened to the sliding platform, causing a disconnect. This informs the Itsy Bitsy processor that the Rover is departing the payload bay. The solenoids will be delayed in "closing" in order to provide ample time for the Rover to depart; however, the time delay will be minimized to prevent the solenoid from overheating due to prolonged activation. The connector will consist of 3 terminals: a common ground, an enable pin, and a trigger pin. The enable pin will be set high when the rover enters the deployment state, and the trigger pin will be set high when the deployment command is received. Resistors are included on the rover's end of the connection to provide current protection to each processor's pins.

5.3.2 Nose Cone Ejection

To aid the deployment of the LSRS, the nose cone will be jettisoned from the launch vehicle at 400 ft. AGL after main deployment has occurred to satsify NASA Requirement 4.3.6. The system will be located on the fore bulkhead in the payload bay as seen in Figure 95. The fore bulkhead of the payload bay serves to separate the LSRS from the nose cone, thus creating a pressure chamber. The bulkhead is pressed against the sliding platform and the aluminum stopper of the LSRS. A lip on the nose cone contacts the opposite side of the bulkhead and seals the pressure chamber from the LSRS. A PerfectFlite Stratologger SL100 altimeter was chosen to ignite the black powder charge due to its current selection in the recovery system. It is powered by a 3.7 V LiPo battery and the components are secured to the aft side of the bulkhead. A 0.5

in. PVC pipe is epoxied to the fore section of the bulkhead inside the pressure chamber and will house the black powder charge. Two 1/8 in. kevlar chords attached to eyebolts on either side of the bulkhead will tether the nose cone to the payload bay satisfying NASA Requirement 4.4.2. The kevlar tethers will be epoxied to the inside of the payload bay and the nose cone bulkhead.

(a) Fore (b) Aft

Figure 95: Nose Cone Ejection Assembly

The amount of black powder needed to successfully jettison the nose cone and shear four 2-56 shear pins was calculated in Section 3.8.3.1 of the Recovery System with full detail in Appendix A. Table 53 summarizes the results of the black powder calculations.

Table 53: Nose Cone Black Powder Ejection Charge Summary

Separation	$F(lb_f)$	P (atm)	n_g (mol gas)	$Mass\,4F$ (g)
Nose Cone	286	0.387	0.0148	1.0

FEA studies were conducted on the various components involved during the nose cone jettison event to ensure no damage occurred during the event. From the black powder calculations, an estimated 286 lb_f force was used to verify component integrity during the jettison event. Figures 96, 97, and 98 show the results of the FEA.

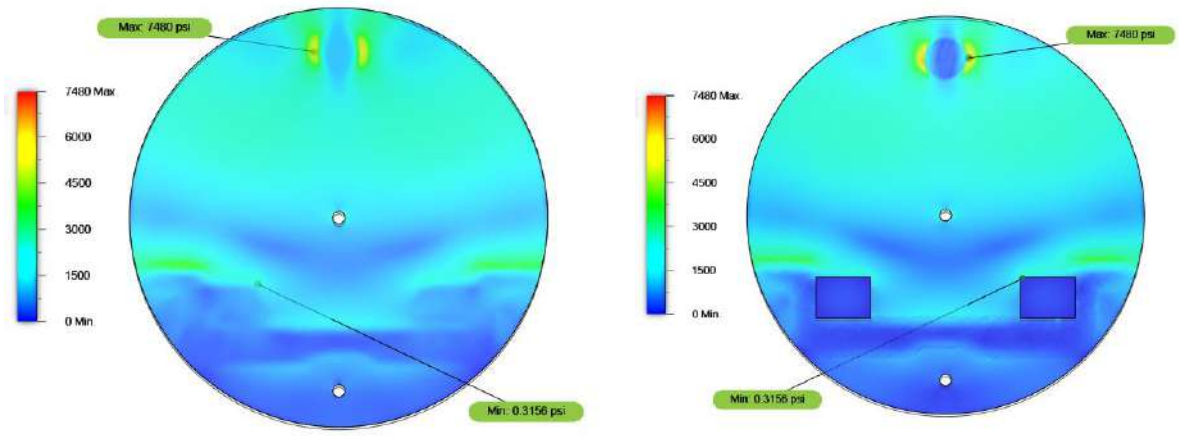

(a) Fore (b) Aft

Figure 96: Finite Element Analysis of Bulkheads

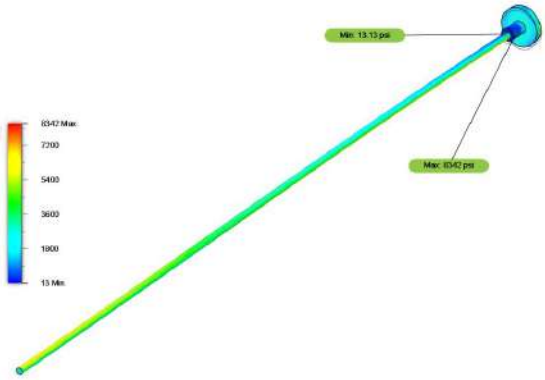

Figure 97: Finite Element Analysis of Stability Rod

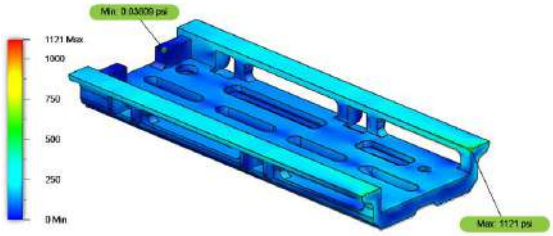

Figure 98: Finite Element Analysis of Sliding Platform

The results of the FEA studies on the jettison event are summarized in Table 54. Factors of Safety were calculated for ASA plastic using a yield stress of 5,000 psi, for 6061 Aluminum using a yield stress of 35,000 psi, and for Garolite G10 using a yield stress of 38,000 psi. The lowest factor of safety was 4.19 for the Stability Rod. These results confirmed a robust design that will succeed in withstanding forces experienced during jettisoning the nose cone.

Table 54

Component	Material	Max Stress (psi)	Factor of Safety
Sliding Platform	ASA	1121	4.46
Stability Rod	6061 Aluminum	8342	4.19
Fore Bulkhead	Garolite G10	7480	5.08

5.3.3 Orientation

The orientation of the LSRS will be accomplished within the payload bay. The platform the LSRS is retained to within the payload bay is secured to the aft bulkhead using a nut and bolt. The bolt is threaded through a flanged bearing that is pressfit into the bulkhead which will allow the platform and thus the LSRS to freely rotate inside the payload bay. An exploded view of the orientation system is shown in Figure 99.

(a) Full (b) Exploded

Figure 99: CAD of Orientation System

During vehicle flight, the LSRS will be secured in place by two rectangular stoppers epoxied to the fore bulkhead. These will fit securely into the corners of the sliding platform as shown in Figure 100. These stoppers will prevent any rotation of the LSRS during flight and will be removed during the nose cone jettison event. The LSRS will freely rotate during the remaining descent and will be correctly oriented once the payload bay has returned to the ground.

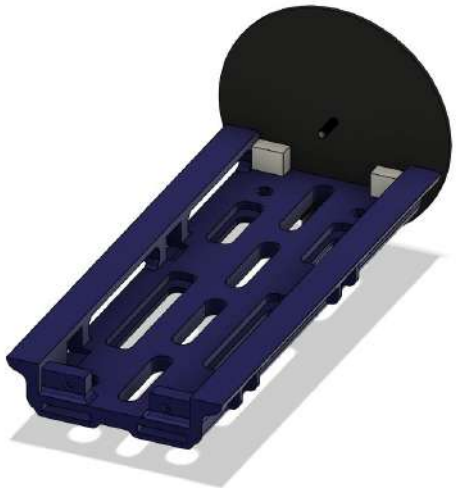

Figure 100: CAD of Orientation featuring Stoppers

A FEA study was conducted on the aft bulkhead and the orientation bearing to ensure reliability of the system. A 260 lb_f load was placed on the contact surfaces of the bearing and

aft bulkhead. This load was conservatively derived from a 37 g acceleration during main parachute deployment.

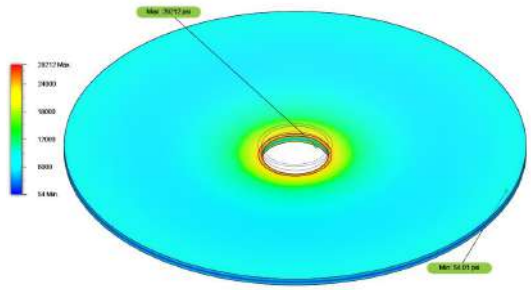

Figure 101: FEA of Aft Bulkhead

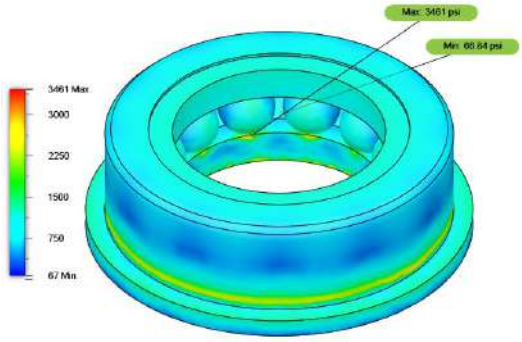

Figure 102: FEA of Orientation Bearing

After conducting the FEA studies, the aft bulkhead experienced a maximum stress of 28,212 psi and the orientation bearing experienced a maximum stress of 3461 psi. Using a yield stress of 38,000 psi for Garolite G10 and 50,800 psi for steel, the aft bulkhead had a FOS of 1.35 and the orientation bearing had a FOS of 14.67. While a FOS of 1.35 is not ideal, the team is confident the G10 fiber glass bulkhead will withstand forces due to previous experiences. Additionally, thicker G10 fiber glass can be purchased to increase strength.

To ensure the LSRS will rotate around the orientation bearing, a center of mass calculation was conducted using Fusion 360 software to verify an off center center of gravity. The results of the calculation can be seen in Figure 103. From this figure, it can be seen that the LSRS will have a center of gravity off center from the rotational axis and will properly orient itself during the recovery of the launch vehicle after jettisoning the nose cone.

Figure 103: LSRS Center of Gravity

5.3.4 UAV and Rover Deployment

Upon successful recovery of the launch vehicle, the Rover and UAV will be free to deploy through the fore end of the payload bay. The ROD system has been designed to enable the Rover to freely translate out of the launch vehicle. The Rover will tow the UAV sled as it translates out

of the payload bay. Once the Rover has towed the sled out of the payload bay, the tow will detach from the Rover and the UAV will deploy to begin searching for the nearest CFEA. The UAV sled is shown below in Figure 104.

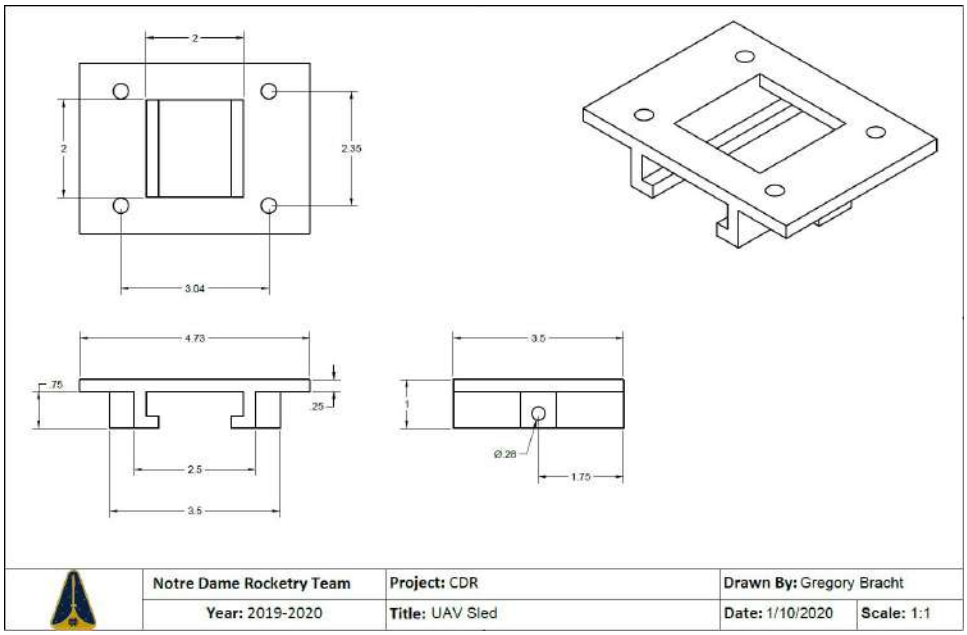

Figure 104: Drawing of UAV Sled

5.4 UAV

The UAV will autonomously locate the CFEA nearest to the launch vehicle's landing site and relay the selected CFEA's GPS coordinates to the ground station. This approach simulates a satellite gathering aerial imagery of a celestial body prior to ground exploration.

Figure 105: CAD Model of UAV

5.4.1 Mechanical Design

The frame of the UAV provides a rigid structure and housing for all the UAV components and electronics and is shown in Figure 106. The frame is made up of two carbon fiber

platforms separated by a set of six aluminum spacers. The four landing struts of the UAV are also manufactured out of aluminum. The use of carbon fiber and aluminum that provide a high strength to weight ratio also minimizes the amount of material used and the overall weight of the frame. A summary of the weight allocation for the UAV frame is shown in Table 55.

Table 55: Weight Allocation of UAV Frame

Component	Quantity	Total Weight
Top Platform	1	1.19 oz
Bottom Platform	1	0.97 oz
6-32 Screws	16	0.38 oz.
Platform Spacers	6	0.68 oz
Landing Struts	4	0.39 oz
Total		3.61 oz

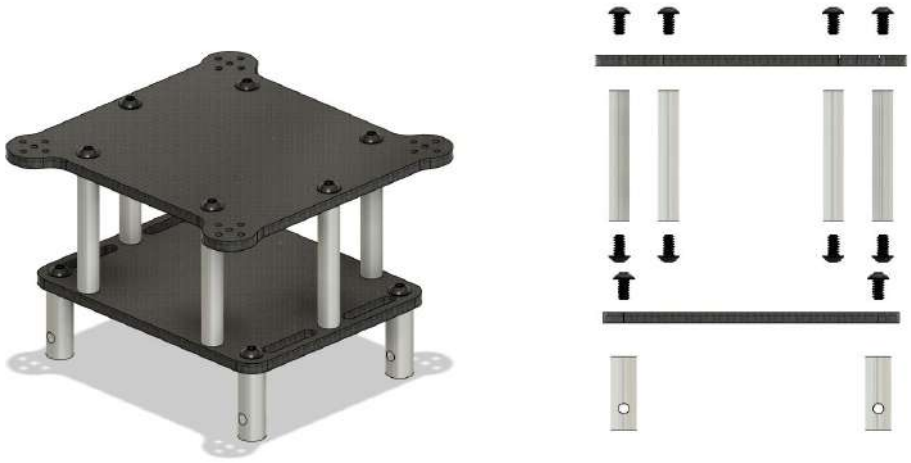

(a) Full (b) Exploded

Figure 106: UAV Frame

A drawing showing the dimensions of the frame can be seen in Figure 107. From this drawing, it can be seen that the UAV meets the dimension requirements outline in Requirement P.10. With the propellers attached to the top of the frame, the UAV has a maximum width and length of 5.45 and 4.8 in. which also meets the dimension requirements. The volume of space between the two platforms will house the battery of the UAV. This provides a secure housing for the battery and protects the battery during any collisions. Two through holes are made towards the bottom of the landing struts to allow the retention pins to retain the UAV in the UAV sled during vehicle flight.

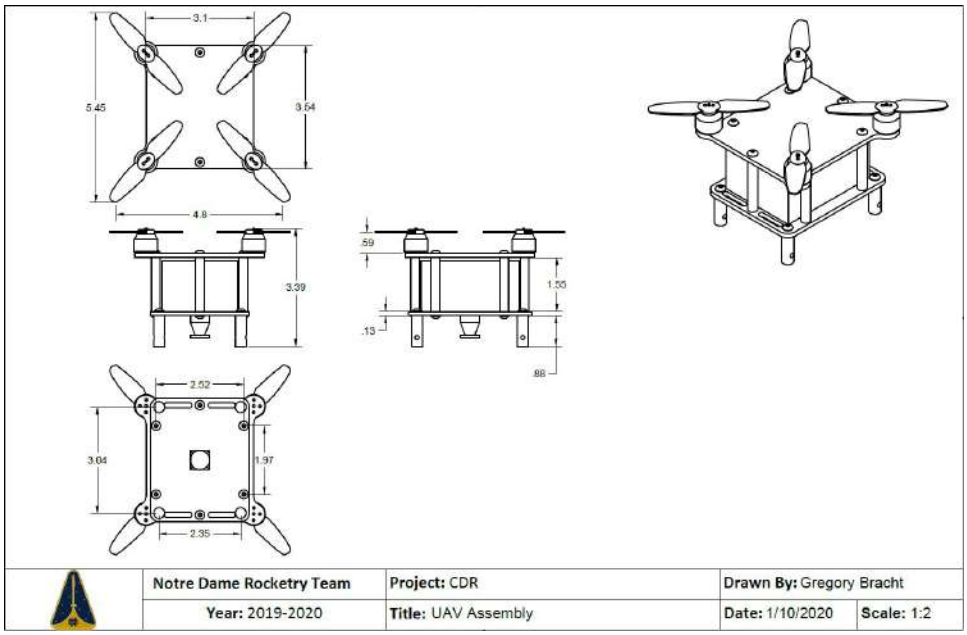

Figure 107: Drawing of UAV Frame

5.4.2 Electrical Design

The UAV is designed around using commercially available electrical components mounted to a custom carbon fiber frame. It includes all components necessary for autonomous flight and communication with the ground station as well as a GPS receiver and a video camera. The UAV receives control signals from the ground station while the camera, GPS, and sensors on-board the UAV transmit data to the ground station.

Table 56: UAV Components List

Component	Selection
Propellers	HQ 3020 3" × 2" Propellers
Motors	RCX H1304 5000Kv Brushless Motor
ESC	Airbot Ori32 BLHeli32 25A 4-in-1 ESC
Battery	Lumenier 3S2P 5000mAh Li-ion Battery
Flight Controller	Airbot Omnibus F4 Nano V6
RC Receiver	TBS Crossfire Nano Rx
Video Transmitter	TBS Unify Pro32 Nano 5G8 400mW Transmitter
Video Transmitter Antenna	Lumenier AXII 2 Right-Angle Stubby 5.8GHz Antenna
Video Camera	Caddx Turbo EOS2 Micro FPV Camera
GPS Module	Matek M8Q-5883 GPS Module

The components listed in Table 56 will be used to construct the UAV. The motors and propellers were selected to output thrust approximately equal to double the weight of the UAV

at maximum power and output thrust roughly equivalent to the UAV's weight at peak efficiency. With a maximum thrust-to-weight ratio of approximately two, the UAV is sufficiently maneuverable to traverse the recovery area quickly and with the motors' peak efficiency located near the speed at which the motors maintain a hover the UAV's flight time is maximized. The battery was selected to maximize flight time by maximizing the capacity of the battery while also keeping the UAV's weight as close to the thrust generated by the motors when operating at their peak efficiency.

The flight controller was selected because it is compact and light, it has a built-in On-Screen Display module that includes sensor data in the video signal, eliminating the need for a separate telemetry transmitter, and it can support enough sensors with its five UART connections and an extra I2C connection to support autonomous flight.Furthermore, it is compatible with Ardupilot flight software, which enables the use of a ground station. The ESCs must be able to supply enough current to the motors while minimizing mass and mounting area. The motors can draw up to 18 amps each, so an ESC that can supply 20-25 amps is ideal. The Airbot Ori32 4-in-1 ESC was selected because it interfaces with the flight controller using an 8-pin cable rather than soldered wires and because it provides the data about the battery voltage and the current drawn by the motors as well as simplifying the wiring configuration of the motors while remaining at approximately the same weight as four individual 20-amp ESCs.

In order to maximize the UAV's flight time, the flight controller will be programmed to wait in an idle state until an enable signal is received from the controller. In this state, current draw to components besides the flight controller is negligible and flight controller current is reduced due to being in an idle state. The ESC, which represents the greatest potential current draw, will not be actively drawing current since it will not be receiving commands from the flight controller during this time.

In compliance with requirement P.12, which establishes a target flight time of 10 minutes, the UAV is projected to have a hover time of just over 15 minutes. The electronics draw about two amps and the motors when hovering draw about four amps each, for a total current draw of approximately 18 amps while hovering. Using a 5000mAh battery, the UAV can hover for about 16.7 minutes before the battery is depleted. The UAV's flight time will be lower than its hover time so the flight time will be measured when the UAV is ready to fly.

The UAV will maintain two connections with the ground station for the duration of its flight, from the time it is powered on at deployment to the its retrieval after the successful completion of the mission. The UAV carries a radio transmitter which maintains a 5.8GHz connection for the camera feed and sensor data as well as a radio receiver which receives control signals from the ground station. The 5.8GHz connection's baud rate is sufficient to carry the video feed transmitted from the UAV to the ground station, while the 915MHz connection requires less power to maintain communications between the UAV and the ground station at the same distance, which reduces energy consumption on board the UAV and improves reliability of the connection while complying with Requirement 2.22.9, which limits the maximum power of any single transmitter to 250mW.

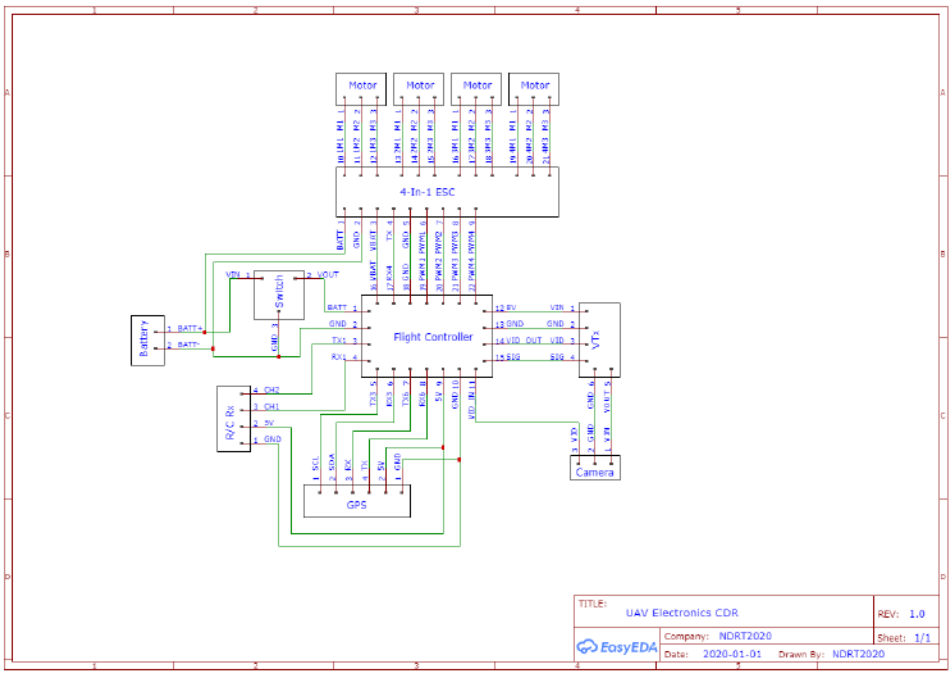

Figure 108: UAV Electrical Schematic

5.4.3 Target Detection

The Target Detection system is responsible for aiding the UAV in finding the location of the Competition Future Excursion Area (CFEA). When the UAV deploys from the rocket, it will fly up and navigate to the CFEA in order to send navigation instructions back to the Rover. In order to create fully autonomous flight, the UAV must be able to fly in a search pattern and identify the CFEA upon capturing an image of it. Directions will be sent to the UAV instructing it to fly in a specified search pattern, and video will be sent back to a ground station to be analyzed in order to detect and navigate towards the target. Two separate algorithms are required for the operation of this system, one that uses computer vision to actually locate the target and one that specifies the flight plan which optimally searches for the target.

5.4.3.1 Detection Algorithm

While flying in a search pattern, the video from the UAV will be constantly analyzed to determine the existence of the CFEA in the frame. This analysis will be done on the ground station using the OpenCV library in Python. In designing this system, the team has relied on footage taken from a drone by last year's team, and will be capturing additional footage in the coming months to further refine the system. An example of this kind of image can be seen in Figure 110.

The images have been collected at various altitudes, from multiple angles, against multiple different backdrops, and in a variety of weather conditions. They have been manually annotated with a program, found in Appendix X which allows the user to specify a polygonal mask by clicking on its vertices. These annotations are then used to create a dataset which can

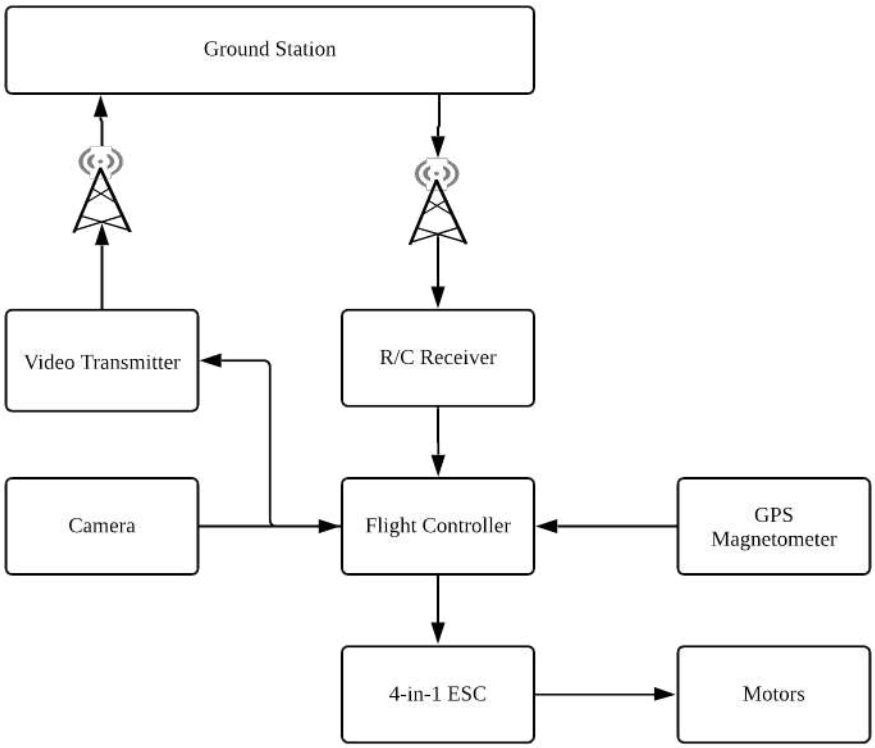

Figure 109: UAV Data Flow Diagram

be used to determine the most effective transformations which can be applied to an input image to create a similar output object mask. This is done using the intersection over union error metric, specified in Equation 32.

$$E = \frac{|A \cap I|}{|A \cup I|} \tag{32}$$

E	Error
A	Set of Pixels in Manually Delineated CFEA
I	Set of Pixels in Algorithm Delineated CFEA

This metric awards algorithms which identify most of the target without identifying areas outside of the target. With this metric, different algorithms and combinations can be directly compared to one another in an empirical way.

The team is considering several different features in the creation of an accurate target detection system. One key feature to consider is color. The CFEA is a distinct shade of yellow, and that shade is different from its surroundings. Because of this, a rough approximation of the location of the target in a frame can be found by considering pixels whose numeric values fall within a certain range. However, there is no guarantee that the standard red, green, and blue (RGB) spectrum is the best color space for this task. Because of this, the team will

Figure 110: A possible target image.

consider alternate spaces as well. For example, the Hue Saturation Value (HSV) space is able to consistently identify similar colors across a range of different brightness levels. Figure 111 illustrates this difference.

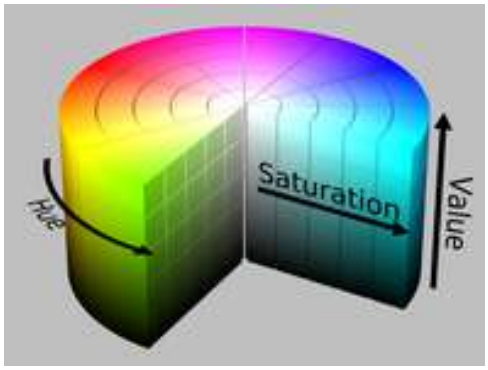

Figure 111: HSV Spectrum.

A yellow tarp, for example, may have a constant hue under widely varying saturations and values. Focusing analysis on the hue channel can make the system more robust. The team will consider every reasonable color space implemented in the OpenCV library. Selection will be limited to the color space that maximizes the intersection over union.

While the color thresholding will be able to give a rough idea of the location of the sample retrieval area, the statistical nature of the analysis will lead to an object mask that is grainy. In order to create a more cohesive image to be better analyzed geometrically, morphological operations are applied to fill in any holes or remove any extraneous pixels. Figure 112 shows an example of this:

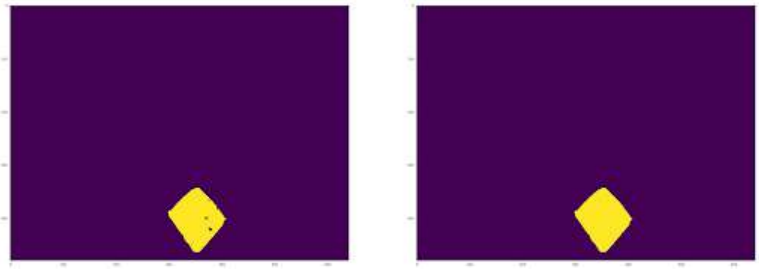

Figure 112: Left: Thresholded image before morphology. Right: Thresholded image after morphology.

Figure 112 was created by applying the dilation, closing, and erosion operations to a color thresholded image. Each of these operations take the form of a convolution with a set kernel. These operations can erode false positive pixels and fill in false negative pixels, leading to a more cohesive image for geometric analysis.

The team will also be analyzing geometric features of the image after color features have been used to create the object mask. In running tests on color detection software, the team noticed that a nearby fence, which had a similar color to that of the target, was registering several false positives for the algorithm. It would detect fence and target and have no way of differentiating the two. This issue could potentially result in the UAV behaving in unexpected and unwanted ways while trying to navigate to the target. In order to circumvent this issue, several geometric features are analyzed. These features include aspect ratio (the width divided by the height of the bounding rectangle), extent (area divided by bounding rectangle area), solidity (area divided by float area), compactness (perimeter squared divided by area), eccentricity (major axis divided by minor axis), and the logarithm of the Hu Moments, a set of features which are transformation-invariant. A square tarp with a circular hole cut in the center has a distinct shape, so machine learning techniques like the support-vector machine can be used to determine the existence of the tarp from its geometric features.

The control flow of the algorithm can be seen in Figure 113.

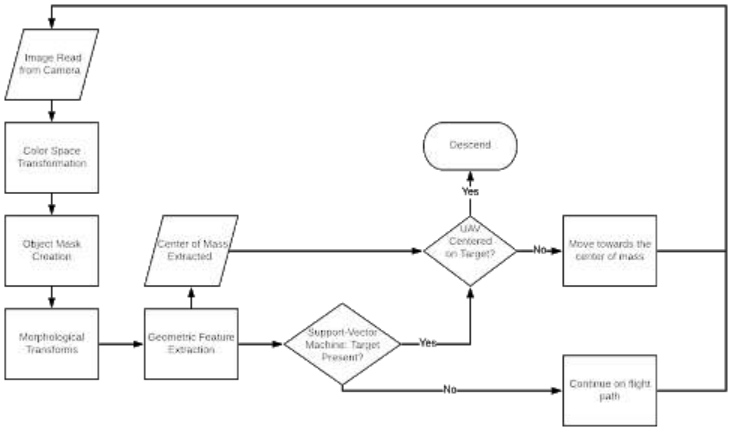

Figure 113: Target Detection control flow.

Figure 113 shows that several transformations are applied to the input image to create the output directions and a decision on the existence of the target. This pipeline can then be integrated with the search algorithm to allow the UAV to reliably locate the CFEA and guide the rover there.

5.4.3.2 Search Algorithm

In order to determine an optimal flight path for the UAV, a Monte Carlo simulation was constructed which scatters five targets randomly around a one mile by one mile field. A “drone” agent is then placed randomly within that field. The agent executes a predefined flight plan

which operates in fixed 5-foot steps. At each step, the agent checks whether a target is within its field of view, and if so the simulation ends, returning the number of steps taken to find a target. Otherwise, the flight path continues until the agent exceeds the bounds of the field. This process is repeated five thousand times for each possible flight path to generate an accurate success rate and search time distribution for each flight path.

For the sake of a lower processing time, a few simplifying assumptions were made. Namely, that the targets and the camera's field of view (FOV) are circular rather than rectangular regions. The circular targets' radius was chosen so as to have an equivalent area to the 10x10 real targets. The camera's FOV was based on the field of view of the UAV camera selected at PDR, the Caddx Turbo EOS2. The simulated FOV angle of 120 degrees is approximately the average of the EOS2's horizontal and vertical FOV angles, respectively 160 and 90 degrees. Finally, a target was determined to be "detected" if its angular size within the camera exceeded 5°, which is the approximate lower bound of the target detection pipeline the team implemented last year.

The team chose three different flight paths as ideal candidates to cover the entire field quickly and completely. All three paths were tested at a fixed height of 40 feet, which was experimentally determined to be the greatest height at which targets could be reliably identified. The first path is a linear sweep of the field, making horizontal passes back and forth across the field's length until the entire field has been scanned. The second path is a spiral proceeding outwards from the center of the field. The final path is a series of "pie slices," proceeding from the center of the field to its edge and back. All three approaches are illustrated in Figure 114.

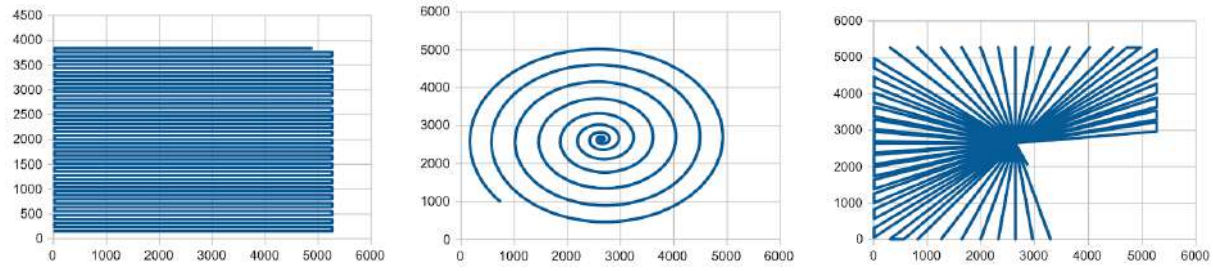

Figure 114: From the left, graphs of the linear sweep, outward spiral, and pie sweep flight paths.

Each path's Monte Carlo simulation was repeated twice, once with a purely random distribution of targets and once with a distribution that forced targets to be at least 1000 feet apart from each other. The results of these simulations were plotted as histograms, which can be seen in Figure 115, Figure 116, and Figure 117.

In short, this summary indicates that the Linear Sweep path has a nearly perfect success rate, while taking between 15,000 and 20,000 steps on average. On the other hand, the Outward Spiral method only has roughly a 50% success rate, in exchange for an average path length of 7,000 to 8,500 steps. The Pie Sweep method has a fairly high, 90% success rate, but takes even longer than the Linear Sweep method. Each "step" is 5 feet long, so even the Outward Spiral method requires approximately 40,000 feet or 8 miles of flight distance to find a target. With

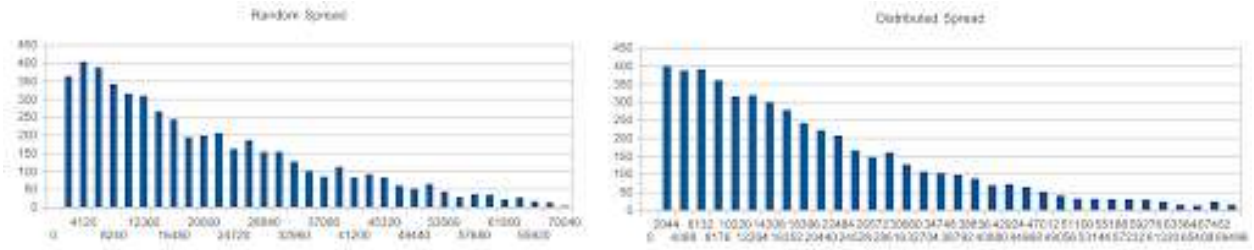

Figure 115: Histograms of Linear Sweep results.

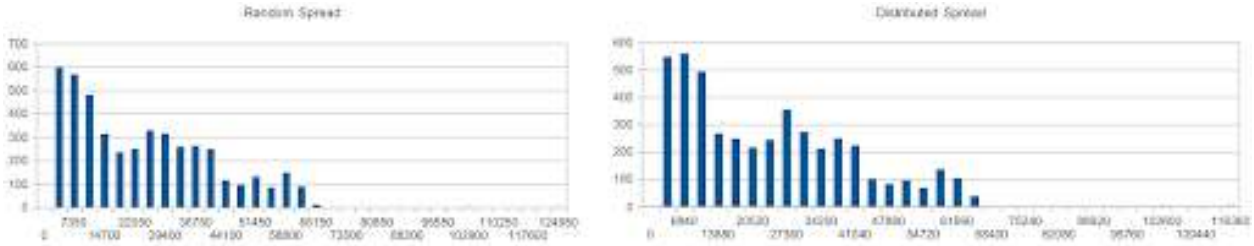

Figure 116: Histograms of Outward Spiral results.

only 15 minutes of flight time, this requires a sustained flight speed of 32 mph or 47 ft/s. While that may be feasible, it pushes the limits of what the mechanical design is expected to achieve with only a 50% chance of success.

Because of this, the team has chosen to implement a more informed search protocol, based on a probability map of the field. This map will identify regions of the field which are likely and unlikely to contain a target. It will be constructed by hand based on aerial photos of the launch site, then cross-checked on the day of launch. The UAV, then, will use GPS to traverse to the nearest likely area, then scan that area with a Linear Sweep flight path. Figure 118 lays out this traversal algorithm in more detail.

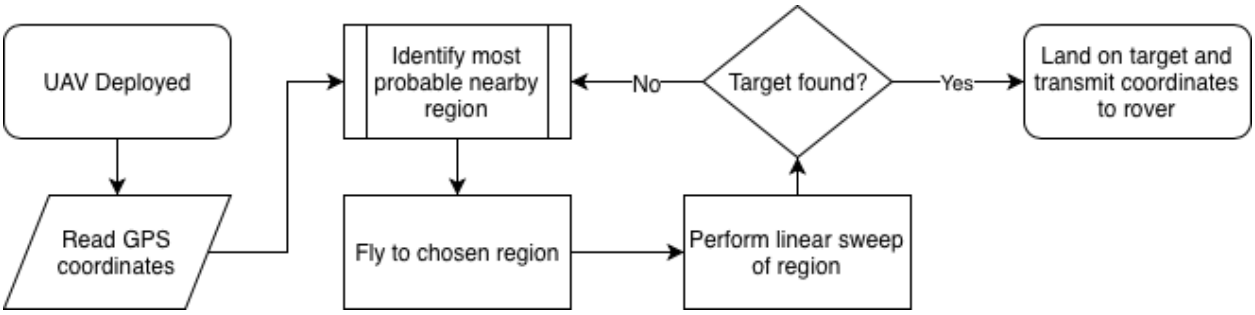

Figure 118: Flowchart of informed search algorithms.

5.4.3.3 Ground Station Relay

The ground station will serve as a command center for both the UAV and the rover, governing both autonomous and manual operations. The primary hardware will be a Raspberry Pi 4B.The Pi was chosen for its processing power, along with its greater user control than microprocessors like the Arduino series and greater hardware compatibility than a PC. It additionally has a relatively low price point. This Pi will be connected to a monitor and

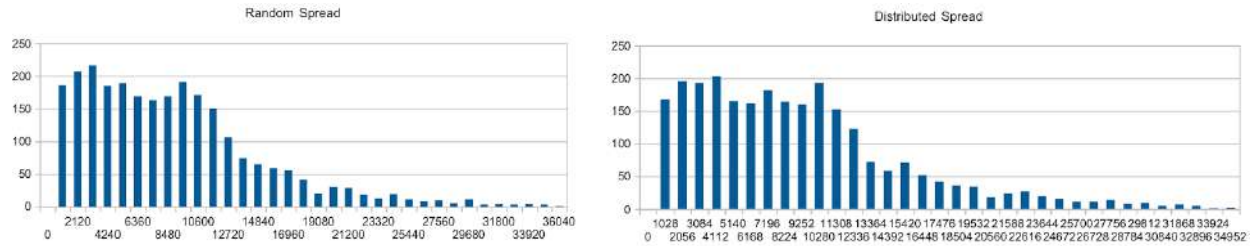

Figure 117: Histograms of Pie Sweep results.

keyboard to display the status of both vehicles and receive user input. It will additionally be equipped with two radio transceivers, one for the rover and one for the UAV. Additionally, it will be equipped with a dedicated receiver for the UAV's video feed. The rover will be using the Adafruit RFM9x long-range radio module, so the ground station will use a second RFM9x module for straightforward compatibility. The RFM9 module is pictured in Figure 129.

As the UAV is using commercial flight controller and radio communication modules, similar modules have been chosen on the ground station for compatibility. The Team Blacksheep (TBS) Crossfire Micro TX has been chosen for primary communications with the UAV. It has built-in telemetry support and is designed for long-range communications. This module will be used with a TBS Diamond antenna, which is designed for communication with low-flying RC aircraft. These devices are shown in Figure 119.

Figure 119: From the left, RFM9x ,TBS Crossfire Micro TX, and TBS Diamond antenna.

Additionally, the ground station will be equipped with the TBS Dominator Rx module, using the included patch antenna. This module is designed for receiving an A/V signal, with the capability to work on a number of different channels. It is pictured in Figure 120.

The primary purpose of the ground station is autonomous control of both the UAV and the rover. Both the target detection and search algorithms detailed in Sections 5.3.3.1 and 5.3.3.2 will be running on the ground station's Raspberry Pi. Control instructions based on those algorithms will be sent to the UAV and rover, using the Mavlink protocol. This is a standard drone communication protocol, and it will be adapted for use by the rover as well. Additionally, if the target detection pipeline executes more slowly than the rate of input from the UAV camera, additional Raspberry Pi 4Bs will be added to the system to form a computing cluster which can process input more quickly.

The Adafruit RFM9x module is designed for line-of-sight communication, which cannot be guaranteed from the fixed position of the ground station. Therefore, this module will use a

Figure 120: TBS Dominator Rx Video Receiver

second TBS Diamond antenna, for improved near-ground communications. Additionally, if testing indicates this system is inadequate, a way station will be implemented for communication with the rover, similar to the system being used with the rocket's telemetry.

The ground station's LCD monitor will display the video feed from the UAV, along with telemetry information from both vehicles. By default, both UAV and rover will behave entirely autonomously, but the ground station will have the ability to switch either vehicle over to manual control. Manual control of the UAV will be accomplished at the ground station via an independent FrSky Taranis X9D Plus 2.4 GHz radio transmitter, pictured in Figure 121. An operator will be able to control the UAV with this transmitter while watching the ground station's incoming video feed.

Figure 121: FrSky Taranis X9D Plus Radio Transmitter

The rover's manual control will be accomplished via a game controller interfaced to a simple arduino uno circuit with an RFM95W transceiver matching the one on the rover. When manual control of the rover is required, the ground station will cease sending commands, allowing a team of operators to walk out to the rover's location and complete the sample retrieval process using the Bluetooth controller. A simple schematic of the manual controller is shown in figure 122.

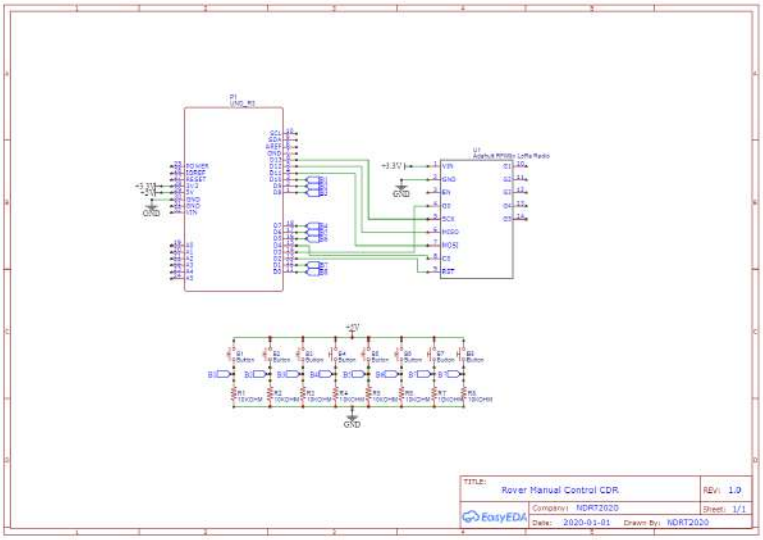

Figure 122: Manual Controller Schematic

5.5 Rover

The rover is a critical part of the payload mission, and is intended to drive the sample retrieval system to the recovery area in order to retrieve a 10 milliliter sample of lunar ice. This year, the team embraced the challenge of designing the rover to autonomously process location data recovered from a UAV in order to navigate to the sample site, similar to how real extraterrestrial payloads must process data from various sources like satellites. The rover is comprised of various subsystems required to provide the mechanical functionality to traverse the launch field, recover the sample, and all necessary electronics for controlling these processes and autonomously responding to data from the UAV or a manual operator.

5.5.1 Mechanical Design

The rover is designed to be strong and lightweight to meet the requirements of the lunar sample recovery mission, which is why the team has chosen the eccentric crank rover as the final mechanical design. No major changes were made to the eccentricity of its motion since PDR. The current overall mechanical design for the rover can be found in Figure 123.

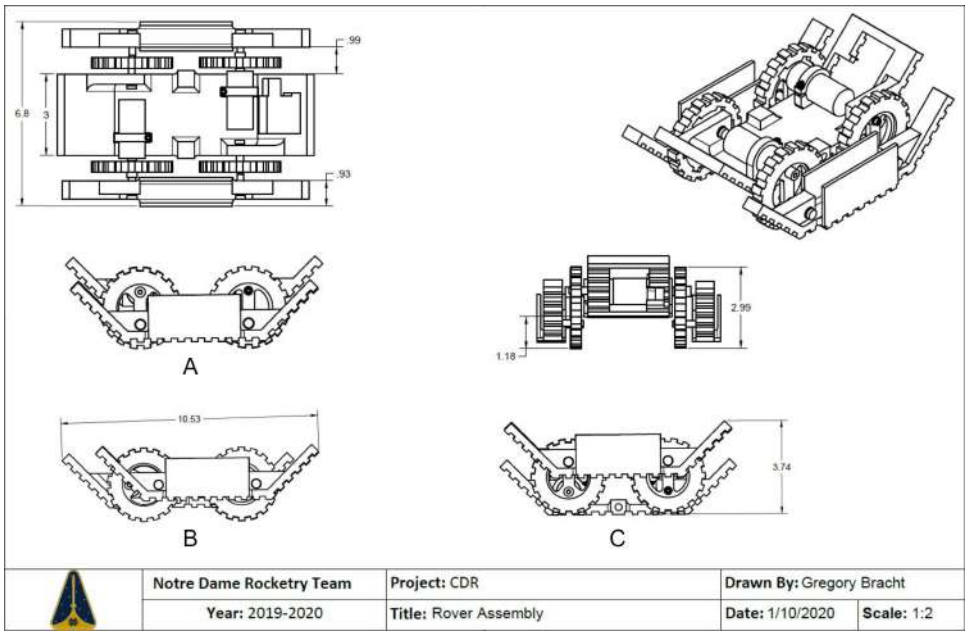

Figure 123: Mechanical Design of the Rover in Translation Configurations

The largest envelope that the rover creates is 6.25 x 10.53 x 3.74 in. An important note to make about the eccentric crank rover is that its envelope is not constant due to its eccentricity. Special care therefore needs to be taken to ensure that the rover can fit securely into the launch vehicle in all of its configurations. During flight the rover will be in configuration C. This position is characterized by the rover body being at its lowest position. This configuration was chosen to best secure the rover with the retention system under the rover.

The design for the main body of the rover consists of a flat section and an angled section at each end. The flat portion in the middle of the body contains the two motors that will be used to drive the rover, along with the electronics that will be used to control it. The motors that have been chosen for the rover are two DC spur gear motors. Table 57 shows important parameters for the selected motors.

Table 57: 98 rpm Econ Gear Motor Parameters

Parameter	Value
Voltage Range	6-18 V
No Load Speed	98 rpm
No Load Current	0.1 A
Stall Current	3.8 A
Stall Torque	524.32 oz.-in.

A DC motor was chosen because of its high startup torque, and relative cheapness. A spur gear motor was chosen, because of the need to have a motor speed of around 60 rpms for the crank wheels. This is a much lower operational speed than a conventional DC motor. This rotational speed was determined based on traveling a max distance of 2,500 ft, within the hour

of allocated time for the sample retrieval. It was determined that having an integrated spur gearing system would be cheaper and lighter than designing an entirely new one. For a DC motor, the torque speed is linear, and it is therefore relatively simple to calculate the operating torque. The method used to calculate the operating torque is seen in Equation 33.

$$T_m = T_s(1 - \frac{\omega}{\omega_f}) \tag{33}$$

Where T_s is the stall torque, ω_f is the no load speed, and ω is the desired operating speed of 60 rpms. From this equation it was determined that each DC motor will have an operating torque of 207 oz-in. For a small and light rover this is more than enough power to drive through the toughest of environmental conditions. These motors are relatively light, and therefore it is acceptable to use an overly powerful motor for the system. In order to hold the motor in place on the rover body, a 25 mm bore clamp will be used. This component was chosen because of its relatively low profile, and easy assembly and disassembly of the rover body. Only one 6-32 screw needs to be tightened to secure the motor, making it a very easy component to handle. To transmit torque from the motor to crank wheel, the hub of the crank wheel will be pressure fit onto the motor shaft. A 4-40 set screw will also be tightened onto the motor shaft to further increase the allowable torque. The team was originally planning on solely using a set screw, but found that due to its small size, it did not have enough holding power. Figure 124 shows how the motor will interface with the crank wheel.

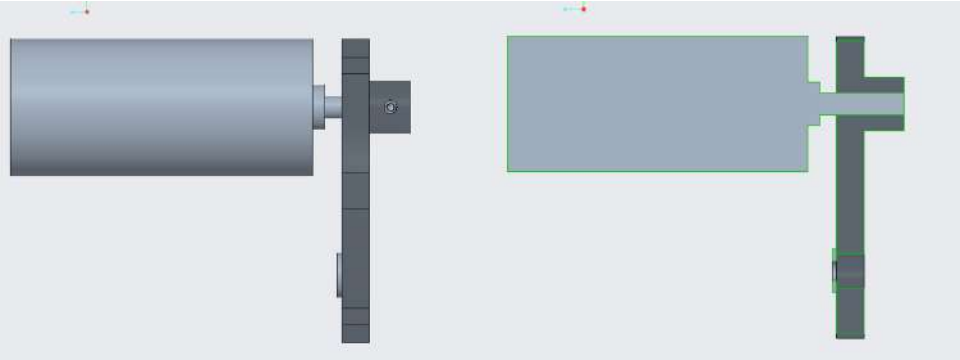

Figure 124: Diagram for how the DC motors will interface with the crank wheel. This system will utilize a pressure fit and set screws to ensure torque transmission.

The body and the two links of the rover will be made out of 3D printed ASA plastic. The team can rapidly prototype the rover body and links with available 3D printers, which is greatly beneficial in the testing process. The team has had prior success utilizing 3D printers in payload design, and is therefore confident in the success of this design criteria. Extensive FEA analysis has also been performed to ensure a safe and successful launch and landing. The body and links have treads designed into the bottom to maximize traction of the system. The terrain the rover will have to traverse to the lunar ice collection site will be muddy, so a treaded system will greatly improve the rover's ability to navigate the terrain.

The crank wheel design is considerably the most complex aspect of the mechanical design of the rover, due to the rigorous environmental conditions that the component will undergo.

The crank wheel will consist of a 6061-aluminum hub fitted with two aluminum shafts. This assembly will be press fit into an HDPE outer wheel, which will also have splines machined into the hub and outer wheel to allow greater transmission of torque. Figure 125 shows an exploded view of the wheel assembly.

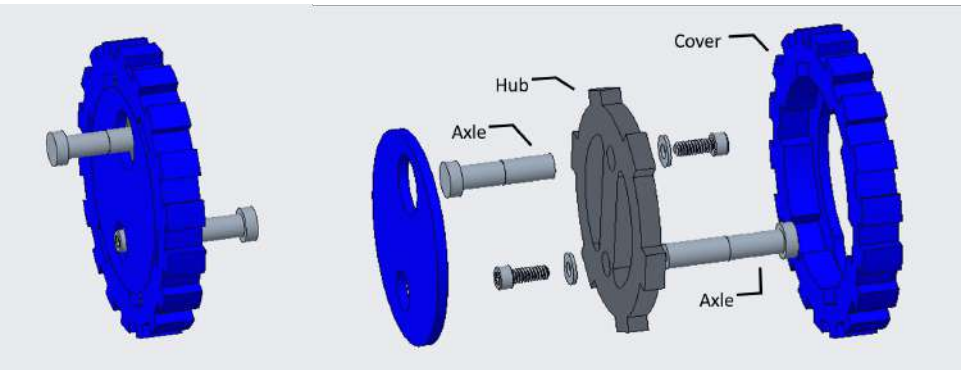

Figure 125: Exploded view of the passive wheel assembly of the motor. Note the splines on the hub and the wheel cover used to secure the assembly together.

As seen from Figure 125 the axles are attached to the hub with a bolt and washer assembly. This was chosen over a more permanent connection for ease of maintenance on the system. It was necessary to make the hub and axles of the crank wheel out of aluminum due to the large accelerations seen from the system during main deployment. Any plastic deformation of the axle during the flight would result in a critical mission failure. The crank wheel will also serve as the attachment point for the payload retention system. Any failure in this system would result in a serious safety hazard to the launch vehicle and others. The higher Young's Modulus and yield strength of aluminum when compared to plastics will greatly mitigate the likelihood of this occurring. 6061 aluminum is also considerably lighter than other materials of similar strengths, such as stainless steel. The outer wheel was chosen to be HDPE largely because the entire wheel assembly could not be made out of aluminum due to weight requirements. HDPE was chosen over 3D printed PLA due to its higher ductility. HDPE will be able to have some plastic deformation, and still be a functional system. To secure the crank wheels to the rest of the rover body, two different methods are being utilized. One is to machine a shoulder onto the crank wheel axle, and the other is placing shaft collars on the axles. Both of these methods fully limit axle motion on its axis.

Due to the rigorous environmental conditions the rover experiences during flight, finite element analysis was performed on many of the components. The Fusion 360 simulation environment was used to perform all analyses. The worst environmental conditions the rover will experience during flight is during main parachute deployment, where the launch vehicle experiences upwards of 37 g's of acceleration. One of the most critical components of the rover is the crank wheel, and for the FEA it was assumed that each crank wheel experiences an equal portion of the acceleration shock load. The hubs outer faces were assumed to be fixed, and this was the only grounded constraint of the analysis. This is a conservative approach, as in reality the outer wheel cover will absorb some stresses, and the hub is not entirely fixed. Two point masses were created to represent the main rover body and link that interact with the crank

wheel. This acceleration was performed for the X, Y, and Z axes individually to ensure that the crank wheel can handle main deployment in all configurations. The results of the FEA can be found in Figure 127.

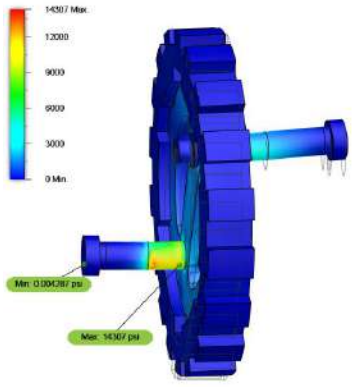

Figure 126: FEA of Crank

The highest stress that the crank wheel experienced in this analysis was 14,307 psi. For 6061 aluminum with a yield strength of 35,000 psi, this results in a safety factor of 2.44. The maximum deflection of the axles was found to be 0.007 inches, which is negligible. Additional FEA simulations were conducted on the links and body of the Rover. The results of the body FEA can be seen in Figure 93 in Section 5.3.1. A 37 g acceleration was used to generate the force experienced by the link and came from the battery located in the slot. Figure 127 shows the results of the FEA.

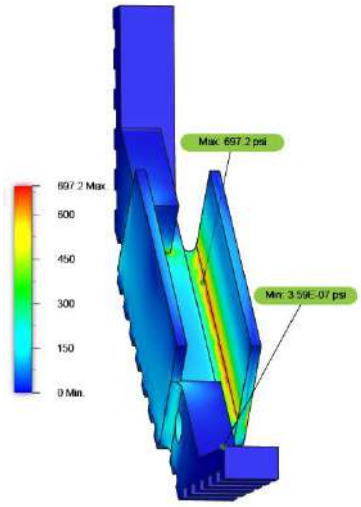

Figure 127: FEA of the Rover Body and Link.

The highest stress experienced in this analysis was 697.2 psi, which results in a safety factor of 7.17 for ASA with a yield strength of 5,000 psi. This safety factor is very conservative. The maximum deflection was found to be 0.003 inches, which is negligible. Beyond FEA, extensive testing will be performed on the rover to ensure it can effectively navigate all the way to the sample sites.

5.5.2 Electrical Design

The rover payload electronics will integrate the system inputs and outputs for control of the payload. The major components consist of: an MCU, an RF transceiver, a GPS module, an IMU, a motor controller and two drive motors, and two sample retrieval servo motors.

5.5.2.1 Microcontroller

The Microchip PIC32MX795F512H was selected as the MCU that will control the rover system. The PIC32 provides 6 UART modules, 4 SPI modules, 5 I2C modules, 5 pulse width modulation (PWM) pins, and a maximum of 53 GPIO pins. This provides ample pins for the rover system, which will utilize one I2C module, two UART modules, one SPI module, and four PWM signals. The PIC32MX will be configured using PICKIT3 programming modules available to the team through the Notre Dame Electrical Engineering design labs and programmed using Microchip's MPLAB X software. A block diagram of the interface protocols used with the PIC32 are shown in figure 128.

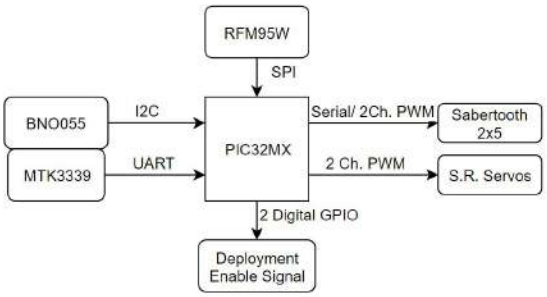

Figure 128: Component Communication

5.5.2.2 RF Transceiver

The rover will receive commands through a Hope RF RFM95W radio module, shown below in figure 129. This module was chosen based on its long range (LoRa) module with a range of 1.25 miles, license-free ISM 915 MHz band operation, 100mW power rating in order to fulfill requirement 2.22.9, and SPI interfacing to the MCU. One module will be integrated into the design of the rover electronics board, and another transmitting module will be used to send signals from the ground station for manual control and delivering the GPS coordinates of the UAV to the Rover.

5.5.2.3 Rover GPS

The MTK3339 GPS module from GlobalTop Technology was selected to provide location information for the rover. This module provides a built in ceramic antenna for tracking from GPS satellites with automatic switching capability and a -165 dBm sensitivity to maintain connection. The 10 Hz refresh rate will be sufficient for the speed of the rover and the 70 mW power rating will allow for longer operation. The GPS module is shown below in figure 129.

5.5.2.4 Rover IMU

The Bosch BNO055 inertial measurement unit (IMU) was selected to collect acceleration and magnetometer measurements. This package allows for multiple sensor measurements to be collected into a single component package over a single I2C interface to the PIC32. The acceleration data will be used to measure if the rover is moving as well as detect orientation prior to deployment. The magnetometer data will be used to determine the compass orientation of the rover in order to correct the orientation and head in the direction of the UAV transmitted GPS coordinate. A strong benefit of this package is that it is designed to perform data fusion of the acceleration and magnetometer data, allowing it to provide tilt-compensated compass data. An external 32kHz oscillator will be used to provide more accurate performance from the BNO055. The BNO055 integrated circuit packaging is shown below in figure 129.

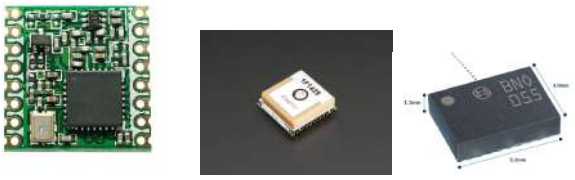

Figure 129: From the left, RFM95W Radio Module, MTK3339 GPS Module, BNO055 IMU

5.5.2.5 Rover Drive Motors and Motor Controller

The Actobotics 98RPM Econ Gear Motor from Servo City was selected to provide actuation for the drivetrain of the rover. These motors were selected due to their small size and high torque of 524 oz-in at stall. The motor draws a mere 0.10 A at no load and 3.8 A at stall, which is lower than many competing options and provides flexibility in choosing from numerous available motor controllers meeting these specifications. Two motors will be used in total, one on each side, and each motor weighs 0.20 pounds. The Econ Gear Motor is shown below in figure 130.

The Sabertooth 2x5 Motor Controller was selected to control the Econ Gear Motors. The Sabertooth 2x5 motor controller was selected to control the drive motors for the rover. This controller can provide 5 amps of continuous current and 10 amps of peak current to two motor channels, which is enough to safely supply up to the 3.8A stall current of the drive motors without burning out the motor controller. The motor controller has a voltage rating of 6-18V, which exactly matches the accepted input range for the selected motor. This motor controller also provides flexibility in control methods, as the board can receive commands via either pulse width modulation (PWM) signals or a serial interface sending a set of bits identifying the speed at which to run each motor. The Sabertooth also incorporates circuit protections to avoid operation while overheating or drawing too much current. The Sabertooth can be seen below in figure 130.

Because the Sabertooth operates at 5V and the PIC32 operates at 3.3V logic, a logic shifter is being used to ensure compatibility between the two devices. The Texas Instruments

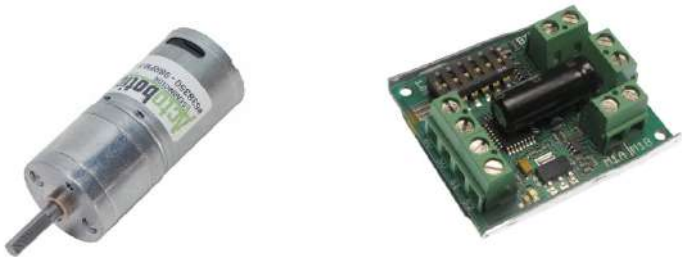

Figure 130: From the left, Econ Gear Motor and Sabertooth 2x5 Motor Controller

SN74LVC8T245 8-Bit dual-supply bus transceiver with configurable voltage-level shifting has been selected to provide this logic shift. This will safely allow serial communication between 3.3V and 5V devices. This chip provides 8 channels, of which 6 will be used. Two channels will be used for the serial communication with the Sabertooth, two channels will be configured to PWM pins for the Sabertooth as an alternative control option, and two channels will be used to send PWM signals to the servo motors used for the sample retrieval, which rely on 5 V signals.

5.5.2.6 Rover Power System

The nominal operating voltage of the selected motors is 12V, with an input range of 6-18V. Hence an 11.1V battery was selected for the Rover. The Rover will be powered by two 11.1V batteries, with one battery mounting on each side rail to distribute weight as described in the mechanical design. Tenergy 11.1V Li-Ion batteries with a 2600 mAh and 5A continuous current rating were selected. This decision was based on the nominal voltage of the motor, the 5A current rating which matches the Sabertooth rating and is over the 3.8A stall current of the motors, providing safety against over-current draw damaging the batteries and causing a safety hazard.

The PIC32 and connected components run at 3.3V logic while the sample retrieval servo motors run at 5V. Thus, voltage regulation is required to power the circuit components off of the 11.1V of the batteries. Due to the large difference in voltage, between 11.1V and 3.3V or 5V, a linear voltage regulator would provide inefficient and reduce the run time of the system. A DC-DC buck converter provides voltage regulation with a much higher efficiency, with the drawback of additional components required to filter noise produced by the switching frequency of the converter. The LM2596 has been selected to provide the voltage conversion and regulation for 3.3 and 5V. The LM2596 operates at a 150kHz switching frequency and can convert voltages from a range up to 40V and supply up to 3A which is sufficient for the battery and circuit components.

A table of the major operating currents of the rover are found in table 58. The average current draw of the rover while driving is 4184.4 mA. Given the 5200 mAh total capacity of the two batteries, this gives the system an approximate run-time of 75 minutes while driving at a half-stall load on the motors. When idle, the motors draw only 10mA, resulting in a total current draw of 194.4 mA and an idle run-time of 26 hours which is more than sufficient for

remaining idle on the launch pad prior to launch.

Table 58: Rover: Estimated Power Budget

Device/State	Current Draw (mA)
PIC32MX	120
LM2596-3V	10
LM2596-5V	10
BNO055	12.3
MTK3339	20
RFM95W	12.1
2x Motors: half-stall	4000
Total Current:	**4184.4**

5.5.2.7 Circuit Integration

To integrate the various components of the rover electronics, a custom PCB has been designed. The design schematics can be seen below in figures 131, 132, and 133.

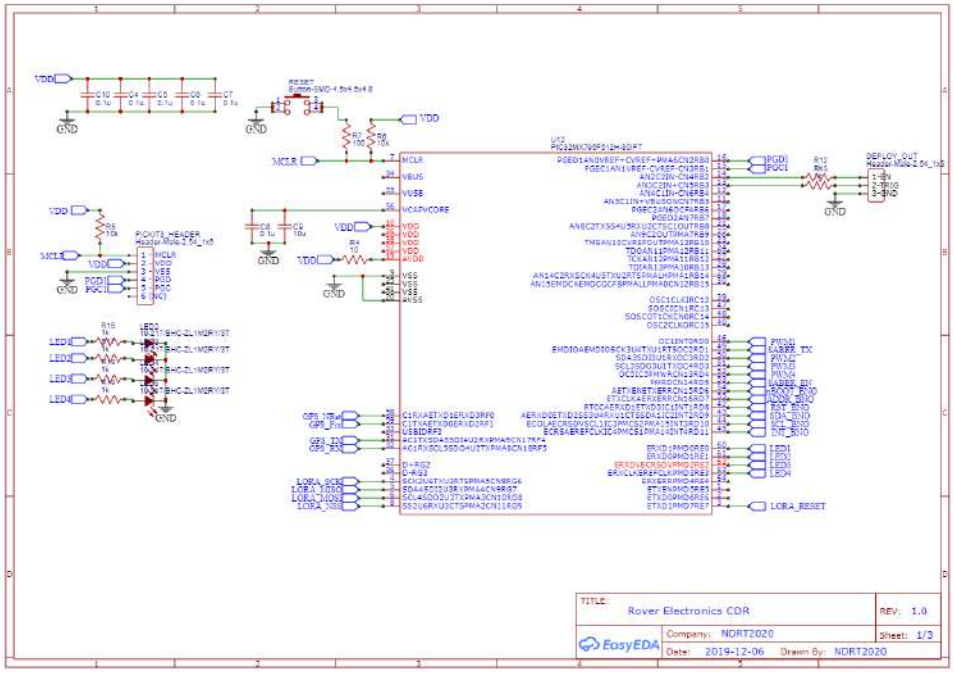

Figure 131: PIC32 Primary Connections Schematic

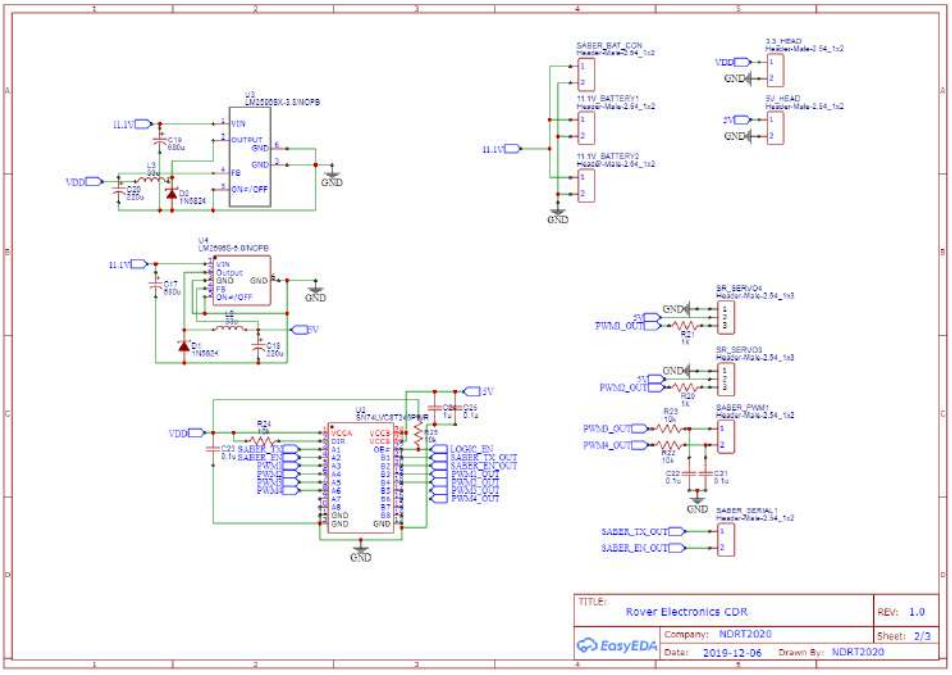

Figure 132: Rover PCB Power Subsystem

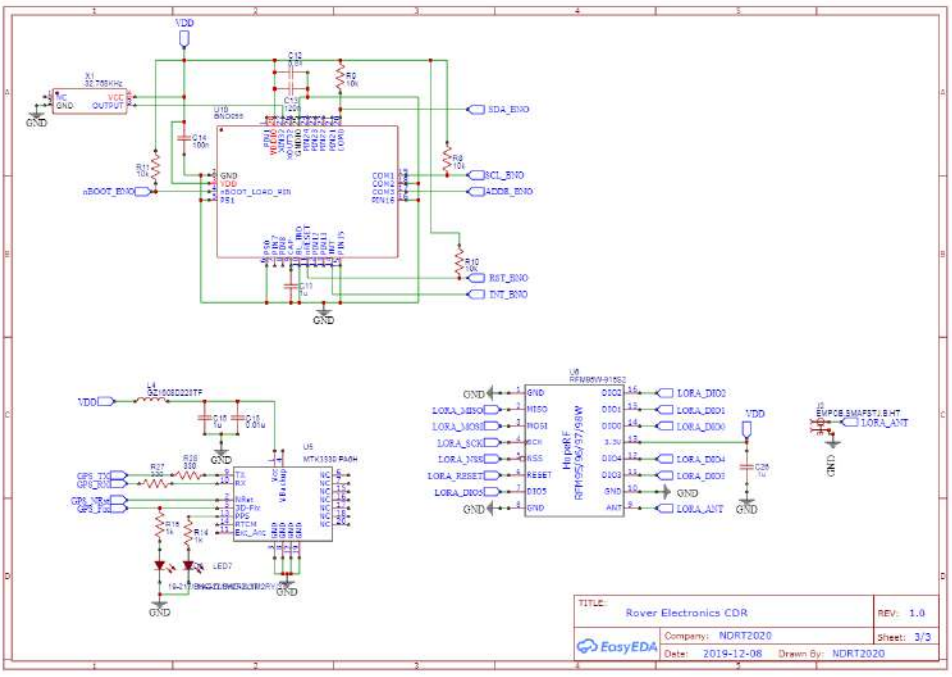

Figure 133: Rover PCB Sensors and Radio Subsystems

5.5.3 Sample Retrieval System

The Sample Retrieval subsystem will be comprised of an Archimedes screw, shown in Figure 134, integrated into the front end of the Rover to gather the lunar ice sample. The screw will be

deployed out of its case using a rack and pinion system into the sample site. It will then rotate based on a PWM signal from the rover processor. The sample will proceed up the screw as it rotates, to be deposited in an enclosed collection bin underneath it.

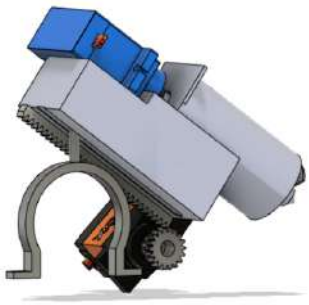

Figure 134: CAD of Sample Retrieval Subsystem

Archimedes screws are historically used with transporting fluids. For this project, the lunar sample is assumed to act fluid-like as it moves across the Archimedes screw. This assumption is grounded upon the fact that the lunar sample is taken to be small, lightweight, with a smooth, low friction surface. These 'grains' of the sample will then be fluid-like. The aforementioned assumption regarding the nature of the lunar sample will be tested to ensure the screw's ability to collect and transport a sample.

5.5.3.1 Archimedes Screw

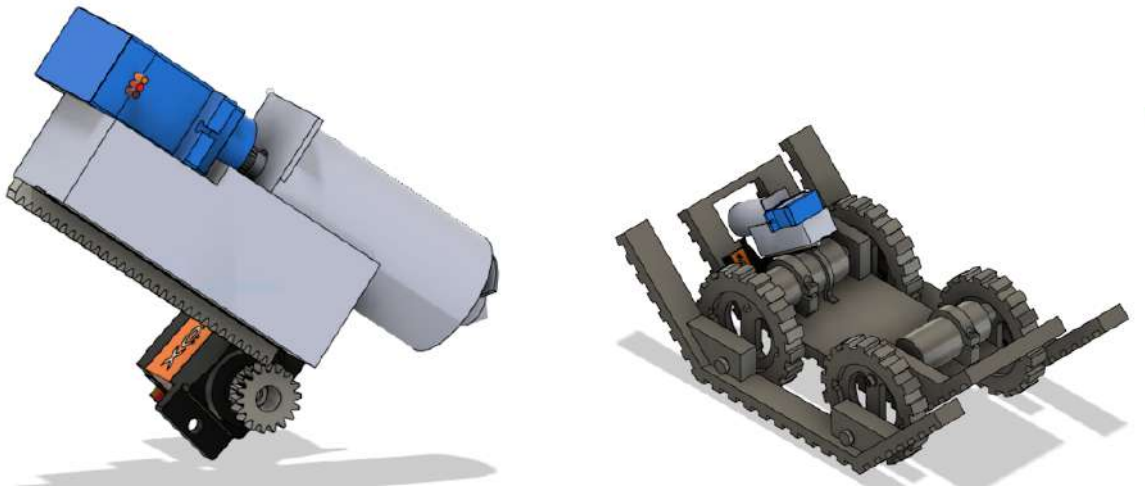

Figure 135: CAD of Archimedes Screw

An Archimedes screw is a helical screw inside a hollow casing (like a tube). These screws have several buckets, bounded pockets of volume along the blade and the tube, that can hold and

translate fluid. One turn of the shaft connected to the screw collects water in the first bucket. As the screw is rotating, the water will travel up to the following buckets (away from the tip of the screw) and more water will be collected in the first bucket. The water will move up the buckets until it exits from the top of the screw. For this subsystem, the sample will be deposited in a hollow box once it reaches the top.

The volume calculation of this hollow box was conducted through a SolidWorks internal region analysis. The volume of the hollow box is 10.26 cubic centimeters. A cubic centimeter is directly identical in volume to a milliliter. Therefore, the (hollow) box volume of 10.26 cubic centimeters is sufficient to store the 10 mL of sample required per NASA Requirement 4.3.3.

5.5.3.2 Rover Integration and Operation

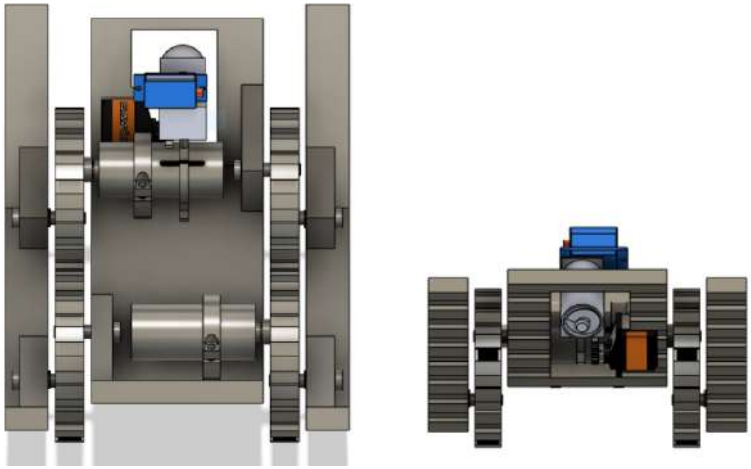

Figure 136: CAD of Archimedes Screw Views

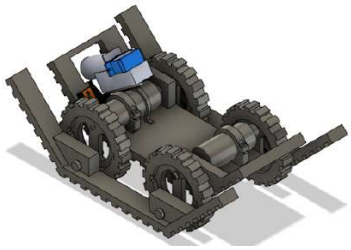

Figure 137: CAD of Archimedes Screw Vehicles Integration

The Archimedes screw will be deployed using a rack and pinion system. A rack and pinion system turns the rotational motion of the pinion into translational motion for the rack. The pinion gear is attached to a high torque motor that is embedded in the front side of the rover base plate. The rack is attached underneath the hollow box of the screw. As the pinion turns, the screw moves down towards the sample. The screw system is supported on the right by a peg

attached to the rover base. Once in contact with the sample, the Adafruit continuous motor will rotate the screw picking up the sample and forcing it to travel up the blade and the case. Then, the sample will fall into the hollow box underneath the tube through a hole situated at the top. This storage method will make the sample easy to contain and transport. Once the screw has collected the 10 milliliters, the pinion will rotate the opposite direction to retract the screw back into the rover.

5.5.4 Rover Software

Software for the rover will be hosted on the PIC32 processor controlling the rover. The software shall be written and compiled in the C language using Microchip's MPLABX program designed to interface with PIC processors. A PICkit3 in-circuit debugger will be used to program the PIC32 and debug the software during testing.

5.5.4.1 Control Flowchart

The rover will go through a few different stages during the mission. Initially, the rover will be in an idle state, secured in the launch vehicle. The rover will use the on-board accelerometer to determine that the launch vehicle has landed, enabling the receiving of a deployment signal with a specific code over radio. This will result in a signal from the rover's PIC32 to the retention electronic system's Itsy Bitsy processor initiating deployment by retracting the retention solenoids and allowing the rover and UAV to drive out of the launch vehicle. As the vehicle departs the launch vehicle, quick disconnect wire connectors that attach the rover to the retention electronics will be pulled apart by the rover departing the launch vehicle, allowing it to leave unobstructed.

After departing the launch vehicle, the UAV will begin its mission sequence. During that time, the Rover will initiate and confirm sensor readings function nominally. If sensors fail, red LEDs on the rover will indicate the need to enter manual control mode which will be done using a manual controller. If sensors are nominal, the rover awaits a confirmation signal from the ground station with GPS coordinates of the UAV at the sample area.

Once the GPS coordinates are retrieved, the rover software will calculate the necessary heading needed for the rover to reach the target area. A simple proportional-integral controller will be used to respond to the error between the current heading measured by the BNO055 and the needed heading. The rover will begin traveling toward the sample area until GPS indicates the rover has reached the sample area where it will initiate the sample retrieval process. Once complete, the rover will drive until GPS indicates the rover has traveled outside the area. A flowchart for the control system can be seen below in figure 138.

5.5.4.2 Rover Compass Heading Calculation

Using the GPS coordinates provided by the UAV and the ones recorded by the GPS module on board the rover, the rover software will calculate the necessary bearing using the formula in equation 34.

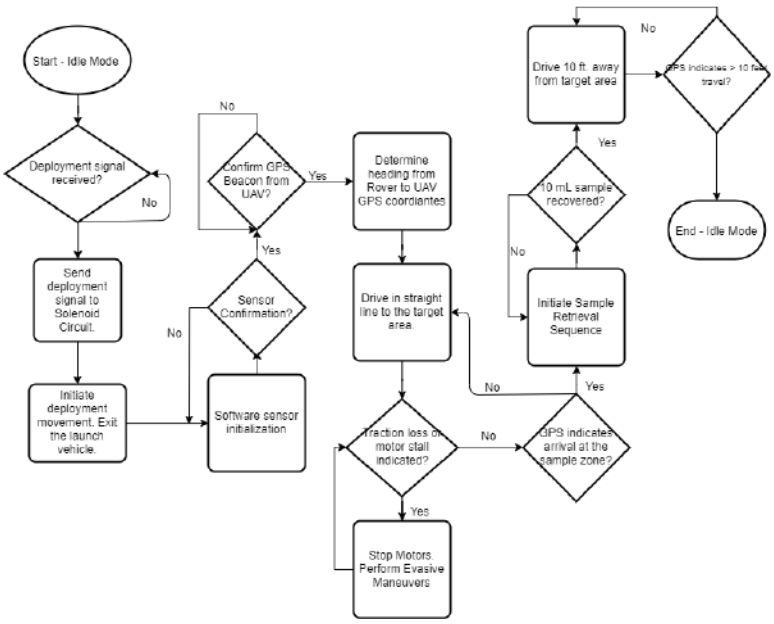

Figure 138: Rover Software Control Flowchart

$$\theta = \text{atan2}(\sin(\Delta\lambda) * \cos(\phi_2), \cos(\phi_1) * \sin(\phi_2) - \sin(\phi_1) * \cos(\phi_2) * \cos(\Delta\lambda)) \tag{34}$$

Where ϕ_1,λ_1 is the start point, ϕ_2,λ_2 the end point, and $\Delta\lambda$ is the difference in longitude. The on board BNO055 inertial measurement unit will be used to calculate the current heading of the rover. The BNO055 shall be configured and calibrated in the COMPASS mode as outlined in section 3.3 of its datasheet. This will allow the BNO055 to fuse data from the magnetometer and accelerometer to provide tilt compensated compass data for calculating heading by taking the inverse tangent of the X and Y components of the magnetometer data.

Once the BNO055 has calculated the rover heading, a simple proportional-integral controller will be used to determine the appropriate response of the rover motors to the error of the current heading and the desired heading for the sample retrieval site.

6 Project Plan

6.1 Testing

The testing plans and progress for each subsection are summarized in Table 59. Testing manuals for each test are included in Sections 6.1.1-6.1.6

Table 59: Testing Plan

System	Test	Test ID	Requirements Verified	Status
Launch Vehicle	Subscale Wind Tunnel Testing	LVT1	2.17.1	Pass
	Subscale Launches	LVT2	2.17.1	Pass
	Bulkhead Solids Testing	LVT3	2.4	Incomplete
	Full Scale Vehicle Test Flight	LVT4	2.18	Incomplete
	Shake Test	LVT5	2.4	Incomplete
	Center of Gravity Test	LVT6	2.18	Incomplete
Recovery	Black Powder Testing	RT1	3.2	Incomplete
	Altimeter Testing	RT2	3.4	Incomplete
	Telemetry Range and Antenna Test	RT3	2.18.2	Incomplete
Payload: Deployment	Free Rotation of Platform	PDT1	P.21	Incomplete
	Solenoid Actuation	PDT2	P.22	Incomplete
	Vibration & Motion Restriction of Rover and UAV	PDT3	P.22	Incomplete
	Deployment of Rover and UAV	PDT4	P.22	Incomplete
Payload: UAV	Manual Flight	PUT1	P.14	Incomplete
	Autonomous Flight	PUT2	P.13	Incomplete
	Trnsmit Video to G.S.	PUT3	P.23	Incomplete
	Detection of Simulated CFEA	PUT4	P.23	Incomplete
	Landing Location Identification	PUT5	P.24	Incomplete
	Detection of CFEA with UAV	PUT6	P.23	Incomplete
Payload: Rover	Electrical Connections	PRT1	P.4	Incomplete
ABS	Subscale Launch	ABT1	V.4	Pass
	Mechanism and Motor Ground Testing	ABT2	V.4	Incomplete
	Control Structure Ground Testing	ABT3	V.4	Incomplete

6.1.1 Launch Vehicle Testing

LVT1: Subscale Wind Tunnel Testing

Objective:

To obtain an experimental drag coefficient for the launch vehicle with air braking tabs at (1) no extension, (2) half-extension, and (3) full-extension. Drag may be scaled to model full-scale vehicle flights.

Tested Items:

- Sub-scale vehicle with no tab extension (no actuation)
- Sub-scale vehicle with half tab extension (half-actuation)
- Sub-scale vehicle with full tab extension (full-actuation)

Motivation:

- To ensure that the subscale launch vehicle can withstand the wind conditions it may face during testing
- To calculate the airspeed around the rocket, the induced drag, the drag coefficient, and Reynold's number.

Success Criteria:

Table 60: Test ID Success Criteria

Requirement ID	Description	Pass/Fail Criteria	Result
2.17.1.	The subscale model should resemble and perform very similarly to the full-scale model.	Success - Dimensionless parameters, such as coefficient of drag, are consistent between wind tunnel and simulated data. Fail - Wind tunnel data is inconsistent with theoretical and subscale data.	Pass

Test Procedure:

Equipment:

- 2 ft x 2 ft x 6 ft subsonic tunnel in Hessert Laboratory with test article mount (see schematic in Figure 26)
- Aerodynamics Lab DAQ Utility
- Sub-scale vehicle
- 3D printed ring simulating unactuated air braking tabs
- 3D printed tabs simulating air braking tab half-actuation
- 3D printed tabs simulating air braking tab full-actuation
- 3D printed bracket

Setup:

1. Create CAD model of bracket to mate with the test article mount inside the wind tunnel (used to suspend the launch vehicle in the subsonic wind tunnel)
2. 3D print bracket
3. Epoxy bracket inside the body tube of the launch vehicle
4. Perform nine 10-second tests per level of actuation (no tabs, half tabs, and full tabs)

Safety Notes:

- Ensured subscale test article was completely intact via visual and shake tests for damage
- Ensured test section was clear
- Ensured wind tunnel door was sealed shut prior to running tests
- Team members stood at a safe distance from the wind tunnel when testing was underway

Procedure:

1. Attach 3D printed ring simulating unactuated air braking tabs to the subscale vehicle
2. Insert vehicle into wind tunnel, parallel to the flow
3. Connect the epoxied bracket on the launch vehicle to the test article mount inside the wind tunnel
4. Close the wind tunnel door, ensuring its seal
5. Team members step away from door
6. Increase wind tunnel airspeed speed to ~1.3 m/s under the supervision of NDRT graduate advisor, Emma Farnan
7. Record data at given speed for 10 s
8. Increase wind tunnel airspeed speed to ~3.6 m/s under the supervision of NDRT graduate advisor, Emma Farnan
9. Record data at given speed for 10 s
10. Increase wind tunnel airspeed speed to ~7.5 m/s under the supervision of NDRT graduate advisor, Emma Farnan
11. Record data at given speed for 10 s
12. Increase wind tunnel airspeed speed to ~11.6 m/s under the supervision of NDRT graduate advisor, Emma Farnan
13. Record data at given speed for 10 s
14. Increase wind tunnel airspeed speed to ~15.7 m/s under the supervision of NDRT graduate advisor, Emma Farnan
15. Record data at given speed for 10 s
16. Increase wind tunnel airspeed speed to ~20.0 m/s under the supervision of NDRT graduate advisor, Emma Farnan
17. Record data at given speed for 10 s
18. Increase wind tunnel airspeed speed to ~24.2 m/s under the supervision of NDRT graduate advisor, Emma Farnan
19. Record data at given speed for 10 s
20. Increase wind tunnel airspeed speed to ~28.6 m/s under the supervision of NDRT graduate advisor, Emma Farnan
21. Record data at given speed for 10 s
22. Increase wind tunnel airspeed speed to ~32.9 m/s under the supervision of NDRT graduate advisor, Emma Farnan
23. Record data at given speed for 10 s
24. Decrease wind tunnel airspeed to 0 m/s under supervision of NDRT graduate advisor, Emma Farnan
25. Disconnect launch vehicle from test article mount
26. Remove launch vehicle from wind tunnel
27. Attach 3D printed tabs simulating air braking tab half-actuation to subscale vehicle
28. Repeat steps 2-26
29. Attach 3D printed tabs simulating air braking tab full-actuation to subscale vehicle
30. Repeat steps 2-26
31. Shut down wind tunnel under supervision of NDRT graduate advisor, Emma Farnan

Results: The tests involving tab extensions yield meaningful data. The data collected showed that the tabs had a negligible effect on drag. In some cases, the tabs reduced drag. Reasons for

the discrepancy include noise and a thick boundary layer due to low speed winds (testing had a maximum airspeed of 32.9 m/s while subscale simulations had a maximum airspeed of 89.9 m/s). Data collected for the drag coefficient of the launch vehicle itself is useful because the thick boundary layer launch vehicle does not affect the rocket in its entirety.

LVT2: Subscale Launches

Objective:

Verify the stability and geometry of the launch vehicle.

Tested Items:

- Sub-scale launch with no tab extension
- Sub-scale launch with half tab extension
- Sub-scale launch with full tab extension

Motivation:

- To verify the flight characteristics of the proposed launch vehicle
- To verify the effectiveness of the ABS drag tabs

Success Criteria:

Table 61: LVT2 Success Criteria

Requirement ID	Description	Pass/Fail Criteria	Result
2.17.1.	The subscale model should resemble and perform very similarly to the full-scale model.	Success - The subscale vehicle is launched and recovered AND is undamaged and relaunchable. Fail - Launch vehicle becomes damaged due to launch or recovery such that it cannot be launched again in the same day OR launch vehicle deviates significantly from expected launch profile.	Pass

Test Procedure:

Equipment:

- Subscale vehicle
- Launch rail
- Subscale Motor

Setup:

1. Attach recovery shock cord to fin can and bottom of recovery tube
2. Insert fire retardant, biodegradable insulation into top of fin can
3. Fold parachute and insert into top of fin can
4. Join fin can and recovery tube via coupler for a friction fit
5. Insert motor into motor mount and secure with motor retainer
6. Activate sensors and insert into top of recovery tube
7. Join payload tube and recovery tube via coupler and secure with set screw

Safety Notes:

- Only launch manager can handle motor
- Listen to RSO instructions at all times

Procedure:

- Slide rail buttons onto launch rail, and set launch rail pitch
- Secure ignition wiring onto motor
- Launch vehicle
- Recover landed vehicle and retrieve flight data from sensors

Results: The subscale launch vehicle successfully launched and landed for three separate flights on December 7, 2019. Altimeter data for each sensor was collected and the vehicle followed the expected flight path. Full subscale results can be seen in Section 3.6.3.

LVT3: Bulkhead Solids Testing

Objective:

To verify bulkhead material selection for strengh to withstand respective forces.

Tested Items:

- 0.25 in. plywood bulkhead
- 0.125 in. G10 fiberglass bulkhead

Motivation:

- To guide decision on bulkhead material selection
- To ensure that bulkheads can sustain their intended loads without damage

Success Criteria:

Table 62: LVT3 Success Criteria

Requirement ID	Description	Pass/Fail Criteria	Result
2.4	Vehicle must be able to be recovered without damage and relaunched in the same day.	Success - Strength properties of various bulkhead materials are verified AND suitable material choices are confirmed. Fail - Strength properties of various bulkhead materials are not verified OR improper material choice was made based on load results.	Incomplete

Test Procedure:

Equipment:

- Carbon fiber couplers with bulkheads to be tested epoxied inside
- Load frame

Setup:

- Mix epoxy and spread out in a ring in the coupler
- Slide bulkhead over ring
- Fillet each side of the seam with epoxy
- Leave to dry for 24 hours

Safety Notes:

- It is unsafe to handle epoxy without gloves
- Stand a safe distance away from the force frame while testing is underway, as coupler and bulkhead have potential to break

Procedure:

- Load coupler and bulkhead onto force frame
- Gradually increase force upon bulkhead until signs of structural failure show, such as cracked bulkhead or separation at the epoxy seam
- Record force at failure
- Repeat for each bulkhead

Results: Results to be collected 01/15/2020 - 01/24/2020.

LVT4: Full Scale Test Flight

Objective:

To validate the launch vehicle's stability, structural integrity, recovery systems, payload systems, and the team's ability to prepare the launch vehicle for flight.

Tested Items:

- Vehicle airframe performance
- ABS performance
- LSRS performance
- Telemetry module performance
- Recovery system performance
- Launch procedure streamline

Motivation:

- To ensure a successful mission with all requirements met and all subsystem designs validated

Success Criteria:

Table 63: Test ID Success Criteria

Requirement ID	Description	Pass/Fail Criteria	Result
2.18	All teams will complete demonstration flights as outlined in Req. 2.18.1-2.18.2.4	Success - Launch confirms that hardware is functioning properly AND flight is stable AND no damage is sustained AND payload system accomplishes simulated mission. Fail - Hardware does not function properly OR flight is unstable OR damage is sustained OR payload is not flown OR payload does not accomplish mission successfully	Incomplete

Test Procedure:

Equipment:

- Nose cone
- Payload bay
- Transition Section
- Recovery Tube
- Fin can
- Shear pins
- Locking screws
- Motor (2)
- Motor Casing
- Motor Retainer
- Eyebolts
- Camera
- Washers
- Nuts
- Screws
- Motor retainer

Setup:

- Inspect each body tube for deformations or cracks to ensure there is no damage
- Check adhesives and connectors at each connection to make sure they are strong
- Inspect fins for any cracks or deformations
- Recovery Integration (See Recovery Checklist)
- Insert ABS into fincan by matching the notches to the internal dowel rod in the body tube
- The removable bulkhead at the top of the system is then secured using four button head screws.
- Inspect the drag tab cutouts in the fin can to ensure that the tabs are visible and have clearance to extend
- Place one 10 washer and lock nut on each of the threaded rods at the top of the forward ABS bulkhead to secure them to the fin can
- Inspect through the barometric vent holes to ensure that the LEDs are still lit and indicate the system is not prematurely in the launched state
- If the LEDs indicate a premature launched state, the system must be removed and reset.
- Make a final inspection of the system's installation for any obvious defects or abnormalities
- Attach loose end of drogue shock cord to the ABS top bulkhead eyebolt
- Secure fin can to recovery tube using shear pins
- Use twist to lock mechanism to screw telemetry system into nose cone
- Secure the lock by aligning the two eye bolts and tying them with Kevlar cord
- Slide sliding payload platform into slots on stationary platform
- Thread nuts and bolts through holes on platform
  The next steps should ONLY be performed by the Launch Manager Dave Brunsting. Gloves and safety glasses should be worn.
- Create one ejection charge using an e-match and black powder. Ensure that the e-match loose wires are shunted together to prevent accidental ignition of the black powder
- Re-check to ensure that the battery box switch is in the "off" position
- Connect the loose ejection charge wire to its corresponding lever wire
- Place the ejection charge in its corresponding PVC charge well
- Cover each charge well with painters tape to keep the charge in place
- Ensure all wire holes are plugged with sealing clay
  This concludes the steps that must be performed by the Launch Manager
- Press fit nose cone between the sliding bulkhead and the inner diameter of the payload bay body tube. Be careful to align the shear pin holes.

- Place shear pins in holes
- Insert the MicroSD card into the back of the camera
- Press power button
- Wait for steady yellow light from camera
- Press the recording button (button with the camera symbol).
- If camera is flashing yellow, then the camera is recording
- Insert the camera into the transition section slot so that the lens is facing downward
- On the edge closest to the lens, place three small washers and loosely fit a lock nut onto the tie rod
- On the edge further from the lens, place the medium washer and then two small washers and loosely fit the lock nut on the tie rod
- If the camera does not fit, or has too much space to move, repeat previous four steps
- If a proper fit is achieved, tighten the lock nuts with crescent wrench
- Perform shake test of assembly to ensure secure connection
  The next steps should ONLY be performed by the Launch Manager Dave Brunsting. Gloves and safety glasses should be worn.
- Remove the motor from its packaging
- Check that the motor is properly assembled according to manufacturer's instructions and inspect the motor for defects
- Insert the propellant into the casing, ensuring that the two spacers precede the propellant
- Screw on the rear closure
- Insert the motor into the rocket, ensuring proper motor direction
- Attach the motor retainer
- Check for a secure fit
  This concludes the steps that must be performed by the Launch Manager
- The Cg and stability check should be performed by the Vehicles lead
- Perform center of gravity (Cg) test to ensure the center of gravity matches the simulated Cg by placing the fully assembled vehicle on a thin wooden stand so that it is cantilevered on both sides. Move the vehicle until it perfectly balances.
- Mark the measured Cg and simulated Cg on the vehicle
- Mark the simulated center of pressure (Cp) on the vehicle
- Ensure calculated stability corresponds to predicted value
- Ballast as necessary to maintain a stability margin of >2 calipers or within 10% of predicted margin (whichever is greater)
- Register with LCO and RSO at the launch site
- Lower the launch rail such that it is parallel to the ground
- Align the rail buttons with the rail and slide the vehicle onto the rail with the fin can towards the ground
- Set rail angle to be perpendicular to the ground with an added maximum 7 degrees into the wind
- Allow payload and subsystem teams to activate systems
  The next steps should ONLY be performed by the Launch Manager Dave Brunsting. Heat resistant gloves and safety glasses should be worn.
- Clear all personnel except for the Launch Manager
- Check that the ignition wires, connected to the launch control system, do not have a live

voltage across them. This can be done by lightly touching the clips to each other while away from the vehicle, watching for sparks. If no sparks are thrown it is safe to proceed.
- Remove the igniter clips from the igniter
- Ensure that the igniter has properly exposed ends which are split apart
- Insert the igniter into the motor
- Attach the clips to the igniter, ensuring good contact
- Clear the launch are of all personnel and maintain the distance as designated by the RSO in accordance with NAR/TRA regulations
- If motor does not ignite when planned, wait for RSO instruction to approach

Safety Notes:

- Only launch manager can handle motor
- Only launch manager can handle black powder
- When launch manager is handling motor or black powder, all others are to stand a safe distance away
- Everyone must listen to range officer at all times

Procedure:

Results: Results to be collected on 02/08/2020, 02/15/2020, and/or 02/29/2020.

LVT5: Shake Test

Objective:

To verify that all vehicle components are secured to the airframe properly

Tested Items:

- No vehicle components within the airframe rattle around when the launch vehicle is shaken

Motivation:

- To prevent any launch vehicle components from becoming damaged in flight

Success Criteria:

Table 64: LVT5 Success Criteria

Requirement ID	Description	Pass/Fail Criteria	Result
2.4	Launch vehicle is not damaged in flight and can be relaunched.	Success - Launch vehicle is fully assembled and no components rattle around. Fail - One or more components are rattling around.	Incomplete

Test Procedure:

Equipment:

- NDRT Launch Vehicle

Setup:

- Assemble vehicle following the procedure described in LVT4

Safety Notes:

- Shaking launch vehicle is prone to dropping and therefore can potentially become damaged
- anyone in general vicinity of launch vehicle can be hit by shaking vehicle

Procedure:

- Shake launch vehicle
- Listen for any rattling parts

Results: Results to be collected prior to launch.

LVT6: Center of Gravity Test

Objective:

To verify that actual vehicle stability aligns with simulated vehicle stability.

Tested Items:

- Center of gravity

Motivation:

- To prevent launch vehicle from being over or under stable during flight

Success Criteria:

Table 65: LVT6 Success Criteria

Requirement ID	Description	Pass/Fail Criteria	Result
2.18	Vehicle must have stable flight	Success - Launch vehicle center of gravity places the stability margin between 2.45 and 2.75. Fail - Launch vehicle center of gravity places the stability margin outside of the acceptable range of 2.45-2.75.	Incomplete

Test Procedure:

Equipment:

- NDRT Launch Vehicle
- Laser cut vehicle stand

Setup:

- Assemble vehicle following the procedure described in LVT4

Safety Notes:

- N/A

Procedure:

- Place launch vehicle on stand and find the spot where the vehicle balances on the stand
- measure distance to tip of nosecone from that location
- calculate actual stability margin

Results: Results to be collected prior to launch.

6.1.2 Recovery Testing

RT1: Black Powder Separation Testing

Objective:

To verify that the calculated quantities of black powder are sufficient to shear the retaining shear pins and separate the vehicle sections.

Tested Items:

- Deployment of the recovery parachutes
- Nose Cone Ejection for payload deployment

Motivation:

- Ensure personnel safety during vehicle launch
- Verify accuracy of black powder calculation techniques
- Ensure success of payload deployment

Success Criteria:

Table 66: RT1 Success Criteria

Requirement ID	Description	Pass/Fail Criteria	Result
3.2	Each team must perform a successful ground ejection test for both the drogue and main parachutes.	Success - All vehicle sections completely separate after black powder ignition and all parachutes end the test outside the vehicle. Fail - Vehicle sections do not completely separate or at least on parachute remains inside the vehicle after test conclusion.	Incomplete

Test Procedure:

Equipment:

- Fully constructed vehicle airframe
- # 2-56 Nylon shear pin (x10)
- ABS Removable Bulkhead and Screws
- All components of CRAM
- 3/8 in. Eyebolts (x2)
- Recovery Coupling Nut
- Wago 221 Lever Nuts (x2)
- Main Parachute
- Drogue Parachute
- Pilot Chute
- 35 ft. Shock Cord (x2)
- 3/8 in. Quicklinks (x6)
- Nomex Blanket (x2)

- Deployment Bag
- Shooter's wire, approx. 45ft
- Sealing Clay
- 9v Battery

Setup:

1. Fold the main and drogue parachutes according to the parachute folding procedures described in Section .
2. Fold the two shock cords according to the shock cord folding procedures described in Section .
3. Secure the ABS removable bulkhead in the fin can using the associated screws

Safety Notes:

- This test involves the use of black powder, a potentially dangerous energetic. The team launch manager, Dave Brunsting, should prepare and install all black powder charges, as well as intitiate the charges during testing.
- During black powder ignition, a perimeter of at least 10 ft. around the vehicle must be maintained by all personnel. Larger perimeters may be established at the discretion of the launch manager.

Procedure:

1. Tape two 6 in. pairs of shooter's wire to one of the switch port cutouts on the inside of the CRAM body, such that they are both capable of being accessed from outside of the rocket after CRAM installation. Ensure that each pair of shooter's wire is twisted together at the switch port.
2. Run one pair of shooter's wire through one of the wire holes in the CRAM top bulkhead. Run the other pair through a wire hole in the CRAM bottom bulkhead.
3. Bolt the CRAM bulkheads on to the CRAM body and thread the eyebolts into the inset coupling nut.
4. Seal any holes remaining holes in the top or bottom bulkheads using clay.
5. Have the team launch manager prepare three black powder charges: a 4.5g charge for the main parachute compartment and two 1 g charges, one for the drogue compartment and one for nose cone ejection.
6. Have the team launch manager install the black powder charges in the CRAM charge wells, connecting to the fed shooter wire using the Wago lever nuts.
7. Twist the assembled CRAM into the matching adapter in the recovery tube.
8. Using quicklinks, connect both shock cords to their respective eyebolts. The drogue harness should connect between the CRAM bottom bulkhead and the ABS bulkhead, and the main harness should connect between the CRAM top bulkhead and the main parachute bulkhead, in the transition section of the vehicle.
9. Connect the folded parachutes to their respective shock cords using quicklinks.
10. Insert the parachutes into the vehicle, taking care to ensure that the parachutes are completely covered by either a Nomex blanket or deployment bag.
11. Assemble the rest of the vehicle.
12. Insert shear pins into the drilled holes in the airframe, two between the recovery tube and

the fin can and four between the recovery tube and the transition section.
13. Connect two 15 ft lengths of shooter wire to the exposed wires taped to the CRAM switch ports.
14. Rest the vehicle horizontally on wood supports.
15. Establish a minimum 10 ft. perimeter around the vehicle
16. The launch manager should connect the first pair of shooter wire to a 9v battery, igniting the drogue ejection charge.
17. Repeat with the main parachute ejection charge.
18. When the team launch manager has given the all-clear, approach the vehicle to check for successful separation and main parachute deployment.
19. Repeat steps 1-18 with the Nose Cone ejection charge, taking all the same safety precautions and following the direction of the team launch manager.

Results: Results to be obtained by February 8, 2020.

RT2: Altimeter Testing

Objective:

To ensure the altimeters are properly powered and respond as expected to flight events.

Tested Items:

- Featherweight Raven3
- Perfectflite Stratologger SL100

Motivation:

- Ensure personnel safety during launch
- Verify reliability of recovery electronics

Success Criteria:

Table 67: RT2 Success Criteria

Requirement ID	Description	Pass/Fail Criteria	Result
3.4	Both drogue and main parachute deployment must be initiated by a commercial altimeter.	Success - The both the drogue and main e-match substitutes successfully light on both altimeters. Fail - At least one e-match substitute does not light at its expected time	Incomplete

Test Procedure:

Equipment:

- Raven3 Altimeter
- Stratologger SL100 Altimeter
- Assembled Altimeter Perfboards w/ Attached Switches (x2)
- 3.7 v LiPo Batteries, 170 mah (x2)
- Small Incandescent Bulbs (x4)
- Stranded Wire, 6 in. (x8)
- USB-MicroUSB cord

- Stratologger Interface Adapter
- Laptop with Perfectflite DataCap software and Featherweight Iterface Software

Setup:

1. Ensure that the recovery switches are already installed and soldered in place on the Altimeter Perfboards, ready to accept the altimeters.
2. Install the altimeters onto the altimeter perfobaord with the attached screw terminals.
3. Use the stranded wire to connect each of the small incandecent bulbs to the altimeters, in the places described in the recovery circuit diagrams. These will act as e-match substitutes.

Safety Notes: This test involves the use of lithium-polymer batteries, which can be volatile and potentially dangerous if used incorrectly. Never short the leads on a LiPo battery. Keep the batteries in a fire-proof LiPo bag when not in use.

Procedure:

1. Plug each battery's JST connector into its associated port on both of the perfboards.
2. Power on the altimeters using the recovery activation switches.
3. Plug the Raven altimeter into the laptop using the MicroUSB cable and start the Featherweight Interface Software.
4. Begin a simulated flight using the altimeter software.
5. Watch the drogue e-match substitute. For a successful test, it should light up as the simulated vehicle passes its apogee.
6. After the simulated vehicle passes its apogee, watch the main e-match substitute. In a successful test, this should light up before the simulated vehicle reaches 500 ft. AGL.
7. Repeat steps 3-6 using the Stratologger altimeter in place of the Raven, The Stratologger Interface Adapter in place of the MicroUSB cable, and the Perfectflite DataCap software in place of the Featherweight interface software.

Results: Results will be obtained by January 31.

RT3: Telemetry Range and Antenna Test

Objective:

To ensure that the telemetry system will reliably transmit data from the launch vehicle during the entirety of the mission.

Tested Items:

- Laptops
- Receiver prototype module
- Transmitter prototype module
- Transmitter dipole antenna
- Receiver patch antenna

Motivation:

- To validate the telemetry system design
- To ensure sufficient range of the telemetry system

Success Criteria:

Table 68: RT3 Success Criteria

Requirement ID	Description	Pass/Fail Criteria	Result
	This test ensures that the telemetry system is functional and can function within range of the launch vehicle	Success - At 1 mile, the transmission success rate is above 90% AND the received packet data error rate is below 10%. Fail - At 1 mile, the transmission success rate is below 90% OR the received packet data error rate is below 10%.	Incomplete

Test Procedure:

Equipment:

- 2 Laptops
- Receiver prototype module
- Transmitter prototype module
- Transmitter dipole antenna
- Receiver patch antenna
- 1 ft^2 piece of fiberglass
- 1 ft^2 piece of ABS plastic

Setup:

Two prototype transmitters will be placed at various distances and will attempt to transmit packets between the modules. Line of sight will be maintained between the transmitter module and receiver module to mimic the line-of-sight transmission that will occur during vehicle flight. Transmissions will occur at distances of 0.5 mile, 0.75 miles, and one mile. The antennas for the transmitter and receiver modules will both be placed approximately 5 ft above the ground. They will be powered from the laptops that will be used to collect the data. Because path loss is higher for transmissions close to the ground, this test is expected to be a worse-case scenario in terms of operating conditions.

Safety Notes:

- All LiPo batteries must be transported in fireproof battery bags. Connections should be inspected before testing.

Procedure:

1. Take the two prototype transceiver modules and separate them by approximately 0.5 mi with guaranteed line-of-sight.
2. Position the antennas in the upright position approximately 5 ft above the ground
3. Tilt the transmitter dipole antenna at approximately 60°to the receiver antenna.
4. Attempt to transmit a packet from the transmitter prototype.
5. Check to ensure that the packet was received by the receiver.
6. Save the contents for further analysis.
7. Repeat for a total of 20 trials.
8. Perform another 20 trials while placing a 1 ft^2 piece of ABS plastic of plastic in front of the transmitter antenna.
9. Perform another 20 trials while placing a 1 ft^2 piece of fiberglass in front of the transmitter antenna.

10. Repeat all 60 trials at 0.75 mi and 1 mi.
11. Sum the number of packets that were received by the receiver prototype and the number of packets that contained data transmission error. Calculate a transmission success rate and a packet data error rate.

Results: This test will be completed by January 18-31.

6.1.3 Payload: Deployment Testing

PD1: Free Rotation of Platform

Objective:

To ensure the payload platform can rotate freely with minimal friction inside the payload bay for orientation purposes.

Tested Items:

- Payload platform and bearing system

Motivation:

- To validate the orientation system design and its loaded CG

Success Criteria:

Table 69: PD1 Success Criteria

Requirement ID	Description	Pass/Fail Criteria	Result
P.21	The deployment system must be able to orient with the platform reaching equilibrium at its lowest point with respect to the ground regardless original orientation.	Success - The payload platform freely rotates AND reaches equilibrium at its lowest point. Fail - The platform cannot freely rotate OR does not reach equilibrium at its lowest point	Incomplete

Test Procedure:

Equipment:

- Payload bay tube
- Fore sliding platform
- Aft stationary platform assembly
- Ballast for UAV and Rover
- UAV
- Rover
- Clamps
- Mounting rig
- Solenoids

Setup: This test will take place in three phases: a simulated rig with ballast, a simulated rig with the UAV and rover and the full assembly. The setup for the simulated rig will be to have the whole configuration outside the body tube to observe the test and more easily modify it if changes are necessary. This will consist of a sturdy mount that the aft bulkhead will be securely clamped to so that it is completely immobile. The sliding platform will then be secured onto the stationary platform with bolts. Ballast will be taped to the fixture to simulate the UAV and rover. For the second trial, the ballast will be replaced with the UAV and rover. The setup for the full assembly will consist of all the parts being secure within the body tube as they would be in the full scale flight.

Safety Notes:

- Inspect batteries before use. All LiPo batteries not in use should be transported in fire proof battery bags.

Procedure:

1. The system is placed at a random orientation.
2. The platform will be released by hand.
3. When the platform reaches equilibrium, the location will be noted.
4. Repeat this with each configuration.

Results: The test will be completed from January 18-31.

PD2: Solenoid Actuation

Objective:

To ensure that the solenoids actuate properly for deployment and retention of the Rover and UAV sled.

Tested Items:

- Attafruit Medium Solenoids
- UAV Sled
- Rover Body

Motivation:

- To validate the actuation mechanism of the solenoids
- To verify the solenoid properly fits into the UAV Sled and Rover Body

Success Criteria:

Table 70: PD2 Success Criteria

Requirement ID	Description	Pass/Fail Criteria	Result
P.22	The ROD system restricts motion in all directions until signalled to deploy the Rover and UAV	Success - The solenoids ALL retract out of the pin slots AND remain retracted for 30 s AND then re-extend into the pin slots. Fail - Some OR All solenoids do not retract out of the pin slots OR do not remain retracted for 30 s, OR do not re-extend into the pin slots	Incomplete

Test Procedure:

Equipment:

- Solenoids
- UAV Sled
- Rover Body
- Battery
- Microcontroller
- Clamps

Setup:

This test will have two stages: testing solenoid actuation into the Rover Body and testing solenoid actuation into the UAV sled. A simple code will be written and uploaded to a microcontroller that will retract the solenoids for 30 s and then extend to solenoids for 45 s to allow time for the solenoids to cool. The UAV Sled and Rover Body will first be clamped down and held in place. Then the solenoids will be inserted into the respective pin slots and be clamped down as well. Once the solenoids are in place, they will be connected to the microcontroller.

Safety Notes:

- Inspect batteries before use. All LiPo batteries not in use should be transported in fire proof battery bags.
- Special care will be taken towards the longevity of the solenoid retraction to prevent overheating.

Procedure:

1. The solenoids will be inserted into the pin slots.
2. The retraction program will be initiated on the microcontroller.
3. The time between retraction and extension will be timed.
4. The solenoid pin will be inspected after solenoid extension.

Results: To be completed between January 18-31.

PD3: Vibration and Motion Restriction of Rover and UAV

Objective:

To validate the retention system and ensure the UAV, Rover, and all components will not move during flight.

Tested Items:

- Solenoids
- Stationary platform
- Sliding platform
- UAV sled
- Rover
- UAV
- ROD system

Motivation:

- To ensure that the full payload will be retained during launch, flight, and recovery
- To validate the mechanical fail-safe of the solenoids and that they remain stationary during launch, flight, and recovery

Success Criteria:

Table 71: PD3 Success Criteria

Requirement ID	Description	Pass/Fail Criteria	Result
P.22 4.3.7.1	The deployment system must restrict motion of the Rover and UAV in all directions until the deployment sequence is initiated.	Success - ALL of the payload components are fully retained Fail - Some OR all of the components are not fully retained.	Incomplete

Test Procedure:

Equipment:

- Solenoids
- UAV Sled
- Rover
- Sliding Platform
- Stationary Platform
- UAV
- Nuts and Bolts

Setup:

The Solenoids will be properly inserted into the slots on the sliding platform. The UAV sled with the UAV and the Rover will be placed into position on the platform and the solenoids will be inserted into the respective slots. The sliding platform will then be slide onto the stationary platform and be secured using the nuts and bolts.

Safety Notes:

- Inspect all ASA components for cracks and deformation.
- Ensure all components are connected securely.

Procedure:

1. Verify all connections and retention pins are properly placed
2. Hold the stationary platform where the bearing would be located
3. Slowly and cautiously rotate the platform
4. Verify minimal motion of the payload

Results: To be completed between February 2-8.

PD4: Deployment of Rover and UAV

Objective:

To ensure that the Rover and UAV can successfully deploy after landing and orientation.

Tested Items:

- Rover design
- UAV sled & sled/platform interface
- Hope FR RFM95W radio module
- Rover crank mechanism

Motivation:

- To validate the deployment signal reception to initiate Rover motion
- To validate the clearance, friction, and stability of the Rover towing mechanism

Success Criteria:

Table 72: PD4 Success Criteria

Requirement ID	Description	Pass/Fail Criteria	Result
P.22	The Rover and UAV remain retained until receiving the activation signal	Success - The Rover receives the activation signal AND successfully tows the UAV out of the payload bay. Fail - The signal does not activate the Rover OR the Rover cannot successfully tow the UAV out of the payload bay	Incomplete

Test Procedure:

Equipment:

- UAV
- UAV Sled
- Rover
- Sliding Platform
- Stationary Platform
- Solenoids
- Nuts and Bolts
- Ground Station
- Batteries
- Payload Bay

Setup:

The Solenoids will be properly inserted into the slots on the sliding platform. The UAV sled with the UAV and the Rover will be placed into position on the platform and the solenoids will be inserted into the respective slots. The sliding platform will then be slide onto the stationary platform and be secured using the nuts and bolts. The Rover, UAV, and ROD systems will be connected to the respective batteries. The Ground station will be powered on and communication established with each system.

Safety Notes:

- Inspect batteries before use. All LiPo batteries not in use should be transported in fire proof battery bags.
- Special care will be taken towards the longevity of the solenoid retraction to prevent overheating.

Procedure:

1. Verify all connections and retention pins are properly placed
2. Verify proper connection between components
3. Initiate deployment sequence

Results: To be completed between February 2-8.

6.1.4 Payload: Rover Testing

PRT1: Electrical Connections

Objective:

To validate the electrical connections of the rover electrical components, success of components communication protocols, and radio communication to the rover.

Tested Items:

- Power Distribution
- I2C, SPI, UART, PWM protocols
- Radio receiving

Motivation:

- To verify the connections and operations of the rover electrical components and board fabrication.

Success Criteria:

Table 73: PRT1 Success Criteria

Requirement ID	Description	Pass/Fail Criteria	Result
P.4	Electrical boards shall be isolated to prevent electrical shorts and ensure signal connections and communication protocols.	Success - A successful test shall verify the correct voltage readings on the PCB, verify sensor readings to the PIC32 memory, verify radio communication to the rover, and verify PWM output waveforms. Fail - The test shall fail if any of the voltage readings, sensor readings, radio receiving, or PWM outputs do not match valid and accepted values.	Incomplete

Test Procedure:

Equipment:

- Fully assembled rover printed circuit board (PCB)
- Two 11.1 V Li-Ion batteries
- 8 Channel Saleae Logic Analyzer
- Laptop with MPLABX installed
- PICKIT3 debugger
- Multimeter
- Radio test station circuit with Arduino Uno and RFM95W.

Setup: The rover printed circuit board (PCB) in its fully assembled state shall be placed securely on an electrostatic discharge (ESD) mat or handled with ESD gloves for the outdoor GPS test step. Connect the USB end of the PICkit3 to the laptop and start MPLABX. Do not connect the PICkit3 until instructed in the procedure. Connect the Saleae Logic Analyzer to the

laptop and begin the Logic program. Turn on the multimeter. Place the two 11.1V batteries on the ESD mat and do not connect to the board until instructed in the procedure.

Safety Notes: Batteries should be stored in a Li-Po safe bag at all times when not in use. At any time a battery is out of the safe bag, safety glasses must be worn. Handle all components on an ESD mat with appropriate wrist strap grounding. For the outdoor GPS test item, transport the circuit using an ESD bag and handle the circuit wearing ESD gloves. Ensure batteries are connected according to their proper polarity to avoid damage to the battery and circuit.

Procedure:

1. Connect the two 11.1V batteries to their corresponding header connectors. CAUTION: Batteries must be connected in the proper polarity indicated or damage may occur to board components.
2. Set the multimeter to measure a DC voltage. Connect the multimeter ground lead to the ground of the 3.3V two pin header, and the positive lead to the positive of the 3.3V pin header. Verify the multimeter reads +3.3V. Repeat for the 5V and 11.1V (Sabertooth) two pin headers.
3. Connect the PICkit3 to the corresponding header on the rover PCB. Download the test program to configure the PIC32 and send a single command over I2C to the BNO055 to read acceleration and magnetometer values and store in an appropriate register. Verify the presence of a valid reading.
4. Download the test program to the PIC32 to communicate with the GPS module over UART. The GPS module should automatically begin transmitting readings when measured. Verify GPS readings are properly stored in the PIC32 register within 5 minutes of outdoor runtime.
5. Power on RFM95W test stand connected to a lab PC. Download onto the Arduino Uno a program to begin transmitting the command “The quick brown fox jumps over the lazy dog 0123456789”. Download the test program to the PIC32 to set the radio module to receive mode over SPI. Verify the reception of the test signal stored in a register.
6. Connect GND pin of the Saleae Logic Analyzer to one of the GND header pins on the board. Connect pins 0 and 1 of the logic analyzer to PWM pin, pin 3, on each of the sample retrieval servo connectors. Connect pins 2 and 3 to the pins of the Sabertooth PWM connector. Download the program to the PIC32 to output a 50% duty cycle PWM signal on each of the PWM pins. Verify the expected 5V signal output on the logic analyzer. Repeat with a 25%, 75%, and 100% duty cycle.

Results: This result has not yet been completed. This test shall be completed upon assembly of the rover PCB in the coming weeks.

6.1.5 Payload: UAV Testing

PUT1: Manual Flight

Objective:

To ensure that the UAV manual override is functional and that successful flight can be achieved.

Tested Items:

- Flight controller
- RC transmitter
- UAV RC receiver
- UAV flight stability
- UAV flight maneuvers

Motivation:

- To validate the manual override function of the UAV
- To ensure the UAV flight is stable
- To validate that the desired flight maneuvers are successful

Success Criteria:

Table 74: PUT1 Success Criteria

Requirement ID	Description	Pass/Fail Criteria	Result
P.14	The UAV must have a manual override switch.	Success - The UAV is manually flown and performs all desired maneuvers AND the UAV has stable flight. Fail - The UAV cannot be manually flown OR cannot perform desired flight maneuvers OR is unstable during flight.	Incomplete

Test Procedure:

Equipment:

- UAV
- Controller
- RC Transmitter

Setup:

1. Ensure that area is free of bystanders and hazards to the UAV (e.g. trees and poles).
2. Power on UAV and ensure that the RC transmitter and receiver are connected. If they do not, follow the manufacturer's directions to bind them.

Safety Notes: Ensure that all nearby personnel, including the UAV operator, maintain a safe distance from the UAV at all times and that the test is not conducted in the vicinity of bystanders. Proper PPE (safety glasses) must be worn while the UAV is powered.

Procedure:

1. Gradually apply throttle to UAV until it begins to lift off.
2. Continue applying constant throttle until UAV reaches an altitude of five feet, then maintain a hover for five seconds.
3. Fly the UAV ten feet in a straight line.
4. Rotate the UAV 90° in place.
5. Land the UAV safely and ensure that the motors stop rotating before approaching the UAV.

Results: To be completed January 18-31.

PUT2: Autonomous Flight

Objective:
To validate the UAV autonomous flight capabilities and ensure stable flight.

Tested Items:

- UAV receiver from ground station signal and autonomous response
- UAV flight stability
- UAV flight maneuvers

Motivation:

- To validate the UAV's autonomous flight capabilities
- To ensure the UAV's flight is stable
- To validate that the desired flight maneuvers are successful

Success Criteria:

Table 75: PUT2 Success Criteria

Requirement ID	Description	Pass/Fail Criteria	Result
P.13	The UAV must use a commercial flight controller	Success - The UAV receives and obeys commands from the ground station AND has a stable flight with successful flight maneuvers. Fail - The UAV does not follow ground station commands OR has unstable flight	Incomplete

Test Procedure:

Equipment:

- UAV
- UAV RC receiver
- Ground station
- Ground station RC transmitter
- Manual controller
- Manual controller RC transmitter

Setup:

- Ensure that the test area is free of bystanders and hazards to the UAV, such as trees and poles.
- Turn on UAV and ensure that the UAV's receiver is connected to both the manual controller's transmitter and the ground station's transmitter.

Safety Notes: Ensure that manual override switch is functional before testing autonomous flight. All personnel must remain a safe distance from the UAV while the UAV is powered on.

Procedure: Program the UAV to do the following autonomously:

1. Take off from the ground
2. Ascend to an altitude of five feet
3. Hover at this altitude for five seconds

4. Travel in a straight line for ten feet
5. Rotate 90° in place
6. Continue in the same direction for ten feet
7. Land safely and shut down motors

Results: To be completed January 18-31.

PUT3: Transmit Video to Ground Station

Objective:

To ensure successful video transmission from the UAV to the ground station for target detection.

Tested Items:

- Ground station video receiver
- UAV video transmitter

Motivation:

- To ensure successful video transmission, including sensor data
- To validate target detection system

Success Criteria:

Table 76: PUT3 Success Criteria

Requirement ID	Description	Pass/Fail Criteria	Result
P.23	The Target Detection system must correctly identify the closest CFEA.	Success - The UAV transmits video during flight AND the ground station successfully receives the video AND the ground station successfully reads sensor data from the UAV. Fail - The UAV cannot transmit video during flight OR the ground station cannot receive video OR ground station cannot read sensor data	Incomplete

Test Procedure:

Equipment:

- Ground station video receiver
- Ground station display
- UAV video transmitter

Setup:

1. Place ground station and UAV approximately 25 feet apart and power on both systems.
2. Ensure that the ground station's video receiver connects to the UAV's video transmitter and the ground station's display is connected to the video receiver.

Safety Notes: Ensure that sufficient distance is between the ground station and the UAV so as to avoid overloading the video receiver. Because the RC transmitters for the ground station and the manual controller are powered down, the UAV is safe to approach but should still be handled with caution.

Procedure:

1. Ensure that the video feed from the UAV's camera is visible on the ground station's display.
2. Explore Ardupilot's On-Screen Display settings to ensure that the ground station is receiving sensor data from the UAV and that all sensors are connected properly and configured correctly in Ardupilot.

Results:

PUT4: Detection of Simulated CFEA

Objective:

To verify that the target detection system can detect the CFEA.

Tested Items:

- UAV CADDX Turbo EOS2 camera
- Target detection code

Motivation:

- To validate the target detection system algorithm and design

Success Criteria:

Table 77: PUT4 Success Criteria

Requirement ID	Description	Pass/Fail Criteria	Result
P.23	The target detection system must correctly identify the closest CFEA	Success - The target detection algorithm correctly identifies the CFEA. Fail - The target detection system does not correctly identify the CFEA.	Incomplete

Test Procedure:

Equipment:

- UAV
- Ground station
- Manual controller
- CFEA

Setup:

1. Prepare area for UAV flight (ensure that area is clear of bystanders and hazards).
2. Place CFEA near designated UAV launch site.
3. Prepare UAV and ground station for takeoff (power both systems on and ensure RC and video connections function properly).

Safety Notes: Ensure that all personnel remain a safe distance from the UAV at all times.

Procedure:

1. Ensure that the ground station display shows the video feed from the UAV.
2. Launch UAV to an altitude of 25 feet.

3. Fly UAV to CFEA while observer watches the ground station's display to ensure that a false CFEA detection is not reported prematurely.
4. With CFEA in frame, observer ensures that CFEA detection algorithm successfully identifies CFEA.
5. Land UAV on CFEA and shut down motors.

Results: To be completed January 18-31.

PUT5: Landing Location Identification

Objective:

To ensure that the target detection system correctly identifies the farthest corner from the launch vehicle landing site of the CFEA for UAV landing.

Tested Items:

- Target detection algorithm

Motivation:

- To ensure that the UAV will land far away from the operating area of the Rover

Success Criteria:

Table 78: PUT5 Success Criteria

Requirement ID	Description	Pass/Fail Criteria	Result
P.24	Target Detection identifies correct corner of CFEA to land on.	Success - The target detection system correctly identifies the proper landing corner of the CFEA Fail - The target detection system does not identify the proper landing corner of the CFEA.	Incomplete

Test Procedure:

Equipment:

- UAV
- Ground station
- Manual controller
- CFEA

Setup:

1. Prepare area for UAV flight (ensure that area is clear of bystanders and hazards).
2. Place CFEA near designated UAV launch site.
3. Prepare UAV and ground station for takeoff (power both systems on and ensure RC and video connections function properly).

Safety Notes: Ensure that all personnel remain a safe distance from the UAV at all times.

Procedure:

1. Ensure that the ground station display shows the video feed from the UAV.
2. Launch UAV to an altitude of 25 feet.

3. Fly UAV to CFEA while observer watches the ground station's display to ensure that a false CFEA detection is not reported prematurely.
4. With CFEA in frame, observer ensures that CFEA detection algorithm successfully identifies CFEA.
5. Use ground station display to land UAV on CFEA at position designated by CFEA detection algorithm.
6. Land UAV on CFEA and shut down motors.
7. Verify that CFEA detection algorithm selected correct corner of CFEA.

Results: To be completed February 2-8.

PUT6: Detection of a Simulated CFEA with UAV

Objective:

To validate the target detection system when receiving video from the UAV

Tested Items:

- Target detection algorithm

Motivation:

- To verify the success of the CFEA detection with data from the UAV

Success Criteria:

Table 79: PUT6 Success Criteria

Requirement ID	Description	Pass/Fail Criteria	Result
P.23	Target Detection correctly identifies the closest CFEA.	Success - The CFEA is correctly identified from the ground with the UAV camera station Fail - The CFEA is not correctly identified.	Incomplete

Test Procedure:

Equipment:

- CFEA
- Camera

Setup:

Safety Notes:

Procedure:

1. Place CFEA in sunny area.
2. Capture several images of CFEA from different angles and showing all or part of CFEA.
3. Move CFEA to shaded and semi-shaded areas, repeating step 2 each time.
4. Analyze results

Results: To be complete February 2-8.

6.1.6 ABS Testing

ABT1: Sub-scale Launch

Objective:

To verify that the addition of drag tabs to the sub-scale launch vehicle decreases apogee while maintaining stability, and to test the functionality of the chosen sensors and microcontroller.

Tested Items:

- Apogee change of sub-scale launch vehicle when drag tabs are implemented
- Stability of flight when drag tabs are implemented
- Capabilities of BNO055 accelerometer, MPL3115 barometer, ADXL345, and Raspberry Pi microcontroller working in sequence

Motivation:

- To verify that the addition of drag tabs lowers the apogee of the launch vehicle as expected
- To ensure that the addition of drag tabs does not cause instability during flight
- To verify that the chosen sensors and microcontroller work in sequence to provide sensible flight data at an acceptable frequency

Success Criteria:

Table 80: ABT1 Success Criteria

Requirement ID	Description	Pass/Fail Criteria	Result
V.4	The addition of the drag tabs will lower the apogee of the launch vehicle.	Success - The recorded apogee for half extension and full extension each subsequently decrease apogee by 80 feet or more. Fail - There is no significant apogee decrease resulting from the addition of the drag tabs.	Pass
V.10, V.14	The addition of the drag tabs will not negatively affect the stability of the launch vehicle.	Success - The launch vehicle undergoes successful flights with the drag tabs attached. Fail - The launch vehicle experiences an unstable flight and fails with the drag tabs attached.	Pass
N/A	The ABS sensors and microcontroller collect data effectively.	Success - The data collected by the sensors is sensible, and is collected at a frequency of at least 50 Hz. Fail - The data collected by the sensors is not physically accurate, or the data is collected at a frequency below 50 Hz.	Pass

Test Procedure:

Equipment:

- Sub-scale launch vehicle
- 3 removable couplers with 2:5 scale drag tab models
- Sensor sled with Raspberry Pi, BNO055, MPL3115, ADXL345, and 3.7V 250 mAh battery attached

- Computer with micro SD card reader

Setup: Two sets of 2:5 scale model drag tabs were fabricated out of Nylon 6/6 to best replicate the induced drag that will be generated with full-scale ABS. One model represents the drag tabs at full extension, and the other represents them at half extension. These were epoxied to removable couplers that could be attached and removed at the CP of the sub-scale launch vehicle, along with a third coupler that sat flush to the vehicle body to represent flight without ABS. The fabricated sub-scale drag tabs are shown in Figure 139, and are shown epoxied to the coupler in Figure 140. Additionally, a sensor sled was constructed out of balsa wood to house the microcontroller, battery, and sensors for ABS, as well as all Recovery electronics. It consisted of two bulkheads and a 5 in. web to which all components were secured. This sensor sled was integrated into the sub-scale launch vehicle in the payload bay, and was secured by a screw at its aft bulkhead.

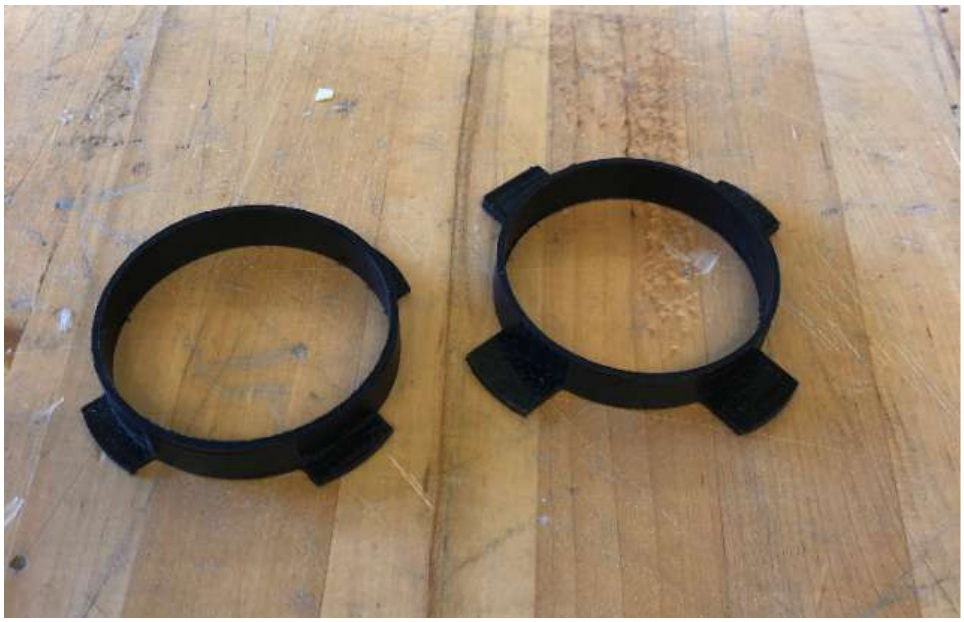

Figure 139: Sub-scale drag tabs

Figure 140: Sub-scale drag tabs on coupler

Safety Notes: Before and after flight, it was essential to inspect the LiPo battery for damage, swelling, or other abnormalities. If any of these were to be observed, the battery would be placed in a fireproof battery bag.

Procedure: The full sub-scale launch procedure is outlined in the Vehicles Test Plan section. Three sub-scale launches were conducted, one with each coupler, in order to represent a flight without ABS, a flight with drag tabs at half extension, and a flight with drag tabs at full extension. For each of these flights, the LiPo battery was plugged into the power booster, and an LED verified that power was being supplied and that the Raspberry Pi was taking data from the sensors. After this, the sensor sled was integrated into the launch vehicle as described in the Setup section, and the launch was conducted. Once the vehicle was recovered, the sensor sled was extracted, and the battery was unplugged. The micro SD card was plugged into a computer to verify that data was collected as expected. This procedure was then repeated for two more flights with the other two couplers attached.

Results: Upon inspection of the sensor data, the ability of the ABS to decrease the apogee of the launch vehicle was verified. For reference, the recorded apogees for each of the launches is shown in Table 81.

Table 81: Recorded Altitude at Apogee for Sub-scale Flights

Flight	No Tabs	Half Tabs	Full Tabs
Altitude (ft)	1366	1126.5	1010

The stability of the launch vehicle was not compromised by the implementation of the drag tabs, as was seen in the steady flight path shown by the sensor data, and the visibly stable flight observed at launch. The sensors successfully collected data at a sampling rate of above 50 Hz, and the data is physically sensible.

ABT2: Mechanism and Motor Ground Test

Objective:

To verify that the fully constructed mechanism and motor will function together as intended to produce drag tab actuation.

Tested Items:

- Servo motor rotation angles in response to PWM signals
- Drag tab extension resulting from servo motor rotation
- Servo motor ability to overcome the internal friction of the mechanism

Success Criteria:

Table 82: ABT2 Success Criteria

Requirement ID	Description	Pass/Fail Criteria	Result
V.4	The servo motor will rotate to the expected angle for a given PWM signal.	Success - When the PWM signal is sent, the servo motor rotates to the correct angle despite resistance from mechanism friction. Fail - The servo motor rotates to an angle too small, or the servo motor stalls due to inability to overcome internal friction.	Incomplete

Test Procedure:

Equipment:

- Fully constructed ABS
- Raspberry Pi programmed to take a simulated flight as an input at 100 Hz

Setup: The Raspberry Pi will be programmed to output PWM signals that are expected to produce known rotation amounts. It will be connected to the servo motor according to the circuit diagram, and the servo motor will be connected to the mechanism central hub.

Safety Notes: A safe distance must be kept from the mechanism during the test, as injury could result from the rapidly moving components. Ensure that power is cut from the servo motor before handling the mechanism.

Procedure: Upon booting up the Raspberry Pi by plugging in the battery to its power booster, a series of PWM signals will be sent to the servo motor. Visual inspection will verify whether the correct servo rotation angle, and resulting drag tab extension, were achieved.

Results: The test will be performed once the full-scale construction of the mechanism is completed. Results must be verified before the first full-scale flight attempt on February 8th.

ABT3: Control Structure Ground Test

Objective:

To verify that the fully constructed ABS is able to filter noisy data and undergo an entire simulated flight in which it needs to decrease velocity using the PID control law.

Tested Items:

- Kalman filter
- Flight stage awareness
- Response of the mechanism to a simulated flight

Success Criteria:

Table 83: ABT3 Success Criteria

Requirement ID	Description	Pass/Fail Criteria	Result
N/A	The Kalman filter successfully eliminates noise in flight data.	Success - Flight data passed through the Kalman filter is smoothed out and does not include extraneous data points. Fail - The Kalman filter is unable to eliminate noise in flight data.	Pass
V.4	The system successfully responds to an entire simulated flight	Success - The PID algorithm produces drag tab extensions in response to the inputted flight data. Fail - The drag tabs do not fully retract when needed, or they do not actuate correctly in response to the simulated flight.	Incomplete

Test Procedure:

Equipment:

- Fully constructed mechanism and servo motor
- Raspberry Pi programmed to output specific PWM signals

Setup: The entire system will be constructed exactly as it will be for full-scale flight. A simulated flight with noise inserted will be uploaded to the Raspberry Pi to be read in place of real-time sensor data.

Safety Notes: A safe distance must be kept from the system during the test, as injury could result from the rapidly moving components. Ensure that the program on the Raspberry Pi has ended before handling the system.

Procedure: Upon booting up the Raspberry Pi by plugging in the battery to its power booster and flipping the "ARM" switch, simulated flight data will be passed through the Kalman filter which was previously verified. The system will experience the same launch cycle it should see in a real flight, and will keep track of the flight state that it is in. During the burnout to apogee phase, the team will visually verify that the drag tabs are actuating in response to the simulated velocity, which will be an overshoot of the desired velocity. After the program is finished, the output data will be inspected to ensure that the drag tabs were fully retracted during all flight states except for burnout to apogee. The data will also be inspected to ensure that the drag tab extensions make sense given the velocity overshoots.

Results: The test will be performed once the full-scale construction of the mechanism is completed. Results must be verified before the first full-scale flight attempt on February 8th.

6.2 Requirements & Verifications

6.2.1 NASA Requirements

Table 84: General Requirements

Requirement		Verification Method				Verification Plan	Status
ID	Description	A	I	D	T		
1.1	Students on the team will do 100% of the project and flight preparation (except for items to be done by the team's mentor). Teams will submit new work.		X	X		NDRT is completely student led. Team officers will delegate all work to student members and verify students conduct all activities except those that mentors are required to conduct (i.e. assembling motors, handling ejection charges).	Complete
1.2	The team will provide and maintain a project plan to include, but not limited to the following items: project milestones, budget and community support, checklists, personnel assignments, STEM engagement events, and risks and mitigations.			X		Team captains are actively maintaining a project plan including a GANTT chart for scheduling milestone targets, team budget, and software such as Slack for organization and task delegation.	In Progress
1.3	Foreign National (FN) team members must be identified by the Preliminary Design Review (PDR) and may or may not have access to certain activities during launch week due to security restrictions. In addition, FN's may be separated from their team during certain activities on site at Marshall Space Flight Center.		X			Design team leads will collect team member information, inform Foreign Nationals of the launch week restrictions, and ensure all Foreign Nationals attending launch week are properly registered in time to attend available activities.	Complete
1.4	The team must identify all team members attending launch week activities by CDR. Team members will include: Students actively engaged in the project throughout the entire year, one mentor, and no more than two adult educators.		X			Team members, mentors, and educators will be required to express interest in attending launch week prior to CDR submission.	Complete
1.5	The team will engage a minimum of 200 participants in educational, hands-on STEM activities by FRR.			X		An Educational Outreach officer has been elected and will communicate outreach activities with community partners and team members. Educational Engagement Activity Reports will accurately describe outreach activities and community impact.	Complete
1.6	The team will establish a social media presence to inform the public about team activities.			X		A Social Media Manager has been elected and will maintain the team's online presence and interaction with the public.	Complete
1.7	Teams will email all deliverables to the NASA project management team by the deadline specified in the handbook for each milestone.		X			Team Captains will confirm deliverables are delivered via email by the deadline and will confirm receipt with the NASA project management team.	In Progress
1.8	All deliverables must be in PDF format.		X			Documentation will be prepared using Overleaf and Google Suite products accessed via an academic license. All documentation shall be compiled into a PDF format.	Complete
1.9	In every report, teams will provide a table of contents including major sections and their respective sub-sections.		X			Documentation prepared using Overleaf will contain a table of contents and sections will be updated automatically to ensure accuracy.	Complete
1.10	In every report, the team will include the page number at the bottom of the page.		X			Documentation prepared using Overleaf will be formatted to include the page number at the bottom of the page.	Complete
1.11	The team will provide any computer equipment necessary to perform a video teleconference with the review panel.		X	X		NDRT maintains a set of teleconferencing equipment and will verify its functionality prior to each presentation. The team will reserve a room in the college of engineering two weeks prior to each presentation.	In Progress
1.12	All teams will be required to use the launch pads provided by Student Launch's launch services provider.			X		The launch vehicle shall be designed to launch with the required launch pads and rails as provided by the launch service provider.	Complete
1.13	Each team must identify a "mentor" as defined in the Student Launch Handbook.		X			NDRT works with a mentor who meets all requirements.	Complete

Table 85: NASA Launch Vehicle Requirements

Requirement		Verification Method				Verification Plan	Status
ID	Description	A	I	D	T		
2.1	The vehicle will deliver the payload to an apogee altitude between 3,500 and 5,500 ft AGL.	X		X	X	Accurate simulations of the vehicle design will be created in RockSim and OpenRocket to project the vehicle apogee and ensure the vehicle will be within the required range and projected to hit the set apogee target. Test flights will be performed to demonstrate this.	In Progress
2.2	Teams shall identify their target altitude goal at the PDR milestone. The declared target altitude will be used to determine the team's altitude score during Launch Week.	X	X			Analysis of the preliminary vehicle and payload design and dimensions were used to set the final target altitude. The target altitude was declared in the PDR report to be 4,444 ft.	Complete
2.3	The vehicle will carry one commercially available, barometric altimeter for recording the official altitude used in determining the Altitude Award winner.		X			The team will select a commercially available barometric altimeter and verify with team mentors and launch managers that the selected altimeter is a reliable selection. The team will be using three altimeters for deployment redundancy, so one altimeter will be identified to the launch managers as the scoring altimeter.	In Progress
2.4	The launch vehicle will be designed to be recoverable and reusable.			X	X	The vehicle will be designed to be reusable. Extensive ground testing of recovery and payload systems will be conducted to ensure written procedures allow for a recoverable and reusable vehicle and payload. This will be verified during full scale flight tests.	In Progress
2.5	The launch vehicle will have a maximum of 4 independent sections.		X			The team will verify during the design and fabrication phases of development that the vehicle has a maximum of 4 independent sections.	In Progress
2.5.1	Coupler/airframe shoulders which are located at in-flight separation points will be at least 1 body diameter in length.		X			Team will verify that coupler/airframe shoulders at in-flight separation points are at least 1 body diameter in length.	In Progress
2.5.2	Nosecone shoulders which are located at in-flight separation points will be at least 1/2 body diameter in length.		X			Team will verify that nosecone shoulders at in-flight separation points will be at least 1/2 body diameter in length.	In Progress
2.6	The launch vehicle will be capable of being prepared for flight at the launch site within 2 hours of the time the FAA flight waiver opens.			X	X	Systems and Safety team will prepare launch day procedures which shall be fully practiced (with the exception of arming any energetics) prior to the first launch day. Full scale test flights will be used to ensure the vehicle is prepared within 2 hours.	In Progress
2.7	The launch vehicle and payload will be capable of remaining in launch-ready configuration on the pad for a minimum of 2 hours without losing the functionality of any critical on-board components.	X			X	During the design phase analysis will be conducted on the power draw of system components and available capacity of on-board batteries. Testing of the vehicle and payload systems will be performed to ensure they are capable of remaining in a launch-ready configuration for at least 3 hours while still having enough capacity to perform the maximum length of the mission without risk of losing power.	In Progress
2.8	The launch vehicle will be capable of being launched by a standard 12 V DC firing system, provided by the NASA-designated launch services provider.		X	X		The vehicle will be designed to launch with a standard 12 V DC firing system. The team will work with our launch manager to ensure compatibility prior to demonstration flights.	In Progress
2.9	The launch vehicle will require no external circuitry or special ground support equipment to initiate launch (other than what is provided by the launch services provider).		X	X		The team will work with the launch manager to ensure compatibility without external circuitry.	In Progress
2.10	The launch vehicle will use a commercially available solid motor propulsion system using APCP, which is approved and certified by the NAR, TRA, and/or the CAR.		X			The team will review NAR, TRA, and CAR certifications to ensure the selected motor is in compliance.	In Progress
2.10.1	Final motor choices will be declared by the CDR milestone.		X			Final motor is the L1395 Blue Streak	Complete
2.10.2	Any motor change after CDR must be approved by the NASA RSO and will only be approved if the change is for the sole purpose of increasing the safety margin.		X	X		All motor changes requested after the CDR milestone will be requested with accompanying analysis demonstrating a safety derived reasoning. The team accepts a penalty regardless of the reasoning if the change is approved.	In Progress
2.11	The launch vehicle will be limited to a single stage.		X			The team shall design the vehicle as a single stage with a motor in accordance with Req. 2.10	In progress
2.12	The total impulse provided by a University launch vehicle will not exceed 5,120 Ns (L-class).		X			As a University launch team, the team shall select a motor providing a total impulse which does not exceed 5,120 Ns (L class).	In Progress
2.13	Pressure vessels on the vehicle will be approved by the RSO and will meet the criteria outlined in Req. 2.13.1-2.13.3.		X			The pressure vessels will be inspected and approved by the RSO prior to launch.	In Progress
2.13.1	The minimum pressure vessel FOS will be 4:1 with supporting design documentation included in all milestone reviews.	X				The team shall design all pressure vessels on the vehicle with a minimum FOS of 4:1 with supporting analysis.	In Progress
2.13.2	Each pressure vessel will include a pressure relief valve that sees the full pressure of the tank and is capable of withstanding the maximum pressure and flow rate of the tank.	X				All pressure vessels will include pressure relief valves. Analysis will be performed to ensure the valve sees the full pressure of the tank and is capable of withstanding maximum pressure and flow rates.	In Progress

Requirement		Verification Method				Verification Plan	Status
ID	Description	A	I	D	T		
2.13.3	The full pedigree of the tank will be described, including the application for which the tank was designed and the history of the tank as defined in the NASA SL Handbook.		X			Documentation shall be maintained on the history of the tank, including all information described in the NASA SL Handbook.	In Progress
2.14	The launch vehicle will have a minimum static stability margin of 2.0 at the point of rail exit.	X				The team shall analyze the vehicle design using software such as OpenRocket and RockSim to verify a static stability margin of 2.0 at the point of rail exit.	In Progress
2.15	Any structural protuberance on the rocket will be located aft of the burnout center of gravity.	X	X		X	All structural protuberance on the vehicle including but not limited to ABS shall be located aft of the burnout center of gravity as determined by analysis and center of gravity testing.	In Progress
2.16	The launch vehicle will accelerate to a minimum velocity of 52 fps at rail exit.	X		X	X	Vehicle design softwares OpenRocket and RockSim shall be used to ensure the vehicle will accelerate to a minimum velocity of 52 fps at the rail exit. This will be demonstrated at full scale launches by analyzing recorded flight data.	In Progress
2.17	All teams will successfully launch and recover a subscale model of their rocket prior to CDR.			X		The team has launched and recovered a subscale model of the rocket prior to CDR.	Complete
2.17.1	The subscale model should resemble and perform as similarly as possible to the full-scale model, however, the full-scale will not be used as the subscale model.		X			The subscale model was designed to be as accurately resembling the full scale model as possible, and was a separate vehicle from the full scale.	Complete
2.17.2	The subscale model will carry an altimeter capable of recording the model's apogee altitude.		X			The subscale model was designed with a payload section for carrying the same altimeter selected for scoring purposes in the full scale rocket.	Complete
2.17.3	The subscale rocket must be a newly constructed rocket, designed and built specifically for this year's project.		X			Team leaders ensured that the subscale rocket was newly constructed based on this year's design.	Complete
2.17.4	Proof of a successful flight shall be supplied in the CDR report.		X			A post launch assessment with test results and altimeter data has been published in this report	Complete
2.18	All teams will complete demonstration flights as outlined in Req. 2.18.1-1.18.2.4.			X		The team shall complete demonstration flights under the supervision of team launch manager Dave Brunsting and the RSO.	Incomplete
2.18.1	All teams will successfully launch and recover their full-scale rocket prior to FRR in its final flight configuration. The rocket flown must be the same rocket to be flown on launch day. The criteria outlined in Req. 2.18.1.1-2.18.19 must be met. Req. details can be found in the NASA SL Handbook.			X		The full scale vehicle shall be launched and safely recovered prior to FRR to verify the vehicle metrics listed in the NASA SL Handbook. The rocket flown shall be the final fight configuration and all major vehicle or payload changes shall be approved by the NASA Student Launch team and require a re-flight in accordance with the vehicle demonstration deadlines.	Incomplete
2.18.1.1	The vehicle and recovery system will have functioned as designed.			X		The vehicle and recovery system shall function safely as designed and meet the relevant launch requirements as determined by collected flight data.	In Progress
2.18.1.2	The full-scale rocket must be a newly constructed rocket, designed and built specifically for this year's project.		X			Team leaders shall ensure that the full-scale rocket is newly constructed, designed and built for this year.	In Progress
2.18.1.3	The payload does not have to be flown during the full-scale Vehicle Demonstration Flight. Req. 2.18.1.3.1 and 2.18.1.3.2 still apply.		X			The team shall inspect whether the payload is flight-ready prior to the full-scale demonstration flight.	Incomplete
2.18.1.3.1	If the payload is not flown, mass simulators will be used to simulate the payload mass.			X		If the payload is not flown, an appropriate mass simulator will be secured in the same section as the payload to simulate payload mass.	Incomplete
2.18.1.3.2	The mass simulators will be located in the same approximate location on the rocket as the missing payload mass.			X		Mass simulators shall be secured in the same approximate location as the payload.	Incomplete
2.18.1.4	If the payload changes the external surfaces of the rocket or manages the total energy of the vehicle, those systems will be active during the full-scale Vehicle Demonstration Flight.			X		All payload systems which alter the external surfaces of the rocket or manage the total vehicle energy shall be active during full-scale demonstration flights.	Incomplete
2.18.1.5	Teams shall fly the launch day motor for the Vehicle Demonstration Flight. The team may request a waiver for the use of an alternative motor in advance if the home launch field cannot support the full impulse of the launch day motor or in other extenuating circumstances.		X			Team shall fly the selected launch day motor for the demonstration flight. The team shall request a waiver for using an alternative motor well in advance of the flight if extenuating circumstances arise. Team shall consult with launch manager Dave Brunsting prior to making any such request.	Incomplete
2.18.1.6	The vehicle must be flown in its fully ballasted configuration during the full-scale test flight. Additional ballast may not be added without a re-flight of the full-scale launch vehicle.			X		The vehicle shall be flown in its fully ballasted configuration during the full-scale test flight. The team will minimize the amount of ballast required during the design and launch preparation phases.	Incomplete
2.18.1.7	After successfully completing the full-scale demonstration flight, the launch vehicle or any of its components will not be modified without the concurrence of the NASA RSO.		X			Systems and Safety officers shall enforce requirements that the launch vehicle and its components are not handled or modified by team members following flight without the approval of the NASA or local launch site RSO.	In Progress
2.18.1.8	Proof of a successful flight shall be supplied in the FRR report. Altimeter data output is required to meet this requirement.			X		A post launch assessment with test results and altimeter data shall be supplied in the FRR report.	Incomplete

Requirement		Verification Method				Verification Plan	Status
ID	Description	A	I	D	T		
2.18.1.9	Vehicle Demonstration flights must be completed by the FRR submission deadline. No exceptions will be made. If the Student Launch office determines that a Vehicle Demonstration Re-flight is necessary, then an extension may be granted (for re-flight only). Teams completing a required re-flight must submit an FRR Addendum by the FRR Addendum deadline.		X			The team shall conduct a vehicle demonstration flight prior to the FRR deadlines. The team acknowledges that no exceptions shall be made and extensions shall only be considered for re-flights seeking to demonstrate improved vehicle safety and payload functionality.	Incomplete
2.18.2	Payload Demonstration Flight - All teams will successfully launch and recover their full-scale rocket containing the completed payload prior to the Payload Demonstration Flight deadline, further described in the NASA SL Handbook. Requirements 2.18.2.1-2.18.2.4 shall be met.		X			he team shall complete a payload demonstration flight prior to the Payload Demonstration Flight deadline.	Incomplete
2.18.2.1	The payload must be fully retained until the intended point of deployment (if applicable), all retention mechanisms must function as designed, and the retention mechanism must not sustain damage requiring repair.		X	X		The payload shall be designed to be fully retained until the intended point of deployment and all retention mechanisms must function as designed without sustaining damage requiring repair inhibiting the reusability of the payload and vehicle, in accordance with Req. 2.4. This will be demonstrated during the full-scale flight tests.	In Progress
2.18.2.2	The payload flown must be the final, active version.		X			The team shall fly the final active payload. Any changes to the payload following the flight will require NASA Student Launch team approval and re-flight in accordance with the demonstration flight deadlines.	Incomplete
2.18.2.3	If the above criteria are met during the original Vehicle Demonstration Flight, occurring prior to the FRR deadline and the information is included in the FRR package, the additional flight and FRR Addendum are not required.		X			The team shall review the requirements and flight performance following the Vehicle Demonstration flight and determine if an additional flight is required.	Incomplete
2.18.2.4	Payload Demonstration Flights must be completed by the FRR Addendum deadline.		X			The team shall complete payload demonstration flights prior to the FRR Addendum deadline. The team acknowledges no extensions will be granted.	Incomplete
2.19	An FRR Addendum will be required for any team completing a Payload Demonstration Flight or NASA required Vehicle Demonstration Re-flight after the submission of the FRR Report.		X			The team shall complete an FRR Addendum for any payload demonstration or vehicle demonstration re-flights after the FRR deadline.	Incomplete
2.19.1	Teams required to complete a Vehicle Demonstration Re-Flight and failing to submit the FRR Addendum by the deadline will not be permitted to fly the vehicle at launch week.		X			The team shall complete a vehicle demonstration re-flight and FRR addendum by the deadline as necessary or forfeit the permission to fly at launch week.	Incomplete
2.19.2	Teams who successfully complete a Vehicle Demonstration Flight but fail to qualify the payload by satisfactorily completing the Payload Demonstration Flight requirement will not be permitted to fly the payload at launch week.		X			The team shall complete a successful payload demonstration flight prior to the Payload Demonstration Flight deadline.	Incomplete
2.19.3	Teams who complete a Payload Demonstration Flight which is not fully successful may petition the NASA RSO for permission to fly the payload at launch week.		X			If the payload demonstration flight is not fully successful, the team shall assess the failures and petition the NASA RSO for permission to fly the paylaod at launch week by preparing documentation about the failures, their risk analysis, and steps that can be taken to resolve the failures safely prior to launch week.	Incomplete
2.20	The team's name and launch day contact information shall be in or on the rocket airframe as well as in or on any section of the vehicle that separates during flight and is not tethered to the main airframe. This information shall be included in a manner that allows the information to be retrieved without the need to open or separate the vehicle.		X			he team shall include team information including name and contact information on the external of the vehicle by incorporating the information into the vehicle paint or applying external labels.	Incomplete
2.21	All Lithium Polymer batteries will be sufficiently protected from impact with the ground and will be brightly colored, clearly marked as a fire hazard, and easily distinguishable from other payload hardware.		X			The Safety and Systems team shall verify that all lithium polymer batteries in the vehicle are sufficiently protected from impact with the ground and shall be clearly labeled with bright colors as a fire hazard. The team shall use fire-proof lithium polymer battery carrying cases for transporting and storing batteries before and after the flight.	Incomplete
2.22	Vehicle Prohibitions		X			The listed vehicle prohibitions shall be inspected prior to all flights to ensure the vehicle is in compliance.	Incomplete
2.22.1	The launch vehicle will not utilize forward canards. Camera housings will be exempted, provided the team can show that the housing(s) causes minimal aerodynamic effect on the rocket's stability.	X		X		The vehicle will not utilize forward canards. If camera housings are used the team shall provide computational fluid dynamics (CFD) analysis and a subscale launch demonstrating the housing does not affect vehicle stability.	Incomplete
2.22.2	The launch vehicle will not utilize forward firing motors.		X			The vehicle will not utilize forward firing motors.	Complete

Requirement		Verification Method				Verification Plan	Status
ID	Description	A	I	D	T		
2.22.3	The launch vehicle will not utilize motors that expel titanium sponges.		X			The vehicle motor documentation shall be inspected to verify it does not expel titanium sponges. This shall be verified with the approval of team launch manager Dave Brunsting.	Incomplete
2.22.4	The launch vehicle will not utilize hybrid motors.		X			The vehicle shall not utilize hybrid motors.	Complete
2.22.5	The launch vehicle will not utilize a cluster of motors.		X			The vehicle shall not utilize a cluster of motors. See Section 3 for details on the motor selection.	Complete
2.22.6	The launch vehicle will not utilize friction fitting for motors.		X			The vehicle shall not utilize friction fitting for motors.	Complete
2.22.7	The launch vehicle will not exceed Mach 1 at any point during flight.	X		X		The launch vehicle shall not exceed Mach 1 at any point during flight as determined by OpenRocket and RockSim analysis, and demonstrated by analyzing the recorded flight data.	In Progress
2.22.8	Vehicle ballast will not exceed 10% of the total unballasted weight of the rocket as it would sit on the pad.		X			The vehicle ballast will not exceed 10% of the total unballasted weight of the rocket as it would sit on the pad.	In Progress
2.22.9	Transmissions from onboard transmitters will not exceed 250 mW of power (per transmitter).	X			X	Transmissions from onboard transmitters shall not exceed 250 mW of power as determined by the specifications of on-board transmitters and relevant testing.	In Progress
2.22.10	Transmitters will not create excessive interference. Teams will utilize unique frequencies, handshake/passcode systems, or other means to mitigate interference caused to or received from other teams.		X		X	Transmitters shall not create excessive interference and shall be utilize unique frequencies or other means to limit interference and shall be tested prior to launch week.	In Progress
2.22.11	Excessive and/or dense metal will not be utilized in the construction of the vehicle. Use of lightweight metal will be permitted but limited to the amount necessary to ensure structural integrity of the airframe under the expected operating stresses.		X			Excessive and/or dense metal shall not be utlized in the construction of the vehicle unless approved by the NASA Student Launch team and team launch manager Dave Brunsting limited to the amount necessary to ensure structural integrity.	In Progress

Table 86: NASA Recovery Requirements

Requirement		Verification Method				Verification Plan	Status
ID	Description	A	I	D	T		
3.1	The launch vehicle will stage the deployment of its recovery devices, where a drogue parachute is deployed at apogee, and a main parachute is deployed at a lower altitude. Tumble or streamer recovery from apogee to main parachute deployment is also permissible, provided that kinetic energy during drogue stage descent is reasonable, as deemed by the RSO.		X			The launch vehicle will contain two separate parachute bays, one for the drogue parachute and one for the main. Each of the altimeters will be programmed to eject the drogue parachute at or shortly after rocket apogee, and the main parachute at a lower altitude.	In Progress
3.1.1	The main parachute shall be deployed no lower than 500 feet.			X	X	All of the recovery altimeters will be programmed to eject the main parachute at an altitude of 500 ft or greater, verified with simulated flight tests and vehicle demonstration flights.	In Progress
3.1.2	The apogee event may contain a delay of no more than 2 seconds.		X			All of the recovery altimeters will be programmed to eject the drogue parachute at apogee or between 0 and 2 s after apogee.	In Progress
3.1.3	Motor ejection is not a permissible form of primary or secondary deployment.		X			All recovery ejection charges will be controlled by commercial altimeters.	In Progress
3.2	Each team must perform a successful ground ejection test for both the drogue and main parachutes. This must be done prior to the initial subscale and full-scale launches.				X	Before any rocket launch by the team, a ground separation test will be performed on the rocket using an ejection charge of the same type and size to be used for the launch.	In Progress
3.3	Each independent section of the launch vehicle will have a maximum kinetic energy of 75 ft-lb_f at landing.	X		X		The main parachute will be appropriately sized such that the largest section falls with a kinetic energy under 75 ft-lb_f under main parachute. The expected descent velocity has been simulated using OpenRocket and a custom Matlab simulator. Descent velocity data will also be taken during test launches to confirm simulation accuracy and ensure compliance with descent kinetic energy requirements.	In Progress
3.4	The recovery subsystem will contain redundant, commercially available altimeters.		X		X	The recovery ejection charges will be controlled by two Featherweight Raven3 altimeters and one PerfectFlite Stratologger SL100 altimeter.	In Progress
3.5	Each altimeter will have a dedicated power supply, and all recovery electronics will be powered by commercially available batteries.		X				In Progress
3.6	Each altimeter will be armed by a dedicated mechanical arming switch that is accessible from the exterior of the rocket airframe when the rocket is in the launch configuration on the launch pad.		X				In Progress
3.7	Each arming switch will be capable of being locked in the ON position for launch (i.e. cannot be disarmed due to flight forces).		X		X		In Progress
3.8	The recovery subsystem electrical circuits will be completely independent of any payload electrical circuits.		X		X	In simulated launch environment, the full function of the recovery electronics will be tested without the payload present to ensure independence from the payload.	In Progress
3.9	Removable shear pins will be used for both the main parachute compartment and the drogue parachute compartment.		X			The same number and configuration of shear pins will be used to secure the parachute compartments during ground separation tests and full launches. See Section 3.8.2 for details.	Incomplete
3.10	The recovery area will be limited to a 2,500 ft radius from the launch pads.	X		X	X	The drift distance of the rocket after apogee was simulated in both OpenRocket and a custom Matlab simulator at a variety of wind speeds up to 20 mph. The drift distance of the rocket after apogee during the test launch will be recorded to ensure accuracy of the simulations and compliance with competition rules.	In Progress
3.11	Descent time will be limited to 90 seconds (apogee to touch down).	X		X	X	The descent time after apogee was simulated using OpenRocket and a custom Matlab simulator. The descent time after apogee will also be measured during test launch to ensure accuracy of simulations and compliance with competition rules.	In Progress
3.12	An electronic tracking device will be installed in the launch vehicle and will transmit the position of the tethered vehicle or any independent section to a ground receiver.		X	X		The launch vehicle will contain an active GPS transmitter during test launch, which will be used to track the location of the tethered vehicle after launch.	Incomplete
3.12.1	Any rocket section or payload component, which lands untethered to the launch vehicle, will contain an active electronic tracking device.		X			All sections of the rocket will be tethered together, with a single dedicated GPS transmitter in one of the sections.	Incomplete
3.12.2	The electronic tracking device(s) will be fully functional during the official flight on launch day.			X	X	The GPS transmitter will be tested for functionality before the official flight on launch day.	Incomplete
3.13	The recovery subsystem electronics will not be adversely affected by any other on-board electronic devices during flight (from launch until landing).			X	X	The rocket will be flown with all electronics active during a test launch before competition. Altimeter data will be inspected afterwords for any evidence of adverse effects.	Incomplete

Requirement		Verification Method				Verification Plan	Status
ID	Description	A	I	D	T		
3.13.1	The recovery subsystem altimeters will be physically located in a separate compartment within the vehicle from any other radio frequency transmitting device and/or magnetic wave producing device.		X			The recovery electronics will be mounted in a recovery bay separate from the payload and any RF or EM transmitters or receivers.	In Progress
3.13.2	The recovery subsystem electronics will be shielded from all onboard transmitting devices to avoid inadvertent excitation of the recovery subsystem electronics.		X			A conductive Faraday cage will encase the recovery altimeters to prevent interference by any outside transmitters.	In Progress
3.13.3	The recovery subsystem electronics will be shielded from all onboard devices which may generate magnetic waves to avoid inadvertent excitation of the recovery subsystem.		X			A conductive Faraday cage will encase the recovery altimeters to prevent interference by any internal magnetic wave producing devices.	In Progress
3.13.4	The recovery system electronics will be shielded from any other onboard devices which may adversely affect the proper operation of the recovery system electronics.		X			A conductive Faraday cage will encase the recovery altimeters to prevent interference by any internal transmitters and other electronics.	In Progress

Table 87: NASA Payload Requirements

Requirement		Verification Method				Verification Plan	Status
ID	Description	A	I	D	T		
4	All payload designs must be approved by NASA. NASA reserves the authority to require a team to modify or change a payload, as deemed necessary by the Review Panel, even after a proposal has been awarded.			X		The team acknowledges that designs must be approved by NASA and that NASA may request design changes.	Complete
4.2	University teams will design a system capable of being launched in a high power rocket, landing safely, and recovering simulated lunar ice from one of several locations on the surface of the launch field. The methods utilized will be at the teams' discretion and will be permitted so long as the designs are deemed safe, obey FAA and legal requirements, and adhere to the intent of the challenge. An additional experiment is allowed, and may be flown, but will not contribute to scoring. If the team chooses to fly an additional experiment, they will provide the appropriate documentation in all design reports so the experiment may be reviewed for flight safety.		X			The team shall be competing in the university division and shall design a payload which meets the listed requirement. The team shall have discretion to design the payload but shall work with team mentors to verify the design is safe, meets FAA requirements, and adheres to the requirements of the challenge. An additional experiment will be flown (ABS), and is thoroughly documented in Section 3.7.6.	In Progress
4.3.1	The launch vehicle will be launched from the NASA-designated launch area using the provided Launch pad. All hardware utilized at the recovery site must launch on or within the launch vehicle.		X			The launch vehicle will be launched from the NASA designated launch area using the provided launch pad. All hardware utilized at the recovery site shall be launched on or within the vehicle.	In Progress
4.3.2	Five recovery areas will be located on the surface of the launch field. Teams may recover a sample from any of the recovery areas. Each recovery site will be at least 3 ft in diameter and contain sample material extending from ground level to at least 2 in. below the surface.			X		The team shall design the payload to be capable of travelling to one of the recovery areas and recover a sample extending at least 2 inches below the surface.	In Progress
4.3.3	The recovered ice sample will be a minimum of 10 mL.			X		The payload will be designed to be capable of recovering an ice sample with a minimum volume of 10 mL.	In Progress
4.3.4	Once the sample is recovered, it must be stored and transported at least 10 linear ft from the recovery area.			X		The payload will be designed to be capable of transporting the recovered sample at least 10 linear ft from the recovery area.	In Progress
4.3.5	Teams must abide by all FAA and NAR rules and regulations.		X			The team shall abide by all FAA and NAR rules and regulations. The team shall conduct a review with the team launch manager prior to the launch day to verify all regulations are met.	In Progress
4.3.6	Black powder and/or similar energetics are only permitted for deployment of in-flight recovery systems. Any ground deployments must utilize mechanical systems.		X			The payload deployment shall utilize an in-flight black powder nose cone ejection system. See Section 5.3.2 for details.	In Progress
4.3.7	Any part of the payload or vehicle that is designed to be deployed, whether on the ground or in the air, must be fully retained until it is deployed as designed.			X	X	The payload shall be designed to be fully retained until it is deployed as designed. This shall be verified in tests prior to launches and demonstrated during the demonstration flights.	In Progress
4.3.7.1	A mechanical retention system will be designed to prohibit premature deployment.	X				The mechanical system was designed to prohibit premature deployment and has been analyzed using methods such as FEA to determine forces on the system to avoid premature deployment. See Section 5 for details on the retention system design and analysis.	Complete
4.3.7.2	The retention system will be robust enough to successfully endure flight forces experienced during both typical and atypical flights.			X	X	The retention system shall be subjected to shake tests to ensure the system is capable of enduring typical and atypical flight forces while still being reusable per Req. 2.4.	In Progress
4.3.7.3	The designed system will be fail-safe.		X		X	The retention system is designed to be fail-safe to ensure that failure of any system components does not result in the payload being damaged or released prematurely. The system shall be designed with redundancy and thoroughly tested to avoid failures.	In Progress
4.3.7.4	Exclusive use of shear pins will not meet Req. 4.3.7.		X			The team will not exclusively use shear pins for retention. See Section 5.3.1 for retention design details.	Complete
4.4.1	Any experiment element that is jettisoned during the recovery phase will receive real-time RSO permission prior to initiating the jettison event.		X			The payload will be completely retained during flight and recovery.	Complete
4.4.2	UAV payloads, if designed to be deployed during descent, will be tethered to the vehicle with a remotely controlled release mechanism until the RSO has given permission to release the UAV.		X	X		The payload will be completely retained during flight and recovery.	Complete
4.4.3	Teams flying UAVs will abide by all applicable FAA regulations, including the FAA's Special Rule for Model Aircraft.		X			The team shall abide by all FAA regulations and shall carefully review the regulations during each step of the development process.	In Progress

Requirement		Verification Method				Verification Plan	Status
ID	Description	A	I	D	T		
4.4.4	Any UAV weighing more than .55 lbs. will be registered with the FAA and the registration number marked on the vehicle.		X			The team UAV weighing more than 0.55 lbs will be registered with the FAA and the registration number marked on the vehicle.	In Progress

Table 88: NASA Safety Requirements

Requirement		Verification Method				Verification Plan	Status
ID	Description	A	I	D	T		
5.1	Each team will use a launch and safety checklist. The final checklists will be included in the FRR report and used during the LRR and any launch day operations.		X			The team shall write and maintain a launch and safety checklist which shall be included in the FRR and LRR reports. The Safety and Systems team shall lead development and enforcement of these safety procedures.	In Progress
5.2	Each team must identify a student safety officer who will be responsible for all items in Req. 5.3.		X			The team has elected Brooke Mumma to serve as the safety officer who will lead the Safety and Systems team. As such she shall be responsible for all safety matters in accordance with Req. 5.3.	Complete
5.3	The role and responsibilities of the safety officer will include, but are not limited to those listed in Req. 5.3.1-5.3.4.		X			The safety officer shall manage the responsibilities listed.	In Progress
5.3.1.1-5.3.1.9	The safety officer shall monitor team activities with an emphasis on safety during design of vehicle and payload, construction of vehicle and payload components, assembly of vehicle and payload, ground testing of vehicle and payload, full-scale launch test(s), subscale launch test(s), launch day, recovery activities, and STEM engagement activities.		X			The safety officer shall monitor all listed team activities during the full development cycle of the team throughout the year. The safety officer shall focus on the safety of the team and shall have the discretion to maintain enforcement methods for handling safety violations.	In Progress
5.3.2	The safety officer shall implement procedures developed by the team for construction, assembly, launch, and recovery activities.		X			The Safety and Systems team shall manage the design teams in writing procedures for construction, assembly, launch, and recovery activities and shall ensure the procedures meet safety requirements following a standardized format set by the team.	In Progress
5.3.3	The safety officer shall manage and maintain current revisions of the team's hazard analyses, failure modes analyses, procedures, and MSDS/chemical inventory data.		X			The Safety and Systems team shall maintain the team's hazard analyses, failure mode analyses, procedures, and MSDS inventory data. The team shall conduct frequent revision meetings.	In Progress
5.3.4	The safety officer assist in the writing and development of the team's hazard analyses, failure modes analyses, and procedures.		X			The Safety and Systems team shall lead writing and development of the analyses and procedures listed.	In Progress
5.4	During test flights, teams will abide by the rules and guidance of the local rocketry club's RSO. The allowance of certain vehicle configurations and/or payloads at the NASA Student Launch does not give explicit or implicit authority for teams to fly those vehicle configurations and/or payloads at other club launches. Teams should communicate their intentions to the local club's President or Prefect and RSO before attending any NAR or TRA launch.		X			The Safety and Systems lead, team captains, and team launch manager shall communicate with the local RSO to ensure the vehicle meets all local configuration requirements and address any safety concerns of the local RSO.	In Progress
5.5	Teams will abide by all rules set forth by the FAA.		X			The team shall abide by all FAA rules and regulations and will conduct frequent reviews to ensure continued compliance.	In Progress

6.2.2 Team Derived Requirements

Table 89: Derived Launch Vehicle Requirements

Requirement				Verification Method				Verification Plan	Status
ID	NASA Parent ID	Description	Justification	A	I	D	T		
V.1	X	The vehicle will have two in-flight separation points to allow for a drogue and main parachute deployment and an additional access point for ABS integration.	Drogue parachute necessary to slow vehicle and decrease drift		X			The design of the rocket will have three separation points, two covered by bulkhead for recovery and a third for ABS integration.	In Progress
V.2	X	The weight distribution throughout the vehicle will be kept the closest possible to constant.	Decrease parachute size		X			An updated weight budget for the launch vehicle will be kept updated at all times.	In Progress
V.3	2.22.8	The vehicle must have a fully designed and integrated ballast area at the rocket's Cg to diminish ballast's effect in the vehicle's stability. The ballast area must hold up to 10% of total vehicle weight.	In the case that payloads are under weight budget, ballasting will be necessary to meet target apogee		X			The ballast area will be designed to fit in the area closest to the rocket's Cg.	In Progress
V.4	2.1, 2.2	The vehicle is designed to reach a 4,444 ft altitude.	Target apogee must be set by the team	X			X	Simulation software will be used to verify vehicle designs reach a 4,100 ft. apogee in a simulated environment, and full scale test flights shall be used to verify the accuracy of the simulation and completion of the requirement.	In Progress
V.5	X	The payload bay shall be a fiber glass body tube with an 8 in. OD and 20 in length.	Payload bay must be radio transparent for signals to payload		X			The team designed the rocket to provide the required dimensions for the payload system. See Section 3.3.2 for design details.	In Progress
V.6	X	ABS must be secured to the rest of the vehicle and fill the full aft diameter of the rocket.	Avoid force unbalance due to movement of payload		X			ABS will be designed for ideal integration into the aft part of the rocket. See Section X for details on ABS design.	In Progress
V.7	X	The vehicle shall not exceed a maximum length of 12 ft.	Vehicle must be easily transported		X			The total length of the full scale rocket will be measured when construction material is delivered.	Incomplete
V.7.1	X	The recovery body tube will not exceed a maximum length of 48 in.	Length budget to fulfull V.7	X				The recovery body tube was designed under that length, shown in Section 3.2. Measurements will be made during fabrication to confirm that this requirement is met.	In Progress
V.7.2	X	ABS will not exceed 11.5 inches in length to fulfill V.7.		X				ABS was designed within this length restriction. See Section 3.7.6 for design details. Measurements will be made during fabrication to confirm that this requirement is met.	In Progress
V.8	2.2	The vehicle shall not exceed a maximum weight of 70 lbs.	Vehicle must be able to achieve target apogee			X		The launch vehicle will be weighted with all of the systems before launch.	Incomplete
V.8.1	X	ABS will not exceed 70 oz in weight.	Weight budget to fulfill V.8		X			ABS was designed to weigh less than 70 oz. Design details can be found in Section 3.7.3.3. Measurements will be made during fabrication to confirm that this requirement is met.	In Progress
V.9	X	The vehicle must house a camera that looks downward with an angle of visibility that includes ABS.	Allows view of ABS tab extension and retraction		X			A housing area will be integrated and a securing mechanism will be designed to safely hold the camera in place. See Section 9 for design details.	In Progress
V.10	2.14	The stability margin of the vehicle with the motor must be between 2 and 3 calibers.	Avoid any possibility of vehicle tilting into the wind	X		X		Flight simulation applications will be used to design for a 2-3 caliber stability margin and before test flights the actual Cg will be measured to calculate the stability margin.	In Progress
V.11	4.2	The motor selection must tend towards overshooting rather than undershooting the target apogee.	Allow use of ABS	X		X		The motor selection will be based on flight simulations and test flights will determine predicted vs actual apogee. See Appendix B.3 for simulation details.	In Progress

Requirement				Verification Method				Verification Plan	Status
ID	NASA Parent ID	Description	Justification	A	I	D	T		
V.12	X	Epoxied bulkheads must be able to hold the load of drogue and main parachute deployments.	Load bearing bulkheads must not break under max load				X	Solid testing will be designed to test max force that an epoxied bulkhead can withstand.	In Progress
V.13	X	Removable bulkhead attached to ABS must be able to withstand the load of drogue and main parachute deployments.	Failure of the bulkhead or the securing screws would prevent the ability to execute a successful landing	X				Analysis of the stresses experienced by the bulkhead and screws during deployment will help determine material and dimensional requirements to ensure these components will not fail.	In Progress
V.14	X	The ABS drag tabs must extend at a location no greater than 1 in. from the CP.	The induced drag force shall not result in destabilizing moments		X			The integration design of ABS will focus on the location of the tabs in relation to the CP, shown in Section 3.2. Measurements will be made during fabrication to confirm that this requirement is met.	In Progress

Table 90: Derived Recovery Requirements

Requirement				Verification Method				Verification Plan	Status
ID	NASA Parent ID	Description	Justification	A	I	D	T		
R.1	3.6, 3.7	Recovery ejection charges shall be capable of being “safed," such that at least 2 independent actions are necessary before the altimeter is fully armed.	To ensure that the black powder ejection charges do not ignite early and injure personnel			X		Two switches of different types will be placed in series with the powering battery such that both switches need to be closed before the altimeter fully arms. See Section 3.8.2 for switch details.	In Progress
R.2	X	The parachutes, shroud lines, and shock cordage shall be protected from potential damage due to the ejection charges.	Ejection charges can burn the parachute, reducing its ability to successfully slow down the rocket			X	X	A Nomex deployment bag will be used to contain the folded main and drogue parachutes to protect them from the ejection charges. Ground separation tests will be performed to ensure adequate parachute protection before launch.	Incomplete
R.3	X	The altimeter bay shall be removable such that rocket apogee/flight data can be quickly retrieved after successful recovery with minimal tools.	A removable altimeter bay allows for quicker assembly and retrieval, allowing for quicker launch turnarounds.				X	The recovery altimeters will be contained in the CRAM, which will be easily removed from the rocket via a twist-to-lock mechanism. Altimeter retrieval demonstration shall be performed such that the altimeters are removed from the landed, separated rocket in 5 minutes or less.	In Progress
R.4	3.4	System shall be redundant such that any 2 component failures (such as altimeter malfunction, battery disconnect, or defective E-match) does not compromise the ability to safely recover the vehicle and complete the mission.	Redundant components increase the reliability of the recovery system and decrease the likelihood of parachute deployment failure			X		Three independent altimeters are used to control parachute deployment, with each altimeter fully capable of deploying both parachutes at the proper times.	In Progress
R.5	X	The altimeter compartment shall be sealed off from the parachute compartment to prevent the ejection charges from damaging the electronics.	Ejection charges can damage exposed altimeters and hinder main parachute deployment			X	X	Ground separation testing will reveal any gas escape out the altimeter ports, and altimeter data will be analyzed after test flight for sudden dips in altitude just after apogee, which is indicative of the ejection charge gasses entering the altimeter bay.	Incomplete
R.6	X	The recovery system shall be capable of being “safed" after landing, in the event that an ejection charge has failed to deploy.	A method of external safety allows for safe retrieval of the rocket in the case of a live deployment charge.			X	X	In a simulated launch environment, an attempt will be made to initiate the ejection charge with one of the stops in place.	Incomplete
R.7		On-vehicle telemetry shall weigh less than 3 lbs	Weight budget ensures apogee is reached			X		Weight will be measured	In Progress
R.8		On-vehicle telemetry shall be packaged in nose cone	Adequate space must be available for other subsystems, specifically for the LSRS			X		CAD Model will be used to verify the size of the final system	In Progress
R.9		Portable power sources shall keep on-vehicle telemetry and relay station operational for well over the mission time	Telemetry goals cannot be met under power shortage	X				From calculations of max. current draw from the system, selected batteries will yield operational times orders of magnitude beyond mission time	In Progress
R.10		On-vehicle telemetry shall store all transmitted data locally	Verifies that data was not corrupted in the wireless link			X		Sample data will be stored on the SD card before flight, and it will be verified that it can be read from a laptop; during test launches, on-vehicle stored data will be read and inspected after launch	In Progress
R.11		On-vehicle telemetry shall transmit reliably over an approximate range of 5500 ft through empty atmosphere	Ensures data is able to be transmitted to the relay station throughout entirity of the flight of the vehicle				X	Transmitter Range Test	In Progress
R.12		Telemetry relay station shall transmit reliably over an approximate range of 2500 ft at ground level	Ensures data can be transmitted from the relay station to the ground station			X	X	Transmitter Range Test	In Progress

Requirement				Verification Method				Verification Plan	Status
ID	NASA Parent ID	Description	Justification	A	I	D	T		
R.13		Ground station GUI shall report GPS data (latitude, longitude, altitude), accelerometer data (three axis acceleration, angular velocity, vehicle orientation), and altimeter data (vehicle altitude) as received	GUI should report a live view of the current status of the vehicle		X			Data received by the ground station will be accurately displayed by the GUI by inspection	In Progress

Table 91: Derived Payload Requirements

Requirement				Verification Method				Verification Plan	Status
ID	NASA Parent ID	Description	Justification	A	I	D	T		
P.1		The Rover must not have an overall width larger than 6 in.	Constraining the Rover to a 6 in. maximum width gives the other subsystems a dimension to design around		X			All Rover body designs will be constrained to a width of 6 in.	In Progress
P.2		The Rover must be able to overcome small obstacles such as rocks, corn stalks, and crop rows.	The terrain where the launch will be conducted is not flat and easy to navigate, so the Rover should be able to overcome any obstacles it may encounter.			X	X	The translation mechanism will be tested traversing multiple types of obstacles	In Progress
P.3		The Rover must be able to traverse through mud, puddles, corn stalks, and corn fields.	The state of the terrain is variable and the rover should be designed to overcome any terrain it may experience.			X	X	The rover will be tested traversing through various terrains that may be present at the launch including mud, puddles, and high cut corn	Incomplete
P.4		The Rover must hold and protect the electronics in a water proof container.	Making the Rover water resistant will enable it to travel through puddles rather than going around them and wasting time.		X	X	X	All containers that will house electronics will be water tested to ensure there are no leaks.	In Progress
P.5		The Rover must not weigh more than 40 oz.	Constraining the Rover to a maximum weight will prevent the payload from going over weight		X			An up to date weight budget of all components will be maintained to keep track of the weight of the systems.	In Progress
P.6		The Rover must have a minimum operating time of 20 min.	A 20 min operating time will provide adequate time for the Rover to traverse to the closest FEA			X	X	Operating time calculations will be conducted at various design milestones to verify the selected components will enable the Rover to operate for a minimum of 20 min.	In Progress
P.7		The Rover must have a manual override switch.	A manual override enables the operator to take control of the Rover should an error occur in the control code.		X	X	X	All control software will be required to have a manual override built into the code.	In Progress
P.8		The Rover will remain dormant until receiving the initiation signal from the UAV.	A low power mode will conserve the battery life of the Rover prior to deploying.			X	X	Various testing will be conducted with the Rover in the low power mode to ensure that no external force or signal will bring the Rover out of the dormant state.	In Progress
P.9		The UAV must be no larger than 4 in x 4 in.	This constraint enables the UAV to fit inside the payload bay without the need for moving arms.		X			The UAV design was restrained to 4 in x 4 in. See Section 5.4.1 for UAV design details.	Complete
P.10		The UAV frame must protect the battery.	Damage to the battery can result in catastrophic failure		X	X		All UAV frame designs will be required to have no moving parts and all components will need to be statically secured. See Section 5.4.1 for design details.	In Progress
P.11		The UAV must weigh under 2.4 oz.	Constraining the UAV to a maximum weight will prevent the payload from going over weight.		X			An up to date weight budget of all components will be maintained to keep track of the weight of the systems.	In Progress
P.12	X	The UAV must have a minimum flight time of 10 min.	A 10 minute flight time will provide adequate time for the UAV to search the area around the Rover.			X		Flight time calculations will be conducted at various design milestones to verify the selected components and the selected frame design will enable the UAV to fly for a minimum of 10 min.	In Progress
P.13		The UAV must use a commercial flight controller.	Using a commercially available flight controller expedites the flight software development process		X			A commercial flight controller for the UAV has been selected.	Complete
P.14	X	The UAV must have a manual override switch.	A manual override enables the operator to take control of the UAV should an error occur in the flight code		X	X	X	All flight software will be required to have a manual override built into the code.	In Progress
P.15	4.3.3	The Sample Retrieval system must recover a minimum sample size of 15 mL	Having a sample size target over the required sample size will ensure the retrieval of a 10 mL sample			X	X	The system has been designed to collect 15 mL of sample. The system will be extensively tested to ensure it consistently retrieves a sample no smaller than 15 mL.	In Progress

Requirement				Verification Method				Verification Plan	Status
ID	NASA Parent ID	Description	Justification	A	I	D	T		
P.16		The Sample Retrieval system must be able to correctly orient itself for retrieval operations.	A self orienting sample retrieval system will allow the rover to be in any position while the retrieval system is operating			X	X	The retrieval system will be extensively tested to verify it can correctly orient itself to perform the retrieval operations consistently and reliably.	Incomplete
P.17	4.3.4	The Sample Retrieval system must retain and protect the recovered sample from spillage and contamination.	Securing the sample once it is collected will ensure successful deliver of the sample from the CFEA.		X	X	X	The sample container will be water tested to ensure no contaminants can leak into the container and the container will be tested through sample retrieval simulations to ensure no amount of sample can spill out of the container during the translation of the Rover.	Incomplete
P.18		The Sample Retrieval system must interface with the Rover electronics.	Reduces system complexity and reduces the risk of failure			X	X	The sample retrieval team will communicate regularly with the Rover electronic team to ensure that the retrieval system can integrate into the electronic system of the Rover.	In Progress
P.19		The Sample Retrieval system must be easily integrated with the Rover frame.	Reduces system complexity and reduces the risk of failure		X	X		The team is utilizing Fusion 360 and cloud based models to ensure all assemblies use up to date models and all systems integrate together.	In Progress
P.20	4.3.7.3	The Deployment system must have multiple fail-safes.	Will ensure system success despite a component failure within the system	X		X	X	All designs of the deployment system will include a minimum of two redundant locking mechanisms for restricting motion of components in the bulkhead of the vehicle. See Section 5.3 for deployment design details.	In Progress
P.21		The Deployment system must be able to correctly orient the Rover and UAV regardless of the landing position of the upper section of the vehicle.	The orientation of the Rover is paramount to mission success			X	X	The orientation system will be extensively tested with the bulkhead section of the vehicle to ensure that it consistently and reliably orients the Rover and UAV for multiple orientations and landings of the bulkhead section of the vehicle.	In Progress
P.22	4.3.7.1	The deployment system must restrict motion of the Rover and UAV in all directions until the deployment sequence is initiated.	Flight stability is dependent on all components in the payload bay remaining locked in place			X	X	All designs of the deployment system will be required to restrict motion of the Rover and UAV in the X, Y, and Z directions. All motion restricting designs will be extensively tested to verify proper functionality.	In Progress
P.23		The target detection system must correctly identify the closest CFEA.	Minimize travel time and distance for the Rover.			X	PUT???	The target detection software will be tested to consistently locate the closest CFEA during multiple simulations in which fluorescent material will be placed on multiple types of terrain. See Section 5.4.2 for system details.	In Progress
P.24		The target detection system must identify the corner of the FEA that is furthest from the Rover.	Reduced risk of the Rover driving over the UAV			X	PUT???	The target detection software will be tested to correctly and reliably identify the corner of the FEA that is furthest from the Rover.	In Progress

Table 92: Derived Systems and Safety Requirements

Requirement				Verification Method				Verification Plan	Status
ID	NASA Parent ID	Description	Justification	A	I	D	T		
S.1	5.3.1.7	Prior to any launch, team members shall be briefed and tested about safety and procedures in accordance with NAR/TAR and NDRT regulations.	To ensure the safety of team personnel, members must be informed of the hazards at launch and proper procedures		X			Attendance will be taken at pre-launch briefings and any members not in attendance will not be eligible to attend the launch. Members failing to pass the safety quiz will not be eligible to attend the launch.	In Progress
S.2	5.3.1.2	Prior to construction of subsection components and the full assembly, schematics and procedures shall be published to ensure correct and safe manufacturing and assembly techniques.	Provides clarity which makes the construction process safer and more efficient.		X			Schematics will be created based on finalized 3D models and available in the workshop prior to any construction.	In Progress
S.3	5.3.3	The team shall maintain updated records of the team's hazard analyses, failure modes analyses, procedures, and MSDS/chemical inventory data and will use this information to drive design, construction, and testing decisions.	Allows the team to make safer and improved decisions		X			Documentation will be available, reviewed, and updated on a regular basis. The most current version will be available on the team shared drive.	In Progress
S.4	5.3.1.2	Each NDRT member participating in construction shall be certified on the machines and tools used in accordance to the Notre Dame Student Fabrication Lab standards.	Requiring certifications for workshop tools ensures that members learn the proper technique and are informed of workshop hazards.		X			Members will receive a card that indicates which tools they are certified on. Each team member must present this card to a team officer before working on any construction.	In Progress
S.5	5.3.1.4	Each subsection of the vehicle and payload shall be tested individually before the full scale test.	Allows the team to identify and correct errors prior to full-scale testing, increasing probability of a successful mission.		X			The Safety and Systems Team will work with each design team to develop testing plans and rigs prior to conducting tests. The physical copy of the testing plan will be used for running the test, and the test results will be filed digitally.	In Progress
S.6	5.3.1.4	The team will develop detailed test procedures at the component and full-scale level to ensure that the designs are robust and reliable.	Allows for standardization of documentation and streamlined communication; ensures that members go into testing fully prepared.		X			A generic test procedure format will be available to the technical leads to modify. Each subsystem will present their testing results prior to full scale assembly.	In Progress

6.3 Project Budget

The Notre Dame Rocketry Team has budgeted $20,753 for this year's NASA Student Launch. Itemized budgets with allocations outlined in Table 94 are kept up to date by each lead. The captain monitors the overall budget. Each purchase is carefully researched to ensure the selection of the most reliable and affordable vendor. Per General Requirement 1.2, updates and modifications to the budget will continue until the submission of the final budget summary in PLAR.

6.3.1 Project Sponsorship

The Notre Dame Rocketry Team's participation in the NASA Student Launch would not be possible without the support of our generous sponsors. Table 93 catalogs the contributors to Notre Dame's project.

Table 93: NDRT 2019-2020 Sponsorship

Funding Source	**Amount**
Carryover (2018/19)	$2,722
Team Merchandise	$160
ND Day Fundraising	$671
The Boeing Company	$10,000
Pratt & Whitney	$5,000
ND EE Department	$1,000
Jim Lampariello (Blue Origin Systems Engineer)	$1,000
GE Aviation	$200
TOTAL FUNDING	**$20,753**

As shown in Table 93, corporate sponsorship constitutes the primary revenue source for the team. This year's corporate sponsors include The Boeing Company, Pratt & Whitney, NDRT's founder Jim Lampariello, and GE Aviation. The Notre Dame Rocketry Team is pursuing funding from AIS Healthcare for the remainder of the year.

6.3.2 Project Revenue Allocation

NDRT has allocated approximately 40% of the budget to Vehicle Design, which encompasses the Air Braking System and the Recovery Subsystem. At $2,000, the Lunar Sample Retrieval System was allocated approximately 10% of the budget. Funding for travel to the competition comprises approximately 43% of the budget. Because purchases cannot be made until the Notre Dame Rocketry Team receives approval from both the Notre Dame Aerospace and Mechanical Engineering Department and the Notre Dame Student Affairs

Office, Table 94 lists the projected Competition Travel purchases. Purchases for Competition Travel include team lodging, mentor lodging, gasoline, vehicle rental, and meals for the team. The remaining 7% of the $20,753 was apportioned to Systems & Safety, STEM Engagement, and miscellaneous purchases such as networking dinners with donors and car repairs for test launch travels. Table 94 outlines NDRT's current revenue allocation.

Table 94: NDRT 2019-2020 Project Allocation

Allocation	**Amount**	**Spent**	**Percent Spent**
Vehicle Design	$5,000	$2,731.06	54.62%
Air Braking System	$1,300	$555.92	42.76%
Recovery Subsystem	$2,000	$1,183.95	59.20%
LSRS	$2,000	$1,800.06	90.00%
Systems & Safety	$650	$113.22	17.42%
STEM Engagement	$300	$18.43	6.14%
Competition Travel	$9,000	$8,999.78	100%
Miscellaneous Expenses	$500	$458.96	91.79%
TOTAL ALLOCATION	**$20,750**	**$15,861.38**	**76.44%**

6.3.3 Line Item Budgets

Table 95 details NDRT's project revenue allocation. Listed are the items that the team has purchased thus far. Table 95 presents the purchased materials for the Recovery Subsystem, Systems & Safety, Vehicle Design, LSRS, ABS, and STEM Engagement. Also included in the table are Miscellaneous Expenses and Competition Travel expenses. Items highlighted in light blue in the Total Cost column are projected expenses for purchase in mid-January.

Table 95: Itemized Budget. Prices highlighted in light blue indicate projected purchases for mid-January.

Recovery Subsystem Components	Vendor	Description	Qty	Price per Unit	Total Cost
3.7 V 170 mAh LiPo	Wing Deli Storefront	Rechargeable Battery Pack	5	$7.48	$37.40
UP-S6 1 s LiPo Battery Charger	Crazepony-Power	LiPo Battery Charger	1	$24.21	$24.21
AC to DC Power Adapter 12 V	Crazepony-Power	Power Cord for Charger	1	$11.56	$11.56
Through Mount Slotted Switch	Aerocon Systems	Switch for Recovery Activation	3	$9.01	$27.03
Magnetic Switch	Featherweight Altimeters	Switch for Recovery Activation	3	$28.34	$85.02
JST PH 2.0 MM Connectors, 30 sets	LATTECH	Connectors for Batteries	1	$7.99	$7.99

CAM-M8C-0-10 GPS	Digi-Key	RF Receiver, GLONASS, GNSS, GPS 1.575 GHz-167 dBm	1	$25.00	$25.00
KX222-1054 Accelerometer	Digi-Key	Accelerometer	1	$9.41	$9.41
BNO055 Accelerometer	Digi-Key	Accelerometer	1	$11.16	$11.16
MPL3115A2 Altimeter	Digi-Key	Altimeter	1	$5.80	$5.80
3.7 V 2500 mAh Lithium Ion Polymer Battery	Adafruit	Lithium Ion Polymer Battery	2	$14.95	$29.90
32-bit PIC32 Microcontroller	Microchip Technology	Microcontroller	3	$4.00	$12.00
ADF7030-1 RF Transceiver	Mouser Electronics	Transceiver	3	$5.10	$15.30
HMC452ST89 1 W Power Amplifier	Analog Devices	Power Amplifier	2	$11.71	$23.42
ANT-433-MHW-SMA-S 433 MHz Antenna	Digi-Key	Antenna	1	$15.04	$15.04
128 GB Micro SD Card - SDSQUAR-128G-GN6MA	SanDisk	Memory Card	1	$19.49	$19.49
FTDI FT230XS-R USB to UART	Mouser Electronics	USB Interface	1	$2.04	$2.04
ADF7030-1 EZ-KIT Evaluation & Development Kit	In House	Evaluation board	1	$0.00	$0.00
ADZS-UCM3029EZLITE Motherboard	In House	Motherboard	1	$0.00	$0.00
Oak Board, 1 in. x 8 in.	Home Depot	CRAM body and adapter material	8	$5.76	$46.08
$\frac{1}{8}$ in. Garolite G10	McMaster-Carr	CRAM bulkhead material	1	$16.26	$16.26
$\frac{1}{4}$-20 Hex Head Screws, 10 pack	McMaster-Carr	Bolts for CRAM	1	$7.12	$7.12
$\frac{1}{4}$-20 Hex Nuts, 100 pack	McMaster-Carr	Nuts for CRAM	1	$3.98	$3.98
$\frac{3}{8}$ Extreme-Strength Steel Coupling Nut	McMaster-Carr	Eyebolt Coupling Nut	1	$36.45	$36.45
$\frac{3}{8}$ Zinc-Plated Steel Eyebolt	McMaster-Carr	Recovery Eyebolts	4	$13.93	$55.72
$\frac{3}{8}$ Stainless Steel Quicklink	FruityChutes	Recovery Quicklinks	6	$10.50	$63.00
IFC-120-S	FruityChutes	Main Parachute	1	$541.97	$541.97
6 in. 13 in. Deployment Bag	FruityChutes	Protection for Main Parachute	1	$51.60	$51.60
		TOTAL COST			**$1183.95**
		Budget Allocation			$2000.00

		Margin			$816.05
Systems & Safety Components	Vendor	Description	Qty	Price per Unit	Total Cost
Vinyl Gloves (200)	Walmart	PPE	1	$11.98	$11.98
Face Masks (5)	Walmart	PPE	4	$0.97	$3.88
Lysol Wipes	Walmart	Cleaning	1	$2.98	$2.98
$\frac{1}{8}$ Wood Board	Home Depot	Miscellaneous Tooling	1	$11.74	$11.74
Drill Bit Set	Amazon	Tooling	1	$29.99	$29.99
Dremmel Bit Set	Amazon	Tooling	1	$35.97	$35.97
Micro Cotton Swab Tips (400)	Preskboo	Epoxy Applicators	1	$16.68	$16.68
		TOTAL COST			**$113.22**
		Budget Allocation			$650.00
		Margin			$536.78
Vehicle Design Components	Vendor	Description	Qty	Price Per Unit	Total Cost
RockSim Licenses	Apogee Components	General	4	$20.00	$80.00
G80T-7 Motors	Apogee Components	Subscale	3	$35.30	$105.90
Motor Retainer	Apogee Components	Subscale	1	$10.00	$10.00
Nose Cones 11.25 in. long	Apogee Components	Subscale	2	$22.19	$44.38
Payload Bay (3 in. tube)	Apogee Components	Subscale	1	$11.17	$11.17
66 mm Tubing	Apogee Components	Subscale	1	$13.00	$13.00
Balsa Sheet	Apogee Components	Subscale	1	$1.76	$1.76
Couplers	Apogee Components	Subscale	5	$16.75	$83.75
Motor Mount (29 mm Tubing)	Apogee Components	Subscale	1	$4.99	$4.99
Epoxy Clay	Apogee Components	Subscale	1	$14.95	$14.95
Taxes & Shipping	Apogee Components	Subscale	1	$86.48	$86.48
$\frac{1}{8}$ in. Plywood	Home Depot	Subscale	1	$11.74	$11.74
RocketPoxy	Apogee Components	Solid Testing	1	$43.75	$43.75

Fiberglass Bulkhead	Apogee Components	Solid Testing	3	$9.80	$29.40
Taxes & Shipping	Apogee Components	Solid Testing	1	$17.41	$17.41
G80 Motors	Impulse Buys Motor Dealer	Subscale	2	$30.00	$60.00
FIN-2SQFT-125	Public Missiles	Full-Scale: G10 Sheet for Fins	3	$67.89	$203.67
CFAF-3.0-PRMx60 (0.054 thickness)	Public Missiles	Full-Scale: Carbon Fiber Motor Mount	1	$229.95	$229.95
CFAF-6.0-PRMx60 (0.054 thickness)	Public Missiles	Full-Scale: Carbon Fiber Tubing	2	$439.95	$879.90
CFCT-6.0x11.75 (0.056 thickness)	Public Missiles	Full-Scale: Carbon Fiber Tubing	2	$94.95	$189.90
CF Airframe Cutting	Public Missiles	Full-Scale: Custom Cuts	3	$6.00	$18.00
CF Airframe Slotting	Public Missiles	Full-Scale: Custom Slots	8	$6.00	$48.00
8 in. G12 Airframe	Madcow Rocketry	Payload Bay Fiberglass Tubing	1	$340.00	$388.00
G10 Fiberglass CR	Apogee Components	Fin Can Centering Rings	2	$19.95	$39.90
Motor Retainer	Apogee Components	Full-Scale Motor	1	$56.67	$56.67
Fiberglass Tube Bulkhead	Apogee Components	ABS Aft Bulkhead	1	$9.80	$9.80
1515 Large Rail Buttons	Apogee Components	Rail Buttons	1	$11.17	$11.17
$\frac{3}{16}$ in. Fiberglass Sheet	McMaster-Carr	Bulkhead for Main Parachute	1	$29.80	$29.80
316 Stainless Steel Washer 2" OD	McMaster-Carr	Washer for Main Deployment	1	$7.62	$7.62
		TOTAL COST			**$2731.06**
		Allocation			$5000.00
		Margin			$2268.94
Lunar Sample Retrieval System Components	Vendor	Description	Qty	Price Per Unit	Total Cost
98 RPM Econ Gear Motor	ServoCity	Gear Motor	2	$14.99	$36.97
Raspberry Pi 3	CanaKit	Pi 3 with 2.5 A USB Power Supply	1	$49.62	$49.62

16 GB Memory Card	SanDisk	Ultra microSDHC Memory Card with Adapter	1	$5.79	$5.79
$\frac{1}{4}$ in. OD Retaining Ring	McMaster-Carr	Ring	1	$8.13	$15.45
$\frac{1}{4}$ in. ID PTFE Tube	McMaster-Carr	Tubing	1	$11.20	$20.12
25 mm Bore Motor Mount	ServoCity	Motor Mount	2	$5.99	$18.97
4-40 Set Screws	McMaster-Carr	Set Screws	1	$3.17	$3.17
Plastic Washers	McMaster-Carr	Washers	1	$3.00	$3.00
6-32 $\frac{3}{8}$ in. Socket Head Bolts	McMaster-Carr	Bolts	1	$8.86	$8.86
6061 $\frac{7}{16}$ in. Rod	McMaster-Carr	Rod	1	$13.19	$13.19
6061 0.625 in. x 3 in. Flat Bar	Grainger Industrial Supply	Bar	1	$2.87	$2.87
Glass Beads	Fire Mountain Gems and Beads, Inc.	Lunar Ice	15	$2.25	$42.52
HDPE Sheet	McMaster-Carr	HDPE	1	$14.25	$14.25
$\frac{1}{4}$ in. Shaft Collar	Ruland Manufacturing Co., Inc.	Collar	4	$6.36	$25.44
Plastic Gear	McMaster-Carr	Gear	1	$2.46	$2.46
Plastic Rack	McMaster-Carr	Rack	1	$3.69	$3.69
High Speed Micro Servo	AMain Hobbies	Servo	1	$29.99	$29.99
Micro CR Motor	Adafruit Industries	Motor	1	$7.50	$7.50
Flight Controller	GetFPV	F4 Nano	1	$29.99	$29.99
Adafruit Itsy Bitsy 3 V	Adafruit Industries	Microcontroller Board	1	$9.95	$9.95
Retention Solenoid	Adafruit Industries	Medium Push Pull Solenoid	4	$7.50	$30.00
Transistor for Solenoid	SparkFun Electronics	Transistor	4	$0.95	$3.80
Diodes for Solenoid	Adafruit Industries	Diodes	1	$1.50	$1.50
5V Regulator for Solenoid	Adafruit Industries	Regulator	4	$0.75	$3.00
Tenergy Li-Ion 11.1 V 2600 mAh	Tenergy Power	Rover Battery	2	$41.99	$83.98
Sabertooth 2x5	RobotShop	Motor Driver	1	$57.95	$57.95
Ori32 BLHeli32	GetFPV	Electronic Speed Controller	1	$39.99	$39.99
Caddx Turbo EOS2 Micro Camera	GetFPV	Camera	1	$15.99	$15.99

TBS Crossfire Nano Receiver	GetFPV	Receiver	1	$29.99	$29.99
Matek M8Q-5883 GPS	GetFPV	GPS	1	$32.99	$32.99
TBS Unify Pro32 Video Transmitter	GetFPV	Transmitter	1	$29.95	$29.95
Lumenier AXII 5.8 GHz Antenna	GetFPV	UAV Antenna	1	$19.99	$19.99
TBS Crossfire TX Bluetooth	GetFPV	Bluetooth	1	$149.99	$149.99
Lumenier AXII LR Antenna	GetFPV	Ground Station Antenna	1	$19.99	$19.99
Propellers	BetaFPV	UAV Props	1	$8.99	$8.99
RCX H1304 Motor	MyRcMart	Motor	4	$9.99	$39.96
RC832 Receiver	AKK	Receiver	1	$16.99	$16.99
3DR Telemetry Kit	ReadytoSky	Telemetry	1	$24.99	$24.99
Lumenier 3S2P Battery	GetFPV	UAV Battery	1	$39.99	$39.99
Bulkhead Bearing	McMaster-Carr	Bearing	1	$13.24	$13.24
3D Printed Parts	Innovation Park	Payload Custom Prints	1	$650.00	$650.00
BNO055	Digi-Key	Accelerometer, Gyroscope, Magnetometer, 9 Axis	1	$11.16	$11.16
MTK3339	Adafruit Industries	GPS Module	1	$29.95	$29.95
RFM95W-915S2 LoRa Module	Digi-Key	Radio Module	1	$13.57	$13.57
32 kHz Crystal Oscillator	Digi-Key	Crystal Oscillator	1	$1.19	$1.19
3.3 V DC-DC Converter	Digi-Key	Converter	1	$4.91	$4.91
5 V DC-DC Converter	Digi-Key	Converter	1	$4.91	$4.91
Logic Converter 3.3 V-5 V	Digi-Key	Converter	1	$1.05	$1.05
PCB Manufacturing	Osh Park	PCB	1	$75.00	$75.00
		TOTAL COST			**$1800.06**
		Allocation			$2000.00
		Margin			$199.94
ABS Components	Vendor	Description	Qty	Price Per Unit	Total Cost
MPL3115A2 - I2C Barometric Pressure, Altitude, Temperature Sensor	Adafruit Industries	Barometric pressure sensor	1	$21.55	$21.55
9-DOF Absolute Orientation IMU Fusion Breakout - BNO055	Adafruit Industries	Accelerometer and gyroscope	1	$33.76	$33.76

Wear-Resistant Black Nylon Sheet, 6 in. x 6 in. x $\frac{1}{2}$ in.	McMaster-Carr	Nylon sheet for sub-scale drag tabs	1	$22.94	$22.94
Raspberry Pi Zero	Adafruit Industries	Microcontroller	1	$16.25	$16.25
Raspberry Pi 3 Power Supply 5 V 2.5 A Micro USB AC Adapter Charger US Plug	Amazon LLC	Plug for powering Raspberry Pi from wall	1	$10.69	$10.69
Adafruit PowerBoost 500 Basic - 5 V USB Boost @ 500 mA from 1.8 V+	RM Gadgets	Power booster for powering Raspberry Pi with battery	1	$12.35	$12.35
AmazonBasics High-Speed Mini-HDMI to HDMI TV Adapter Cable - 6 Feet	Amazon LLC	HDMI cable for connecting Raspberry Pi to monitor	1	$7.48	$7.48
1578 Lithium Ion Polymer Battery - 3.7 V 500 mAh	Adafruit Industries	Batteries for sub-scale	2	$10.06	$20.12
2-Port USB Hub 1 Male to 2 Female USB y Splitter Cable	Amazon LLC	USB splitter to connect mouse and keyboard to Raspberry Pi	1	$8.99	$8.99
Male Micro USB 2.0 to Female USB	Amazon LLC	USB adapter for Raspberry Pi	1	$5.97	$5.97
Multipurpose 6061 Aluminum, 1 in. Thick x 2-$\frac{1}{2}$ in. Wide, 1 Foot Long	McMaster-Carr	Aluminum to fabricate mechanism	1	$23.16	$23.16
Multipurpose 6061 Aluminum, $\frac{1}{4}$ in. Thick x 1-$\frac{1}{2}$ in. Wide, 1 Foot Long	McMaster-Carr	Aluminum to fabricate mechanism	1	$3.68	$3.68
Slippery MDS-Filled Wear-Resistant Nylon Sheet, 12 in. x 12 in. x $\frac{1}{4}$	McMaster-Carr	Nylon to fabricate drag tabs	1	$30.31	$30.31
Slippery MDS-Filled Wear-Resistant Nylon Sheet, 12 in. x 12 in. x $\frac{1}{2}$ in.	McMaster-Carr	Nylon to fabricate slotted deck for drag tabs	1	$55.76	$55.76
Ultra-Low-Profile Precision Shoulder Screw, Slotted, $\frac{1}{4}$ in. Shoulder Diameter, $\frac{1}{2}$ in. Shoulder Length, 10-32 Thread	McMaster-Carr	Shoulder screws for mechanism	8	$4.55	$36.40
Low-Strength Steel Threaded Rod, $\frac{1}{4}$ in.-20 Thread Size, 1 Foot Long	McMaster-Carr	Threaded rods for structure	4	$0.64	$2.56
Birch Rod, 36 in. Long, $\frac{1}{2}$ in. Diameter	McMaster-Carr	Dowel rod for alignment	1	$7.45	$7.45

Steel Locknut with External-Tooth Lock Washer, Zinc-Plated, $\frac{1}{4}$ in.-20 Thread Size	McMaster-Carr	Lock nuts for attaching decks to threaded rods	1	$5.42	$5.42
Ball Bearing, Open, Trade Number R10, for $\frac{5}{8}$ in. Shaft Diameter	McMaster-Carr	Ball bearing for mechanism	2	$6.66	$13.32
RCD 36845 D-845WP 32-Bit Monster Torque Waterproof Steel Gear Servo	Hitec	Servo motor	1	$94.31	$94.31
7.4 V 350 mAh 2S Lipo Battery 25C with USB charger	CBB Store	Pack of 2 batteries for servo motor	1	$19.99	$19.99
3.7 V 450 mAh 502535 Lipo battery Rechargeable Lithium Polymer ion	Wing Deli	Batteries for full-scale electronics	3	$6.49	$19.47
T453 6-Port LiPo Battery Charger	Tenergy	Charger for LiPo batteries	1	$8.99	$8.99
PCB Manufacturing	Osh Park	PCB	1	$75.00	$75.00
		TOTAL COST			**$555.92**
		Allocation			$1300.00
		Margin			$744.08
STEM Engagement Components	Vendor	Description	Qty	Price Per Unit	Total Cost
Straws	Walgreens	Mission to Mars	1	$2.29	$2.29
Trashbags	Walgreens	Mission to Mars	1	$4.49	$4.49
LifeSavers Candy	CVS	Mission to Mars	1	$2.69	$2.69
Rubber Bands	CVS	Mission to Mars	1	$1.69	$1.69
Candy Canes (large)	Walgreens	Mission to Mars	2	$1.99	$3.98
Candy Canes (small)	Walgreens	Mission to Mars	1	$3.29	$3.29
		TOTAL COST			**$18.43**
		Allocation			$300.00
		Margin			$281.57
Miscellaneous Expenses	Vendor	Description	Qty	Price Per Unit	Total Cost
Proposal Dinner	Bruno's Pizza	Lead Compiling Session	1	$49.26	$49.26
Preliminary Design Review Dinner	Bruno's Pizza	Lead Compiling Session	1	$27.24	$27.24
Boeing Meet & Greet	Chick-Fil-A	Session with Pat Dolan	1	$177.57	$177.57

Test Launch Tire Repair	Discount Tire	Test Launch Flat Tire	1	$204.89	$204.89
		TOTAL COST			**$458.96**
		Allocation			$500.00
		Margin			$41.04
Competition Travel Expenses	Vendor	Description	Qty	Price Per Unit	Total Cost
Team Lodging	Airbnb	Rental Home for 4 Nights of Launch Week	4	$725	$2900.00
Team Vehicle Rental	Notre Dame Transportation Services	Mini-Van Rentals	5	$275.00	$1375.00
Team Mentor Hotel	Marriott Hotels	Hotel Room for 4 Nights of Launch Week	4	$88.00	$352.00
Gasoline	Gas Stations en route	Fuel for 5 Mini-Vans per mile	470	$2.61	$1226.70
Food	Restaurants en route and in Alabama	Food budget per member for the entirety of the competition	28	$112.36	$3146.08
		TOTAL COST			**$8999.78**
		Allocation			$9000
		Margin			$0.22

6.4 Project Timeline

The project plan adheres to NASA-specified milestones through the completion of team-derived tasks. The following figures outline timelines for Vehicle Design (Figure 141), the Recovery Subsystem (Figure 142), the Lunar Sample Retrieval System (Figure 143), the Air Braking System (Figure 144), Systems & Safety (Figure 145), and STEM Engagement (Figure 146). Timelines pictured begin at the beginning of the University of Notre Dame's semester on January 14 (except the timelines for LSRS and ABS, which begin on January 13). All tasks and milestones before this date have been completed, as displayed in the progress column.

6.4.1 Vehicle Design Timeline

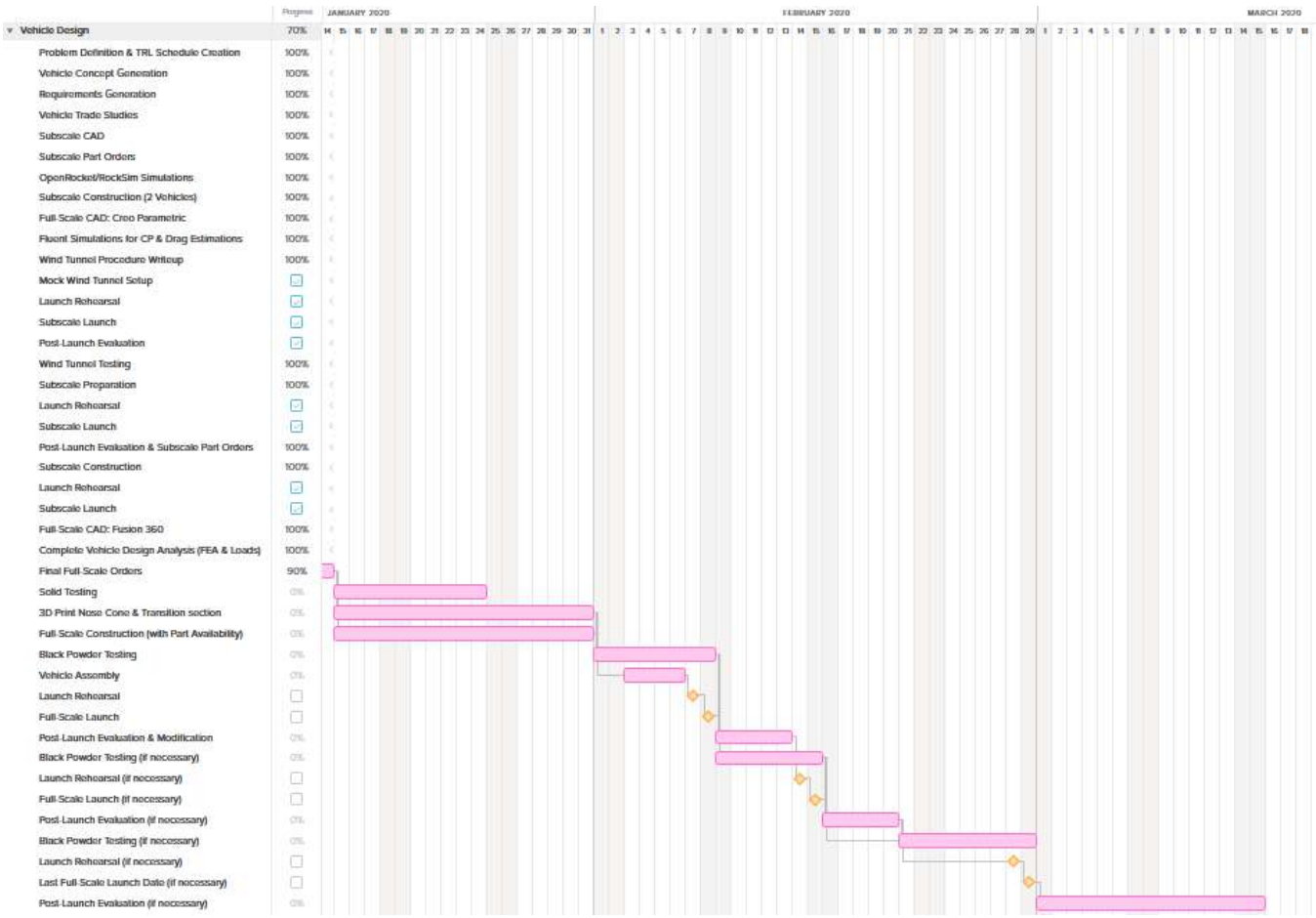

Figure 141: Second Semester Timeline for the Vehicle Design Team.

6.4.2 Recovery Subsystem Timeline

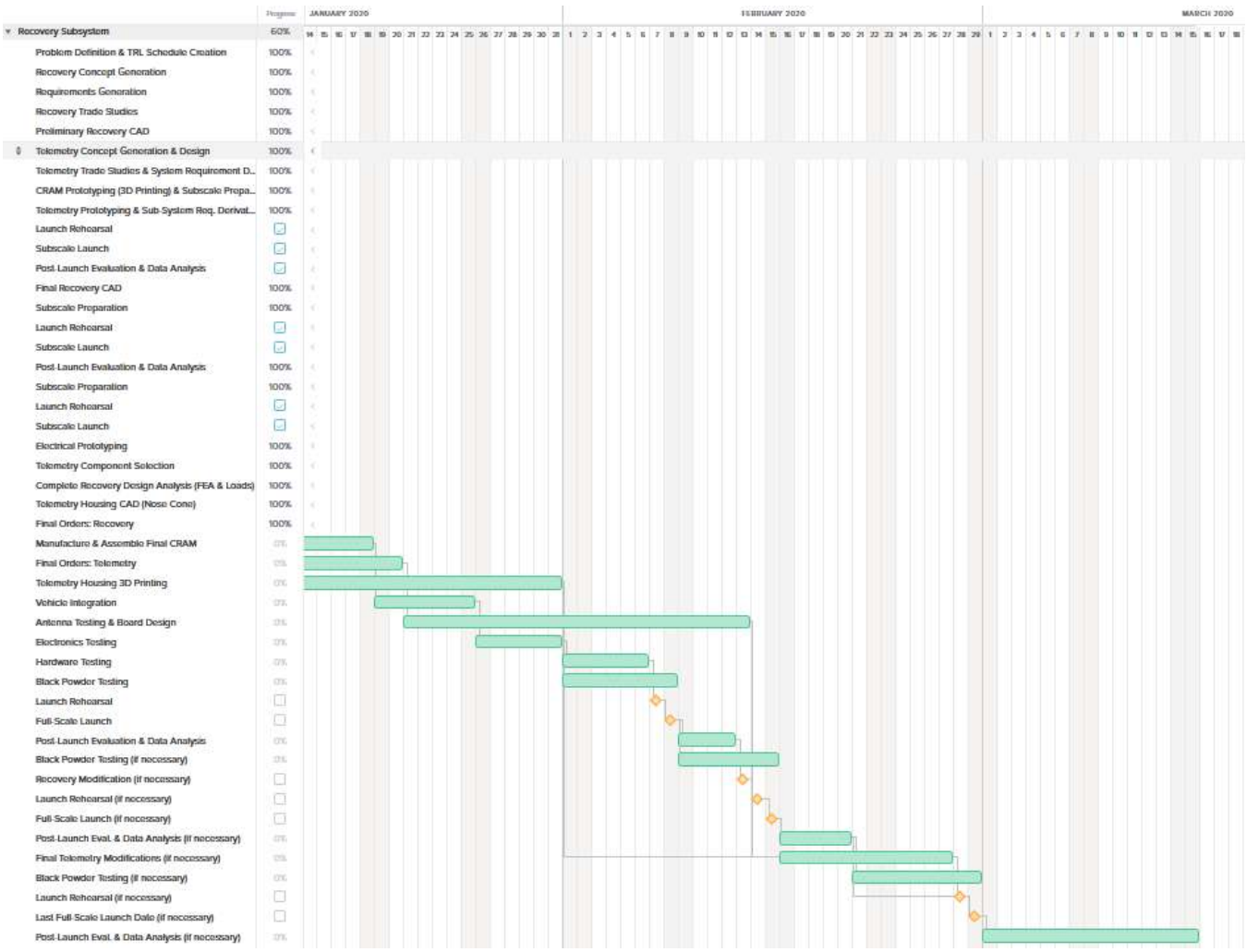

Figure 142: Second Semester Timeline for the Recovery Team.

6.4.3 Lunar Sample Retrieval System Timeline

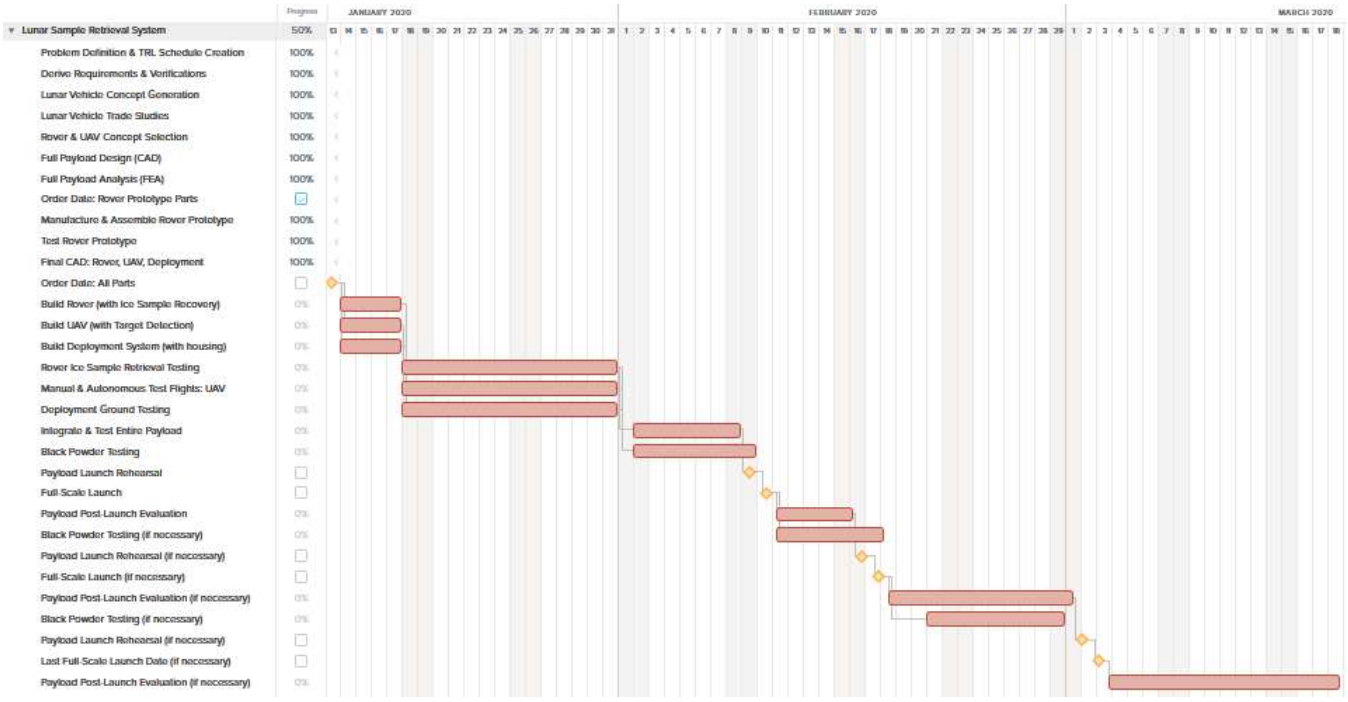

Figure 143: Second Semester Timeline for the Lunar Sample Retrieval System Team.

6.4.4 Air Braking System Timeline

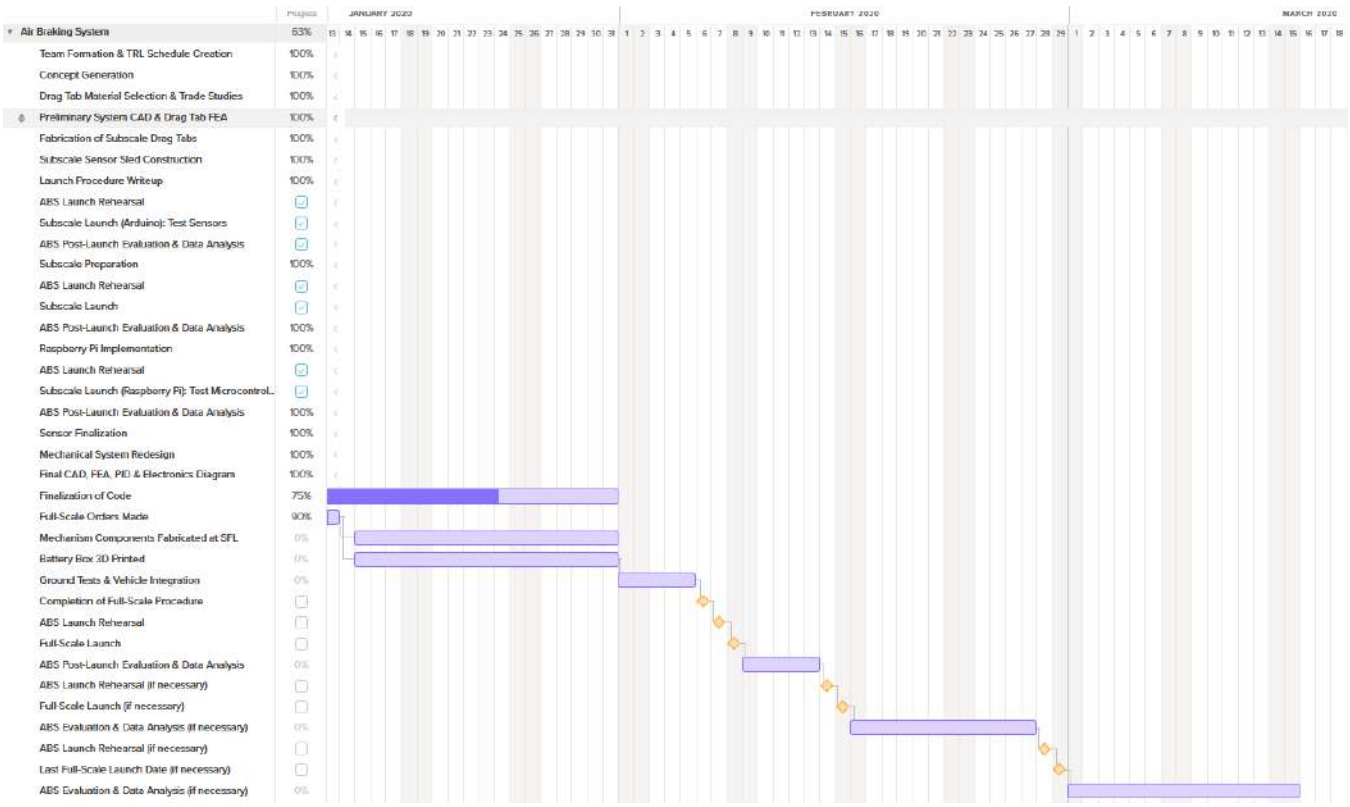

Figure 144: Second Semester Timeline for the Air Braking System Team. The team is ahead of schedule in finalizing their Kalman Filter, 4th Order Runge-Kutta, and PID codes.

6.4.5 Systems & Safety Timeline

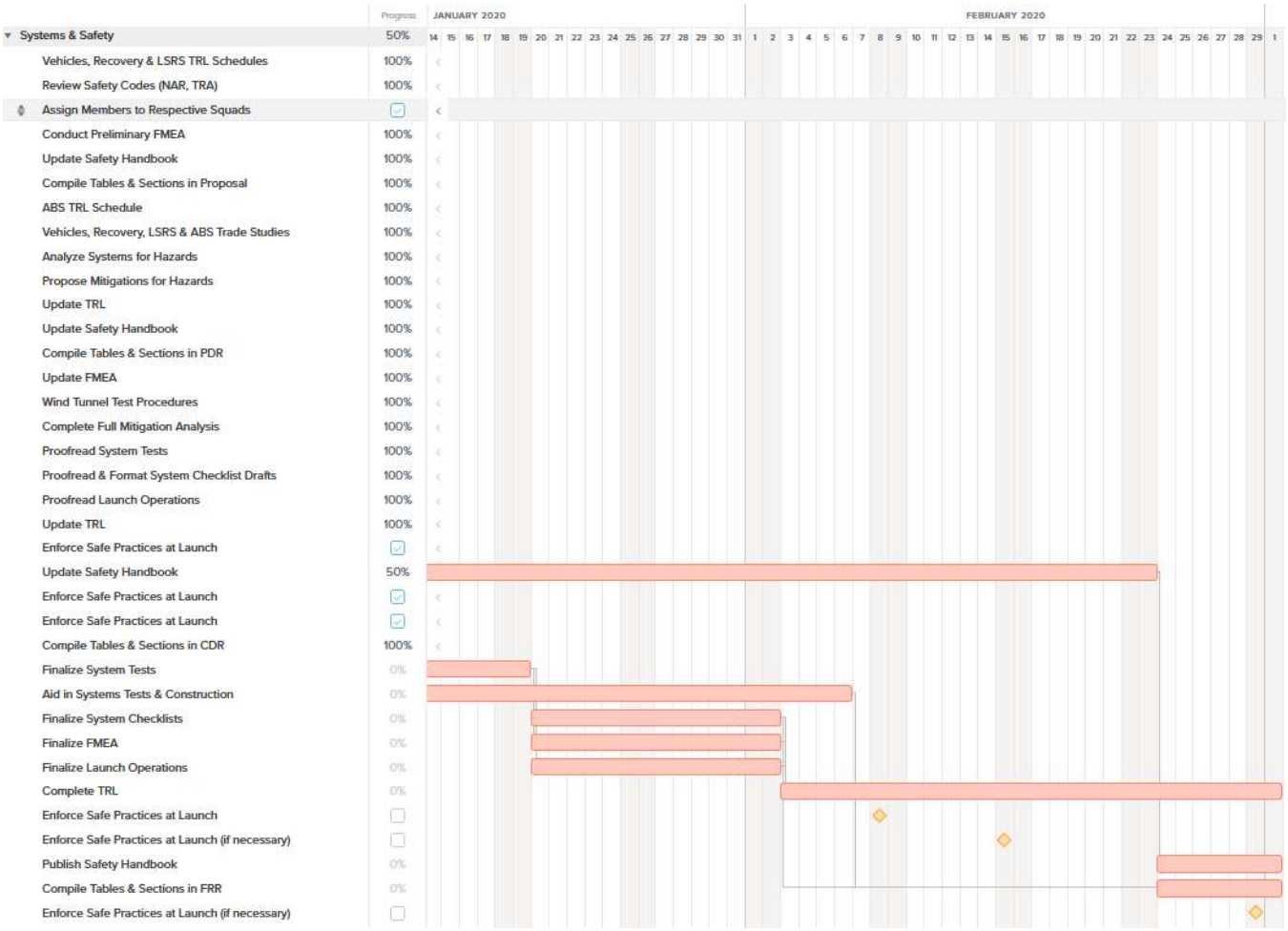

Figure 145: Second Semester Timeline for the Systems & Safety Team.

6.4.6 STEM Engagement Timeline

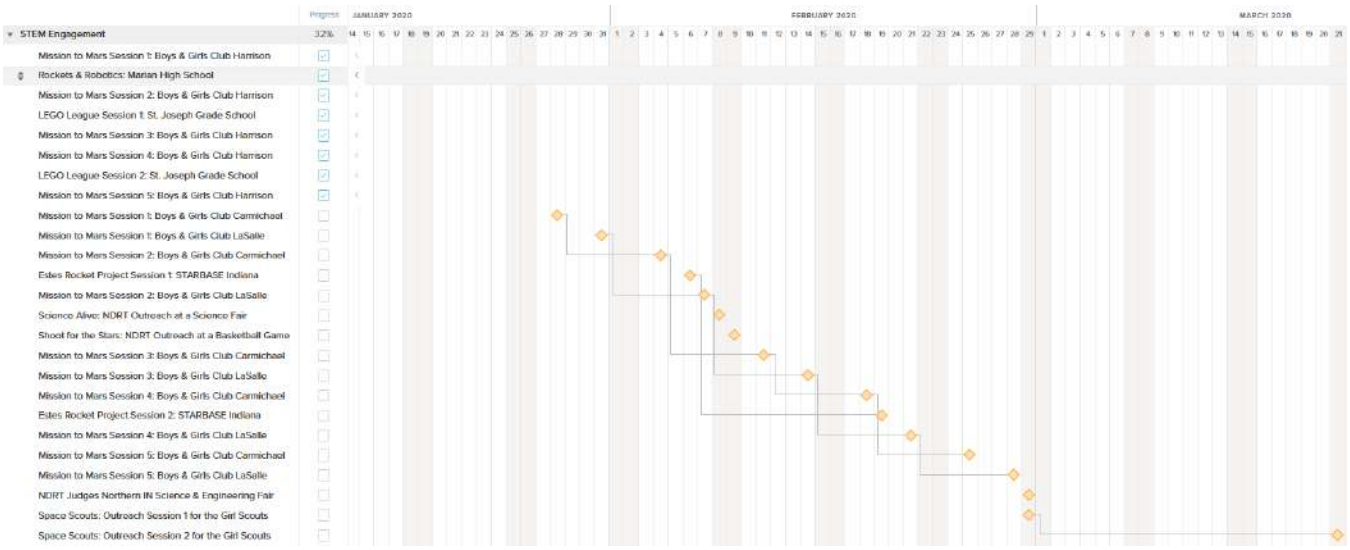

Figure 146: Second Semester Timeline for STEM Engagement.

6.4.6.1 STEM Engagement Project Descriptions

This year, the Notre Dame Rocketry Team will continue its involvement with the community and efforts to encourage excellence in STEM through Educational outreach and mentorship. In the past, the team participated in events working directly with students to promote excellence in STEM and teamwork. These events featured hands-on activities, one on one interaction between team member and student, and curriculum tailored to the age level. The team plans to continue working with several of the same organizations as in years past, including The Boys and Girls Club of St. Joseph County, the Society of Women's Engineers, and the Girl Scouts of Northern Indiana. In addition, the team intends on extending its reach into the community and working with students from local parishes and schools. Activities will span over a wide age range, ranging from 3rd to 12th grade. Several larger events that proved to be successful in the past will be repeated, such as the Science Alive! fair held at the St. Joseph County Library, the 5 week programs with the Boys and Girls Club, and the Girl Scout day. With such a push for volunteer opportunities by members of the team, the team is overcoming the proposal goal of 500 students, and aiming to reach at least 2000 by the time of competition. Additionally, the team implemented a new mentorship program between returners and new members, which will help promote STEM and rocketry internally. It will not only be a resource for the sharing of knowledge, but also a way to foster relationships and good team unity. The effort to educate and support between team members will strengthen leadership skills and build confidence in one's knowledge of the field. This program will make members better mentors, teachers, and project leaders. It will allow them to make an even larger impact on the community, fostering relationships with youth and encouraging the future of science, technology, engineering, and mathematics. Through the demonstration of scientific experiments, presentations, and mentorship, NDRT plans to have an incredibly successful year; with the incredible dedication of team members and their efforts to promote creativity,

innovation and inspiration, this goal will be achievable.

Mission to Mars: The Mission to Mars program is designed for a 5 week curriculum. It is unique to this year's objective of building a Lunar Vehicle system and will provide students with an understanding of planetary surface exploration. The first lesson provides background information on Mars, including the physical features, the location, and the atmosphere, through the form of a Bingo game. Students then discuss with NDRT members what a vehicle would need to survive in these conditions in terms of fuel capacity, weight, durability, size, etc. The second lesson is a modified version of the NASA *Touchdown* exercise, teaching the principles of landing on different surfaces and shock absorbent systems in order to protect fragile cargo. Students drop test systems constructed of paper cups with marshmallow "astronauts" from a designated height and then discuss their results. The third lesson teaches the importance of communication and conciseness in missions through the NASA *Rover Races* lesson. Students work to complete a set course with a small team, where only the leader of the team dictates commands. The fourth lesson challenges students to apply knowledge of the factors learned in previous lessons through the design of a rubber band powered vehicle. The focus is on structure, size, and ability to operate. Students will test the vehicles for functionality, efficiency, and design. NDRT members assist in leading these tests and discuss with the students upon completion. The fifth lesson is an overall collaboration of all lessons, providing a review and evaluation of what the students learned in the form of a Mars Jeopardy game.

Rockets & Robotics: Following the team's goal of establishing connections around the community, the event allows NDRT members to meet with students from the Marian Catholic High School Rocketry and Robotics team. Ranging from freshmen to seniors, the students shared their experiences as part of the high school rocketry and robotics team. NDRT members gave a short presentation about the mission of the team and a summary of the Student Launch Initiative. Emphasis was placed on the implementation of the engineering design process and the mentorship that is required to successfully complete the task. Students were then given the chance to ask questions to the NDRT members, whether about rocketry and robotics, college, the competition rocket, and more.

Building Connections with LEGO League: The NDRT met with the St. Joseph Grade School LEGO League team in an effort to learn more about the local community and work with a local school. In a series of two events, NDRT members established connections with students ranging from grades 5-8. These events focused on mentoring the students through learning about their LEGO league projects, working with them to refine designs, and providing them with additional challenges as teambuilding and brainstorming exercises.

Estes Rocket Project: In a partnership with STARBASE Indiana, a Department of Defense funded STEM engagement foundation, NDRT will present to 5th grade students from local underprivileged schools. The presentation will include a summary of the Student Launch Initiative, background information about rocketry, and a brief demonstration using an Estes rocket. This presentation is a fantastic opportunity to foster relationships between NDRT members and students from around the community who may not otherwise have exposure to STEM or access to STEM activities.

Space Scouts: In partnership with the Girl Scouts of Northern Indiana, the NDRT will host two events that will provide a series of rocketry related activities and challenges. The specific lesson is still being determined.

Shoot for the Stars: The NDRT will provide rocketry related challenges and teambuilding exercises hosted at a booth during a Notre Dame basketball game. The specific lesson is still being determined.

A Full Black Powder Calculations

Initial Separation Event: Drogue Parachute Deployment

$$F = (\tau)(A_s)(n) = (10{,}000\,\text{psi})(\frac{\pi}{4}(0.086\text{ (in.)})^2)(2\text{ Shear Pins}) = 116\,\text{lb}_\text{f}$$

$$P = \frac{F}{A_b} = \frac{116\,\text{lb}_\text{f}}{\frac{\pi}{4}(6\text{ in.})^2} = 4.1\text{ psi} = 0.28\text{ atm}$$

$$\text{Chamber Volume} = \frac{\pi}{4}(\text{bulkhead diameter (in.)}^2)(\text{height (in.)}^2)$$
$$= \frac{\pi}{4}(6\text{ (in.)}^2)(11\text{ (in.)}) = 311\text{ (in.)}^3 = 5.1\text{ L}$$

$$n_g = \frac{PV}{RT} = \frac{(0.28\text{ atm})(5.1\text{ L})}{(0.082057\text{ (L*atm/mol/K)})(1837.2\text{ K})} = 0.0095\text{ moles gas}$$

$$\frac{0.0095\text{ moles gas}}{1} \times \frac{2\text{ mol KNO}_3}{4\text{ mol gas}} \times \frac{101.1\text{ g KNO}_3}{1\text{ mol KNO}_3} = 0.48\text{ g KNO}_3$$

$$\frac{0.0095\text{ moles gas}}{1} \times \frac{1\text{ mol S}}{4\text{ mol gas}} \times \frac{32.1\text{ g S}}{1\text{ mol S}} = 0.076\text{ g S}$$

$$\frac{0.0095\text{ moles gas}}{1} \times \frac{3\text{ mol C}}{4\text{ mol gas}} \times \frac{12.0\text{ g C}}{1\text{ mol C}} = 0.085\text{ g C}$$

$$0.48\text{ g KNO}_3 + 0.076\text{ g S} + 0.085\text{ g C} = 0.64\text{ g Black Powder}$$

With a FOS of 25%, $\boxed{0.8\text{ g}}$ of black powder is needed for the initial separation event. This will be rounded to 1 g of black powder for ease of measuring in the launch field.

Secondary Separation Event: Main Parachute Deployment

$$F = (\tau)(A_s)(n) = (10{,}000\,\text{psi})(\frac{\pi}{4}(0.086\text{ (in.)})^2)(4\text{ Shear Pins}) = 232\,\text{lb}_\text{f}$$

$$P = \frac{F}{A_b} = \frac{232\,\text{lb}_\text{f}}{\frac{\pi}{4}(6\text{ in.})^2} = 8.2\text{ psi} = 0.56\text{ atm}$$

$$\text{Chamber Volume} = \frac{\pi}{4}(\text{bulkhead diameter (in.)}^2)(\text{height (in.)}^2)$$
$$= \frac{\pi}{4}(6\text{ (in.)}^2)(31\text{ (in.)}) = 876\text{ (in.)}^3 = 14.3\text{ L}$$

$$n_g = \frac{PV}{RT} = \frac{(0.56\text{ atm})(14.3\text{ L})}{(0.082057\text{ (L*atm/mol/K)})(1837.2\text{ K})} = 0.053\text{ moles gas}$$

$$\frac{0.053\text{ moles gas}}{1} \times \frac{2\text{ mol KNO}_3}{4\text{ mol gas}} \times \frac{101.1\text{ g KNO}_3}{1\text{ mol KNO}_3} = 2.7\text{ g KNO}_3$$

$$\frac{0.053\text{ moles gas}}{1} \times \frac{1\text{ mol S}}{4\text{ mol gas}} \times \frac{32.1\text{ g S}}{1\text{ mol S}} = 0.43\text{ g S}$$

$$\frac{0.053\text{ moles gas}}{1} \times \frac{3\text{ mol C}}{4\text{ mol gas}} \times \frac{12.0\text{ g C}}{1\text{ mol C}} = 0.48\text{ g C}$$

$$2.7\text{ g KNO}_3 + 0.43\text{ g S} + 0.48\text{ g C} = 3.6\text{ g Black Powder}$$

With a FOS of 25%, $\boxed{4.5\text{ g}}$ of black powder is needed for the secondary separation event. This will be rounded to 5 g of black powder for ease of measuring in the launch field.

Tertiary Separation Event: Nose Cone Ejection for Payload Deployment

$$F = (\tau)(A_s)(n) = (10{,}000\ psi)(\frac{\pi}{4}(0.112\ in.)^2)(2\ Shear\ Pins) = 197\ lb_f$$

$$P = \frac{F}{A_b} = \frac{197\ lb_f}{\frac{\pi}{4}(4.5\ in.)^2} = 12.4\ psi = 0.843\ atm$$

$$Chamber\ Volume = \frac{\pi}{4}(bulkhead\ diameter\ (in.)^2)(height\ (in.)^2)$$

$$= \frac{\pi}{4}(4.5\ (in.)^2)(3\ (in.)) = 47.7\ (in.)^3 = 0.782\ L$$

$$n_g = \frac{PV}{RT} = \frac{(0.843\ atm)(0.782\ L)}{(0.082057\ (L*atm/mol/K))(1837.2\ K)} = 0.004372\ moles\ gas$$

$$\frac{0.004372\ mol\ gas}{1} \times \frac{2\ mol\ KNO_3}{4\ mol\ gas} \times \frac{101.1\ g\ KNO_3}{1\ mol\ KNO_3} = 0.221\ g\ KNO_3$$

$$\frac{0.004372\ mol\ gas}{1} \times \frac{1\ mol\ S}{4\ mol\ gas} \times \frac{32.1\ g\ S}{1\ mol\ S} = 0.0351\ g\ S$$

$$\frac{0.004372\ mol\ gas}{1} \times \frac{3\ mol\ C}{4\ mol\ gas} \times \frac{12.0\ g\ C}{1\ mol\ C} = 0.0393\ g\ C$$

$$0.221\ g\ KNO_3 + 0.0351\ g\ S + 0.0393\ g\ C = 0.295\ g\ Black\ Powder$$

With a FOS of 20%, $\boxed{0.354\ \text{g}}$ of black powder are needed for the tertiary separation event.

Summary of Black Powder Charges

Table 96: Summary of Black Powder Charges

Separation Event	Amount of Black Powder
Initial (Drogue)	1 g Black Powder
Secondary (Main)	5 g Black Powder
Tertiary (Nose Cone)	0.354 g Black Powder

B ABS

B.1 Kalman Filter Python Script

```
import numpy as np
import matplotlib.pyplot as plt
import openpyxl
"""
Variables:
x-state vector
phi-state transition matrix
H-state to sensor matrix
"""
#Constructs a matrix to move from the body frame to the inertial frame
def body_to_inertial(roll,pitch,yaw):
    c = lambda x: np.cos(x)
    s = lambda x: np.sin(x)
    out = np.zeros((3,3))
    out[0,0] = c(yaw)*c(pitch)
    out[0,1] = c(yaw)*s(roll)*s(pitch)-c(roll)*s(yaw)
    out[0,2] = s(roll)*s(yaw)+c(roll)*c(yaw)*s(pitch)
    out[1,0] = c(pitch)*s(yaw)
    out[1,1] = c(roll)*c(yaw)+s(roll)*s(yaw)*s(pitch)
    out[1,2] = c(roll)*s(yaw)*s(pitch)-c(yaw)*s(roll)
    out[2,0] = -s(pitch)
    out[2,1] = c(pitch)*s(roll)
    out[2,2] = c(roll)*c(pitch)
    return out
#Transforms body acceleration to inertial acceleration
def accel_trans(a,roll,pitch,yaw):
    R = body_to_inertial(roll,pitch,yaw)
    #R = inertial_to_body(roll,pitch,yaw)
    a_trans = R@a
    return a_trans
#Implements the Kalman Filter-May later be replaced by the FilterPy Library
class Kalman():
    def __init__(self,var_m,var_s,var_a):
        self.T = 0
        self.x = np.array([0,0,0])
        self.gen_phi()
        self.H = np.array([[1,0,0],
                           [0,0,1]])
        self.Q = np.array([[0,0,0],
                           [0,0,0],
                           [0,0,var_m]])
        self.R = np.array([[var_s,0],
                           [0,var_a]])
```

```
        self.P = np.zeros((3,3))
        self.K = np.zeros((3,2))
        self.I = np.eye(3)
    #Generate the transition matrix from the ∆ t
    def gen_phi(self):
        self.phi = np.array([[1,self.T,self.T**2/2],
                             [0,1,self.T],
                             [0,0,1]])
    #Updates the state
    def update_state(self,in_z,∆_t): #in_z is input sensor readings
        self.T = ∆_t
        self.gen_phi()
        xhatpre = self.phi@self.x
        xhatpost = xhatpre+self.K@(in_z-self.H@xhatpre)
        Pkpre = self.phi@self.P@self.phi.T+self.Q
        Pkpost = (self.I-self.K@self.H)@Pkpre
        Kk = Pkpre@self.H.T@np.linalg.inv(self.H@Pkpre@self.H.T+self.R)
        self.x = xhatpost
        self.P = Pkpost
        self.K = Kk
    #Outputs the current state
    def current_state(self):
        return self.x
#reads in a row of the sheet and creates a measurement
def create_measurement(row,sheet):
    #Read in BNO Absolute Orientation and convert to radians
    roll = sheet['H'+str(row)].value*np.pi/180
    pitch = sheet['I'+str(row)].value*np.pi/180
    yaw = sheet['J'+str(row)].value*np.pi/180
    #Read in altitude
    y = sheet['N'+str(row)].value
    #Read in ADXL Acceleration and translate to vertical
    ax = sheet['O'+str(row)].value
    ay = sheet['P'+str(row)].value
    az = sheet['Q'+str(row)].value
    a_trans = accel_trans(np.array([ax,ay,az]),roll,pitch,yaw)
    return np.array([y,a_trans[1]])
if __name__ == '__main__':
    wb = openpyxl.load_workbook('NoTab.xlsx')
    sheet = wb['Filtered Data']
    #Set the parameters of the variances
    var_m = 3
    var_s = .1
    var_a = 5
    filty = Kalman(var_m,var_s,var_a)
    states = []
    x_rec = []
    a_rec = []
    prev_t = sheet['A2'].value
    for i in range(2,200):#len([i for i in sheet.rows])):
        z = create_measurement(i,sheet)
```

```
        t = sheet['A'+str(i)].value
        ∆_t = t - prev_t
        prev_t = t
        filty.update_state(z,∆_t)
        states.append(filty.current_state())
        x_rec.append(z[0])
        a_rec.append(z[1])
    #Plot Output
    states = np.array(states)
    plt.clf()
    plt.subplot(131)
    plt.plot(x_rec,label='Sensor Position')
    plt.plot(states[:,0],label='Kalman Position')
    plt.legend()
    plt.subplot(132)
    plt.plot(states[:,1],label='Kalman Velocity')
    plt.legend()
    plt.subplot(133)
    plt.plot(a_rec,label='Sensor Acceleration')
    plt.plot(states[:,2],label='Kalman Acceleration')
    plt.legend()
    plt.show()
```

B.2 PID Algorithm

```
%% PID
% Set gains
kP = 2; % Proportional Gain
kD = 0.5; % Derivative Gain
kI = 0.05; % Integral Gain

%% Load ideal flight path
ideal = load('Ideal_Flight_Profile.csv');
yi = ideal(:,1); % altitude of ideal flight
vi = ideal(:,2); % vertical velocity of ideal flight
ymax = 4444; % target altitude

%% Given Quantities
mr = 831/(16*32.2); % Mass of rocket (oz converted to slugs)
g = 32.2; % [ft/s^2]
Cd_r = 0.30; % drag coefficient of rocket based on wind tunnel test
Cd_t = 2.06; % drag coefficient of drag tabs based on CFD results
Dr = (8/12); % Largest diameter of rocket [ft]
Ar = (pi/4)*Dr^2; % Incident area of rocket due to largest diameter [ft^2]
At = 4*1*1.995/144; %[ft^2] full extension area of tabs
rho = 0.0023769; % density of air [slug/ft^3]
```

```
theta = 10*pi/180; % fixed flight angle (degrees converted to radians)
dt = .01; %timestep

%% Conditions at burnout
    iCnt = 2; % start main loop counter
    y(iCnt) = 975.48; % altitude at burnout (this can be changed)
    y(iCnt-1) = y(iCnt);
    v(iCnt) = max(vi); % velocity at burnout (this can be changed)
    v(iCnt-1) = v(iCnt);
    phi(iCnt) = 0; % tabs are fully retracted at the start
    t(iCnt) = 0;
    err1(iCnt) = v(iCnt)-max(vi);
    phi(iCnt+1) = 0;

while (v(iCnt) > 0) % run until apogee is reached
    % Do one step of numerical integration of the rocket's position
    [y,v,phi] = rocketKutta(y,v,theta,phi,dt,rho,Ar,Cd_r,Cd_t,g,mr,iCnt);

    % increment main loop counter
    iCnt = iCnt + 1;

    % Increment time vector
    t(iCnt) = t(iCnt-1) + dt;

%Find error between new position and road
    err1(iCnt) = error1(y,v,yi,vi,iCnt,ymax);

%Find the approximate derivative to the error function
    % Compute approximate derivative of the error term using backward
    % finite difference technique
    derivError = derror(y,err1,iCnt);

%Find the approximate integral to the error function
    % Compute the approximate integral of the error function
    intError = ierror(y,err1,iCnt);

%%  PID control law for shaft angle
    % Compute new value for phi using PID control law
    phi(iCnt) = kP*err1(iCnt) + kD*derivError + kI*intError;
end
```

B.3 4th Order Runge-Kutta Flight Simulation

```
function [y,v,phi] = rocketKutta(y,v,theta,phi,dt,rho,Ar,Cd_r,Cd_t,g,mr,...
iCnt)
% rocketKutta performs one time step of the 4th order Runge-Kutta method
```

```
% numerical approximation for marching forward the equation
% of motion for the rocket.  It includes limits on the shaft angle
% and limits on change in shaft angle per time step based on the motor
% and mechanism design.

% Set parameters
maxPhi = 63.5*pi/180; % maximum absolute value of phi in radians

% Compute the maximum amount the shaft can turn in one time step
maxDeltaPhi = 60*pi/180/.17*dt; %(rad)

% Find the current array counter
iCnt = length(y);

% compute the change in phi between timesteps
ΔPhi = phi(iCnt) - phi(iCnt-1);
% If the Δ phi is too great change to max allowable
if abs(ΔPhi) > maxDeltaPhi
    if ΔPhi < 0
        phi(iCnt) = phi(iCnt-1) - maxDeltaPhi ;
    else
        phi(iCnt) = phi(iCnt-1) + maxDeltaPhi ;
    end
    disp(['Change in steering angle per timestep too great at...
    (',num2str(y(iCnt)),',',num2str(v(iCnt)),').']);
end

% Now check limits on phi. If phi is out of its max, change commanded phi
% to the limits.

if phi(iCnt) < 0
    phi(iCnt) = 0;
elseif phi(iCnt) > maxPhi
    phi(iCnt) = maxPhi;
    %flag = 3;
    disp(['Shaft angle too great. It was set to 63.5 degrees at...
    (',num2str(y(iCnt)),',',num2str(v(iCnt)),').']);
end

% Perform 4th order Runge-Kutta to find new position and velocity
    L= (-9.16e-7)*rad2deg(phi(iCnt))^3 + (-1.66e-4)*rad2deg(phi(iCnt))^2...
    + 0.0317*rad2deg(phi(iCnt)) - 0.00131; % extension of tabs based on phi
    At = 4*L*1.995/144; % Resulting area of tabs [ft^2]
    k11 = v(iCnt)*dt;
    k21 = (-((rho*Ar*Cd_r)/(2*mr*cos(theta)))*(v(iCnt)^2) -...
    ((rho*At*Cd_t)/(2*mr*cos(theta)))*(v(iCnt)^2) - g)*dt;
    k12 = (v(iCnt) + 0.5*k21)*dt;
    k22 = (-((rho*Ar*Cd_r)/(2*mr*cos(theta)))*((v(iCnt)+0.5*k21)^2) -...
    ((rho*At*Cd_t)/(2*mr*cos(theta)))*((v(iCnt)+0.5*k21)^2) - g)*dt;
    k13 = (v(iCnt) + 0.5*k22)*dt;
    k23 = (-((rho*Ar*Cd_r)/(2*mr*cos(theta)))*((v(iCnt)+0.5*k22)^2) -...
```

```
55      ((rho*At*Cd_t)/(2*mr*cos(theta)))*((v(iCnt)+0.5*k22)^2) - g)*dt;
56      k14 = (v(iCnt) + k23)*dt;
57      k24 = (-((rho*Ar*Cd_r)/(2*mr*cos(theta)))*((v(iCnt)+k23)^2) -...
58      ((rho*At*Cd_t)/(2*mr*cos(theta)))*((v(iCnt)+k23)^2) - g)*dt;
59
60      y(iCnt+1) = y(iCnt) + (1/6)*(k11 + 2*k12 + 2*k13 + k14);
61      v(iCnt+1) = v(iCnt) + (1/6)*(k21 + 2*k22 + 2*k23 + k24);
62      phi(iCnt+1) = phi(iCnt);
```

B.4 PID Error Functions

```
1  function [err1] = error1(y,v,yi,vi,iCnt,ymax)
2
3  yr = y(iCnt);
4  yid = yi(1);
5  i = 1;
6
7  while (yid ≤ yr) && (i < length(yi)) % search the whole vector until the
8  %altitudes approx. match
9      if i < length(yi)
10         yid = yi(i);
11         i = i+1;
12     else
13        yid = ymax;
14     end
15 end
16
17 m = (vi(i) - vi(i-1)) / (yi(i) - yi(i-1));
18 videal = m*(y(iCnt) - yi(i-1)) + vi(i-1); % calc ideal velocity at this
19 %altitude (linear approx)
20 vrocket = v(iCnt); % velocity of rocket at this point
21 err1 = vrocket - videal;
22
23 if yid < 1000
24     err1 = 0; % does not work until alt = 1000 feet to avoid
25     %"early burnout" issue
26 end
27
28 function [derivError] = derror(y,err1,iCnt)
29
30 derivError = (err1(iCnt)-err1(iCnt-1))/(y(iCnt)-y(iCnt-1));
31
32 function [intError] = ierror(y,err1,iCnt)
33
34 intError=0;
35 for i=2:iCnt
```

```
36      if err1(i) ≥.1 || err1(i)≤-.1
37          intError= intError + (y(i)-y(i-1))*(err1(i)+err1(i-1))/2;
38      else
39          intError=0;
40      end
41  end
```

C Some team's stuff...

C.1 Kewl Complicated Algorithm Code

```
% This is the formatting for MATLAB code
% It is snackilicious
i = 1;
for i = 1:100
    disp('yeah')
    i = i + 1;
end
```

D Another team's stuff...

D.1 Anotha Kewl Complicated Algorithm Code

```
% This is the formatting for MATLAB code
% It is snackilicious
i = 1;
for i = 1:100
    disp('yeah')
    i = i + 1;
end
```

E References